UNICAMP

SUSANA PEREIRA DE JESUS

MODELAGEM DA CINÉTICA DE TRANSFERÊNCIA DE MASSA NO PROCESSO DE EXTRAÇÃO SUPERCRÍTICA A PARTIR DE PRODUTOS NATURAIS

MODELING OF THE MASS TRANSFER KINETICS IN SUPERCRITICAL FLUID EXTRACTION OF NATURAL PRODUCTS

Campinas
2015

UNIVERSIDADE ESTADUAL DE CAMPINAS

FACULDADE DE ENGENHARIA DE ALIMENTOS

SUSANA PEREIRA DE JESUS

MODELAGEM DA CINÉTICA DE TRANSFERÊNCIA DE MASSA NO PROCESSO DE EXTRAÇÃO SUPERCRÍTICA A PARTIR DE PRODUTOS NATURAIS

MODELING OF THE MASS TRANSFER KINETICS IN SUPERCRITICAL FLUID EXTRACTION OF NATURAL PRODUCTS

Tese apresentada ao Programa de Pós-Graduação em Engenharia de Alimentos da Faculdade de Engenharia de Alimentos da Universidade Estadual de Campinas como parte dos requisitos exigidos para a obtenção do título de Doutora em Engenharia de Alimentos.

Thesis presented to the Food Engineering Postgraduation Programme of the School of Food Engineering of the University of Campinas in partial fulfillment of the requirements for the degree of Ph.D. in Food Engineering.

Orientadora: Profª. Drª. Maria Angela de Almeida Meireles

ESTE EXEMPLAR CORRESPONDE À VERSÃO FINAL DA TESE DEFENDIDA PELA ALUNA SUSANA PEREIRA DE JESUS E ORIENTADA PELA PROF^A. DR^A. MARIA ANGELA DE ALMEIDA MEIRELES.

Assinatura do orientador

Campinas
2015

Ficha catalográfica
Universidade Estadual de Campinas
Biblioteca da Faculdade de Engenharia de Alimentos
Claudia Aparecida Romano - CRB 8/5816

J499m Jesus, Susana Pereira de, 1984-
Modelagem da cinética de transferência de massa no processo de extração supercrítica a partir de produtos naturais / Susana Pereira de Jesus. – Campinas, SP : [s.n.], 2015.

Orientador: Maria Angela de Almeida Meireles.
Tese (doutorado) – Universidade Estadual de Campinas, Faculdade de Engenharia de Alimentos.

1. Modelagem matemática. 2. Transferência de massa. 3. Extração com fluido supercrítico. I. Meireles, Maria Angela de Almeida. II. Universidade Estadual de Campinas. Faculdade de Engenharia de Alimentos. III. Título.

Informações para Biblioteca Digital

Título em outro idioma: Modeling of the mass transfer kinetics in supercritical fluid extraction of natural products
Palavras-chave em inglês:
Mathematical modeling
Mass transfer
Supercritical fluid extraction
Área de concentração: Engenharia de Alimentos
Titulação: Doutora em Engenharia de Alimentos
Banca examinadora:
Maria Angela de Almeida Meireles [Orientador]
Haiko Hense
Isabel Cristina do Nascimento Debien
Priscilla Carvalho Veggi
Rodrigo Nunes Cavalcanti
Data de defesa: 25-02-2015
Programa de Pós-Graduação: Engenharia de Alimentos

BANCA EXAMINADORA

____

Prof[a]. Dr[a]. Maria Angela de Almeida Meireles
DEA/FEA/UNICAMP (Orientadora)

____

Prof. Dr. Haiko Hense
EQA/CTC/UFSC (Titular)

____

Dr[a]. Isabel Cristina do Nascimento Debien
DEA/FEA/UNICAMP (Titular)

____

Dr[a]. Priscilla Carvalho Veggi
Politécnica/USP (Titular)

____

Dr. Rodrigo Nunes Cavalcanti
DEA/FEA/UNICAMP (Titular)

____

Prof[a]. Dr[a]. Cintia Bernardo Gonçalves
FZEA/USP (Suplente)

____

Prof. Dr. Fernando Antonio Cabral
DEA/FEA/UNICAMP (Suplente)

____

Prof. Dr. Julian Martínez
DEA/FEA/UNICAMP (Suplente)

TESE DE DOUTORADO

Autora: Susana Pereira de Jesus

Título: Modelagem da cinética de transferência de massa no processo de extração supercrítica a partir de produtos naturais

Orientadora: Prof[a]. Dr[a]. Maria Angela de Almeida Meireles

---

RESUMO

A extração supercrítica consiste em uma operação unitária de separação na qual o solvente é um fluido no estado supercrítico, sendo que o dióxido de carbono (CO_2) é o mais utilizado. Destaca-se por ser reconhecida como uma tecnologia limpa, alternativa aos métodos convencionais que em geral utilizam solventes orgânicos prejudiciais à saúde e ao meio-ambiente. O processo de extração supercrítica tem sido extensivamente estudado pela comunidade científica nas últimas décadas, o que resultou na construção de um sólido conhecimento sobre os principais fundamentos envolvidos neste processo, além da formação de uma ampla base de dados para descrever o comportamento de diferentes sistemas (CO_2 + matriz sólida). É uma técnica de extração a alta pressão que começou a ser utilizada em escala comercial na década de 1980 e, desde então, o número de plantas em operação é crescente em algumas regiões como Europa, Ásia e Estados Unidos. Apesar disso, continua a ser considerada uma tecnologia emergente e inovadora, visto que os métodos convencionais ainda são predominantes em diversas aplicações industriais e, em muitos países (como é o caso do Brasil), a técnica ainda não é utilizada em escala comercial. A viabilidade técnica do processo de extração supercrítica já está consolidada e a tecnologia encontra-se disponível comercialmente. Além disso, pesquisadores da área afirmam que a técnica pode ser economicamente competitiva, dependendo da área de aplicação e do produto de interesse. Entretanto, a questão econômica ainda é considerada como o principal empecilho à disseminação desta técnica, pois os custos de investimento associados a uma planta de alta pressão são altos quando comparados à instalação de plantas que operam em baixas pressões. Diante deste cenário, considera-se importante a investigação de métodos de cálculo (modelagem e simulação) que possam ser aplicados no sentido de estimar parâmetros para design de processo e aumento de escala, os quais são requeridos em estudos de viabilidade econômica. No presente trabalho, dados disponíveis na literatura foram utilizados para estudar a modelagem matemática da transferência de massa no processo de extração supercrítica. Para tanto, dados cinéticos de matérias-primas diversas foram ajustados por meio da aplicação de diferentes modelos, tendo como foco avaliar a versatilidade e aplicabilidade dos mesmos em termos de design de processo. Os resultados demonstraram que o modelo spline e o modelo de Sovová foram eficientes na descrição quantitativa da curva de extração, além de apresentarem versatilidade para ajustar curvas com formatos diferenciados. O modelo spline apresentou os melhores ajustes e também menores erros na descrição da etapa CER (*Constant Extraction Rate*), a qual é a mais importante em termos de design de processo.

Palavras chave: modelagem matemática, transferência de massa, extração com fluido supercrítico.

DOCTORAL THESIS

Author: Susana Pereira de Jesus

Title: Modeling of the mass transfer kinetics in supercritical fluid extraction of natural products

Supervisor: Dr[a]. Maria Angela de Almeida Meireles

ABSTRACT

Supercritical fluid extraction (SFE) is a solid-fluid separation technique in which the solvent is a fluid in the supercritical state, and the supercritical carbon dioxide (CO_2) is the most used solvent. It is recognized as a green technology and a versatile alternative to conventional extraction methods, which generally use organic solvents that are harmful to human health and environment. The SFE process has been extensively studied by scientific community in the last decades. As a consequence, a solid knowledge about the fundamental concepts has been developed, and there is a huge amount of data to describe the behavior of different systems (CO_2 + solid matrix). It is a high pressure extraction method that has been carried out on a commercial scale since the 1980s. From that point on, a growing number of industrial plants have been operating in Europe, Asia, and USA. However, SFE can still be considered an emerging technology since the conventional methods remain the most used in various applications. Besides, this technique has yet not been applied on a commercial scale in several countries, such as Brazil. The technical feasibility of SFE process is consolidated and the industrial-scale technology is commercially available. Researchers in this field claim that costs of SFE may be commercially competitive, depending on application area and target products. Nonetheless, the economic aspects are still considered an obstacle in SFE technology dissemination. This happens especially because a high pressure process requires higher investment costs than a conventional low pressure plant. In this scenario, it is important to investigate calculation methods (modeling and simulation) that may be applied to estimate parameters for process design and scale-up, which are key points in studies of economic viability. In this work, the mathematical modeling of SFE mass transfer was investigated by using experimental data from literature. Then, different models were applied to fit the kinetic data of SFE from various raw materials. The main purpose was to evaluate the models by considering their versatility and applicability in terms of process design. The results showed that spline and Sovová's models have been very effective in describing the quantitative behavior of the extraction curves. Moreover, these models presented versatility in fitting different curve shapes. The spline model provided the best fits as well as the lowest residual errors in the CER (*Constant Extraction Rate*) period, which is the most important region for process design purposes.

Keywords: mathematical modeling, mass transfer, supercritical fluid extraction.

SUMÁRIO

AGRADECIMENTOS

Ao Programa de Pós-Graduação em Engenharia de Alimentos do DEA/FEA/Unicamp, pela oportunidade de realização desta tese de doutorado.

Ao Conselho Nacional de Desenvolvimento Científico e Tecnológico (CNPq), pelo financiamento deste trabalho por meio da concessão da bolsa de doutorado (Processo: 141828/2010-2).

À Prof[a]. Dr[a]. Maria Angela de Almeida Meireles, pela orientação e valiosos ensinamentos, assim como pelo apoio, paciência e compreensão durante todo o período do curso de doutorado.

Ao Prof. Dr. Julian Martínez, pela imensa colaboração e diversos auxílios acerca dos temas modelagem matemática e transferência de massa.

Ao Prof. Dr. Haiko Hense, pelo apoio e parceria na elaboração de um dos artigos apresentados nesta tese.

Aos membros da banca examinadora, pela disponibilidade e contribuições feitas ao texto deste trabalho.

À minha família e amigos especiais, pelo carinho, suporte e incentivo em todas as situações e diante de todas as dificuldades.

LISTA DE FIGURAS

LISTA DE TABELAS

LISTA DE ABREVIATURAS E SIGLAS

CER = taxa de extração constante (*Constant Extraction Rate*)

COM = custo de manufatura (*Cost Of Manufacturing*)

CO_2 = dióxido de carbono

DC = controlado pela difusão (*Diffusion-Controlled*)

db = base seca (*dry basis*)

DEA = Departamento de Engenharia de Alimentos

FEA = Faculdade de Engenharia de Alimentos

FER = taxa decrescente de extração (*Falling Extraction Rate*)

GRAS = geralmente reconhecido como seguro (*Generally Recognized as Safe)*

GYI = isotermas de rendimento global (*Global Yield Isotherms*)

LASEFI = Laboratório de Tecnologia Supercrítica: extração, fracionamento e identificação de extratos vegetais

MSE = erro médio quadrático (*Mean Square Error*)

OEC = curva global de extração (*Overall Extraction Curve*)

ORR = taxa de recuperação do γ-oryzanol (*γ-Oryzanol Recovery Rate*)

P_C = pressão crítica

P_i = pressão de inversão (*crossover pressure*)

RBO = óleo de farelo de arroz (*Rice Bran Oil*)

RBOS = borra de neutralização do óleo de farelo de arroz (*Rice Bran Oil Soapstock*)

SC-CO_2 = dióxido de carbono supercrítico

SCF = fluido supercrítico (*Supercritical Fluid*)

SFE = extração supercrítica (*Supercritical Fluid Extraction*)

SSR = soma de quadrados dos resíduos (*Sum of Squared Residuals*)

T_C = temperatura crítica

wb = base úmida (*wet basis*)

z = direção axial

LISTA DE SÍMBOLOS

A_S = área de seção transversal [m^2]

a_1, a_2 e a_3 = parâmetros ajustáveis do modelo spline [kg/s], tal que (a_1), (a_1+a_2) e (a_1+a_2+a_3) são os coeficientes angulares das retas nº 1, 2 e 3, respectivamente

b_0 = parâmetro ajustável do modelo spline [kg]: coeficiente linear da reta nº 1

C_1 = parâmetro ajustável do modelo empírico [s]: sem significado físico

C_2 = parâmetro ajustável do modelo logístico [s^{-1}]: sem significado físico

D_{aX} = coeficiente de difusão na fase sólida [m^2/s]

D_{aY} = coeficiente de dispersão na fase fluida [m^2/s]

d_B = diâmetro do leito de extração [m]

D_{ef} = parâmetro ajustável do modelo difusivo [m^2/s]: coeficiente efetivo de difusão do soluto na matriz sólida

d_P = diâmetro médio de partícula [m]

F = massa de matéria-prima alimentada [kg]

F_{DRY} = massa de matéria-prima alimentada - em base seca [kg]

H_B = altura do leito de extração [m]

J(X,Y) = termo de transferência de massa interfacial [s^{-1}]

k_{XA} ou k_S = parâmetro ajustável do modelo de Sovová [s^{-1}]: coeficiente de transferência de massa na fase sólida

k_{YA} ou k_F = parâmetro ajustável do modelo de Sovová [s^{-1}]: coeficiente de transferência de massa na fase fluida

P = pressão [MPa]

M_{CER} = taxa de extração da etapa CER [kg/s]

m_{EXT} = massa de extrato [kg]

m_{IS} = massa de sólido inerte [kg]

Q_{CO2} = vazão mássica de solvente [kg/s]

r = raio da partícula [m]

R_{CER} = rendimento de extração da etapa CER [%; kg/kg]

S = massa de solvente [kg]

S/F = massa de solvente/massa de matéria-prima [kg/kg]

T = temperatura [K]

t = tempo de extração [s]

t_1 e t_2 = parâmetros ajustáveis do modelo spline [s]: interceptos entre as retas nº1 e nº2 e as retas nº2 e nº3, respectivamente

t_{CER} = tempo de duração da etapa CER [s]

t_{CER2} = intercepto (ponto de cruzamento) entre as retas nº1 e nº3 do modelo spline [s]

t_{FER} = tempo de duração da etapa FER [s]

t_m = parâmetro ajustável do modelo logístico [s]: sem significado físico

u_i = velocidade intersticial do solvente no leito de extração [m/s]

X = razão mássica de soluto na fase sólida [kg/kg]

X_0 = rendimento global ou razão mássica inicial (t = 0) de soluto na fase sólida [kg/kg]

X_K = parâmetro ajustável do modelo de Sovová [kg/kg]: razão mássica de soluto de difícil acesso

X_P = razão mássica de soluto de fácil acesso [kg/kg]

Y = razão mássica de soluto na fase fluida [kg/kg]

Y_{CER} = razão mássica de soluto na saída do extrator durante a etapa CER [kg/kg]

Y^* = solubilidade do extrato na fase fluida [kg/kg]

ε = porosidade do leito [adimensional]

ρ_A = densidade aparente do leito [kg/m^3]

ρ_{CO2} e ρ_S = densidade do CO_2 e da matriz sólida, respectivamente [kg/m^3]

CAPÍTULO 1 – INTRODUÇÃO GERAL E OBJETIVOS

1.1 INTRODUÇÃO

A extração supercrítica (SFE - *Supercritical Fluid Extraction*) é uma técnica de separação sólido-fluido na qual o solvente é um fluido no estado supercrítico, ou seja, um fluido cujos valores de temperatura e pressão estão acima da temperatura crítica (T_C) e da pressão crítica (P_C), respectivamente (Brunner, 1994). O dióxido de carbono (CO_2) é o solvente mais utilizado, por diversas características importantes, tais como: é classificado como GRAS (*Generally Recognized as Safe*); o estado supercrítico é atingido em baixa temperatura [T_C = 31,05 ^oC (Sandler, 1999)] e condições amenas de pressão [P_C = 7,38 MPa (Sandler, 1999)]; é relativamente barato, facilmente encontrado com grau de pureza elevado e também seguro para a manipulação (atóxico e não inflamável) (Brunner, 2005; Rosa e Meireles, 2009). A SFE é, portanto, um método de extração a alta pressão alternativo aos processos convencionais conduzidos em baixas pressões. Em termos de processo, as vantagens da extração com CO_2 supercrítico são bem conhecidas. Entre elas destacam-se: fácil separação da mistura solvente-extrato, seletividade ajustável de acordo com as condições de temperatura e pressão, possibilidade de reciclo do solvente e baixo consumo energético na planta industrial. Além disso, em termos de produto, os extratos obtidos destacam-se por apresentar elevada qualidade, pois as condições de processo podem ser ajustadas de forma a preservar e concentrar compostos com propriedades funcionais interessantes.

De forma geral, a investigação do processo de SFE pode ser dividida em quatro etapas fundamentais:

1) *estudo do comportamento termodinâmico do sistema*: é realizado com base em experimentos para determinação da solubilidade e/ou obtenção das isotermas de rendimento global (GYI – *Global Yield Isotherms*). Nesta etapa, o

objetivo principal consiste em selecionar as condições de temperatura e pressão mais adequadas para a obtenção dos compostos de interesse;

2) *estudo da cinética de transferência de massa*: é feito por meio de experimentos cinéticos que visam à determinação da curva global de extração (OEC - *Overall Extraction Curve*);
3) *estudo do aumento de escala:* consiste na determinação experimental de dados em escala piloto (grande escala) e comparação dos mesmos com os dados obtidos em escala laboratorial (pequena escala);
4) *simulação e análise econômica do processo*: uma vez que um critério efetivo de aumento de escala é definido, o passo seguinte consiste em fazer a simulação do processo SFE em escala industrial e cálculo do custo de manufatura (COM – *Cost Of Manufacturing*).

As isotermas de rendimento global são um conjunto de experimentos nos quais uma extração exaustiva é conduzida a fim de esgotar todo o material extraível presente na matriz sólida, numa dada condição de temperatura e pressão. Nestes experimentos utiliza-se uma quantidade pequena de matéria-prima e uma única coleta do extrato é feita ao final do tempo total de processo, pois se deseja determinar o rendimento da extração e as características químicas e de bioatividade do extrato. Vários experimentos são realizados usando diferentes combinações de temperatura e pressão, tendo como foco avaliar qual a influência que estas variáveis termodinâmicas exercem na SFE a partir de uma determinada matéria-prima. Ambas as variáveis (temperatura e pressão) estão diretamente relacionadas com duas propriedades importantes: densidade do solvente e pressão de vapor do soluto. Estas duas propriedades são as que determinam qual a seletividade do fluido supercrítico e qual a solubilidade do extrato no fluido em questão. Cabe ressaltar ainda que, dependendo do grau de polaridade dos solutos que se deseja extrair, pode ser necessário avaliar também a adição de um cossolvente de caráter polar (etanol ou água, por exemplo) em diferentes concentrações. Os extratos são avaliados em termos de rendimento (cálculo do rendimento da extração) e composição (análise do perfil de composição química, determinação da concentração de algum composto alvo e/ou avaliação de propriedades bioativas). O objetivo é determinar as condições de processo nas quais os compostos de interesse sejam obtidos em maior quantidade e/ou com maior grau de pureza.

Depois de selecionados os parâmetros temperatura e pressão, o passo seguinte consiste no estudo da transferência de massa, a qual é avaliada por meio da obtenção de curvas globais de extração (OECs). Estas curvas são obtidas a partir de experimentos cinéticos nos quais a massa de extrato é coletada e quantificada em intervalos de tempos pré-determinados. Neste caso é recomendado utilizar uma maior quantidade de matéria-prima, pois a finalidade é obter uma curva com vários pontos experimentais, sendo que a extração deve ser conduzida até atingir (ou se aproximar de) uma assíntota. Os dados do experimento cinético são usados para a construção da OEC, que é um gráfico da massa acumulada de extrato em função do tempo de extração (ou quantidade de solvente). Na literatura existem diversos modelos disponíveis para a descrição da OEC, sendo que alguns são baseados em equações empíricas e outros baseados nas equações do balanço de massa. A maior parte dos modelos se enquadra na segunda categoria e, neste caso, cada autor faz sua própria interpretação dos mecanismos de transferência de massa que ocorrem dentro do leito de extração (Martínez *et al.*, 2007). Entre os modelos propostos por diferentes autores, existem tanto equações muito simples quanto equações altamente complexas. A seleção do modelo mais adequado deve ser feita em função do sistema (matriz sólida + solvente) em estudo e também do propósito da investigação (precisão requerida nos cálculos de um determinado projeto). Além disso, as disponibilidades tanto de dados experimentais quanto de softwares para cálculo precisam ser levadas em consideração.

A modelagem da OEC consiste em uma ferramenta que pode ser utilizada para estabelecer uma conexão entre a etapa 2 e as etapas 3 e 4. O modelo matemático é aplicado no ajuste de dados experimentais obtidos para a OEC em escala laboratorial (etapa 2). O estudo da modelagem auxilia na interpretação da cinética de transferência de massa, a qual é fundamental a fim de se definir quais mecanismos de transporte de massa são mais importantes no decorrer do processo de extração. Além disso, o objetivo principal da modelagem matemática da OEC é a determinação de parâmetros que possam ser aplicados em estudos de aumento de escala (etapa 3) e/ou estudos de simulação e análise econômica (etapa 4). O propósito da etapa 3 é conhecer quais parâmetros permanecem constantes (ou como estes parâmetros variam) no processo de transposição de pequena para grande escala, sendo que as informações obtidas podem ser usadas para a definição de critérios de aumento de escala que sejam aplicáveis ao sistema em questão. Na etapa 4, o objetivo da simulação consiste em predizer os dados de processo que são necessários para a investigação da viabilidade econômica. Os cálculos de simulação e análise econômica podem ser feitos a partir da utilização de softwares disponíveis comercialmente, tal como o *SuperPro Designer*® (Intelligen, Inc., EUA).

A extração supercrítica é uma operação unitária que começou a ser aplicada em escala comercial na década de 1980 (Brunner, 1994). Desde então, este processo tem sido extensivamente estudado por diferentes pesquisadores ao redor do mundo. O sólido conhecimento adquirido sobre a técnica permite aos pesquisadores da área afirmar que a SFE já está consolidada como um processo viável tecnicamente e, além disso, tem grande potencial para se tornar economicamente competitiva em muitas situações. Prova disso é a quantidade crescente de plantas industriais em operação, sendo que estas estão distribuídas basicamente na Europa, Ásia e Estados Unidos (Brunner, 2005). Adicionalmente, é interessante ressaltar que a tecnologia já está disponível comercialmente, sendo que empresas que trabalham nessa área oferecem opções de equipamentos tanto para plantas com design padrão (projetos previamente desenvolvidos) quanto para plantas customizadas (projetos a serem desenvolvidos de acordo com a necessidade específica do cliente) (Brunner, 2005).

No entanto, ainda que o conhecimento do fenômeno e a tecnologia de processo já estejam consolidados, a realidade é que muitos países (como o Brasil, por exemplo) não possuem plantas de SFE operando em escala industrial. Portanto, de forma geral, as técnicas convencionais continuam sendo predominantes nas mais diversas aplicações das operações unitárias de separação sólido-fluido. Assim sendo, a SFE ainda hoje é considerada uma tecnologia alternativa, inovadora e emergente. Isso acontece principalmente porque o custo de instalação para plantas que operem com altas pressões é alto quando comparado ao custo de instalação das plantas que operam a baixa pressão. Entretanto, estudos de viabilidade econômica mostram que vários outros custos (além da instalação) devem ser considerados a fim de se obter predições do custo de manufatura do produto e tempo de retorno do investimento (Rosa e Meireles, 2005; Albuquerque e Meireles, 2012). Considerando o contexto mencionado, fica claro que um dos grandes desafios atuais é encontrar meios de avaliar a viabilidade econômica do processo de SFE. Por isso é fundamental que os pesquisadores da área realizem trabalhos no sentido de propor métodos experimentais e/ou métodos de cálculo (modelagem e simulação) direcionados à obtenção de parâmetros para design de processo e aumento de escala, os quais são necessários para a investigação da análise econômica do processo.

O grupo de pesquisa LASEFI (DEA/FEA/Unicamp) se destaca dentro do cenário mundial no que diz respeito ao desenvolvimento de conhecimento na área específica de SFE. Desde a sua fundação (1984) até os dias atuais, o LASEFI tem investigado intensivamente diversos aspectos relacionados à SFE a partir de matrizes vegetais diversas. No começo, o foco dos estudos era direcionado à investigação, compreensão e descrição dos fenômenos físicos envolvidos na SFE. Uma vez que essa parte do conhecimento foi consolidada, os esforços passaram a ser direcionados ao desenvolvimento de métodos experimentais que permitissem, de forma prática e segura, a obtenção de dados de processo para diferentes sistemas. Como resultado, uma ampla base de dados foi construída para um número expressivo de matérias-primas diversificadas, trabalho este que continua até hoje. Nos últimos anos, os estudos têm contemplado não apenas a obtenção de dados experimentais em pequena escala, mas também a busca constante de informações sobre design de processo, aumento de escala e análise econômica. No presente trabalho, dados cinéticos de matérias-primas diversas foram utilizados para estudar a modelagem matemática de OECs por meio da aplicação de diferentes modelos disponíveis na literatura.

1.2 Objetivos

O objetivo geral deste trabalho foi estudar a modelagem da transferência de massa no processo de extração supercrítica, tendo como propósito avaliar a versatilidade dos modelos e aplicabilidade dos mesmos em termos de design de processo.

Os principais objetivos específicos encontram-se listados a seguir:

a) fazer uma revisão bibliográfica geral sobre o processo SFE, levando em consideração conceitos fundamentais consolidados e também o estado atual da arte;
b) investigar a modelagem matemática da OEC em diferentes sistemas (matriz vegetal + CO_2), tendo como foco a utilização de modelos simplificados (complexidade matemática relativamente baixa);
c) estudar em detalhes a descrição da OEC utilizando o modelo *spline*, o qual é descrito por um conjunto de linhas retas;
d) utilizar diferentes modelos (disponíveis na literatura) para ajustar dados cinéticos de um grupo diversificado de matérias-primas, as quais possuem diferentes características específicas e curvas de extração com formatos variados;
e) analisar de forma comparativa os resultados da modelagem por meio da avaliação de três aspectos fundamentais: qualidade do ajuste matemático, versatilidade e aplicabilidade em termos de aumento de escala e design de processo.

1.3 Estrutura da Tese

A estrutura geral do presente trabalho está apresentada de forma esquemática na Figura 1.1.

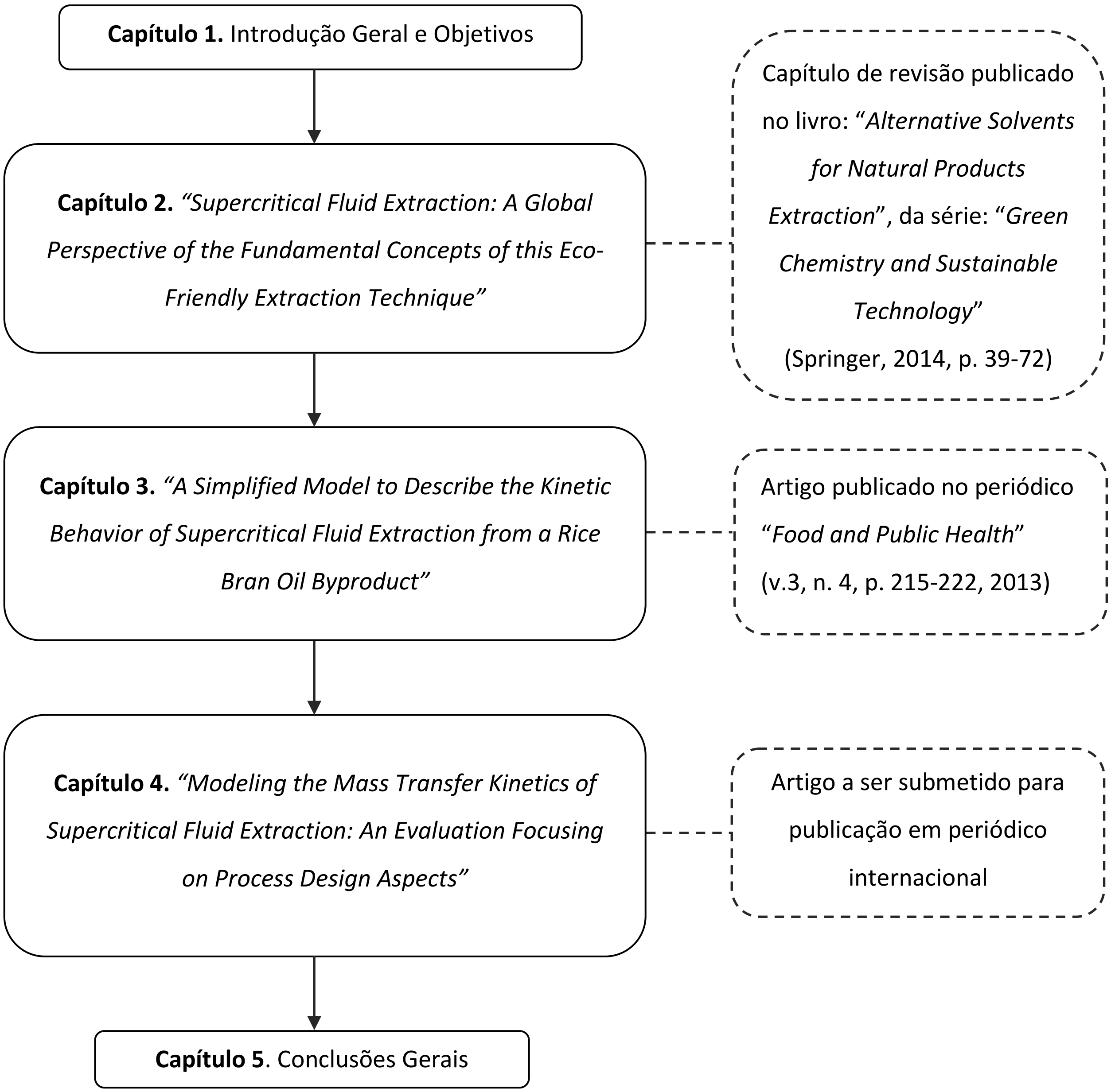

Figura 1.1 Diagrama esquemático dos capítulos apresentados na tese de doutorado

REFERÊNCIAS

ALBUQUERQUE, C. L. C.; MEIRELES, M. A. A. Defatting of annatto seeds using supercritical carbon dioxide as a pretreatment for the production of bixin: Experimental, modeling and economic evaluation of the process. **The Journal of Supercritical Fluids,** v. 66, p. 86-95, 2012.

BRUNNER, G. **Gas extraction: an introduction to fundamentals of supercritical fluids and the application to separation processes**. Darmstadt: Steinkopff, 1994. 387 p.

BRUNNER, G. Supercritical fluids: technology and application to food processing. **Journal of Food Engineering,** v. 67, n. 1–2, p. 21-33, 2005.

MARTÍNEZ, J.; ROSA, P. T. V.; MEIRELES, M. A. A. Extraction of clove and vetiver oils with supercritical carbon dioxide: modeling and simulation. **The Open Chemical Engineering Journal,** v. 1, n. 1, p. 1-7, 2007.

ROSA, P. T. V.; MEIRELES, M. A. A. Rapid estimation of the manufacturing cost of extracts obtained by supercritical fluid extraction. **Journal of Food Engineering,** v. 67, p. 235-240, 2005.

ROSA, P. T. V.; MEIRELES, M. A. A. Fundamentals of supercritical extraction from solid matrices. In: MEIRELES, M. A. A. (Ed.). **Extracting Bioactive Compounds for Food Products: Theory and Application**. Boca Raton: CRC Press –Taylor & Francis Group, 2009. p.272-288.

SANDLER, S. I. **Chemical and engineering thermodynamics**. 3rd ed. New York, NY: John Wiley, 1999. 772 p.

CAPÍTULO 2 – SUPERCRITICAL FLUID EXTRACTION: A GLOBAL PERSPECTIVE OF THE FUNDAMENTAL CONCEPTS OF THIS ECO-FRIENDLY EXTRACTION TECHNIQUE

Susana P. Jesus and M. Angela A. Meireles

Capítulo publicado no livro *Alternative Solvents for Natural Products Extraction*, da série *Green Chemistry and Sustainable Technology*, Editora: Springer Berlin Heidelberg, 2014.

e-ISBN: 978-3-662-43628-8 | DOI: 10.1007/978-3-662-43628-8_3

Chapter 3 – Supercritical Fluid Extraction: A Global Perspective of the Fundamental Concepts of this Eco-Friendly Extraction Technique

Susana P. Jesus and M. Angela A. Meireles[1]

Abstract Supercritical fluid extraction (SFE) is a green technology that has been applied on a commercial scale for more than three decades. SFE is a high-pressure extraction method in which a mixture of solutes is separated from a solid matrix by bringing the mixture into contact with a fluid in the supercritical state. A supercritical fluid has very particular and unique characteristics, which enable its use as an efficient extraction solvent. Carbon dioxide (CO_2) is the most commonly used supercritical fluid and has applications in food, cosmetic, pharmaceutical, and correlated industries. Many research works have already demonstrated that SFE is a technically feasible process that may also be commercially competitive in terms of economic viability. Although SFE is commercially carried out in several countries, it is nonetheless still considered an emerging technology. This emerging status remains associated with SFE technology because the conventional low-pressure extraction methods remain the most frequently used extraction techniques, in particular due to the comparatively low cost of investment that is required for installing a low pressure industrial plant. The physical phenomena that occur during SFE have already been extensively investigated, and there is consensus that SFE is a complex phenomenon that involves multicomponent systems. However, various simplifications can be performed to describe SFE for the purpose of process design. Presently, one of the major challenges for researchers in this area is the proposition of practical procedures (experimental and/or calculation methods) in order to simplify the determination of some process parameters which are required for studies of economic feasibility. This chapter presents the fundamental concepts of SFE and gives special attention to the information that must be available to conduct preliminary studies of process design and cost estimation.

[1] S. P. Jesus · M. A. A. Meireles (✉)

LASEFI/DEA/FEA (School of Food Engineering)/UNICAMP (University of Campinas); Rua Monteiro Lobato, 80; Campinas-SP; CEP:13083-862; Brazil

e-mail: meireles@fea.unicamp.br

F. Chemat and M. Abert Vian (eds.), *Alternative Solvents for Natural Products Extraction*, Green Chemistry and Sustainable Technology,
DOI 10.1007/978-3-662-43628-8__3,

3.1 The Supercritical Fluid Extraction Technique

The consumers' increasing concern about environmental issues and human health has motivated the development of green technologies and the search for natural ingredients with bioactive properties. In fact, the natural products market has presented a progressive and continuous growth in the last decades. Natural matrices are complex multicomponent systems and so the selective separation of specific substances is a difficult task that requires efficient extraction methods [1]. Rostagno and Prado [1] recently published a book that presents a global view of the state-of-the-art techniques for the extraction and processing of natural products. These authors claim that there is a need for more efficient and selective processes, which can improve the overall quality of natural products and also enable the development of innovative products [1]. Nonetheless, most of the industries still use conventional techniques that are based on outdated technologies. Considering this scenario, the Supercritical Fluid Extraction (SFE) is a particularly interesting alternative to extract bioactive compounds from natural sources. Therefore, the SFE process has many potential applications in food, pharmaceutical, and cosmetic industries.

The SFE is a high-pressure extraction method that has been carried out on a commercial scale since the 1980s. The industrial scale applications of SFE comprise the decaffeination of green coffee beans and black tea leaves, the production of hop extracts, the extraction of essential oils, oleoresins and flavoring compounds from herbs and spices, the extraction of high-valued bioactive compounds from different natural matrices, the extraction and fractionation of edible oils, and the removal of pesticides from plant material [2,3]. At the very early stages of this technology, very large vessels (up to 40 m^3) were sometimes built. Later, the extractors' capacity became smaller, and today, most extractor vessels have a volume that is equal to or smaller than 1 m^3 [3].

According to Brunner [3], the costs of SFE processes are competitive. Furthermore, in particular cases, SFE processing is the only way to satisfy the product specifications. A significant number of SFE industrial plants of various capacities have been built since the 1980s. Most of the plants are distributed within Europe, the USA, Japan, and the South East Asian Countries. The state-of-the-art technology that is necessary to design a SFE plant is commercially available. Standard designs can be acquired from many suppliers, and special designs can be custom tailored for a particular process [3].

SFE is a unit operation that performs the separation of a mixture of solutes from a solid matrix by bringing the mixture in contact with a supercritical solvent [4]. The solid material is placed in an extraction cell, forming a fixed bed of solid particles. The supercritical fluid flows continuously through the fixed bed and dissolves the extractable components of the solid [2]. The mixture of solutes that is removed from the solid matrix is named the extract. SFE processes are usually carried out in batch and single-stage modes because solids are difficult to handle continuously in pressurized vessels and separation factors are high [3]. Nonetheless, the modification of the process from batch to continuous mode can be performed by arranging two or more extractors in the process line [5,6]. This change allows the system to operate continuously despite the occurrence of solid matrix exhaustion. Then, the arrangement of *n* extractors (where $n \geq 2$) operating in a parallel configuration results in the continuous production of the extract by intercalating the charge/discharge times of the *n* extractors in the plant. Plant operation in a continuous mode occurs according to the following format: while one extractor is in the charge/discharge step, the other *n-1* extractors are in the extraction step [6]. This operating mode presents the advantages of reducing the process setup time and increasing productivity, which leads to a reduction of the operating costs [3,6].

A simple SFE process comprises two major steps: extraction and separation. In the extraction step, the solvent is fed into the system and is uniformly distributed throughout the extractor. The solvent flows through the solid matrix, extracting the soluble compounds. In the separation step, the loaded solvent (the mixture formed by solvent + extract) is removed from the extraction cell and fed into the separator (flash tank), where the mixture is separated by a rapid reduction of the pressure. The extract precipitates in the separator, while the solvent is removed from the system and is delivered to a recycling step. The solvent is cooled and recompressed and then returns to a storage tank, which feeds the extraction system [2,7]. A schematic diagram of the SFE process is shown in Fig. 3.1.

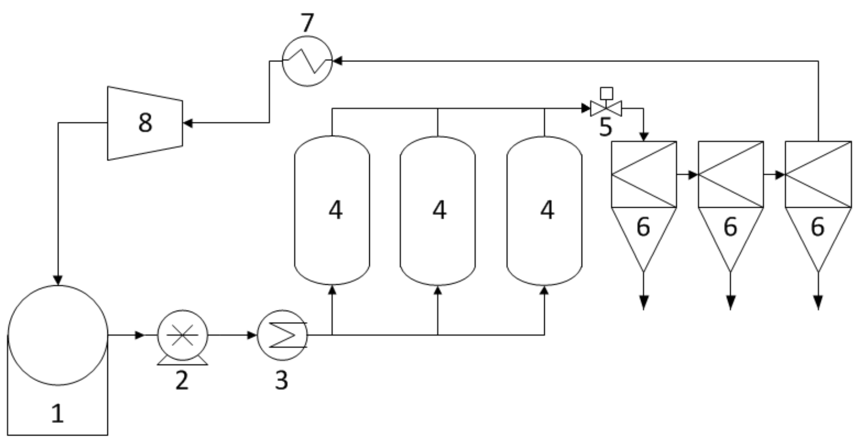

Fig. 3.1 A simplified flowchart of the SFE process (1: CO_2 storage tank; 2: solvent pump; 3: heat exchanger; 4: extractor; 5: pre-expansion valve; 6: separator; 7: cooler; 8: compressor; the system contains several temperature and pressure controllers that are not shown) (adapted from Pereira and Meireles [7], with kind permission from Springer Science and Business Media)

3.2 The Supercritical Fluid

A pure component is considered to be in the supercritical state when both its pressure (P) and temperature (T) are higher than their critical values (P_C and T_C, respectively) [2]. The supercritical region is illustrated in the phase diagrams presented in Fig. 3.2 and Fig. 3.3. In this region, the fluid can be considered either an expanded liquid or a compressed gas [4].

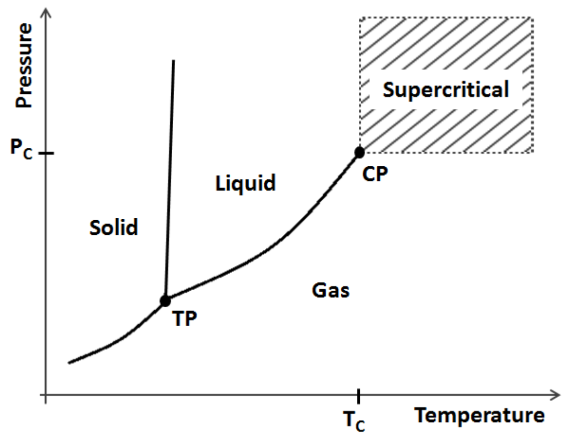

Fig. 3.2 A pure component PxT (pressure versus temperature) diagram: the supercritical region is indicated by the hatched lines (TP: triple point; CP: critical point; P_C: critical pressure, T_C: critical temperature) (adapted from Brunner [2], with kind permission from Springer Science and Business Media)

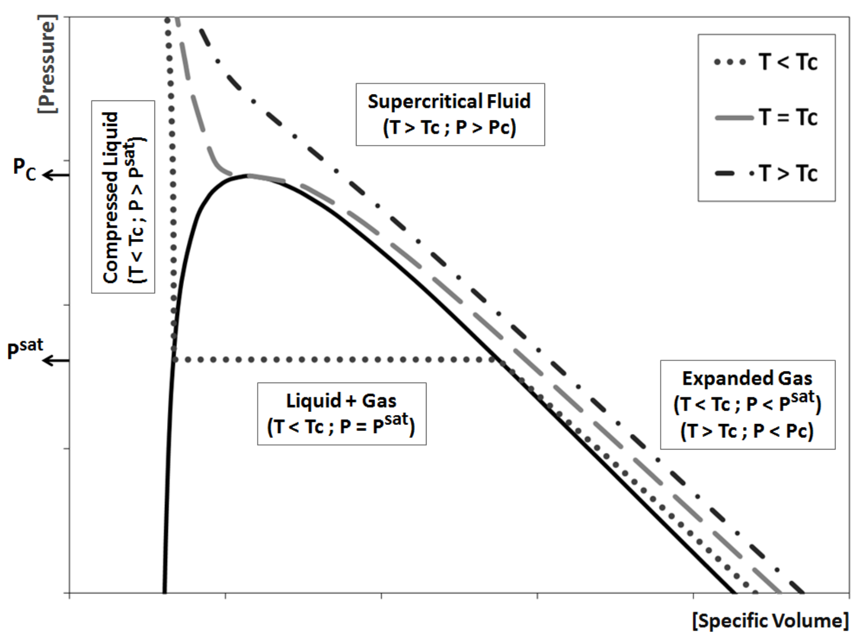

Fig. 3.3 Schematic illustration of a pure component PxV (pressure versus volume) diagram (T: temperature; T_C: critical temperature; P: pressure; P_C: critical pressure; P^{sat}: saturation pressure)

Supercritical fluids (SCFs) show very particular and unique characteristics that enable their use as efficient solvents. The densities of SCFs are relatively high (compared to gases), and consequently, SCFs have high solvation power. Furthermore, the density can be easily tuned by varying the system pressure or temperature.

This particular effect provides these fluids with a certain degree of selectivity, which is useful for the extraction process and allows for easy solvent-solute separation. The separation step can be performed by either decreasing the pressure or increasing the temperature of the mixture (solvent + extract) leaving the extraction column [4]. In the supercritical state, liquid-like densities are approached, while the viscosity is near that of normal gases, and the diffusivity is approximately two orders of magnitude higher than that of the liquid forms [3]. Therefore, in comparison to a gas, a supercritical fluid (SCF) has higher density; in contrast, compared to a liquid, the SCF possesses lower viscosity and a higher diffusion coefficient. All of these characteristics result in a greater solvation power, which allows high extraction rates when SCFs are applied as solvents.

Supercritical carbon dioxide (SC-CO_2) is the most commonly used solvent for applications of SFE in the food, cosmetic, pharmaceutical, and other similar industries. According to Rosa and Meireles [4], two important justifications for the choice of CO_2 are its low critical temperature (T_C = 304.2 K) and mild critical pressure (P_C = 7.38 MPa). Additionally, CO_2 is not only cheap and readily available at high purity but is also safe to handle (non-toxic and non-flammable) and easily removed by simple expansion to common environmental pressure values [3]. Some well-noted advantages of the SFE process are the solvent recycling possibility, low energy consumption, adjustable solvent selectivity, prevention of oxidation reactions, and production of high quality extracts.

The properties of SC-CO_2 can be modified over relatively wide ranges. The solvent power of SC-CO_2 is high for hydrophobic or slightly hydrophilic components and decreases with increasing molecular weight [3]. Generally, when the operational pressure is increased, more hydrophilic compounds can also be extracted. If the goal is the extraction of more hydrophilic compounds, then the solvent polarity can be increased by the addition of a polar solvent. The added solvents are named the cosolvents or modifiers [4]. The cosolvent is generally a solvent of high polarity, such as water or ethanol. These two solvents are conveniently selected because both are classified as GRAS (generally recognized as safe). Therefore, the green concept of supercritical technology is perfectly maintained. The cosolvent takes the form of a compressed liquid (see Fig. 3.3) when held in the usual operational conditions of the SFE process.

3.3 The Solid Matrix

In natural sources, the soluble portion of the solid matrix is generally composed of several different classes of organic compounds. As a result, the extract (or solute) is a complex mixture of chemical species, such as terpenes, terpenoids, flavonoids, alkaloids, and many other compounds [8]. The soluble fraction may be located inside cellular structures and may interact very strongly with the non-soluble components of the raw material. Therefore, vegetable raw materials often pass through a pretreatment process to facilitate solvent access to the solute and to increase the solute-solvent interactions.

3.3.1 Raw Material Pretreatment

In SFE, the raw material commonly passes through a pretreatment stage before it is fed into the fixed bed extractor. Pretreatment is performed to prepare the solid particles, allowing the best possible efficiency to be achieved in the extraction process. In most cases, the pretreatment process comprises one or more of the following steps:

- *Drying*: A drying step is often used to adjust the water content of the solid matrix. If the target compound is a non-polar or slightly polar substance, then the water content is reduced to increase the extraction efficiency. However, if the target compound has a more polar structure, the drying process may not be necessary or adequate. In some cases, the initial water contained in the solid particles can act as a cosolvent and improve the extraction efficiency of certain polar compounds.
- *Milling*: The main purpose of the milling step is the reduction of the solid particle sizes to enlarge the interfacial solid-fluid mass transfer area. Furthermore, the milling process may also cause the destruction of some plant cellular structures and, consequently, facilitate solvent access to the solute. Nonetheless, reducing the particle size also increases the degree of compaction of the solid substrate. Excessive bed compaction must be avoided because it can result in the formation of preferential pathways of solvent access, preventing the solvent from reaching all of the extractable material [5].
- *Sieving*: A sieving step is generally applied to standardize the size of the solid particles. Some particles may be discarded according to the particle diameter range of interest.
- *Chemical reaction*: A reaction step is not commonly applied, but it can be useful in particular cases. A chemical reaction may be performed to free the target solutes and improve the extraction efficiency.

3.4 The Definition of the Pseudo-Ternary System

In SFE from natural matrices, the obtained extracts are complex mixtures composed of different groups of chemical compounds. Therefore, the extract is always a multicomponent system. Additionally, the solid matrix is a very complex mixture that can contain intact cellular structures, as well as broken cellular structures [8,9]. Knowledge of the system's composition and the physical phenomena that occur inside the extraction bed is essential for creating a detailed description of the SFE process. This knowledge is also fundamental to decision making with respect to simplifying the description of the phenomena that take place within the extraction cell. With respect to composition, some assumptions may be used to facilitate the description of the SFE system (solid material + solvent). According to Rodrigues et al. [8], a very simplified picture of the system is developed when it is treated as having been formed by three pseudocomponents (extract + cellulosic structure + solvent), which are defined below:

- *Extract (or solute)*: The extract is a multicomponent mixture composed of the solids that are soluble in the extraction solvent. The extract interacts with both the supercritical solvent and the cellulosic structure [8].
- *Cellulosic structure (or inert material)*: The cellulosic structure is formed by a multicomponent mixture that contains all of the solids that are insoluble in the supercritical solvent. It is crucial to note that although being inert to the solvent action, the cellulosic structure interacts strongly with the extract [8].
- *Solvent*: The solvent can be either a pure component (the fluid in the supercritical state) or a mixture of the supercritical fluid and a cosolvent. In the typical operating conditions of SC-CO_2 extraction, the cosolvent (water, ethanol, among others) is a compressed liquid.

3.5 Thermodynamics Aspects

The design of an engineering project of a SFE system requires knowledge of the limitations that control the extraction process. According to Ferreira and Meireles [10], the constraints of the SFE are related to two aspects: (a) the thermodynamics (solubility and selectivity) and (b) the mass transfer phenomena. A discussion of the first is presented in this section, while the second aspect is treated in Sect. 3.6.

3.5.1 Equilibrium Solubility (Y)*

The driving potential for mass transfer is determined by the difference relative to the equilibrium state. According to Brunner [3], the phase equilibrium provides information regarding (a) the capacity of the supercritical solvent, which is directly related to the solubility of a specific solute in the solvent (the solubility is the amount of a solute that is dissolved by the supercritical solvent at thermodynamic equilibrium), (b) the selectivity of a supercritical solvent, which can be described as the ability of a solvent to selectively dissolve one or more compounds, and (c) the dependence of these two solvent properties on the conditions of state (P and T). If the capacity and selectivity are known, a guess can be made regarding whether a separation problem can be solved using a supercritical solvent [3].

It should be noted that two different approaches can be adopted when considering the equilibrium solubility of an extract within a supercritical fluid, including (a) the solubility of the pseudobinary system (Y_{BIN}^*), which is composed only of the extract + solvent, and (b) the solubility of the pseudoternary system (Y_{TER}^*), as described in Sect. 3.4 (cellulosic structure + extract + solvent). It is well known that the cellulosic structure strongly interacts with the extract. Thus, the solubility of a solute as measured in the pseudobinary system differs significantly from the solubility of the same solute when measured in the pseudoternary system [9]. A good example of the influence of the cellulosic structure on the solubility value is given by Brunner [2]: the solubility of pure caffeine in SC-CO_2 (binary system) is approximately 20 times greater than the solubility of caffeine measured for the pseudoternary system (caffeine + coffee grains + SC-CO_2) at the same conditions of temperature and pressure. Brunner [2] also mentioned that the concentration of caffeine in the supercritical solvent throughout most time of the SFE process is less than 100 ppm. This value is significantly below the solubility of caffeine as measured for the pseudoternary system (Y_{TER}* = 200 ppm at T = 350 K and P = 30 MPa). Then, it can be said that when the solubility of the pseudoternary system is relatively high (as in the caffeine example), the mass ratio of the solute in the fluid phase (Y) will likely be significantly lower than Y_{TER}* during typical SFE operational conditions.

Equilibrium solubility is only reached under specific processing conditions. A detailed discussion of the experimental determination of the pseudoternary solubility is presented by Rodrigues and co-workers [8]. These authors used the dynamic method to measure the pseudoternary solubility of extracts from three vegetable raw materials (clove buds, ginger, and eucalyptus). In the dynamic method, a typical SFE experiment is performed: the solvent is continuously fed into an extraction column at a given pressure and temperature using a solvent flow rate (Q_{CO2}) that assures saturation at the exit of the column [4]. Rodrigues et al. [8] demonstrated that there is a particular solvent flow rate (denoted Q*) at which the equilibrium is achieved and the solubility must be measured. Therefore, the use of the dynamic method requires that a certain set of experiments must be performed to determine the specific solvent flow rate at which the solvent leaves the extraction cell under the saturation condition [11]. This is necessary because, under large flow rates, there is insufficient contact time to guarantee that the solvent is saturated. However, at very low solvent flow rates, axial dispersion may interfere with the measurement of solubility. Hence, there is an optimum solvent flow rate that is a function of the raw material and the thermodynamic state (P and T) used in the SFE process [4,11].

In the dynamic method, the equilibrium solubility is given by the slope of the linear part of the overall extraction curve (OEC) (this curve is discussed extensively in Sect. 3.6.2). The work presented by Rodrigues et al. [8] showed that the experimental determination of Y_{TER}* requires a slow, tedious and costly experimental investigation because it is necessary to determine the CO_2 flow rate that can be used safely for the measurement of the equilibrium solubility [9]. In some works, the solubility is simply calculated by using the slope of the linear part of an OEC determined under a random solvent flow rate (i.e., $Q_{CO2} \neq Q^*$). Meireles [9] state that in this case, the measured value should be referred to as $Y_{S/F}$* and that there is a clear difference between Y_{TER}* and $Y_{S/F}$*. This author also mentioned that the difference can be understood by recalling that to measure the first value (the true solubility in the pseudoternary system), it is expected that equilibrium is achieved during the extraction experiment (i.e., Q_{CO2} must be equal to Q*). In the second case, the "solubility" ($Y_{S/F}$*) is measured at a given solvent to feed (S/F) mass ratio using a random solvent flow rate. In the latter case, there is no guarantee that the saturation of the solvent is reached; thus, the value of $Y_{S/F}$* cannot be treated as the real equilibrium solubility.

3.5.2 Global Yield Isotherms (GYI)

When studying a SFE system, one of the first fundamental steps is the selection of the temperature and pressure parameters, which must be chosen by taking into account the quality and purity of the obtained extract. The quality of an extract is determined by its chemical composition, which is directly related to the selectivity of the solvent. Thus, a set of experiments must be performed based on various combinations of temperature and pressure because both thermodynamic parameters are strongly related to selectivity and solubility. These experiments deliver information regarding the solvent density, which is directly associated with the solvent power and consequently with the adjustable selectivity of SC-CO_2. Moreover, these experiments also provide information regarding the solubility of the solute in the supercritical solvent. According to Carvalho Jr. et al. [12], the investigation of a SFE process requires some knowledge of the behavior of the system of "solid material + CO_2." The interactions of the extract with both the solvent and cellulosic structure are fundamental to understanding the extraction process. However, very little is known regarding these interactions because they involve multicomponent systems of high complexity. The extension of these "solute-solvent" and "solute-cellulosic structure" interactions can be evaluated through two types of experiments: (a) the determination of the solubility of the pseudoternary system (as previously discussed in Sect. 3.5.1) under different conditions of temperature and pressure and (b) the results of the global yield isotherms (GYI) [12]. In GYI experiments, an exhaustive extraction is conducted under different conditions of temperature and pressure.

Meireles [9] claimed that to obtain reliable results for Y_{TER}*, the experiments used to determine solubility must be performed in a SFE unit containing an extractor vessel with a volume of at least 50 cm^3. This requirement is because in these experiments, an overall extraction curve (OEC) (see Sect. 3.6.2) must be built; thus, the use of small amounts of feed material is generally associated with relatively high experimental errors. Moreover, the solubility measurements require difficult experimental work (as discussed in Sect. 3.5.1). However, the GYI experiments are comparatively easy to conduct because they only require an exhaustive extraction. In this case, extractor vessels of small volumes (such as 5 cm^3) and, consequently, small amounts of the feed material can be safely used to perform GYI assays because there is no need to build an OEC [9]. Therefore, taking into account all the aspects cited above, it is apparent that the choices of operating temperature and pressure may be easier upon consideration of the results of GYI experiments.

In terms of the total extraction yield or the yield of a specific target compound, the results from GYI assays are generally plotted on a graph similar to the schematic illustration presented in Fig. 3.4. From this plot, it is possible to evaluate the effects of the parameters temperature and pressure on the extraction yield. Taking into account an isothermal condition, the effect of operational pressure can be understood. It is clear that a rising pressure results in an increasing extraction yield. This effect is attributed to the increase in CO_2 density and, consequently, the enhancement of its solvation power (although, a higher solvation power may be associated with lower selectivity) [13]. The effect of the operational temperature in SFE is typically more complex due to the combination of two variables, density and vapor pressure. The vapor pressure of the solute increases with temperature, causing increased solubility. However, the solvent density decreases with increasing temperature, causing reduced solubility [11]. As a result, these two variables cause inverse effects on the extraction yield. It is well known that the dominant effect depends on the magnitudes of both effects individually.

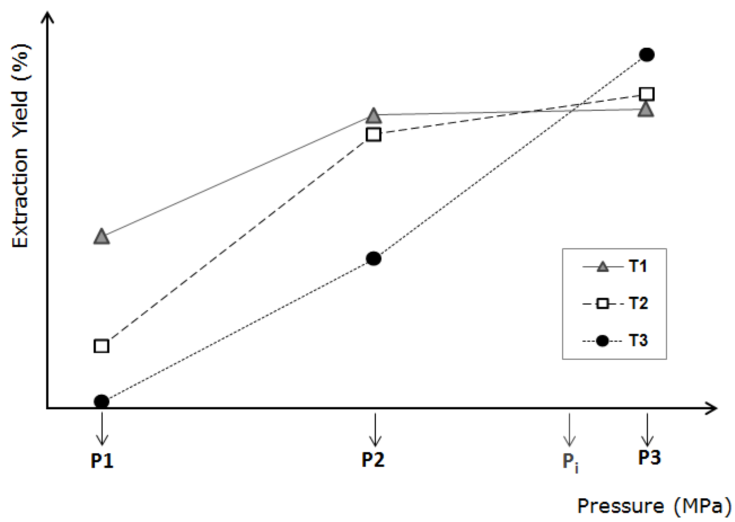

Fig. 3.4 Schematic illustration of the Global Yield Isotherms (T1 < T2 < T3; P1 < P2 < P3; Pi: crossover pressure) (the experimental points were connected by lines only to evidence the crossover point) (adapted from Jesus et al. [13])

At relatively low pressures (P < Pi, according to Fig. 3.4) the effect of solvent density prevails; thus, increasing the temperature results in a reduction of the extraction yield. However, at relatively high pressures (P > Pi, according to Fig. 3.4), the effect of vapor pressure dominates; as a result, increasing the temperature enhances the extraction yield [2,11,13]. The pressure at which the inversion of the dominant mechanism occurs is known as either the crossover point or the crossover pressure. From the GYI graph (Fig. 3.4), it can be said that the crossover pressure (Pi) falls somewhere between P2 and P3. At pressures less than Pi, the solvent density always dominates, while at pressures higher than Pi, the dominant mechanism is the solute vapor pressure. The crossover point is a characteristic of each SFE system (solvent + solute + cellulosic structure) and must be experimentally determined for each distinct pseudoternary system.

Generally, when working with SFE from natural matrices, the major goal is to produce extracts that are enriched in bioactive compounds. As a result, it is important to hold in mind that the selection of the operating temperature and pressure must be made by taking into account the extract characterization in terms of its chemical composition and functional properties. To do so, the extracts obtained in the GYI experiments should be characterized using appropriate methods, such as gas chromatography with flame ionization detection (GC-FID), gas chromatography-mass spectrometry (GC-MS), high-performance liquid chromatography (HPLC), and ultraviolet spectrophotometry, among others [9]. Additionally, the bioactive properties of the material should also be investigated, particularly if the production of nutraceutical products is the purpose of the extraction process.

3.6 Mass Transfer Aspects

The mass transfer mechanisms that occur in SFE from natural solid matrices are not readily understood. The difficulties encountered in describing and modeling the SFE process arise from the fact that SFE involves multicomponent systems with a significant number of components, which can belong to many different chemical classes. Therefore, it is very difficult to establish the interactions between the solvent, the solutes and the solid matrix [10].

3.6.1 The Mass Balance Equations in the Fixed Bed Extractor

The SFE process is generally performed in a fixed bed extractor of cylindrical shape. The solid particles are packed in the extraction cell, forming a fixed bed through which the supercritical solvent is continuously flowed. A schematic representation of the fixed bed extractor is shown in Fig. 3.5.

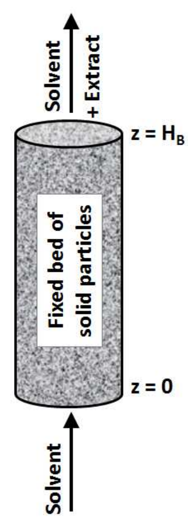

Fig. 3.5 A typical fixed bed extractor of the SFE process (z: axial coordinate, H_B: bed height)

It is crucial to propose simplifications when carrying out calculations of the process design. Some simplifications must be assumed to reduce the problem to one that is mathematically tractable. To simplify the description of the SFE process, the extraction system is usually treated as a pseudoternary (cellulosic structure + extract + solvent) and biphasic system (fluid phase + solid phase). The fluid phase (solvent + extract) and the solid phase (cellulosic structure + extract) are both pseudobinary systems [9,14]. A schematic diagram of the components inside the fixed bed extractor is presented in Fig. 3.6.

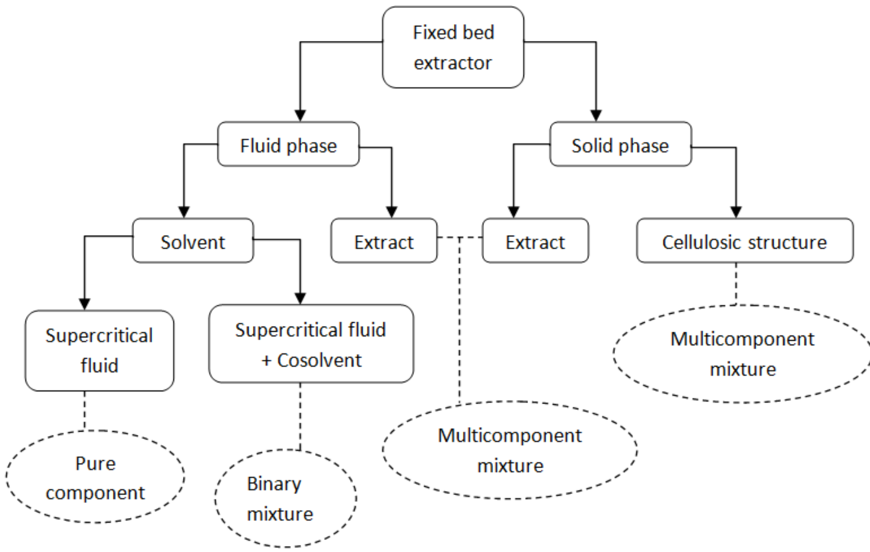

Fig. 3.6 Diagram of the fixed bed extractor composition in SFE from natural matrices

When evaluating the mass balance of SFE, it is typical to assume that the extraction cell is a cylindrical bed in which the solid particles are homogeneously distributed. The solvent flows in the axial direction (z), and the extractor geometry is such that the bed height can be considered infinitely larger than the bed diameter ($H_B >>> d_B$). Then, the terms of the radial (r) and tangential (Θ) directions can be neglected in the mass balance equations. Moreover, the solid and fluid phases can be taken as non-reactive systems. By taking into account all of these assumptions, the mass balance in the extraction bed can be described by Eqs. 3.1 and 3.2 [14,15]. It is interesting to note that in SFE, the fluid phase can be treated as a diluted solution; therefore, the solvent properties can replace the fluid phase properties [10].

- Fluid phase: [Accumulation] + [Convection] = [Dispersion] + [Interfacial Mass Transfer]

$$\frac{\partial Y}{\partial t}+u_i\frac{\partial Y}{\partial z}=\frac{\partial}{\partial z}\left(D_{aY}\frac{\partial Y}{\partial z}\right)+\frac{J(X,Y)}{\varepsilon} \qquad (3.1)$$

- Solid phase: [Accumulation] = [Diffusion] + [Interfacial Mass Transfer]

$$\frac{\partial X}{\partial t} = \frac{\partial}{\partial z}\left(D_{aX} \frac{\partial X}{\partial z} \right) + \frac{J(X,Y)}{(1-\varepsilon)} \frac{\rho_{CO2}}{\rho_S} \qquad (3.2)$$

where Y is the mass ratio of the solute in the fluid phase (kg/kg); X is the mass ratio of the solute in the solid phase (kg/kg); t is the extraction time (s); u_i is the interstitial velocity of the solvent (m/s); z is the axial direction (m); D_{aY} is the dispersion coefficient in the fluid phase (m^2/s); D_{aX} is the diffusion coefficient in the solid phase (m^2/s); ρ_{CO2} is the solvent density (kg/m^3); ρ_S is the true density of the solid matrix (kg/m^3); J(X,Y) is the interfacial mass transfer term (s^{-1}); and ε is the bed porosity (dimensionless).

The mass balance equations of the fluid and solid phases have been applied by several authors who have proposed many mathematical models based on the mass transfer phenomena that occur inside the extraction bed. One of the main differences among the proposed mathematical models is how each author describes the interfacial mass transfer term. This description depends on the personal assumptions that are made by each author when developing a different mass transfer model. Some of the mathematical models available in the literature are discussed in Sect. 3.7.

3.6.2 The Overall Extraction Curve (OEC)

According to Brunner [2], the course of SFE can be evaluated by analyzing the variables of a) the total amount of extract, b) the extraction rate, c) the remaining amount of extract in the solid, and d) the concentration of the extract in the supercritical solvent at the extractor outlet. All of the cited variables can be plotted as a function of the extraction time (or solvent consumption) to obtain curves that give important information regarding the SFE process. In most cases, variable (a) is selected such that the course of the extraction process is followed by determining the accumulated mass of the extract against the extraction time (or solvent consumption). This representation is the most commonly used and is well known as the *overall extraction curve* (OEC). The information provided by the OEC is useful for comparing the extraction results within a series of experiments when using the same solid matrix [2,3].

The mass of the extract that accumulates during the SFE process is typically shaped as shown in the schematic curve presented in Fig. 3.7. The first part (P-I) of the curve is a straight line and, therefore, corresponds to a constant extraction rate period. The second part (P-II) is a non-linear function that approaches a limiting value, that is, the total amount of extractable substances in the solid matrix [2]. Under certain processing conditions (as discussed in Sect. 3.5.1), the slope of the linear part of the graph may be given by the equilibrium solubility. However, it is fundamental to remember that the straight line generally occurs because the mass transfer resistance remains constant in the early stages of the extraction process. Therefore, the presence of the linear region is not proof that equilibrium conditions have been attained during SFE [2,3].

The shape of the OEC depends on the kinetics of solute extraction from the solid matrix and the solvation power of the SC-CO_2, which in turn depends on the operational conditions [3]. The course of the SFE from a solid matrix follows two types of curves for the extraction rate, as can be seen in Fig. 3.8. Curve 1 (C1) represents the extraction rate when a high initial concentration of solute in the solid substrate exists or when the solute is readily available to the solvent. Curve 2 (C2) represents the extraction rate when a low initial concentration of solute exists in the solid substrate or when the solute is not readily available to the solvent. Curve 2 also corresponds to the second part (P-II) of curve 1 because a depletion phase always comes after the first part (P-I, where a constant extract concentration is observed in the fluid phase at the outlet of the extraction cell) [2].

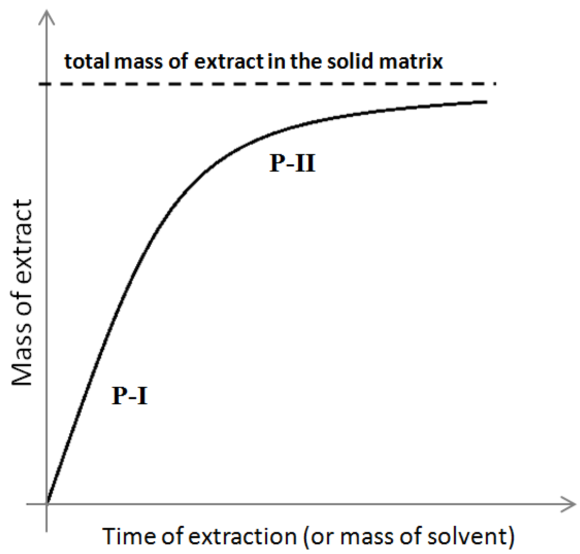

Fig. 3.7 The typical overall extraction curve (OEC) (P-I: part 1, P-II: part II) (adapted from Brunner [2], with kind permission from Springer Science and Business Media)

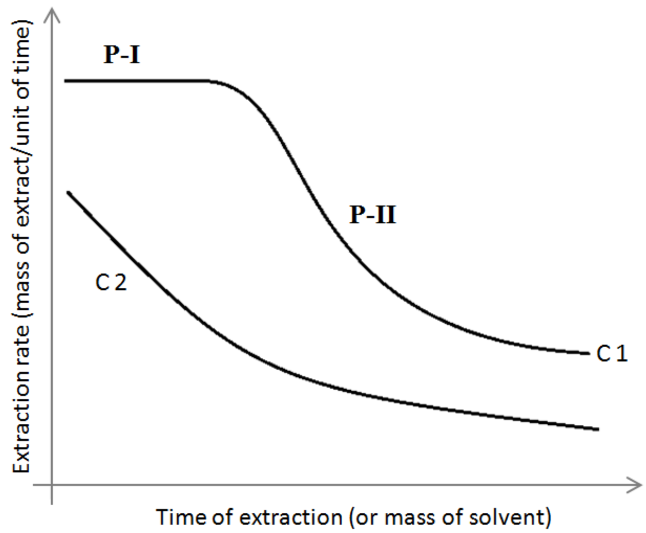

Fig. 3.8 Extraction rate curve: schematic illustration of curve 1 (C1) and curve 2 (C2) as described by Brunner [2] (the OEC from curve 1 has the shape previously presented in Fig. 3.7; P-I: part 1; P-II: part II) (adapted from Brunner [2], with kind permission from Springer Science and Business Media)

According to Brunner [2], the first part (P-I) of curve 1 (C1) has several main characteristics: (a) in the fluid phase, the mass transfer resistance dominates the process, (b) the solute compounds are readily available at the interface solid/fluid, and (c) a constant amount of extract is transferred to the bulk of the supercritical solvent, resulting in a constant concentration at the bed outlet. In the second part (P-II) of curve 1 (C1), as well as in curve 2 (C2), the extract concentration decreases with increasing extraction time due to the increasing mass transfer resistances and the depletion of the extract in the solid phase. The solid matrix will be depleted of the extractable material in the direction of flow. The concentration of extract components increases in the direction of flow both in the SCF and in the solid material [2,3].

3.7 Mathematical Modeling

Mathematical models based on the mass transfer phenomena, or even with merely empirical basis, are important tools in SFE investigations. The mathematical modeling of extraction curves may help develop an understanding of the kinetic behavior of SFE through the definition of extraction rates, steps, time, and/or mass transfer parameters with strong physical meaning [5]. The modeling of OECs helps the determination of the extraction time (cycle time), which is important for achieving the optimal utilization of an industrial scale plant [2]. The main goal of using a mathematical model is the determination of parameters that may be applied to key aspects of process design, such as equipment dimensions, the solvent flow rate, particle size, and the solvent to feed (S/F) mass ratio, among others [16]. Thus, mathematical models can be useful tools for scale-up prediction, process design, and/or cost estimation purposes.

Knowledge of the initial distribution of a solute in the solid substrate directly affects the selection of the models that can adequately describe a given SFE system. The extractable substances may be distributed within the solid matrix in various ways. The solute can be (a) located freely on the surface of the solid material, (b) adsorbed on the outer surface of the solid material, (c) heterogeneously distributed inside the solid particle (located inside the pores or other specific cell structures), or (d) evenly distributed within the solid particles [17].

Many mathematical models have been developed to describe the OEC, ranging from simple equations to very complex equations. Some extensive reviews concerning the mathematical modeling of SFE were presented by Oliveira et al. [18] and Sovová [19], among other authors. In this chapter, it is not our intention to deliver a detailed discussion of all models available in the literature. Thus, we take a classical approach and focus on the fundamental concepts while presenting some well-known models from the SFE literature. According to Reverchon [17], the mathematical models used to describe the OEC can be divided into three main categories based on the approaches of (a) empirical evidence, (b) heat transfer analogy, or (c) differential mass balance integration.

The models developed from the first category are based on the hyperbolic shape of the typical OEC. One example is the model proposed by Esquível et al. [20] for describing the SFE of oil from olive husk. The empirical models use a hyperbolic function to fit the experimental data. The general form of the models from this category can be given by Eq. 3.3 [4].

$$m_{EXT} = X_0 F\left(\frac{t}{C_1 + t}\right) \qquad (3.3)$$

where m_{EXT} is the mass of the extract (kg); t is the time of extraction (s); F is the mass of the feed material (kg); X_0 is the initial mass ratio of the extractable solute in the solid substratum (kg/kg); and the constant C_1 is an adjustable parameter that has no physical meaning (s). The empirical model may give good fits in some particular cases, but it does not give any phenomenological information regarding the SFE process. Thus, this model has limited application in terms of scale-up and process design.

In the second category, an analogy is considered between SFE and the heat transfer by diffusion. In this case, all mass transfer is considered to happen based only on the mechanism of diffusion, allowing an apparent diffusion coefficient to be obtained [4]. The model presented by Crank [21] for the description of heat transfer in a solid particle cooling in a uniform medium was adapted by Reverchon [17] and was used to fit SFE data [15]. Reverchon [17] applied Fick's second law of diffusion to obtain a model that describes the OEC according to Eq. 3.4.

$$m_{EXT} = X_0 F\left[1-\frac{6}{\pi^2}\sum_{n=1}^{\infty}\frac{1}{n^2}\exp\left(\frac{-n^2\pi^2 D_{ef}t}{r^2}\right)\right] \qquad (3.4)$$

where m_{EXT} is the mass of the extract (kg); t is the time of extraction (s); F is the mass of the feed material (kg); X_0 is the initial mass ratio of the extractable solute in the solid substratum (kg/kg); n is an integer number; r is the radius of the spherical particle (m); and D_{ef} is the adjustable parameter, which represents the effective diffusion coefficient of the solute within the solid matrix (m^2/s). The application of the diffusion model is restricted to very few systems because in most cases, it results in a poor fit. This behavior is expected because mass transfer in SFE may not be properly described by diffusion alone because convective mass transport dominates the beginning of the process [4].

The third category comprises the majority of the mathematical models proposed for the description of SFE processes. The starting point is the evaluation of the differential mass balance (see Eqs. 3.1 and 3.2, which were presented in Sect. 3.6.1) inside the fixed bed extractor [4]. Then, each author gives a personal interpretation of the mass transfer phenomena that happen in both the fluid and solid phases. An example from this category is the model presented by Sovová [22], which has been extensively used by various researchers of SFE. A fundamental characteristic of this model is that the solute is distinguished in two different fractions, one present in broken cells and the other in intact cells [4]. As a result, this model was developed for application when the raw material passes through a milling process before extraction (see Sect. 3.3.1). The solute fraction present in the broken cells is denoted as the easily accessible solute (X_P), which is located at the particle surface and is the first fraction extracted. The fraction contained in the intact cells is denoted as the hardly accessible solute (X_K) and is located inside the solid particle. The OEC follows the shape of the type 1 curve (C1) described by Brunner [2] (as discussed in Sect. 3.6.2).

Sovová [22] divided the OEC into three distinguishable regions [10,11] as follows:

- *Constant extraction rate (CER)*: in the CER period, the external surfaces of the solid particles are assumed to be fully covered with the easily accessible solute. In this region, the solute is essentially removed by convection; thus, the mass transfer resistance exists in the fluid phase.
- *Falling extraction rate (FER):* in the FER period, flaws in the superficial solute layer begin to appear and so the hardly accessible solute starts to be extracted. As a result, the solute is extracted by both convection and diffusion mechanisms. This is a transition period that is caused by the continuous depletion of the solute layer in the external surface.
- *Diffusion-controlled (DC)*: in the DC period, the solute at the particle surface is completely exhausted, and only the hardly accessible solute is available for extraction. As a result, mass transfer is controlled by intraparticle diffusion. The mass transfer resistance exists in the solid phase due to the low diffusivity of the solute in the solid matrix.

The model developed by Sovová [22] takes into account the solute solubility (Y*) in the fluid phase and the mass transfer coefficients in both the fluid and solid phases (k_{YA} and k_{XA}, respectively) [10]. This model neglects the terms of dispersion and accumulation in the fluid phase, as well as the diffusion in the solid phase. Accumulation in the fluid phase was disregarded because the residence time of the solvent was considered to be low enough to support this assumption. Hence, the accumulation term was considered only in the solid phase [4]. The model also assumes pseudo-steady state and plug flow. The parameters temperature, pressure, and solvent velocity are taken as constant throughout the entire extraction process. The fixed bed is assumed to be homogeneous with respect to the particle size and the initial solute distributions [10]. The mass balance equations proposed by Sovová [22] are presented in Eqs. 3.5 and 3.6 for the fluid and solid phases, respectively.

$$u_i \frac{\partial Y}{\partial z} = \frac{J(X,Y)}{\varepsilon} \qquad (3.5)$$

$$\frac{\partial X}{\partial t} = \frac{J(X,Y)}{(1-\varepsilon)} \frac{\rho_{CO2}}{\rho_S} \qquad (3.6)$$

where Y and X are the mass ratios of the solute in the fluid and solid phases, respectively (kg/kg); t is the extraction time (s); u_i is the interstitial velocity of the solvent (m/s); ρ_{CO2} and ρ_S are the solvent and solid matrix densities, respectively (kg/m^3); ε is the bed porosity (dimensionless); z is the axial direction (m); and J(X,Y) is the interfacial mass transfer term (s^{-1}) as described by Eqs. 3.7 and 3.8, which must be applied when $X > X_K$ and $X \leq X_K$, respectively. The initial and boundary conditions for the mass balance equations are presented in Eqs. 3.9 and 3.10.

$$J(X,Y) = k_{YA}\left(Y^* - Y\right) \qquad (3.7)$$

$$J(X,Y) = k_{XA} X \left(1 - \frac{Y}{Y^*}\right) \qquad (3.8)$$

$$X(z, t=0) = X_0 \qquad (3.9)$$

$$Y(z=0, t) = 0 \qquad (3.10)$$

Sovová [22] solved the model equations and developed an analytical solution that is presented in Eqs. 3.11, 3.12, and 3.13, which must be applied, respectively, to the CER ($t \leq t_{CER}$), FER ($t_{CER} < t \leq t_{FER}$) and DC regions ($t > t_{FER}$). The extraction times that identify the ends of the CER and FER periods are denoted t_{CER} and t_{FER}, respectively.

$$m_{EXT} = Q_{CO2} Y^* [1 - \exp(-Z)] t \qquad (3.11)$$

$$m_{EXT} = Q_{CO2} Y^* [1 - t_{CER} \exp(Z_W - Z)] \qquad (3.12)$$

$$m_{EXT} = m_{SI} \left\{ X_0 - \frac{Y^*}{W} \ln\left[1 + \exp\left(\frac{WX_0}{Y^*}\right) - 1\right] \exp\left[\frac{WQ_{CO2}}{m_{SI}}(t_{CER} - t)\right]\left(\frac{X_P}{X_0}\right)\right\} \qquad (3.13)$$

Considering that:

$$Z = \frac{m_{IS} k_{YA} \rho_{CO2}}{Q_{CO2}(1-\varepsilon)\rho_S} \qquad (3.14)$$

$$W = \frac{m_{IS} k_{XA}}{Q_{CO2}(1-\varepsilon)} \qquad (3.15)$$

$$Z_W = \frac{ZY^*}{WX_0} \ln\left\{ \frac{X_0 \exp\left[\frac{WQ_{CO2}}{m_{IS}}(t_{CER} - t)\right] - X_K}{X_0 - X_K} \right\} \qquad (3.16)$$

$$t_{CER} = \frac{m_{IS} X_P}{Y^* Z Q_{CO2}} \qquad (3.17)$$

$$t_{FER} = t_{CER} + \frac{m_{IS}}{Q_{CO2} W} \ln\left[\frac{X_K + X_P \exp\left(WX_0 / Y^* \right)}{X_0} \right] \qquad (3.18)$$

$$m_{IS} = F - m_0 = F - (X_0 F) \qquad (3.19)$$

The nomenclature used in Eqs. 3.11 to 3.19 is specified as

m_{EXT} = the mass of the extract (kg);

t = the extraction time (s);

F = the mass of the feed material (kg);

X_0 = the initial mass ratio of extractable solute in the solid substratum (kg/kg);

m_0 = the initial amount of extractable solute in the solid substratum (kg);

m_{IS} = the mass of the inert solid (kg);

Q_{CO2} = the solvent flow rate (kg/s);

ρ_{CO2} and ρ_S = the densities of CO_2 and the solid material, respectively (kg/m^3);

ε = the bed porosity (dimensionless);

Y^* = the solubility of the extract in the supercritical solvent (kg/kg);

X_P = the mass ratio of the easily accessible solute in the solid substratum (kg/kg);

X_K = the mass ratio of the hardly accessible solute in the solid substratum (kg/kg);

k_{YA} and k_{XA} = the mass transfer coefficients in the fluid and solid phases, respectively (s^{-1}).

The application of the model developed by Sovová [22] generally results in good fits to experimental data for many different raw materials. A significant advantage of this model is that it provides a good physical description of the mass transfer phenomena in SFE processes [11]. Therefore, it is a convenient choice for the purposes of process design because the adjustable parameters (k_{YA}, k_{XA}, and X_K) can be applied in scale-up investigations. Years later, Sovová [23] presented another model that is also based on the concept of broken and intact cells. In this new model, the term for accumulation in the fluid phase was considered, and some changes were applied to the term of interfacial mass transfer. As a result, the complexity of the mathematical model increased significantly, and then the model was solved numerically because an analytical solution was no longer suitable [4,23]. Furthermore, the number of adjustable parameters increased and more information was required for the application of the new mathematical model, thereby limiting its practical use.

All of the models discussed thus far assume that the solute is a pseudocomponent. Martínez et al. [24] proposed a model that can be applied under two different assumptions regarding the solute composition, that is, to either a pseudocomponent or a multicomponent system. The assumption of a multicomponent system may be useful if there exists interest in knowing the kinetic behavior of specific compounds that are present in the extract. In this chapter, we present the model for a pseudocomponent solute, and we refer to it as the "logistic model." Further extension of this model to multicomponent systems is easily carried out because the same considerations and analogous equations are used.

According to Martínez et al. [24], the model begins by applying the differential mass balance inside the extraction bed for solid and fluid phases. This author neglected the terms of accumulation and dispersion in the fluid phase because he assumed that both phenomena lack significant influence relative to the convection term. The main peculiarity of this model is the definition of the term of interfacial mass transfer, which is described by one of the solutions from the logistic equation. The model equation for a pseudocomponent system is presented in Eq. 3.20. The logistic model has two adjustable parameters, named C_2 and t_m. No physical meaning is attributed to the first parameter (C_2), while the second (t_m) is defined as the time during which the extraction rate reaches its maximum value [24].

$$m_{EXT} = \frac{X_0 F}{\exp(C_2 t_m)} \left\{ \frac{1+\exp(C_2 t_m)}{1+\exp[C_2 (t_m - 1)]} - 1 \right\} \tag{3.20}$$

where m_{EXT} is the mass of the extract (kg); t is the time of extraction (s); F is the mass of the feed material (kg); X_0 is the initial mass ratio of the extractable solute in the solid substratum (kg/kg); and C_2 (s^{-1}) and t_m (s) are the adjustable parameters.

The logistic model generally provides a relatively good fit to experimental data gleaned from different raw materials. However, when applying this model to common OEC shapes, many authors have obtained negative values for t_m; when this happens, no physical meaning can be attributed to the parameter t_m [13]. The absence of physical meaning brings an empirical character to this model; thus, the model has limited application in terms of process design and scale up.

3.7.1 The Spline Model

Many different mathematical models have been used to describe and understand the kinetics of SFE processes, ranging from simple equations to very complex equations. An example of a simplified approach used to model the extraction curve is the so-called spline model, as presented by Meireles [9]. This model, which has an empirical basis, is based on the assumption that the OEC can be described by a family of N straight lines. The lines from spline model can be calculated using Eq. 3.21 [9,25][2] written for the 1^{st}, 2^{nd}, 3^{rd}, …, and N^{th} lines.

$$m_{EXT} = \left(b_0 - \sum_{i=1}^{i=N-1} t_i a_{i+1} \right) + \sum_{i=1}^{i=N} a_i t \tag{3.21}$$

where m_{EXT} is the mass of the extract (kg); t is the time of extraction (s); N is the number of straight lines; b_0 is the linear coefficient of line 1 (kg); $\sum a_i$ (for i=1 to i=N) are the slopes of lines 1 to N (kg/s); and t_i (for i=1 to i=N-1) is the time in which the intercept between line "i" and line "i+1" occurs (s). Equation 3.21 is greatly

[2] The model presented here (Eq. 3.21) is the revised form of the equations previously published by Meireles [9,25] because, in the original reference [9], typographical errors were present in the equation that describes the spline model.

simplified for two or three straight lines, as presented in Eqs. 3.22, 3.23, and 3.24. When considering an OEC described by 3 straight lines, the m_{EXT} for the three different periods of extraction should be calculated using the following equations [13]:

For the first straight line (**$t \leq t_1$**), the m_{EXT} is obtained by Eq. 3.22:

$$m_{EXT} = b_0 + a_1 t \qquad (3.22)$$

For the second straight line (**$t_1 \leq t \leq t_2$**), the m_{EXT} is obtained by Eq. 3.23:

$$m_{EXT} = (b_0 - t_1 a_2) + (a_1 + a_2)t \qquad (3.23)$$

For the third straight line (**$t \geq t_2$**), the m_{EXT} is obtained by Eq. 3.24:

$$m_{EXT} = (b_0 - t_1 a_2 - t_2 a_3) + (a_1 + a_2 + a_3)t \qquad (3.24)$$

The spline model has been extensively used by our research group (LASEFI/FEA/UNICAMP) to model the kinetic data obtained from SFE studies [11,13,26-28]. This model has been applied based on considerations that the OEC can be described by two or three straight lines, depending on the shape of the extraction curve. Although the use of two straight lines may be adequate in some cases, the model with three lines is more versatile because it can be applied to any possible OEC shape. Moreover, when the OEC is described by three straight lines, it is possible to make a useful analogy with the three different extraction regions (the CER, FER, and DC periods, as previously discussed in Sect. 3.7) that are observed in a typical OEC. In this case, the parameters t_1 and t_2 (from Eqs. 3.23 and 3.24) correspond to t_{CER} and t_{FER}, the extraction times that mark the ends of the CER and FER periods, respectively. A schematic representation of an OEC that was fitted with three lines is presented in Fig. 3.9.

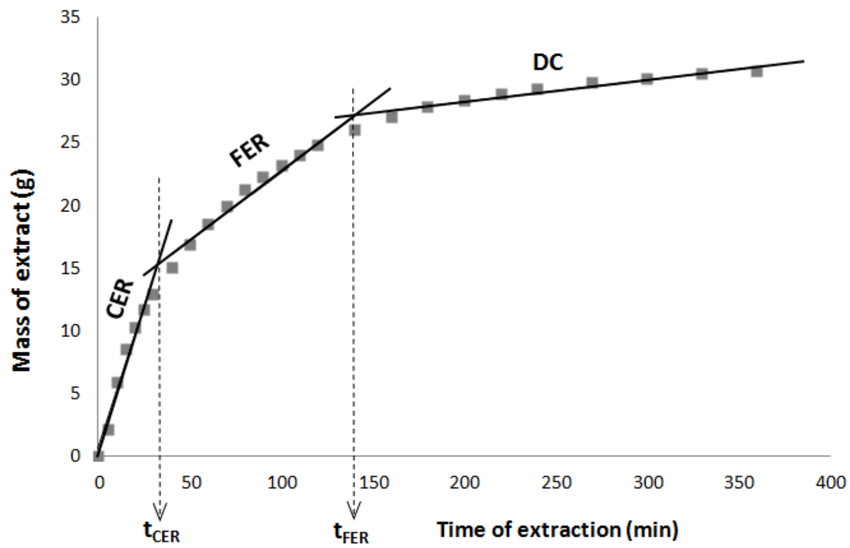

Fig. 3.9 Schematic representation of the spline model: extraction curve of SFE from clove bud (313 K/15 MPa, 226 g of feed material, solvent flow rate = 9.6 x 10^{-5} kg/s) fitted to three straight lines, which were prolonged to evidence the intercept points (t_{CER} and t_{FER}). Experimental data were obtained from Prado [27]. (*CER* constant extraction rate, *FER* falling extraction rate, *DC* diffusion-controlled, t_{CER} is the time spam of the CER period, t_{FER} is the time that marks the end of the FER period)

To fit the experimental OEC to a spline containing three straight lines, a nonlinear fit must be performed since the intercept points (t_{CER} and t_{FER}) are unknown. This can be carried out by using the procedures PROC REG and PROC NLIN of the SAS® software package (SAS Institute Inc., Cary, NC, USA) [13]. According to Jesus et al. [13], the fitted lines may be associated with three different mass transfer mechanisms (as illustrated in Fig. 3.9), following the classic description of the CER, FER and DC periods [22]. Thus the first, second, and third lines can be related to the CER, FER, and DC regions, respectively. When studying SFE kinetics, it is a very common procedure to apply the spline model for the determination of various kinetic parameters that characterize the CER period. These parameters are [9,13] the time span of the CER period (t_{CER}), the extraction rate of the CER period (M_{CER}), the mass ratio of the extract in the fluid phase at the bed outlet (Y_{CER}), the extraction yield of the CER period (R_{CER}), and the solvent-to-feed mass ratio of the CER period (S/F_{CER}). Both t_{CER} (s) and M_{CER} (kg extract/s) are adjustable parameters from the spline model (t_1 and a_1, respectively, as presented in Eq. 3.23). Y_{CER} (kg extract/kg CO_2) is obtained by dividing M_{CER} by the mean solvent flow rate (Q_{CO2}, kg CO_2/s). The parameters R_{CER} (%, kg extract/kg feed material) and S/F_{CER} (kg CO_2/kg feed material) should be calculated using modeled data (the values obtained for t_{CER} and m_{EXT} at the end of the CER period) [13].

The spline model generally presents a good fit to experimental data; thus, it is capable of delivering a good description of the OEC quantitative behavior [13]. Furthermore, although the model possesses an empirical basis and is comparatively simple in terms of its mathematical complexity, it nonetheless delivers helpful information regarding the SFE process. The association that can be made between the first line and the CER period is particularly useful because the CER region is the most important in terms of process design. According to Pereira and Meireles [7], between 50 and 90 % (w/w) of the total amount of extract can be recovered before the end of the CER period. Therefore, for many industrial applications, the extraction process may be ended shortly after t_{CER} because the best operational conditions are likely those in which a significant amount of extract is produced within a relatively short process time [7]. Therefore, the values of t_{CER} and R_{CER} approximately represent the minimum time that a SFE cycle should last and the minimum extraction yield expected under the given process conditions [9].

Some works on scale-up (see Sect. 3.8 for details) have demonstrated that the extraction yields and kinetic behaviors observed in laboratory assays can be reproduced on a pilot scale [16,28-31]. Hence, it is possible that the same extraction yields may be achievable in an industrial plant. In this case, the parameters t_{CER}, $(S/F)_{CER}$, and R_{CER} can be used in preliminary studies of economic feasibility (aspects concerned with cost estimation are discussed in Sect. 3.9). According to Leal [32], when using the spline model, the intersection between lines 1 and 3 (CER and DC, respectively, as illustrated in Fig. 3.9) defines an additional parameter of time, which is named t_{CER2}. This parameter can also be used as a good estimation of the process time in preliminary studies of COM predictions [13,26].

In the literature on SFE, several additional complex mathematical models are presented for the description of the OEC. These models, which have a phenomenological basis, may provide reliable descriptions of the mass transfer mechanisms involved in the extraction process. This means that the adjustable parameters can have significant physical meanings and, as a result, may be used for scale-up purposes. Nonetheless, to apply phenomenological models, additional specific data are required. The model proposed by Sovová [22], for example, requires information concerning the extract solubility (Y*) in supercritical CO_2, representing data that are not always available; in many cases, such data may not be available in the literature, and the associated experimental determination would be a difficult task (as discussed in Sect. 3.5.1). Thus, considering the difficulties encountered in finding specific data for many natural extracts, it is clear that one advantage of the spline model is that only kinetic data are necessary to carry out OEC mathematical modeling. Moreover, even with an empirical basis, this model provides useful and practical information concerning the SFE process, particularly with respect to the CER period.

3.8 Scale-Up

Scale-up is the task of achieving on a larger scale the same process behavior that was previously obtained in laboratory assays by considering the differences that are inherent to the processes conducted on equipment of significantly different sizes [5,30]. By scaling up a process, a product with the same characteristics can ideally be obtained at a larger production rate with no or minimal modifications required. The prediction of a process behavior at the industrial scale is one of the most challenging tasks for food and chemical engineers [5].

After many decades of intensive research, the theoretical basis of SFE is now well established. Hundreds of publications concerning the optimization of process parameters in SFE from different raw materials are reported in published books, articles and patents based on the results obtained on the laboratory scale. However, few data can be found for pilot-plant scales, and less data are available at the industrial scale [5]. Open and accessible knowledge regarding commercial scale processes and equipment is very scarce. Information regarding industrial processes depends on the policies of the companies that use and sell SFE units [33].

The available scale-up data in the open literature are inconclusive, so there is no consensus regarding a general scale-up criterion that may be applicable to SFE from solid matrices [30]. To validate scale-up criteria, it is necessary to assess their applicability to different types of raw materials [34] because the mass transfer mechanisms depend on the specific characteristics of the solid substrates and respective solutes. The works that explore scale-up methods are usually limited to specific raw materials and process conditions; as a result, significant care is necessary when proposing a generalization. The process of defining universal scale-up criteria is very complex. However, when considering the main process parameters of SFE and how they affect extraction yield and kinetics, it may be possible to find ways of achieving some effective scale-up procedures [5].

In SFE, the scale-up objective is the reproduction of the same extraction curve at a larger scale by preserving some of the extraction parameters used at the laboratory scale. Therefore, the biggest challenge is the discovery of which parameters, when conserved, will lead to the same results (extraction rates, yields and chemical compositions of the products) when performing the scale-up procedure. The solution to this type of problem is tricky, and the challenge involves deep knowledge of the limiting factors of the SFE process, which may be based on either thermodynamics or mass transfer [5]. Del Valle et al. [35] suggested that caution is required when working with simple scale-up procedures because in SFE, the relationships between extraction rates and extraction conditions depend on several parameters and may be very complex. Moreover, differences between the mass transfer phenomena may occur when significantly increasing the process scale [35]. However, Prado et al. [30] emphasize that the use of some simple criteria could help the development of easily applicable scale-up methods, which would decrease the time and cost utilized in the design of a SFE process.

According to Clavier and Perrut [36], a simple scale-up procedure for SFE processes can be conducted by following two main steps: (a) perform small-scale experiments to define the optimal extraction conditions by scanning over the operational parameters (different pressures, temperatures, solvent to feed ratios, and others), and then (b) select the scale-up method based on the factors that limit mass transfer during extraction. Depending on the complexity and kinetic limitations of the process, different strategies may be applied to the design of the production unit. The easiest scale-up method consists of holding one or both of the ratios of Q_{CO2}/F and S/F constant, where Q_{CO2} is the solvent flow rate, F is the feed mass in the extractor, and S is the solvent mass required for the extraction [36]. Then, three scale-up criteria can be proposed [36]: (a) in the case of an extraction limited by solubility, the S/F ratio should be held constant between the small and large scales; (b) for a process limited by internal diffusion, the Q_{CO2}/F ratio should be conserved from the small to the large scale; and (c) when both diffusion and solubility are limiting mechanisms, both ratios (S/F and Q_{CO2}/F) should be held constant in the scale-up process.

The Q_{CO2}/F ratio is inversely proportional to the residence time of the solvent inside the extractor, as can be seen in Eq. 3.25. It is important to emphasize that the solvent density (ρ_{CO2}), the bed porosity (ε), and the bed apparent density (ρ_B) should be preserved when studying the above-mentioned scale-up criteria. Therefore, it is clear that the residence time (t_{RES}) will be conserved if the ratio between the solvent flow rate (Q_{CO2}) and the feed mass in the extractor (F) is held constant. Clavier and Perrut [36] note that the contact time between the solvent and solid matrix is a determining factor for processes limited by internal diffusion; as a result, the residence time should be conserved from the small to the large scale.

$$t_{RES} = \frac{\varepsilon \rho_{CO2} F}{\rho_B Q_{CO2}} \qquad (3.25)$$

where t_{RES} is the residence time of the solvent (s); ε is the bed porosity (dimensionless); ρ_{CO2} is the solvent density (kg/m^3); ρ_B is the bed apparent density (kg/m^3); F is the feed mass in the extractor (kg); and Q_{CO2} is the solvent flow rate (kg/s).

The criterion that necessitates maintaining the Q_{CO2}/F ratio as a constant (and consequently preserving the residence time) has been effective when applied to the scale-up of SFE from clove [16], peach almond [31], and striped weakfish wastes [37]. However, it is considered unsatisfactory for the scale-up of SFE data from vetiver roots [16]. This may have resulted from the physical properties of vetiver oil (particularly, its high viscosity), which could have affected the mass transport properties in small-scale experiments and may have contributed to a significant loss of the extract at some locations within the equipment [16]. In the just-mentioned works [16,31,37], the large-scale experiments were conducted on SFE equipment with capacities no larger than 300 cm^3; hence, no assays were performed on pilot-scale units. The same criterion (constant Q_{CO2}/F) was used to investigate the scale-up of SFE from red pepper by performing large-scale experiments in a pilot-plant unit [5]. The authors observed that the extraction curves obtained at the laboratory (300 cm^3 capacity) and pilot (5150 cm^3 capacity) scales exhibited significantly different kinetic behaviors, so the applied scale-up criterion could not be used to accomplish the authors' goal [5]. According to Martínez and Silva [5], the divergences observed between applications at small and large scales may have occurred as a result of bed compaction, variations in the efficiencies during the separation step, distinct bed geometries, and mechanical dragging. Martínez and co-workers [16] also investigated another scale-up proposal that consisted of holding constant the superficial velocity of the solvent; however, this criterion was ineffective because the results obtained for large-scale experiments were far from those achieved for small-scale experiments.

In recent works from our research group, the criterion based on holding constant both the S/F and Q_{CO2}/F ratios has been successfully applied to the scale-up of SFE from different raw materials [27-30]. In these works, the small-scale extraction curves were obtained on laboratory-scale equipment (an extraction vessel measuring 290 cm^3 in volume) and were then used as references for scaling up the SFE process. The large-scale experiments were performed in a pilot-plant unit (an extraction vessel measuring 5150 cm^3 in volume), containing three separators that were arranged in series. The proposed criterion was effective for the scale-up data of SFE from clove [30], sugarcane residue [30], grape seeds [28], ginger [27], and annatto seeds [29]. Taking into account the feed mass in the extractor, a 15-fold scale-up was achieved for clove and sugarcane residue [30], a 17-fold scale-up was performed for grape seeds [28] and ginger [27], and a 12-fold scale-up was accomplished for annatto seeds [29]. The extraction curves obtained in small- and large-scale experiments had similar shapes, but in all cases, the authors found that the pilot-scale yields were higher (ranging from 5 to 20 % higher, depending on the raw material used) than those achieved in the small-scale assays [27-30]. According to Prado et al. [30], the manufacturers of SFE equipment claim that the extraction process is more efficient at larger scales, so the higher yields achieved in pilot-scale experiments are in agreement with the information delivered by manufacturers.

The scale-up procedure suggested by Clavier and Perrut [36] (holding one or both of the S/F and Q_{CO2}/F ratios constant) provides the significant advantage of simplicity. Nonetheless, this approach does not take into account several important factors that may affect the extraction process (radial diffusion, axial mixing, bed compaction, etc.) and is incapable of predicting the effects of using a series of extractors. A refined scale-up method that integrates all of the relevant factors in SFE processes requires a numerical simulation that may estimate any possible plant configuration and may lead to the optimization of industrial units [36].

3.9 Economic Analysis

It is apparent that industries must earn profits, so even the most brilliant technology will never be accepted unless it can provide a product with a price tag that is at least compatible to that of similar products that are already available in the market [38]. This means that demonstrating the economic feasibility of an emerging technology is the only way to attract potential investors. Therefore, researchers should blend their scientific enthusiasm with economic awareness [38] because the cost aspects are fundamental to the process design.

According to Meireles [9], SFE from solid matrices was shown to be a technically feasible process. However, despite the increasing number of industrial plants in operation all over the world, in many regions (Latin America, for example), SFE is not applied on a commercial scale [9]. Thus, although SFE has been used as an industrial operation since the 1980s [2], it can still be considered an emerging technology because the conventional techniques continue to be the most commonly used approaches in various applications of solid-fluid extraction. One reason for this is the restraints imposed by the high investment costs, which are usually associated with the high pressure aspect of the processes [9,39]. Therefore, to spread SFE technology, it is critical to find ways of demonstrating that this technique can be profitable. Indeed, this is a task of major importance with respect to preventing the elimination of SFE at the very early stages of the process design. Hence, efforts must be undertaken to develop simple and reliable methods for estimating the cost of manufacturing (COM) of SFE products because cost information is a determinant factor in the initial stages of business plan analyses [9,40]. Moreover, it is also important to emphasize that a preliminary analysis of the COM must be performed with minimal experimental information [40].

The COM of various SFE extracts has been systematically studied by our research group for more than a decade. Based on the knowledge acquired from this systematic investigation, we can state that the following information must be available to perform cost estimations.

- The *operating conditions of temperature and pressure* should be selected by taking into account the results from GYI experiments (see Sect. 3.5.2). Both parameters are strongly related to equipment specifications and the utilities demand.
- The *extraction yield for a given extraction time and solvent-to-feed ratio*, which are process parameters that should be obtained from the OEC (see Sect. 3.6.2). These parameters are necessary to determine the rates of solvent consumption and extract production, as well as the cycle time.
- The *description of the raw material pretreatment*, which are the process steps that must be conducted prior to the extraction process (as discussed in Sect. 3.3.1). The pretreatment requirements are important for estimating the preprocessing costs.
- The *bed apparent density* is required to calculate the mass of feed material that must be packed into a certain bed volume. If a given production rate is desired, then the plant capacity and the raw material demand can be determined using the bed apparent density.
- The *extract composition* is valuable information, although it is not necessary when calculating the COM. Nonetheless, characterization of the extract, in terms of its chemical compounds and functional properties, is essential information for defining the selling price of SFE products. If a reliable estimation of the selling price can be made, then it is possible to also make a good prediction of the payback period, which is a cost parameter that may attract investors and aid decision-makers.

Rosa and Meireles [39] presented a simple procedure for estimating the COM of extracts obtained by SFE. These authors applied the methodology described by Turton et al. [41], in which the COM is calculated as a sum of the direct costs, fixed costs, and general expenses [9,39]. The direct costs are directly dependent on the production rate, that is, they are composed of the costs of raw materials, operating labor, and utilities, among others. The fixed costs are independent of the production rate and involve taxes, insurance, depreciation, etc. The general expenses are associated with business maintenance, such as administrative costs, research and development, and sales expenses, among others [39]. The three components of the COM (direct costs + fixed costs + general expenses) are then estimated in terms of five main costs, as expressed in the model (Eq. 3.26) proposed by Turton et al. [39,41]:

$$COM = 0.304F_{CI} + 2.73C_{OL} + 1.23(C_{UT} + C_{WT} + C_{RM}) \qquad (3.26)$$

where COM is the cost of manufacturing, which is expressed in US$/kg; F_{CI} is the fixed cost of investment; C_{OL} is the cost of the operating labor; C_{UT} is the cost of the utilities; C_{WT} is the cost of waste treatment; and C_{RM} is the cost of the raw materials.

The fixed cost of investment (F_{CI}) can be calculated on a yearly basis as the product of the total investment by the annual depreciation rate (normally, a 10 % rate is considered). In addition to the expenses associated with equipment and installations, the investment cost should also include the initial amount of CO_2 that is required to fill the solvent reservoir [39]. The cost of operational labor (C_{OL}) is related to the number of workers that are needed to operate the process equipment (extractors, separators, heat exchangers, compressors, pumps, storage tanks, etc.). The cost of the utilities (C_{UT}) is calculated by considering the demand for heating steam, cooling water, and electric power [26,39].

In the SFE of natural products, the raw material is a plant or animal substrate, which may require one or more pretreatment steps (cleaning, selection, drying, milling, etc.) before extraction can be performed. The cost of the raw materials (C_{RM}) is composed of expenses that include the solid substrate (both the solid matrix and all of the pretreatment costs) and the loss of CO_2 during the process. The solvent lost is associated with the leaking of CO_2 from the system, either as a result of dissolution in the extract after the separation process or entrapment in the solid substrate that is removed from the extractor [39]. Rosa and Meireles [39] considered that a factor of 2 % (taking into account the total amount of solvent used in a cycle of extraction) was adequate for estimating the CO_2 lost. Regarding the generation of waste, the only waste accumulated is the exhausted solid, which is harmless and can be reused in other industrial applications or is simply disposed of as an ordinary organic waste [26]. In particular cases, the exhausted solid is the main desired product, as in the removal of caffeine from coffee, the reduction of nicotine in tobacco, and the removal of cholesterol from foods, among others. Therefore, the cost of waste treatment (C_{WT}) can be completely neglected and is assumed to be zero [26,39].

As long as the production requirements of a particular SFE process are known, the optimal configuration of the industrial plant can be determined [36]. A typical SFE unit (see Fig. 3.1) is composed of two or more extraction columns, two or more separators (flash tanks), which are arranged in series to allow a certain degree of extract fractionation, a CO_2 reservoir, a solvent pump, heat exchangers, a compressor for CO_2 recycling, several valves, and temperature and pressure controllers [7,39].

To determine the input and output mass rates and the energy demands of the industrial process, the mass and energy balance equations must be solved. This can be achieved by using software (either home-made or commercial packages) that addresses process engineering calculations. In recent years, our research group has adopted the commercial software SuperPro Designer® (Intelligent Inc., Scotch Plains, NJ, USA) as a useful tool for studying the economic feasibility of SFE [26,28,34,42-46]. This software allows calculations of the process and economic parameters, so it can be used to perform simulations of industrial-scale processes. The COM and the payback period are some of the output data obtained from simulations performed in SuperPro Designer®. According to the Association for the Advancement of Cost Engineering International, cost estimations can be divided into five classes (1–5), which are defined by taking into account the degree of accuracy between the predicted value and the real COM. The class 5 estimation is based on the lowest level of project definition, while the class 1 estimation is closer to the final definition of the industrial project. The SuperPro Designer® software is capable of estimating COMs that may be classified as classes 2–3 [26].

It is well known that the COM of a SFE product is significantly influenced by extraction time (t_{EXT}), which is the time required for one cycle of extraction. Therefore, it is very important to know the extraction curve because kinetic data can be used to estimate the time in which the COM reaches its minimum value. Prado and co-workers [28] studied the economic viability of the production of grape seed oil by SFE. These authors investigated different times of extraction (from 60 to 300 min) and plant capacities (0.005, 0.05, and 0.5 m^3). The minimum COM (12 US$/kg) was found for a plant size of 0.5 m^3 by considering an extraction time equal to 240 min [28]. Taking into account the selling price (40 to 80 US$/kg) of a similar product (grape seed oil obtained by cold pressing), the SFE process was considered to be economically viable [28]. Other examples of recent works in which similar cost analyses were performed are summarized in Table 3.1.

The economic feasibility of a SFE product depends on a comparative analysis between COM and the product's selling price [9,28,39]. If the preliminary COM estimated for a certain extract is lower than the market price of a similar product, then there is a very strong indication that the process under investigation can be economically viable. However, defining a selling price may not be a trivial task because SFE extracts are still innovative products. Therefore, in many situations, an equivalent product is not yet available in the market, preventing a selling price from being accurately determined. Moreover, in the natural products market, the prices are directly dependent on the extract quality, which can be evaluated in terms of its chemical composition and functional properties. Then, depending on the composition and properties of the extract, different selling prices are possible. It is well established that, in most cases, SFE extracts tend to possess quality advantages compared to extracts obtained by other techniques, particularly in comparison to extracts produced with low-pressure solvent techniques. This happens because SFE is a green, selective and mild extraction method, resulting in an extract that is enriched in desirable compounds, free of toxic solvents, and without the loss of compounds due to thermal degradation or oxidative reactions [7]. Thus, SFE products may be given higher prices in comparison to extracts obtained using other extraction methods. Prado and Meireles [45] reported that the selling price of clove oil extracted by SFE is 110 US$/kg, whereas the price of clove volatile oil obtained by steam distillation varies between 26 and 86 US$/kg. Generally, when the SFE product is still not available in the market, the selling prices of oils produced by steam distillation or cold pressing may be used as initial references in the cost analyses of oils obtained by SFE [28,39,45].

Table 3.1 Cost of manufacturing (COM) of extracts obtained by Supercritical Fluid Extraction (SFE)

Raw material	Botanic name	Target compounds	T (K)	P (MPa)	t_{EXT} (min)	S/F (kg/kg)	Yield (%)	COM (US$/kg)	Selling price (US$/kg)	Ref.
clove buds	*Eugenia caryolhyllus*	volatile oil	313	15	52	3.65	14.2	31	100	[45]
grape seeds	*Vitis vinifera*	unsaturated fatty acids and antioxidants	313	35	240	6.6	9.9	12	40 – 80	[28]
annatto seeds	*Bixa orellana*	tocotrienols	313	20	105	8.7	2.75	115	NI	[29]
cashew leaves	*Anacardium occidentale*	volatile oil, flavonoids, alkaloids and anti-oxidant compounds	318	20[a]	47	11.5	1	24	NI	[42]
lemon verbena leaves	*Aloysia triphylla*	volatile oil and flavonoids	333	35	180	9.1	1.8	1070	1375	[34]
mango leaves	*Mangifera indica*	variety of bioactive compounds (flavo-noids, alkaloids, terpenes, terpenoids and antioxidant compounds)	323	30	90	4.2	1.8[b]	92	10 – 500	[46]

T: temperature; P: pressure; t_{EXT}: extraction time; S/F: solvent to feed ratio; NI: not informed; Ref.: reference.

[a] SFE was performed using ethanol (5 %) as a cosolvent.

[b] Approximated value (obtained by visual observation of the overall extraction curve).

In some cases, a preliminary cost analysis can indicate that the COM of a SFE extract is too close to or even higher than the market price of a similar product [39,44]. Even so, it is important to bear in mind that certain considerations must be made before disregarding SFE as a viable process [39]. Some of the important factors that should be considered when evaluating the results obtained in a preliminary cost analysis are listed below [39,44,46]:

- *Optimization of the process parameters*: Generally, further and detailed studies of process parameters can result in significant cost reductions. If the extraction rates are increased, then the extraction time and the COM will be reduced [45]. Additionally, the evaluation of different plant configurations and operating modes (by varying the number and arrangement of extractors) may lead to increasing productivity, which can lead to a decrease in the operating costs and COM [3,6].
- *Different selling prices*: The prices of natural products can vary significantly according to the concentration of one or more target compounds. Extracts obtained by SFE are generally recognized as nutraceutical products; as a result, they may possess special uses and distinct prices. Therefore, the amount and availability of specific bioactive compounds should be carefully evaluated to verify the quality of the product and to specify the market price of the extract [39].
- *Scale increase*: Many authors have demonstrated that the COM of a SFE product tends to be reduced when the plant capacity is increased [26,28,34,42,45,46]. Albuquerque and Meireles [26] reported that the COM (SFE extract obtained from annatto seeds) decreased from 125 to 109 US$/kg as the extraction vessels capacities were increased from 0.1 to 0.5 m^3.
- *Advancements in project detailing*: In a preliminary analysis, the COM tends to be overestimated because the worst-case scenarios are normally assumed to avoid cost underestimations. Uncertainties in the process design are diminished as the project advances, allowing more accurate cost calculations to be performed.

It is common knowledge that high-pressure plants are associated with high investment costs. However, the cost of SFE units has decreased in recent years due to competition between suppliers, which has motivated significant technical improvements and cost reductions [44]. Furthermore, it is important to emphasize that the COM is calculated as a sum of five main costs (as previously presented in Eq. 3.26) [39], hence several other cost aspects (not only the investment costs) must be considered to evaluate the economic feasibility of SFE processes. Many recent works have reported that SFE can be an economically viable method for obtaining bioactive extracts [28,29,34,39,45]. Thus, it is clear that a promising business opportunity is available [9] because SFE has shown true potential as a profitable alternative for the production of high quality and high value-added products.

REFERENCES

1. Rostagno MA, Prado JM (eds) (2013) Natural Product Extraction: Principles and Applications. The Royal Society of Chemistry, Cambridge

2. Brunner G (1994) Gas extraction: an introduction to fundamentals of supercritical fluids and the application to separation processes. Steinkopff, Darmstadt

3. Brunner G (2005) Supercritical fluids: technology and application to food processing. Journal of Food Engineering 67 (1–2):21-33. doi:http://dx.doi.org/10.1016/j.jfoodeng.2004.05.060

4. Rosa PTV, Meireles MAA (2009) Fundamentals of supercritical extraction from solid matrices. In: Meireles MAA (ed) Extracting Bioactive Compounds for Food Products: Theory and Application. CRC Press –Taylor & Francis Group, Boca Raton, pp 272-288

5. Martínez J, Silva LPS (2013) Scale-up of Extraction Processes. In: Rostagno MA, Prado JM (eds) Natural Product Extraction: Principles and Applications. The Royal Society of Chemistry, Cambridge, pp 363-398

6. Moraes MN, Zabot GL, Meireles MAA Assembling of a supercritical fluid extraction equipment to operate in continuous mode. In: III Iberoamerican Conference on Supercritical Fluids, Cartagena de Indias, 1-5 April 2013.

7. Pereira CG, Meireles MAA (2010) Supercritical fluid extraction of bioactive compounds: fundamentals, applications and economic perspectives. Food and Bioprocess Technology 3 (3):340-372. doi:http://dx.doi.org/10.1007/s11947-009-0263-2

8. Rodrigues VM, Sousa EMBD, Monteiro AR, Chiavone-Filho O, Marques MOM, Meireles MAA (2002) Determination of the solubility of extracts from vegetable raw material in pressurized CO_2: a pseudo-ternary mixture formed by cellulosic structure+solute+solvent. The Journal of Supercritical Fluids 22 (1):21-36. doi:http://dx.doi.org/10.1016/S0896-8446(01)00108-5

9. Meireles MAA (2008) Extraction of bioactive compounds from Latin American plants. In: Martinez JL (ed) Supercritical fluid extraction of nutraceuticals and bioactive compounds. CRC Press –Taylor & Francis Group, Boca Raton, pp 243-274

10. Ferreira SRS, Meireles MAA (2002) Modeling the supercritical fluid extraction of black pepper (*Piper nigrum* L.) essential oil. Journal of Food Engineering 54 (4):263-269. doi:http://dx.doi.org/10.1016/S0260-8774(01)00212-6

11. Sousa EM, Chiavone-Filho O, Moreno MT, Silva DN, Marques MOM, Meireles MAA (2002) Experimental results for the extraction of essential oil from *Lippia sidoides* Cham. using pressurized carbon dioxide. Brazilian Journal of chemical engineering 19 (2):229-241. doi:http://dx.doi.org/10.1590/S0104-66322002000200003

12. Carvalho Jr RN, Moura LS, Rosa PTV, Meireles MAA (2005) Supercritical fluid extraction from rosemary (*Rosmarinus officinalis*): Kinetic data, extract's global yield, composition, and antioxidant activity. The Journal of Supercritical Fluids 35 (3):197-204. doi:http://dx.doi.org/10.1016/j.supflu.2005.01.009

13. Jesus SP, Calheiros MN, Hense H, Meireles MAA (2013) A Simplified Model to Describe the Kinetic Behavior of Supercritical Fluid Extraction from a Rice Bran Oil Byproduct. Food and Public Health 3 (4):215-222. doi:http://dx.doi.org/10.5923/j.fph.20130304.05

14. Vasconcellos CMC (2007) Extração supercrítica dos óleos voláteis de *Achyrocline satureioides* (Macela) e *Vetiveria zizaioides* (Vetiver): determinação da cinética de extração e estimativa de custos de manufatura. UNICAMP (University of Campinas), Brazil

15. Martínez J (2005) Extração de óleos voláteis e outros compostos com CO_2 supercrítico: desenvolvimento de uma metodologia de aumento de escala a partir da modelagem matemática do processo e avaliação dos extratos obtidos. UNICAMP (University of Campinas), Brazil

16. Martínez J, Rosa PTV, Meireles MAA (2007) Extraction of clove and vetiver oils with supercritical carbon dioxide: modeling and simulation. The Open Chemical Engineering Journal 1 (1):1-7

17. Reverchon E, Marrone C (1997) Supercritical extraction of clove bud essential oil: isolation and mathematical modeling. Chemical Engineering Science 52 (20):3421-3428. doi:http://dx.doi.org/10.1016/S0009-2509(97)00172-3

18. Oliveira ELG, Silvestre AJD, Silva CM (2011) Review of kinetic models for supercritical fluid extraction. Chemical Engineering Research and Design 89 (7):1104-1117. doi:http://dx.doi.org/10.1016/j.cherd.2010.10.025

19. Sovová H (2012) Modeling the supercritical fluid extraction of essential oils from plant materials. Journal of Chromatography A 1250 (0):27-33. doi:http://dx.doi.org/10.1016/j.chroma.2012.05.014

20. Esquível MM, Bernardo-Gil MG, King MB (1999) Mathematical models for supercritical extraction of olive husk oil. The Journal of Supercritical Fluids 16 (1):43-58. doi:http://dx.doi.org/10.1016/S0896-8446(99)00014-5

21. Crank J (1975) The Mathematics of Diffusion. 2 edn. Oxford University Press, Oxford

22. Sovová H (1994) Rate of the vegetable oil extraction with supercritical CO_2—I. Modelling of extraction curves. Chemical Engineering Science 49 (3):409-414. doi:http://dx.doi.org/10.1016/0009-2509(94)87012-8

23. Sovová H (2005) Mathematical model for supercritical fluid extraction of natural products and extraction curve evaluation. The Journal of Supercritical Fluids 33 (1):35-52. doi:http://dx.doi.org/10.1016/j.supflu.2004.03.005

24. Martínez J, Monteiro AR, Rosa PT, Marques MO, Meireles MAA (2003) Multicomponent model to describe extraction of ginger oleoresin with supercritical carbon dioxide. Industrial & engineering chemistry research 42 (5):1057-1063. doi:http://dx.doi.org/10.1021/ie020694f

25. Meireles MAA (2013) Supercritical CO_2 extraction of bioactive components from algae. In: Domínguez H (ed) Functional ingredients from algae for foods and nutraceuticals. Woodhead Publishing, Cambridge, pp 561-584

26. Albuquerque CLC, Meireles MAA (2012) Defatting of annatto seeds using supercritical carbon dioxide as a pretreatment for the production of bixin: Experimental, modeling and economic evaluation of the process. The Journal of Supercritical Fluids 66 (0):86-95. doi:http://dx.doi.org/10.1016/j.supflu.2012.01.004

27. Prado JM (2010) Estudo do aumento de escala do processo de extração supercrítica em leito fixo. UNICAMP (University of Campinas), Brazil

28. Prado JM, Dalmolin I, Carareto NDD, Basso RC, Meirelles AJA, Vladimir Oliveira J, Batista EAC, Meireles MAA (2012) Supercritical fluid extraction of grape seed: Process scale-up, extract chemical composition and economic evaluation. Journal of Food Engineering 109 (2):249-257. doi:http://dx.doi.org/10.1016/j.jfoodeng.2011.10.007

29. Albuquerque CLC (2013) Obtenção de sementes desengorduradas e de óleo rico em tocotrienóis de urucum por extração supercrítica: estudo dos parâmetros de processo, do aumento de escala e da viabilidade econômica. UNICAMP (University of Campinas), Brazil

30. Prado JM, Prado GHC, Meireles MAA (2011) Scale-up study of supercritical fluid extraction process for clove and sugarcane residue. The Journal of Supercritical Fluids 56 (3):231-237. doi:http://dx.doi.org/10.1016/j.supflu.2010.10.036

31. Mezzomo N, Martínez J, Ferreira SRS (2009) Supercritical fluid extraction of peach (*Prunus persica*) almond oil: Kinetics, mathematical modeling and scale-up. The Journal of Supercritical Fluids 51 (1):10-16. doi:http://dx.doi.org/10.1016/j.supflu.2009.07.008

32. Leal PF (2008) Estudo comparativo entre os custos de manufatura e as propriedades funcionais de óleos voláteis obtidos por extração supercrítica e destilação por arraste a vapor. UNICAMP (University of Campinas), Brazil

33. Brunner G (2010) Applications of supercritical fluids. Annual review of chemical and biomolecular engineering 1:321-342. doi:http://dx.doi.org/10.1146/annurev-chembioeng-073009-101311

34. Prado JM, Veggi PC, Meireles MAA (2013) Supercritical fluid extraction of lemon verbena (*Aloysia triphylla*): Process kinetics and scale-up, extract chemical composition and antioxidant activity, and economic evaluation. Separation Science and Technology 49 (4):569-579. doi:http://dx.doi.org/10.1080/01496395.2013.862278

35. del Valle JM, Rivera O, Mattea M, Ruetsch L, Daghero J, Flores A (2004) Supercritical CO_2 processing of pretreated rosehip seeds: effect of process scale on oil extraction kinetics. The Journal of Supercritical Fluids 31 (2):159-174. doi:http://dx.doi.org/10.1016/j.supflu.2003.11.005

36. Clavier J-Y, Perrut M (2004) Scale-up issues for supercritical fluid processing in compliance with GMP. In: York P, Kompella UB, Shekunov BY (eds) Supercritical Fluid Technology for Drug Product Development. Marcel Dekker Inc., New York, pp 565-601

37. Aguiar AC, Visentainer JV, Martínez J (2012) Extraction from striped weakfish (*Cynoscion striatus*) wastes with pressurized CO_2: Global yield, composition, kinetics and cost estimation. The Journal of Supercritical Fluids 71 (0):1-10. doi:http://dx.doi.org/10.1016/j.supflu.2012.07.005

38. Prasad NK (2012) Downstream Process Technology: A New Horizon In Biotechnology. PHI Learning Private Limited, New Delhi

39. Rosa PTV, Meireles MAA (2005) Rapid estimation of the manufacturing cost of extracts obtained by supercritical fluid extraction. Journal of Food Engineering 67 (1–2):235-240. doi:http://dx.doi.org/10.1016/j.jfoodeng.2004.05.064

40. Meireles MAA (2003) Supercritical extraction from solid: process design data (2001–2003). Current Opinion in Solid State and Materials Science 7 (4–5):321-330. doi:http://dx.doi.org/10.1016/j.cossms.2003.10.008

41. Turton R, Ballie RC, Whiting WB, Shaeiwitz JA (1998) Analysis, synthesis, and design of chemical process. Prentice Hall PTR, Upper Saddle River

42. Leitão NCMCS, Prado GHC, Veggi PC, Meireles MAA, Pereira CG (2013) *Anacardium occidentale* L. leaves extraction via SFE: Global yields, extraction kinetics, mathematical modeling and economic evaluation. The Journal of Supercritical Fluids 78 (0):114-123. doi:http://dx.doi.org/10.1016/j.supflu.2013.03.024

43. Prado IM, Albuquerque CLC, Cavalcanti RN, Meireles MAA Use of a commercial process simulator to estimate the cost of manufacturing (COM) of carotenoids obtained via supercritical technology from palm and buriti trees. In: 9th International Symposium on Supercritical Fluids, Arcachon, 18-20 May 2009.

44. Prado JM, Assis AR, Maróstica-Júnior MR, Meireles MAA (2010) Manufacturing cost of supercritical-extracted oils and carotenoids from amazonian plants. Journal of Food Process Engineering 33 (2):348-369. doi:http://dx.doi.org/10.1111/j.1745-4530.2008.00279.x
45. Prado JM, Meireles MAA Estimation of manufacturing cost of clove (*Eugenia caryophyllus*) extracts obtained by supercritical fluid extraction using a commercial simulator. In: 11th International Congress on Engineering and Food, Atenas, 22-26 May 2011.
46. Prado IM, Prado GHC, Prado JM, Meireles MAA (2013) Supercritical CO_2 and low-pressure solvent extraction of mango (*Mangifera indica*) leaves: Global yield, extraction kinetics, chemical composition and cost of manufacturing. Food and Bioproducts Processing 91 (4):656-664. doi:http://dx.doi.org/10.1016/j.fbp.2013.05.007

CAPÍTULO 3 – A SIMPLIFIED MODEL TO DESCRIBE THE KINETIC BEHAVIOR OF SUPERCRITICAL FLUID EXTRACTION FROM A RICE BRAN OIL BYPRODUCT

Susana P. Jesus, Maurício N. Calheiros, Haiko Hense and M. Angela A. Meireles

Artigo publicado no periódico *Food and Public Health,* v. 3, n. 4, p. 215-222, 2013.

e-ISSN: 2162-8440 | DOI: 10.5923/j.fph.20130304.05

Food and Public Health 2013, 3(4): 215-222
DOI: 10.5923/j.fph.20130304.05

A Simplified Model to Describe the Kinetic Behavior of Supercritical Fluid Extraction from a Rice Bran Oil Byproduct

Susana P. Jesus[1], Maurício N. Calheiros[2], Haiko Hense[2], M. Angela A. Meireles[1,*]

[1]LASEFI/DEA (Department of Food Engineering), FEA (School of Food Engineering), UNICAMP (University of Campinas), Campinas, 13083-862, Brazil
[2] LATESC/EQA (Chemical and Food Engineering Department), UFSC (Federal University of Santa Catarina), Florianópolis, 88040-900, Brazil

Abstract The mathematical modeling of the overall extraction curve (OEC) was performed using experimental data of supercritical fluid extraction (SFE) from a byproduct of the rice bran oil (RBO) industry. The soapstock derived from the RBO deacidification process was used as raw material because it contains a significant amount of γ-oryzanol, which is a valuable natural antioxidant. The main goal of this work was to describe the OEC by a simplified model using the kinetic data obtained for the SFE from rice bran oil soapstock (RBOS). The global yield isotherms (GYI) were used to select the best operational conditions (temperature and pressure) based on the extraction yield and the γ-oryzanol content of the obtained extract. The OEC was fitted to four simplified models and the kinetic parameters which characterize the constant extraction rate (CER) were estimated. The highest values for the extraction yield (12.5 %, w/w), the γ-oryzanol content (16 %, w/w), and the γ-oryzanol recovery rate (55 %, w/w) were found at 30 MPa/333K. The proposed spline model presented the best fit to experimental data and quantitatively described the OEC. The estimated time span of the CER period (t_{CER}) was 70 min and the corresponding solvent to feed (S/F) ratio and extraction yield were 23 and 9.4 %, respectively.

Keywords Overall Extraction Curve, Supercritical Carbon Dioxide, Spline Model, Rice Bran Oil Soapstock, Oryzanol

1. Introduction

Supercritical fluid extraction (SFE) is a versatile and environmentally friendly alternative to conventional extraction processes. Carbon dioxide (CO_2) is the most used supercritical fluid because it has low critical temperature (304.2 K), mild critical pressure (7.38 MPa), and important characteristics such as non-toxic, non-flammable, non-expensive, and readily available at good purity[1]. Some other well noticed advantages of the SFE are the easily solvent elimination, solvent recycling possibility, low energy consumption, adjustable solvent selectivity, and prevention of oxidation reactions[2, 3].

The investigation of the SFE process requires two types of experiments: the global yield isotherms (GYI), and the overall extraction curve (OEC). The GYI are performed in different conditions of temperature (T) and pressure (P) because both parameters are directly related to the adjustable selectivity of supercritical CO_2. Therefore the GYI can be used to select the operational conditions of T and P based on the extraction yield and the chemical composition of the obtained extract[4]. After this selection the OEC must be determined because it brings information about the kinetic behaviorof the SFE process. A typical OEC presents three different regions[4 – 6]: (i) a constant extraction rate (CER) period where the solute contained at the surface of the particles is removed by convection; (ii) a falling extraction rate (FER) period where convection in the fluid phase and diffusion in the solid phase are both important mechanisms; (iii) a diffusion-controlled (DC) period in which the mass transfer is controlled only by the diffusion mechanism.

The mathematical modeling of the OEC allows the determination of the time of extraction (cycle time), which is important for an optimal utilization of the industrial scale plant[7]. In order to achieve this, mathematical models must be evaluated with respect to their applicability in terms of process design. Many mathematical models have been developed to describe the OEC, from simple equations to very complex ones. Meireles[5] presented a simplified model in which the OEC was described by a family of two or three straight lines, where the first line represented the CER period. According to Pereira and Meireles[8] 50 – 90% (w/w) of the total amount of extract can be obtained at the end of

* Corresponding author:
meireles@fea.unicamp.br (M. Angela A. Meireles)
Published online at http://journal.sapub.org/fph

the CER period, what makes this step the most important one in terms of process design. Therefore, for many industrial applications, the extraction process ends shortly after the CER period because the best operational conditions will be those in which a high amount of extract is obtained in a relatively short process time[8]. The previous affirmation justifies why it is usual and important to determine some kinetic parameters which characterize the CER region of the OEC.

Researchers and consumers' interest in the rice bran oil (RBO) have been increasing due to its great potential as a nutraceutical food. The RBO health benefits are usually associated with natural antioxidant components such as tocopherols, tocotrienols and γ-oryzanol[9, 10]. Attention is usually focused on γ-oryzanol (a group of ferulic acid esters of sterols and triterpene alcohols) since it has a powerful antioxidant action[11]. Improvement of the plasma lipid pattern, hypocholesterolemic activity, and treatment of inflammatory processes are some of the health-promoting effects attributed to γ-oryzanol[10, 12]. The antioxidant action has also been associated with the prevention of some cancers[13, 14].

In traditional chemical refining the deacidification is a process step in which the free fat acids are neutralized by addition of an alkali reagent, resulting in neutral oil plus soapstock as a byproduct. The γ-oryzanol content in the crude RBO varies in the range of 1.5 – 2.9 % (w/w)[15]. During deacidification step, however, there is a significant decrease (up to 90 %) in the RBO γ-oryzanol content because it is transferred to the rice bran oil soapstock (RBOS)[10, 16].

According to Paucar-Menacho et al.[15] the typical RBOS contains 1.2 – 3.6 % (w/w, dry basis) of γ-oryzanol. The RBOS has been mostly used to produce soap by detergent industries. Nevertheless, this byproduct has a remarkable potential of being financially profitable since it could be used as a raw material for γ-oryzanol recovering processes[17]. The valuable antioxidant activity presented by γ-oryzanol makes it an interesting substance for wide application by food, cosmetic, and pharmaceutical industries.

Research works reporting the SFE from rice bran using supercritical CO_2 as solvent have already been published, including comparisons between SFE and conventional hexane extraction as well as investigations to optimize the γ-oryzanol content in extracted oil[18 – 21]. There are also reports about the application of conventional extraction techniques for recovering the γ-oryzanol available in the RBOS[22, 23]. However, as far as we know, there are yet no reports about the use of the RBOS as raw material for the supercritical CO_2 extraction. The main goal of this work was to investigate the mathematical modeling of the OEC applying simplified models, as well as the determination of the kinetic parameters from the CER period. For that, we used experimental new data about the SFE using the RBOS as raw material. The GYI were evaluated in order to select the operational conditions (T and P) which maximize the γ-oryzanol recovery in the obtained extracts.

2. Materials and Methods

The experimental assays were performed in the Laboratory of Thermodynamics and Supercritical Technology (LATESC, EQA, UFSC, Florianópolis, Brazil). The details about the applied experimental methodology have been described in the sections 2.1 to 2.4.

2.1. Characterization of the Raw Material

The raw material was a RBOS obtained from IRGOVEL Ltd. (Pelotas, RS, Brazil). The RBOS initial moisture content was determined gravimetrically using a drying oven at 378 K[24]. The γ-oryzanol content (OC) was quantified by high-performance liquid chromatography with UV detection (HPLC-UV), as detailed in section 2.4.

2.2. Pretreatment of the Raw Material

The RBOS pretreatment included three sequential steps: saponification, drying, and crushing. The first step was a saponification reaction, which was based on the methodology proposed by Rao and co-workers[25]. The RBOS saponification was carried out using sodium hydroxide (NaOH) at controlled temperature (363 K) and constant stirring over a period of 1 hour. The proportion of reagents was 1:20 relating NaOH amount to RBOS dried matter content. The excess alkali was neutralized by sodium bicarbonate addition in order to adjust the pH between 9 and 10, which is the optimum pH range for γ-oryzanol extraction from the RBOS[26].

The resultant soap was allowed to air-dry for 2 hours at room temperature. Then the soap was dried in an oven at 388 K for 4 hours. The dried soap was crushed and particles were fractionated in a vibratory sieve shaker (Bertel Metallurgic Ind. Ltd., SP, Brazil). The obtained solid particles were used as the feed material for the SFE experiments.

2.3. Supercritical Fluid Extraction

The SFE equipment was a dynamic extraction unit developed by Zetzl and co-workers[27] at the TechnischeUniversität Hamburg-Harburg (Germany). The details about the unit design as well as the experimental procedures have already been well described in previous works[28, 29]. The extraction solvent was CO_2 99.9 % pure delivered at pressure up to 6 MPa (White Martins, Brazil). The extract was collected in the separator which was an amber glass vial immersed in an ice bath at ambient pressure.

In the GYI assays the operational conditions of pressure and temperature varied according to a 3^2 factorial design. The levels were: 10, 20, and 30 MPa and 303, 318, and 333 K. The mass of feed material (F), the total extraction time, the CO_2 flow rate (Q_{CO2}), and the solvent to feed (S/F) ratio were: 30 g, 240 min, 1.67×10^{-4} kg/s, and S/F=80, respectively. The assays were all performed in duplicates. In the kinetic experiments the extracted mass was collected and quantified in predetermined time intervals and the accumulated mass of extract was plotted as a function of the extraction time (t) to generate the OEC. The kinetic assays were performed using the following operational conditions: F = 30 g, Q_{CO2} = 1.67×10^{-4} kg/s, P = 30 MPa, and T = 333 K.

2.4. Determination of the γ-Oryzanol Content

The γ-oryzanol quantification was performed by HPLC/UV according to Scavariello[30]. The analysis system was composed by: isocratic pump (Perkin Elmer Series 200); ultraviolet (UV)/visible detector (Perkin Elmer LC 290); column (Thermo Electron Corporation LICHROSORB RP 18; 4.6 × 250 mm, 5 mm coupled to a C18-5 pre-column). The UV detector was set at 315 nm and the mobile phase was composed by acetonitrile/methanol/isopropanol (50:45:5 by vol.) at a flow rate of 1.0 mL/min. The samples were diluted in hexane and a volume of 20 μL was injected into the system.

2.5. Calculation of the Extraction Yield and the γ-Oryzanol Recovery Rate

The extraction yield ($X_{0,S/F}$) of the GYI assays (S/F = 80) was calculated by the ratio between the mass of extracted matter and the mass of feed material (wet basis) used to fill the extraction cell. The γ-oryzanol recovery rate (ORR) was obtained by the ratio between the mass of γ-oryzanol in the extract and the mass of γ-oryzanol originally present in the raw material (RBOS) which was treated to produce the SFE feed material (according to the pretreatment described in section 2.2). Thus the ORR was calculated by Equation 1 using experimental data obtained for: $X_{0,S/F}$ (%, w/w), γ-oryzanol content in the extract (OC_{EXT}) (%, w/w), γ-oryzanol content in the RBOS (OC_{RBOS}) (%, w/w), and pretreatment yield (Y_{PT}) (w/w). The pretreatment yield was defined as the ratio between the final mass of solid particles and the initial mass of crude raw material.

$$\mathrm{ORR}\ (\%) = \left(\frac{OC_{EXT}\, X_{0,S/F}\, Y_{PT}}{OC_{RBOS}}\right) \tag{1}$$

2.6. Mathematical Modeling

The extraction curve was obtained by plotting the accumulated mass of extract (or extraction yield) versus the extraction time. The OEC mathematical modeling was evaluated using the following models: empirical model presented by Esquível et al.[31], diffusion model of Crank[32], logistic model presented by Martínez et al.[33], and spline model described by Meireles[5].

The empirical, diffusion and logistic models were fitted to experimental data using the software Mass Transfer (LATESC/EQA/UFSC, Florianópolis, Brazil)[34]. This software was developed in Delphi 7.0 using the maximum likelihood method to minimize the sum of the squares of the residues. The spline modeling was performed by fitting the experimental OEC to a spline containing three straight lines using the procedures PROC REG and PROC NLIN of the SAS software package (version 9.0, SAS Institute Inc., Cary, USA).

The adjustable parameters as well as the equations used in the mathematical modeling are detailed in Table 1.

Table 1. Description of the equations used in the mathematical modeling of the overall extraction curve (OEC)

Model	Equation
Empirical [31]	$m_{EXT} = x_0 F\left(\frac{t}{C_1 + t}\right)$
Diffusion [32]	$m_{EXT} = x_0 F\left[1 - \frac{6}{\pi^2}\sum_{n=1}^{\infty}\frac{1}{n^2}\exp\left(\frac{-n^2\pi^2 D_1 t}{r^2}\right)\right]$
Logistic [33]	$m_{EXT} = \frac{x_0 F}{\exp(C_2 t_m)}\left\{\frac{1+\exp(C_2 t_m)}{1+\exp[C_2(t_m - t)]} - 1\right\}$
Spline [5]	* when $t \le t_{CER}$: $m_{EXT} = b_0 + b_1 t$ * when $t_{CER} < t \le t_{FER}$: $m_{EXT} = b_0 + b_1 t + b_2(t - t_{CER})$ * when $t > t_{FER}$: $m_{EXT} = b_0 + b_1 t + b_2(t - t_{CER}) + b_3(t - t_{FER})$

Nomenclature:
m_{EXT} = mass of extract (g);
F = mass of feed material (g);
x_0 = initial mass ratio of extractable solute in the solid substratum (g/g);
t = time of extraction (min);
C_1 = adjustable parameter of the empiric model: no physical meaning (min);
n = integer number;
D_1 = adjustable parameter of the diffusion model: diffusion coefficient of the solute within the solid substratum (m^2/min);
r = the radius of the sphere particle (m);
C_2 = adjustable parameter of the logistic model: no physical meaning (min^{-1});
t_m = adjustable parameter of the logistic model: instant in which the extraction rate reaches its maximum value (min);
t_{CER} = time span of the CER period (min);
t_{FER} = end of the FER period (min);
b_0 = linear coefficient (zero-order term) of the CER straight line (g);
b_1, b_2 e b_3 = slope coefficients (first-order terms) of the CER, FER, and DC straight lines, respectively (g/min).

2.7. Estimation of the Kinetic Parameters

The experimental OEC was described by a family of three straight lines using a nonlinear fitting performed in the software SAS (as described in the section 2.6). The fitted lines were associated with three different mass transfer mechanisms following the classic descriptions of the CER, FER and DC periods[6]. Thus the first, second, and third lines were respectively identified as the CER, FER, and DC regions. From the spline model the following parameters for the CER period were estimated: the time span of the CER period (t_{CER}), the extraction rate for the CER period (M_{CER}), the mass ratio of extract in the supercritical phase at the bed outlet (Y_{CER}), the extraction yield of the CER period (R_{CER}), and the solvent to feed mass ratio of the CER period (S/F_{CER}). The t_{CER} and M_{CER} (kg extract/s) are both adjustable parameters from the spline model (t_{CER} and b_1, respectively, according to Table 1). The Y_{CER} (kg extract/kg CO_2) was obtained by dividing M_{CER} by the mean solvent flow rate (Q_{CO2}, kg CO_2/s). The parameters R_{CER} (%, kg extract/kg feed material) and S/F_{CER} (kg CO_2/kg feed material) were calculated using modeled data (m_{EXT}) from spline model.

2.8. Statistical Analysis

The statistical analysis of the experimental data was performed through a one-way Analysis of Variance (ANOVA) and Tukey test using the software STATISTICA for Windows (version 7.0, Statsoft Inc., USA). A calculated p-value< 0.05 was considered to be statistically significant.

3. Results and Discussion

3.1. Characterization of the Raw Material

The RBOS characterization analyses resulted in a moisture content of 45 ± 1 % (w/w) and a γ-oryzanol content of 2.7 ± 0.1 % (w/w, dry basis). The determined RBOS moisture content is lower than the ones reported by Narayan et al.[17] (65 – 70 %, w/w) and by Kaewboonnum et al.[22] (57 %, w/w). Such differences in the moisture content are understandable since the RBOS composition depends on operational parameters of the RBO refining process, which usually differ from one industry to another. Some variations in the deacidification step, such as centrifugation time and amount of water and alkali added in the process, as well as rice bran initial composition, have direct influence on the RBOS composition. The obtained γ-oryzanol content (2.7 ± 0.1 %, w/w, dry basis) is in accordance with the range (1.2 – 3.6 %, w/w, dry basis) reported by Paucar-Menacho et al.[15].

3.2. Pretreatment of the Raw Material

Figure 1. Raw material pretreatment: (a) crude rice bran oil soapstock (RBOS); (b) RBOS after saponification and drying steps

The RBOS received from the RBO industry was the crude raw material (Figure 1a) which was pretreated in order to obtain the feed material used in the SFE. The pretreatment was conducted in three steps: saponification, drying, and crushing. The material presented in Figure 1b was the RBOS after the saponification reaction and the drying process. This material was then crushed and the obtained solid particles were fed into the fixed extraction bed.

The solid particles moisture content was less than 3 % (w/w) and the mean particle diameter was 2.4×10^{-4} m. The pretreatment yield (as previously defined in section 2.5) was equal to 0.41 g of solid particles/g of RBOS.

3.3. Extraction Yield, γ-Oryzanol Content, and γ-Oryzanol Recovery Rate

The interactions between the solvent and the various solutes present in the solid substratum are fundamental to understand the SFE process. However, the solid substratum is a complex multicomponent system and very little information is known about these interactions. The extension of these interactions can be measured through the determination of the solubility of the system (solid substratum + CO_2) or through the results of the GYI experiments[35].

The results of the GYI assays are presented (Table 2) in terms of extraction yield, γ-oryzanol content and γ-oryzanol recovery rate. Taking into account an isothermal condition a rising operational pressure resulted in the increase of both the extraction yield and the γ-oryzanol content. This effect can be attributed to the increase in CO_2 density and therefore the enhancement in the solvation power.

Table 2. Results of the global yield isotherms (GYI) assays: extraction yield ($X_{0,S/F}$), γ-oryzanol content (OC) and γ-oryzanol recovery rate (ORR)

P (MPa)	T (K)	ρCO_2 (I) (kg/m^3)	$X_{0,S/F}$ (%, w/w) (II)	OC (%, w/w)	ORR (%, w/w)
10	303	773	$6.1^{a} \pm 0.3$	0.5	0.8
10	318	503	$2.2^{b} \pm 0.2$	0.3	0.2
10	333	291	$0.22^{c} \pm 0.04$	0.03	0.0
20	303	891	$10.4^{d,e} \pm 0.2$	3.4	10
20	318	814	$9.7^{d} \pm 0.1$	2.8	7.4
20	333	725	$5.3^{a} \pm 0.1$	2.4	3.5
30	303	949	$10.6^{d,e} \pm 0.9$	11.8	34
30	318	891	$11.1^{e} \pm 0.4$	13.5	41
30	333	830	$12.5^{f} \pm 0.5$	16.0	55

(I) Carbon dioxide density[36]
(II) Equal letters indicate no statistically significant difference

The effect of the process temperature in the SFE is typically more complex[37, 38] and can be better understood through the analysis of the GYI presented in Figure 2, where a crossover point (near 27 MPa) can be clearly observed. At 10 and 20 MPa the rising temperature produced a decrease in the extraction yields as well as in the γ-oryzanol content of the obtained extracts. This effect is associated with the significant reduction in the solvent density and therefore it is possible to conclude that below crossover pressure the density effect was the dominant mechanism in the SFE process. At 30 MPa, on the other hand, an increase in the process temperature resulted in the enhancement ofthe extraction yield and the γ-oryzanol content. This behavior can be explained because in the highest pressure the CO_2 density changed slightly with temperature, and as a consequence the solute vapor pressure was the dominant mechanism affecting the extraction process.

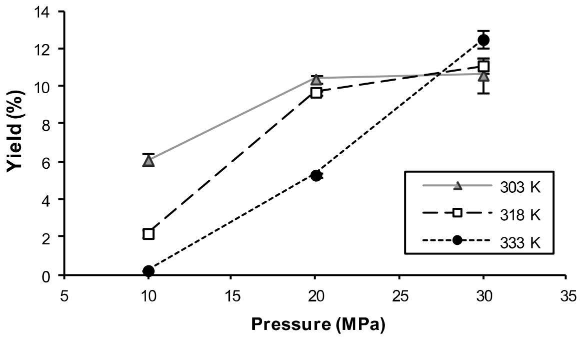

Figure 2. Global yield isotherms (303, 318, and 333 K) obtained in the SFE process (*the experimental points are connected to evidence the isotherms crossover*)

Analogous pressure and temperature effects in the GYI results, as well as the presence of a crossover region, have already been noticed by many authors studying a wide range of raw materials[4, 29, 35, 38 – 39]. It is actually well established in the specific literature that both pressure and temperature are key variables in the SFE process.

The highest OC and ORR values were found at 30 MPa/333 K. The maximum OC (16 %, w/w) obtained in this work was lower than the ones reported by Kumar and co-workers[23] for conventional extraction using various organic solvents. These authors studied the recovery of γ-oryzanol from RBOS through Soxhlet extraction and found a maximum OC (25 %, w/w) when using ethyl acetate as solvent. Higher values for the OC (up to 90 %, w/w) can be obtained when the extract is further purified to achieve higher γ-oryzanol purity. Processes for γ-oryzanol purification usually involve sequential steps including fractional precipitation, crystallization, and/or separation by chromatographic column[22, 25].

The maximum ORR (55 %, w/w) is higher than the value (31 %, w/w) reported by Jesus et al.[40] in a previous work in which a different RBO byproduct was used as feed material for the SFE process. The obtained ORR could not be appropriately compared with some results from other works because it seems that each author calculates the γ-oryzanol recovery based on specific considerations which are usually different from one research group to another. In the present work we defined the ORR by Equation 1, however this kind of information was not found in other authors' works and therefore no additional comparisons were possible.

3.4. Mathematical Modeling and Kinetic Parameters

The experimental and modeled curves are illustrated in Figure 3. The adjustable parameters and the mean square error (MSE) calculated for the applied models are presented in Table 3.

The analysis of the lowest MSE values, as well as the visual observation of Figure 3, indicated that both the spline[5] and logistic[33] models could quantitatively describe the OEC. The distribution of the residuals (Figure 4) confirmed the good fits presented by spline and logistic models.

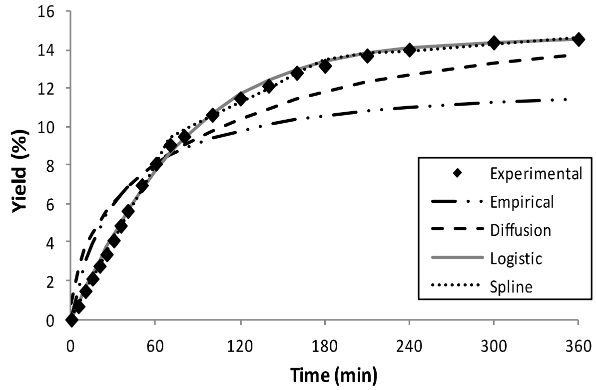

Figure 3. Experimental data (30 MPa/333 K) and modeled extraction curves obtained by empirical[31], diffusion[32], logistic[33], and spline[5] models

The empirical[31] and diffusion[32] models did not present good agreements with experimental data and so could not be used to describe quantitatively the OEC. This performance was already expected taking into account the specific characteristics of these models. Therefore both were applied in this work only for comparison purposes. The empirical model is described by a very simple equation (Table 1) which has just one adjustable parameter and no physical meaning. The diffusion model has some relation with the mass transfer phenomenon but it considers only the diffusion mechanism since the mass balance is applied to the solid phase while fluid phase is neglected. The observation of the experimental curve shape already indicated that the diffusion model would not be adequate since the convective mechanism should not be neglected in the extraction process.

Table 3. Mathematical modeling of the overall extraction curve and kinetic parameters of the constant extraction rate (CER) period

Model	Adjustable parameter(I)	MSE(II)
Empirical[31]	C_1 = 32.8 min	0.332
Diffusion[32]	D_1 = 9.49 x 10^{-12} (m^2/min)	0.192
Logistic[33]	C_2 = 0.0159 (min^{-1}) t_m = – 54.6 (min)	0.004
Spline[5]	b_0 (g) = 0.0386 b_1 (g/min) = 0.0398 b_2 (g/min) = – 0.0288 b_3 (g/min) = – 0.0092 t_{CER} (min) = 70 t_{FER} (min) = 186	0.002
Kinetic parameter		Estimated value
$M_{CER} \times 10^7$ (kg extract/s)		6.63
$Y_{CER} \times 10^3$ (kg extract/kg CO_2)		3.98
R_{CER} (%, kg extract/kg feed)		9.4
$[S/F]_{CER}$ (kg CO_2/kg feed)		23

(I) The description of the adjustable parameters is presented in Table 1
(II) Mean Square Error (MSE)

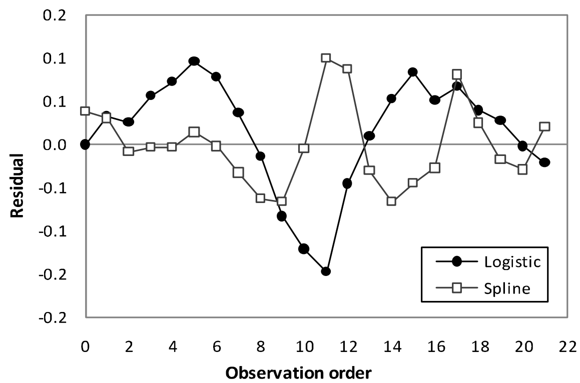

Figure 4. The distribution of the residuals obtained from mathematical modeling using logistic[33] and spline[5] models

According to Martínez et al.[33] the logistic model was developed from the differential mass balance applied inside the extraction bed for solid and fluid phases. The particularity of the logistic model was the definition of the interfacial mass-transfer term, which was described by one of the solutions from the logistic equation. The logistic model has two adjustable parameters named here (Table 1) as C_2 and t_m. No physical meaning was attributed to the first one (C_2), while the second one (t_m) was described as the time in which the extraction rate reaches its maximum value[33]. However, when applying this model to usual OEC shapes, many authors[3, 38 – 40] have obtained negative values for t_m and therefore no physical meaning could be associated to this parameter. Although logistic model provided a good quantitative description of the OEC, the absence of physical meaning turned it into an empirical model. Therefore the logistic model adjustable parameters would not be applicable in terms of process design and scale up.

The spline model presented the lowest MSE value and described very well the OEC quantitative behavior. Besides that, yet being a very simple model in terms of mathematical complexity, the spline model could also be related to the mass transfer phenomena since the experimental and modeled curves showed the distinctive three regions: CER, FER, and DC. The description of the CER period by a straight line was used to estimate the kinetic parameters which are presented in Table 3. The R_{CER} value represented 64 % of the total extraction yield (14.7 %) obtained at the end of the OEC. This is in accordance with the range (50 – 90 %) mentioned by Pereira and Meireles[8] when justifying the relevance of the CER period.

The values of t_{CER} and R_{CER} roughly represent the minimum time a SFE cycle should last and the minimum extraction yield expected at a given process condition (T, P, Q_{CO2}, and solid substratum pretreatment)[5]. The parameters t_{CER}, $(S/F)_{CER}$, and R_{CER} can be used in preliminary studies of the process design by applying the scale up criterion proposed by Prado and co-workers[41 – 42]. This criterion basically consists in maintaining constant the solvent to feed (S/F) ratio and also the process time which was necessary to achieve the respective S/F value. After the scale-up prediction is done the economical viability of the process can be investigated by making the estimation of the cost of manufacturing (COM) as described by Rosa and Meireles[43].

According to Leal[44], the intersection between the lines CER and DC defines an additional parameter of time, which is named as t_{CER2}. This parameter can also be used as a good estimation of the process time for preliminary studies about the COM prediction[4]. The calculated value of the parameter t_{CER2} was 98 min, and the mass of extract obtained at this point was 71 % of the total mass recovered at the final time of extraction. Both the parameters t_{CER} and t_{CER2} can be used as an initial estimative of the cycle time when performing exploratory investigations about the economical viability of the SFE process.

The specific literature about the SFE presents several more complex mathematical models to describe the OEC. The more accurate models can provide a more reliable description of the mass transfer phenomena in the fixed bed extractor. However, the application of these models also requires some additional data which not always are available to the investigated system. One example is the model described by Sovová[6], which requires information about the true density of the solid particles and also about the solubility of the pseudo-binary system formed by extract (a multicomponent mixture of solutes) + CO_2. The data about solubility is not always available and the experimental determination is not an easy or quick procedure. Therefore, when considering the above mentioned scenario, it is possible to say that one advantage of the spline model is that only the kinetic data of the SFE is enough to perform the mathematical modeling of the OEC.

4. Conclusions

The high γ-oryzanol content (2.7 %, w/w, dry basis) detected in the RBOS confirmed its potential as a raw material for γ-oryzanol recovering processes. The analysis of the GYI results (Table 2) indicated that the best operational condition was found at 30 MPa/333 K. The spline model presented the best fit to the OEC and the values calculated for the parameters t_{CER} and t_{FER} were, respectively, 70 and 186 min. At the end of the CER and FER periods the extracted mass was 64 % and 93 % of the total mass obtained at the final time of extraction.The spline model presents a very low mathematical complexity, and despite that can describe very well the OEC when only kinetic data about the investigated system are readily available.

ACKNOWLEDGEMENTS

The authors thank CNPq (477986/2007-2) for the financial support of the experimental work and IRGOVEL Ltd. (Pelotas, RS, Brazil) for the donation of the raw material. Susana P. Jesus thanks CNPq (141828/2010-2) for the doctorate fellowship.

REFERENCES

[1] Paulo T.V. Rosa, M.Angela A. Meireles, "Fundamentals of supercritical extraction from solid matrices", pp. 272-288, in: M.A.A.Meireles (Ed.), "Extracting Bioactive Compounds for Food Products: Theory and Application", CRC Press – Taylor &Francis Group, USA, 2009.

[2] Leandro Danielski,CarstenZetzl, HaikoHense,Gerd Brunner, "A process line for the production of raffinated rice oil from rice bran", Elsevier, The Journal of Supercritical Fluids, vol. 34, pp. 133-141, 2005.

[3] NatáliaMezzomo, Julian Martínez,Sandra R. S. Ferreira, "Supercritical fluid extraction of peach (*Prunuspersica*) almond oil: kinetics, mathematical modeling and scale-up", Elsevier, The Journal of Supercritical Fluids, vol. 51, pp. 10-16, 2009.

[4] Carolina L. C. Albuquerque, M. Angela. A. Meireles, "Defatting of annatto seeds using supercritical carbon dioxide as a pretreatment for the production of bixin: Experimental, modeling and economic evaluation of the process", Elsevier, The Journal of Supercritical Fluids, vol.66, pp. 86-94, 2012.

[5] M. Angela. A. Meireles,"Extraction of bioactive compounds from Latin American plants", pp. 243-274, in: J. Martinez (Ed.) "Supercritical Fluid Extraction of Nutraceuticals and Bioactive Compounds", CRC Press – Taylor & Francis Group, USA, 2008.

[6] Helena Sovová,"Rate of the vegetable oil extraction with supercritical CO_2 – I.Modeling of extraction curves."Elsevier, Chemical Engineering Science, vol. 49, no. 3, pp. 409-414, 1994.

[7] Gerd Brunner, "Gas extraction: an introduction to fundament als of supercritical fluid and the applications to separation processes", 1st ed., Steinkopff, Germany, 1994.

[8] Camila G. Pereira, M. Angela A Meireles, "Supercritical Fluid Extraction of Bioactive Compounds: Fundamentals, Applications and Economic Perspectives". Springer, Food and Bioprocess Technology,vol. 3, pp. 340-372, 2010.

[9] F. T. Orthoefer, "Rice bran oil: healthy lipid source", IFT, Food Technology, vol. 50, pp. 62-64, 1996.

[10] Christianne E. C. Rodrigues, Márcia M. Onoyama, Antonio J. A. Meirelles,"Optimization of the rice bran oil deacidification process by liquid–liquid extraction", Elsevier, Journal of Food Engineering, vol. 73, pp. 370–378, 2006.

[11] Remo Bucci, Andrea D. Magrì, Antonio L. Magrì, Federico Marini,"Comparison of three spectrophotometric methods for the determination of γ-oryzanol in rice bran oil",Springer, Analytical and Bioanalytical Chemistry, vol. 375, pp. 1254-1259, 2003.

[12] Claudia Juliano, Massimo Cossu, Maria C. Alamanni, LuisellaPiu, "Antioxidant activity of gamma-oryzanol: mechanism of action and its effect on oxidative stability of pharmaceutical oils", Elsevier, International Journal of Pharmaceutics, vol. 299, pp. 146-154, 2005.

[13] Carrie K. L. Kong, W. S. Lam, Lawrence C. M. Chiu, Vincent E. C.Ooi, Samuel S. M. Sun, Yum-Shing Wong, "A rice bran polyphenol, cycloartenylferulate, elicits apoptosis in human colorectal adenocarcinoma SW480 and sensitizes metastatic SW620 cells to TRAIL-induced apoptosis", Elsevier, Biochemical Pharmacology, vol. 77, no. 9, pp. 1487-1496, 2009.

[14] V. Van Hoed, G. Depaemelaere, J. Vila Ayala, P. Santiwattana, R. Verhé, W. De Greyt,"Influence of chemical refining on the major and minor components of rice bran oil", AOCS Press, Journal of the American Oil Chemists Society, vol. 83, no. 4, pp. 315-321, 2006.

[15] Luz M. Paucar-Menacho, Leomar H. Silva, Anderson S. Sant'ana, Lireny A. G. Gonçalves,"Refiningofricebranoil (*Oryza sativa* L.) to preserve γ-oryzanol",SBCTA, Ciência e Tecnologia de Alimentos, vol. 27, 45-53, 2007.

[16] L. Rajam, D. R. Soban Kumar, A. Sundaresan, C. Arumughan,"A novel process for physically refining rice bran oil through simultaneous degumming and dewaxing", Springer, Journal of the American Oil Chemists' Society, vol. 82, no. 3, pp.213-220, 2005.

[17] A. V. Narayan, R. S. Barhate, and K. S. M. S. Raghavarao, "Extraction and purification of oryzanol from rice bran oil and rice bran oil soapstock",Springer, Journal of the American Oil Chemists' Society, vol. 83, no.8, pp. 663-670, 2006.

[18] C. Balachandran, P. N. Mayamol, Shiny Thomas, DivyaSukumar, A. Sundaresan, "An ecofriendly approach to process rice bran for high quality rice bran oil using supercritical carbon dioxide for nutraceutical applications", Elsevier, Bioresource Technology, vol. 99, pp. 2905-2912, 2008.

[19] M.S. Kuk, M.K. Dowd,"Supercritical CO_2 extraction of rice bran", Springer, Journal of the American Oil Chemists' Society, vol. 75, no. 5, pp. 623–628, 1998.

[20] Giuseppe Perretti, Enrico Miniati, Luigi Montanari, Paolo Fantozzi,"Improving the value of rice by-products by SFE", Elsevier, The Journal of Supercritical Fluids, vol. 26, pp. 63-67, 2003.

[21] ZhiminXu, J. Samuel Godber,"Comparison of supercritical fluid and solvent extraction methods in extracting γ-oryzanol from rice bran",Springer, Journal of the American Oil Chemists' Society, vol. 77, no. 5, pp. 547-551, 2000.

[22] Pitchanan Kaewboonnum , Janya Vechpanich , Pravit Santiwattana , ArtiwanShotipruk , "γ-oryzanol recovery from rice bran oil soapstock",Taylor & Francis Group, Separation Science and Technology, vol. 45, no. 9, 1186-1195, 2010.

[23] Raj R. Kumar, Purnima K. Tiku, VishveshwaraiahPrakash, "Preferential extractability of γ-oryzanol from dried soapstock using different solvents",Society of Chemical Industry, Journal of the Science of Food and Agriculture, vol. 89, pp. 195-200, 2009.

[24] AOAC, "Official Methods of Analysis", 11th ed., Association of Official Analytical Chemists, USA, 1990.

[25] K. V. S. A. Rao, B. V. S. K. Rao, T.N.B. Kaimal,"Process for the isolation of oryzanols from rice bran oil soapstock", US Patent No 6410762, 2002.

[26] G. S. Seetharamaiah, J. V. Prabhakar,"Oryzanol content of Indian rice bran oil and its extraction from soapstock", Springer, Journal of Food Science and Technology, vol. 23, no.5, pp.270-273, 1986.

[27] CarstenZetzl, Gerd Brunner,M. Angela A. Meireles, "Standardized low cost SFE units for university education and comparative research",in Proceedings of the 6th International Symposium on Supercritical Fluids, Versailles, France, ISBN 2-905-267-37-02, 2003.

[28] Aziza K. Genena, HaikoHense, ArturSmânia Jr., Simone M. Souza,"Rosemary (*Rosmarinusofficinalis*) – a study of the composition, antioxidant and antimicrobial activities of extracts obtained with supercritical carbon dioxide", SBCTA,Ciência e Tecnologia de Alimentos, vol. 28, no. 2,pp. 463-469, 2008.

[29] Eliane M. Z. Michielin, Louisiane F. V. Bresciani, Leandro Danielski, Rosendo A. Yunes, Sandra R. S. Ferreira, "Composition profile of horsetail (*Equisetum giganteum* L.) oleoresin: comparing SFE and organic solvents extraction", Elsevier, The Journal of Supercritical Fluids, vol. 33, pp. 131-138, 2005.

[30] Eliete M. S. Scavariello,"Modificação química e enzimática da borra de neutralização do óleo de farelo de arroz". Ph.D. Thesis, University of Campinas, Brazil, 2002.

[31] M. M. Esquível, M. G. Bernardo-Gil, M. B. King, "Mathematical models for supercritical extraction of olive husk oil", Elsevier, The Journal of Supercritical Fluids, vol. 16, pp. 43-58, 1999.

[32] J. Crank, "The Mathematics of Diffusion", 2nd ed., Claredon Press, United Kingdom, 1975.

[33] Julian Martínez, Alcilene R. Monteiro, Paulo T. V. Rosa, Márcia O. M. Marques, M. Angela A. Meireles, "Multicomp onent model to describe extraction of ginger oleoresin with supercritical carbon dioxide",ACS Publications, Industrial and Engineering Chemistry Research, vol. 42, 1057-1063, 2003.

[34] Jeferson Correia, Eliane M.Z. Michielin, Sandra R.S. Ferreira, "Estudo de modelos de transferência de massa para processos de extração supercritica",Scientificinitiationreport (PIBIC - CNPQ), Federal Universityof Santa Catarina, Brazil, 2006.

[35] Raul N. Carvalho Jr.,Lucinewton S. Moura, Paulo T. V. Rosa, M. Angela.A. Meireles, "Supercritical fluid extraction from rosemary (*Rosmarinusofficinalis*): Kinetic data, extract's global yield, composition, and antioxidant activity", Elsevier,The Journal of Supercritical Fluids, vol. 35, pp. 197-204, 2005.

[36] E.W. Lemmon, M.O. McLinden, D.G. Friend,"Thermophysi cal Properties of Fluid Systems", in NIST Chemistry WebBook, NIST Standard Reference Database Number 69, Eds. P.J. Linstrom and W.G. Mallard, National Institute of Standards and Technology, USA, Online Available: http://webbook.nist.gov.

[37] Leandro Danielski, Luanda M. A. S. Campos, Louisiane F. V. Bresciani, HaikoHense, Rosendo A. Yunes, Sandra R.S. Ferreira,"Marigold (*Calendula officinalis* L.) oleoresin: solubility in $SC\text{-}CO_2$ and composition profile",Elsevier, Chemical Engineering and Processing, vol. 46, pp. 99-106, 2007.

[38] Cíntia S. G. Kitzberger, Rodrigo H. Lomonaco, Eliane M. Z. Michielin, Leandro Danielski, JefersonCorreia, Sandra R.S. Ferreira,"Supercritical fluid extraction of shiitake oil: curve modeling and extract composition",Elsevier, Journal of Food Engineering, vol. 90, pp. 35-43, 2009.

[39] Luanda M. A. S. Campos, Eliane M. Z. Michielin, Leandro Danielski, Sandra R. S. Ferreira,"Experimental data and modeling the supercritical fluid extraction of marigold (*Calendula officinalis*) oleoresin", Elsevier, The Journal of Supercritical Fluids, vol. 34, pp. 163-170, 2005.

[40] Susana P. Jesus, Renato Grimaldi, HaikoHense,"Recovery of γ-oryzanol from rice bran oil byproduct using supercritical fluid extraction",Elsevier, The Journal of Supercritical Fluids, vol. 55, 149-155, 2010.

[41] Juliana M. Prado, Glaucia H. C. Prado, M. Angela. A. Meireles, "Scale-up study of supercritical fluid extraction process for clove and sugarcane residue", Elsevier, TheJournal of Supercritical Fluids, vol. 56, pp. 231-237, 2011.

[42] Juliana M. Prado, IredeDalmolin, Natália D. D. Carareto, Rodrigo C. Basso, Antonio J.A. Meirelles, J. Vladimir Oliveira, Eduardo A. C. Batista, M. Angela A. Meireles, "Supercritical fluid extraction of grape seed: Process scale-up, extract chemical composition and economic evaluation", Elsevier, The Journal of Food Engineering, vol. 109, pp. 249-257, 2012.

[43] Paulo T.V. Rosa, M.Angela A. Meireles,"Rapid estimation of the manufacturing cost of extracts obtained by supercritical fluid extraction", Elsevier, Journal of Food Engineering,vol. 67, pp. 235-240, 2005.

[44] Patrícia F. Leal, "Estudo comparativo entre os custos de manufatura e as propriedades funcionais de óleos voláteis obtidos por extração supercrítica e destilação por arraste a vapor", Ph.D. Thesis, Universityof Campinas,Brazil, 2008.

CAPÍTULO 4 – MODELING THE MASS TRANSFER KINETICS OF SUPERCRITICAL FLUID EXTRACTION: AN EVALUATION FOCUSING ON PROCESS DESIGN ASPECTS

Susana P. Jesus and M. Angela A. Meireles

(Artigo a ser submetido em periódico internacional)

MODELING THE MASS TRANSFER KINETICS OF SUPERCRITICAL FLUID EXTRACTION: AN EVALUATION FOCUSING ON PROCESS DESIGN ASPECTS

Susana P. Jesus and M. Angela A. Meireles*

LASEFI/DEA/FEA (School of Food Engineering)/UNICAMP (University of Campinas); Rua Monteiro Lobato, 80; Campinas-SP; CEP: 13083-862; Brazil. *meireles@fea.unicamp.br

1 INTRODUCTION

Supercritical fluid extraction (SFE) is a solid-fluid separation technique in which the solvent is a fluid in the supercritical state. It is a versatile and environmentally friendly alternative to conventional low pressure extraction methods. Supercritical carbon dioxide (SC-CO_2) is the most commonly used solvent because it has low critical temperature [T_C = 304.2 K (Sandler, 1999)] and mild critical pressure [P_C = 7.38 MPa (Sandler, 1999)]. Additionally, it is not only cheap and readily available at high purity, but also safe to handle (non-toxic and non-flammable) and easily removed by simple expansion to common environmental pressure values (Brunner, 2005; Rosa and Meireles, 2009). Some well-noted advantages of the SFE process are the solvent recycling without any additional treatment (solvent recycling is virtually possible in any process, nonetheless, it may require a purification step), low energy consumption, adjustable solvent selectivity, prevention of oxidation reactions, and the production of high quality extracts (Mezzomo *et al.*, 2009; Jesus *et al.*, 2013).

The SFE process has been applied on a commercial scale since the 80s (Brunner, 1994). According to Brunner (2005), the costs of SFE are competitive and quite a large number of industrial plants have been built during the last decades. These operating plants are mostly distributed in Europe, the USA, Japan, and in the South East Asian Countries (Brunner, 2005). However, none is located in Latin America (Prado *et al.*, 2011). SFE can still be considered an emerging technology since the conventional methods are yet the most used in various applications of solid-fluid extraction. This happens especially because a high pressure process requires higher investment costs than a conventional low pressure plant. Nonetheless, it is well known that several other costs (besides the initial investment) must also be considered to estimate the cost of manufacturing (COM) of some desired product (Rosa and Meireles, 2005). Meireles (2003) affirms that, "in order to avoid the elimination of SFE at the very early stages of the process design, some preliminary analysis of the COM should be done with a minimal of experimental information".

Two types of experimental data must be available in order to make the COM estimation (Meireles, 2008; Albuquerque and Meireles, 2012): global yield isotherms (GYI) and overall extraction curves (OECs). The GYI are determined in different conditions of temperature (T) and pressure (P), because both thermodynamic parameters are strongly related to the solvent selectivity and the solute solubility. Therefore, the GYI are used to select the best operational conditions (T and P) based on the chemical composition of the obtained extract. After this selection, the OECs (accumulated mass of extract versus extraction time) must be determined because they bring information about the kinetic behavior of the SFE process, and thus, of the process yield. A typical overall extraction curve (OEC) may be divided in three distinguishable regions (Sovová, 1994; Ferreira and Meireles, 2002): constant extraction rate (CER), falling extraction rate (FER), and diffusion-controlled (DC) periods. During the CER period, the particles' surfaces are covered with solute, then the so-called *easily accessible solute* (X_P) is removed by convection. In the FER period, there is no more solute covering the entire surface of part of the solid particles, so both convection and diffusion mechanisms are important. This is a transition period that is caused by the continuously depletion of the solute layer in the external surface. In the DC period, the particles surfaces are completely exhausted and only the *hardly accessible solute* (X_K) (i.e. the solute located inside the solid particles) is available for extraction. Therefore the mass transfer is controlled by intraparticle diffusion (Sovová, 1994; Silva and Martínez, 2014).

Nomenclature

a_1, a_2, a_3 = adjustable parameters of spline model (kg/s)	t_{CER} = duration of the CER period (s)
b_0 = adjustable parameter of spline model (kg)	t_{CER2} = intersection point between the lines CER and DC from spline model (s)
C_2 = adjustable parameter of logistic model (no physical meaning) (s^{-1})	$t_{CER\_SP} = t_1 = t_{CER}$ calculated by Spline model (s)
db = dry basis	$t_{CER\_SV} = t_{CER}$ calculated by Sovová's model (s)
d_B = bed diameter (m)	t_{FER} = time that marks the end of the FER period (s)
d_P = mean particle diameter (m)	$t_{FER\_SP} = t_2 = t_{FER}$ calculated by Spline model (s)
D_{ef} = effective diffusion coefficient of the solute within the solid matrix (m^2/s)	t_m = adjustable parameter of logistic model (no physical meaning) (s)
F = mass of feed material (kg)	t_{TOTAL} = total extraction time (s)
F_{DRY} = mass of feed material in dry basis (kg)	t_{RES} = residence time of the solvent (s)
H_B = bed height (m)	t_1 and t_2 = adjustable parameters of spline model (s)
k_F = fluid phase mass transfer coefficient (s^{-1})	u_i = interstitial velocity of the solvent (m/s)
k_S = solid phase mass transfer coefficient (s^{-1})	wb = wet basis
m_0 = initial mass of extractable matter (kg)	X = mass ratio of solute in the solid phase (kg/kg)
m_{EXT} = mass of extract (kg)	X_0 = global yield (kg/kg)
m_{EXT_TOTAL} = total mass of extract (kg)	X_K = intact cells solute ratio (hardly accessible solute) (kg/kg)
M_{CER} = extraction rate of the CER period (kg extract/s)	X_P= broken cells solute ratio (easily accessible solute) (kg/kg)
N = integer number	Y = mass ratio of solute in the fluid phase (kg/kg)
n_e = number of experimental observations	Y_{CER} = Y at the bed outlet during the CER period (kg extract/kg CO_2)
Q_{CO2} = solvent flow rate (kg CO_2/s)	$Y_{CER\_SP} = Y_{CER}$ from spline model (kg/kg)
r = radius of the sphere particle (m)	$Y_{CER\_SV} = Y_{CER}$ from Sovová's model (kg/kg)
R_{CER} = extraction yield of the CER period (%; kg extract/kg feed material)	Y* = extract solubility in the fluid phase (kg solute/kg solvent)
RP = relative porcentage (%; kg extract/kg extract)	z = axial direction
S = mass of solvent (kg)	ε = bed porosity (dimensionless)
S/F = solvent to feed mass ratio (kg/kg)	ρ_A = bed apparent density (kg/m^3)
S/F_{CER} = solvent to feed mass ratio of the CER period (kg CO_2/kg feed material)	ρ_{CO2} = solvent density (kg/m^3)
t = extraction time (s)	ρ_S = solid matrix density (kg/m^3)

Many mathematical models have been developed to describe the OECs, from simple equations to very complex ones. The main purpose of using a mathematical model is the determination of parameters that may be applied for process design aspects, such as extraction time, solvent to feed (S/F) mass ratio, particle size, equipment dimensions, among others (Martínez *et al.*, 2007). Thus, the modeling of the OECs can be a useful tool to determine some parameters that are required for scale up and cost estimation purposes. In order to achieve this, the mathematical models must be evaluated with respect to their applicability in terms of process design. According to Reverchon (1997), the mathematical models used to describe the OECs may be divided into categories based on three main approaches: (1) empirical, (2) heat transfer analogy, (3) differential mass balance integration. The third category comprises the majority of the mathematical models available in the specific literature. The starting point is the evaluation of the differential mass balance inside the fixed bed extractor (Rosa and Meireles, 2009). In this case, each author gives his/her personal interpretation of the mass transfer phenomena that happen in both fluid and solid phases.

Nowadays, one of the crucial challenges in SFE investigation is to propose experimental as well as calculation procedures in order to simplify the determination of process parameters that are required for preliminary studies of process design and economic feasibility. In this work, the mathematical modeling of the SFE mass transfer kinetics was studied by using four different models: diffusion (Crank, 1975), logistic (Martínez *et al.*, 2003), spline (Meireles, 2008), and Sovová's (1994). These models were applied to describe the OECs of six raw materials (clove, ginger, grape seed, lemon verbena, sugarcane residue, and annatto seed), which have specific characteristics and various curve shapes. The main goal was to evaluate the models by considering the versatility to fit different curves and the applicability in terms of process design aspects. A comparative analysis of the obtained results was done to discuss the performance of the investigated models.

2 METHODOLOGY

2.1 Kinetic data

The experimental data were selected from three PhD theses previously developed by members of our research group. The experimental curves presented in Section 3 were built using kinetic data from six different raw materials: clove, ginger, grape seed, and lemon verbena (Prado, 2010), sugarcane residue (Shintaku, 2006; Prado, 2010), and annatto seed (Albuquerque, 2013). All the information about the experimental conditions used to obtain each OEC is summarized in Table 1.

The raw materials passed through drying and milling steps prior to the extraction, except for annatto seeds that were used without passing by any milling process. Most of the raw materials were originally in their natural form, which is the case of clove buds, ginger roots, lemon verbena leaves, and annatto seeds. However, the materials nominated as *grape seed* and *sugarcane residue* were byproducts from the winery and sugar-ethanol industries, as detailed by Prado and co-workers (Prado *et al.*, 2011; Prado *et al.*, 2012). As presented in Table 1 and Figures 9, 11 and 13, there are three OECs obtained by using sugarcane residue as feed material for SFE. The symbols "L-1" and "L-2" refers to two different lots of sugarcane residue, which were used in the experiments performed by Prado (2010) and Shintaku (2006), respectively. The lot L-2 was used to build two extraction curves at 323 K that are named here as "C-1" (P = 20 MPa) and "C-2" (P = 35 MPa), as can be noticed in Table 1.

Table 1 Data from the overall extraction curves (OECs) used in the mathematical modeling study

	Clove[a]	**Ginger**[a]	**Grape seed**[a]	**Lemon verbena**[a]	**Sugarcane residue (L-1)** [a]	**Sugarcane residue (L-2)** [b]		**Annatto seed**[c]
						C-1	**C-2**	
Solid matrix characterization								
Moisture (%)	8.6	8.3	12.0	5.3	0 [g]	ni[h]	ni[h]	8.9
d_p (m)	9.08E-04	7.55E-04	7.79E-04	6.72E-04	7.69E-04	2.80E-04	2.80E-04	3.65E-03
ρ_s (kg/m^3)	1422	1477	1408	1453	1731	1740	1740	1330
Fixed bed characterization								
ρ_A (kg/m^3)	779	728	966	420	302	262	262	648
Posority	0.45	0.51	0.31	0.71	0.83	0.85	0.85	0.52
(H_B/d_B)[d]	2.31	1.65	2.31	2.31	2.31	0.78	0.78	2.10
Operational data								
T (K)	313	313	313	333	333	323	323	313
P (MPa)	15	30	35	35	35	20	35	20
ρ_{CO2} (kg/m^3) [e]	766.5	910.5	935.3	863.5	863.5	785.2	899.8	840.6
F (g) [f]	225.95	149.97	279.97	121.94	87.65	25.00	25.00	171.00
$[S/F]_{TOTAL}$ (wb) [f]	9.18	14.66	12.59	21.14	29.70	59.96	60.48	22.78
t_{TOTAL} (min)	360	360	450	420	360	360	360	335
F_{DRY} (g)	206.51	137.52	246.37	115.48	87.65	ni[h]	ni[h]	155.78
S_{TOTAL} (g)	2073.0	2197.7	3524.8	2577.2	2602.8	1505.5	1512.0	3894.9
Q_{CO2} (kg/s)	9.60E-05	1.02E-04	1.31E-04	1.02E-04	1.20E-04	6.94E-05	7.00E-05	1.94E-04

d_p: mean particle diameter; ρ_S: true density of solid particles; ρ_A: bed apparent density; (H_B/d_B): bed height to diameter ratio; T: temperature; P: pressure; ρ_{CO2}: solvent density; F: mass of feed material (g); wb: wet basis; t_{TOTAL}: total time of extraction; $[S/F]_{TOTAL}$: solvent to feed ratio at $t=t_{TOTAL}$; F_{DRY}: mass of feed material in dry basis; S_{TOTAL}: total amount of solvent; Q_{CO2}: solvent flow rate; L-1: lot used by Prado (2010); L-2: lot used by Shintaku (2006); C-1: curve obtained at 323K/20MPa; C-2: curve obtained at 323K/35MPa. Experimental data from: [a]Prado (2010); [b]Shintaku (2006); [c]Albuquerque (2013). [d]bed diameter (d_B) = 5,42 cm; [e]NIST webbook; [f]mean value of experiments in duplicate; [g]the moisture value was less than 0.6 %; [h]the moisture value was not informed.

2.2 Mathematical modeling

The mathematical modeling of the experimental OECs was performed using four different models: the diffusion model of Crank (1975), the logistic model developed by Martínez and co-workers (Martínez *et al.*, 2003), the spline model described by Meireles (2008), and the model proposed by Sovová (1994). A brief description of these models and the respective fitting procedures are presented in Sections 2.2.1 to 2.2.4. In all cases, the modeling was performed by fitting each pair of duplicates simultaneously, thus providing a unique set of parameters for each OEC. The input data required for the applied models are summarized in Table 2.

Table 2 Required input data and adjustable parameters of the different mathematical models

Model	Input data [g]	Adjustable parameters [g]
Diffusion [a]	m_{EXT}, t, X_0, r	D_{ef}
Logistic [b]	m_{EXT}, t, X_0	C_2, t_m
Spline [c], [e]	m_{EXT}, t	b_0, a_1, a_2, a_3, t_1, t_2
Sovová [d], [f]	m_{EXT}, t, X_0, H_B, d_B, F, d_P, Q_{CO2}, ρ_{CO2}, ρ_S, Y*	k_F, k_S, X_K

[a]Crank (1975); [b] Martínez et al. (2003); [c] Meireles (2008); [d] Sovová (1994).
[e]Initial estimations are required for the parameters t_{CER} and t_{FER}.
[f]Initial estimations (lower and upper limits) are required for the parameters k_F, k_S, and X_K.
[g]The symbols are described in the nomenclature chart.

The initial mass of extractable matter (m_0) is the total amount of extractable solute that is contained in the feed material mass (F) at the beginning of the process (t = 0) at a given extraction condition (T and P). The global yield (X_0), which is defined by Equation 1, represents the total amount of extract that can be recovered when the solid matrix passes through an exhaustive extraction. As presented in Table 2, the parameter X_0 is needed as input data for the diffusion, logistic, and Sovová's models. In this work, the values of X_0 (see Table 3 in Section 2.5) were calculated assuming that the total mass of extract

(m_{EXT_TOTAL}) obtained at the end of the OEC ($t = t_{TOTAL}$) could be used as an estimation of m_0.

$$X_0 = \frac{m_0}{F} \qquad (1)$$

2.2.1 Diffusion model

The diffusion model is described by Equation 2, which is based on an analytical solution presented by Crank (1975) to solve Fick's second law of diffusion. This model has come from an analogy between SFE and the heat transfer phenomenon that occurs when a hot ball is cooled in a uniform medium (Reverchon, 1997). It is a phenomenological model (Sovová, 2012) that considers that the extraction is controlled solely by diffusion in the solid phase, i.e., the process is limited by the mechanism of intraparticle diffusion. Therefore, the mass balance is applied to the solid phase while fluid phase is completely neglected. Only the terms of accumulation and diffusion are taken into account, so the differential mass balance is reduced to Fick's second law of diffusion.

$$m_{EXT} = X_0 F \left[1 - \frac{6}{\pi^2} \sum_{n=1}^{\infty} \frac{1}{n^2} exp\left(\frac{-n^2 \pi^2 D_{ef} t}{r^2}\right)\right] \qquad (2)$$

Where m_{EXT} is the mass of the extract (kg); t is the extraction time (s); F is the mass of the feed material (kg); X_0 is the global yield (kg/kg); r is the radius of the spherical particle (m); and D_{ef} is the adjustable parameter, which represents the effective diffusion coefficient of the solute within the solid matrix (m^2/s).

The diffusion model was fitted to experimental data using the software Mass Transfer (LATESC/EQA/UFSC, Florianópolis, Brazil) (Correia *et al.*, 2006). This software was developed in Delphi 7.0 applying the maximum likelihood method to minimize the objective function, which was the sum of squared residuals (SSR).

2.2.2 Logistic model

The logistic model proposed by Martínez et al. (2003) is presented in Equation 3. In this model, the variation of the extract composition along the process was described by the logistic equation, which is typically applied to model population growth. According to the authors, the starting point to develop the model was a simplification of the differential mass balance in the fluid phase. They considered only the terms of convection and interfacial mass transfer, thus neglecting accumulation and dispersion. Then, one of the solutions of the logistic equation was incorporated into the term of interfacial mass transfer (Martínez *et al.*, 2003). Taking this into account, the logistic model is treated here as an empirical model since the logistic equation has no connection with the phenomenological description of the mass transfer. Therefore, no physical meaning can be attributed to the two adjustable parameters (C_2 and t_m).

$$m_{EXT} = \frac{X_0 F}{exp(C_2 t_m)} \left\{ \frac{1 + \exp(C_2 t_m)}{1 + exp[C_2(t_m - t)]} - 1 \right\} \qquad (3)$$

Where m_{EXT} is the mass of the extract (kg); t is the extraction time (s); F is the mass of the feed material (kg); X_0 is the global yield (kg/kg); and C_2 (s^{-1}) and t_m (s) are the adjustable parameters.

The software Mass Transfer (previously described in Section 2.2.1) was applied for fitting the logistic model to the experimental OEC. Thus, again, the adjustable parameters were estimated by using the maximum likelihood method and the SSR was the objective function.

2.2.3 Spline model

The spline model, as presented by Meireles (2008), has an empirical basis. It is based on the assumption that the OEC can be described by a family of N straight lines. When considering three lines, the spline model is given by a set of three equations.

Therefore, the extracted mass is calculated using Equations 4, 5, and 6, which must be respectively applied to describe the first (**$t \leq t_1$**), second (**$t_1 \leq t \leq t_2$**), and third (**$t \geq t_2$**) lines (Jesus and Meireles, 2014).

$$m_{EXT} = b_0 + a_1 t \qquad (4)$$

$$m_{EXT} = (b_0 - t_1 a_2) + (a_1 + a_2)t \qquad (5)$$

$$m_{EXT} = (b_0 - t_1 a_2 - t_2 a_3) + (a_1 + a_2 + a_3)t \qquad (6)$$

Where: b_0, a_1, a_2, a_3, t_1, and t_2 are the adjustable parameters of the model; m_{EXT} is the mass of the extract (kg); t is the extraction time (s); b_0 is the linear coefficient of line 1 (kg); $\sum a_i$ (for i=1 to i=3) are the slopes of lines 1 to 3 (kg/s), as follows: (a_1), (a_1+a_2), and (a_1+a_2+a_3) are the slope coefficients of lines 1, 2, and 3, respectively; t_1 is the time in which occurs the intercept between lines 1 and 2 (s); t_2 is the time in which occurs the intercept between lines 2 and 3 (s).

The point of using the spline model is the assumption that each straight line represents a different extraction mechanism. Thus, it is usual to consider that the first, second, and third lines can be associated with the CER, FER, and DC periods, respectively (Jesus and Meireles, 2014). In this case, the intercepts t_1 and t_2 are equivalent to t_{CER} (*duration of the CER period*) and t_{FER} (*time that marks the end of the FER period*), respectively. These intercept points are unknown, so a nonlinear fit must be done because the intercepts are adjustable parameters of the model (Freund and Littell, 2000). In this work, the experimental OEC was fitted to a spline containing 3 straight lines by using the procedure PROC NLIN of the SAS® software package (version 9.0, SAS Institute Inc., Cary, USA). The SSR was the minimized objective function. Besides, it is important to mention that the fitting was performed without forcing the model to go through the origin point (0, 0). In other words, the parameter b_0 (linear coefficient of the first line) was not forced to be zero. This procedure was adopted because we chose better fits rather than getting the exact physically correct value for b_0, which should be zero since *"m_{EXT} < 0"* cannot exist and *"m_{EXT} > 0"* is not reasonable because only pure CO_2 was used in the kinetic experiments.

2.2.4 Sovová's model

The model developed by Sovová (1994) is based on the differential mass balance, which is applied inside the extraction bed for solid and fluid phases. It is a phenomenological model that follows the broken and intact cell approach (Sovová, 2012), thus being designed to be used when the raw material pretreatment includes a milling step. According to Sovová (1994), the solute can be divided into two parts: the *easily accessible solute* (X_P) and the *hardly accessible solute* (X_K). The first part (i.e. X_P) covers the particles' surfaces and is directly exposed to the solvent, so it can be easily removed by convection. The second part (i.e. X_K) is retained inside the solid particles, and then the mass transfer depends on the diffusion mechanism.

Sovová's model assumes plug flow, and the fixed bed is considered to be homogeneous with respect to both particle size and initial solute distributions (Ferreira and Meireles, 2002). In the differential mass balance, Sovová (1994) neglected the terms of dispersion and accumulation in the fluid phase as well as the diffusion in the solid phase. Then, the simplified mass balance equations for fluid and solid phases are given by Equations 7 and 8, respectively. The boundary and initial conditions are presented in Equations 9 and 10.

$$u_i \frac{\partial Y}{\partial z} = \frac{J(X,Y)}{\varepsilon} \qquad (7)$$

$$\frac{\partial X}{\partial t} = \frac{J(X,Y)}{(1-\varepsilon)} \frac{\rho_{CO2}}{\rho_S} \qquad (8)$$

$$Y(z=0,t) = 0 \qquad (9)$$

$$X(z, t = 0) = X_0 \qquad (10)$$

Where Y and X are the mass ratios of solute in the fluid and solid phases, respectively; t is the extraction time; u_i is the interstitial velocity of the solvent; ρ_{CO2} and ρ_S are the solvent and solid matrix densities, respectively; ε is the bed porosity; X_0 is the global yield (kg extract/kg feed material); z is the axial direction; and $J(X,Y)$ is the interfacial mass transfer term. Concerning the term of interfacial mass transfer, the definition depends on the solute concentration in the solid phase. Thus, this term is defined either by Equation 11 or Equation 12, which must be respectively applied when $\mathbf{X > X_K}$ or $\mathbf{X \leq X_K}$.

$$J(X > X_K, Y) = k_F(Y^* - Y) \qquad (11)$$

$$J(X \leq X_K, Y) = k_S X\left(1 - \frac{Y}{Y^*}\right) \qquad (12)$$

Where Y^* is the extract solubility in the fluid phase (kg solute/kg solvent); k_F and k_S are the mass transfer coefficients in the fluid and solid phases, respectively.

The model has three adjustable parameters (X_K, k_F, k_S), and all them can be identified in Equations 11 and 12 (Silva and Martínez, 2014). From this point, Sovová (1994) solved analytically the mass balance equations and obtained a set of three equations that can be easily found in the literature (Ferreira and Meireles, 2002; Martínez *et al.*, 2007). Each one of these equations was related to a different extraction period (CER, FER or DC). In this work, however, the simplified mass balance equations were solved numerically using a finite difference method and the extraction curve was obtained by numerical integration, as presented by Silva and Martínez (2014). Then, the model was fitted to experimental data by using a derivative-free algorithm that establishes lower and upper limits for each parameter (Aguiar *et al.*, 2012; Silva and Martínez, 2014). Once again, the SSR was the objective function to be minimized.

2.3 Estimation of kinetic parameters of the CER period

In the spline modeling, the OEC was described by a family of three straight lines using a nonlinear fitting performed in the software SAS (as previously described in Section 2.2.3). Then, the fitted lines were associated with three different mass transfer regions following the classic description of Sovová (1994). Therefore, the first, second, and third lines were respectively identified as the CER, FER, and DC regions. The results of the spline model were used to estimate the following parameters: the duration of the CER period (t_{CER}), the extraction rate of the CER period (M_{CER}), the mass ratio of solute in the fluid phase at the bed outlet during the CER period (Y_{CER}), the extraction yield of the CER period (R_{CER}), and the solvent to feed mass ratio of the CER period (S/F_{CER}). The t_{CER} (s) and M_{CER} (kg extract/s) are both adjustable parameters from spline model (t_1 and a_1, respectively, according to Equations 4 to 6). The Y_{CER} (kg extract/kg CO_2) was obtained by dividing M_{CER} by the mean solvent flow rate (Q_{CO2}, kg CO_2/s) of the CER period. The parameters R_{CER} (%, kg extract/kg feed material) and $[S/F]_{CER}$ (kg CO_2/kg feed material) were calculated using the modeled data (values obtained for t_{CER} and m_{EXT} at the end of the CER period).

2.4 Additional parameters of spline model

According to Leal (2008), the intersection between the lines CER and DC defines an additional parameter of time, which is named as t_{CER2}. This parameter may be used as a good estimation of the process time for preliminary studies about the COM prediction (Albuquerque and Meireles, 2012). The values of t_{CER2} were calculated using the adjustable parameters obtained to describe the straight lines of spline model. Then, three parameters of time (t_{CER}, t_{FER}, and t_{CER-2}) were estimated for each OEC. Nonetheless, these time parameters are directly related to the solvent flow rate used in the kinetic experiments. In order to somehow avoid the influence of the solvent flow rate, it is useful to consider the S/F (solvent to feed) mass ratio. So, we also calculated the parameters S/F

(S/F_{CER}, S/F_{FER}, and S/F_{CER2}) that were related to each time parameter (t_{CER}, t_{FER}, and t_{CER2}, respectively). Besides these, we determined the parameter denoted here as the relative percentage (RP, as defined in Equation 13), which can be connected to each one of the time parameters.

$$RP_K = \frac{m_{EXT\_K}}{m_{EXT\_TOTAL}} \qquad (13)$$

Where RP_K is the relative percentage (%, kg/kg) when $t = t_K$; m_{EXT_K} is the accumulated mass of extract (kg) when $t = t_K$; m_{EXT_TOTAL} is the total mass of extract (kg) obtained at the end of the kinetic experiment; and k is the symbol that identifies the extraction period (CER, FER or CER2).

2.5 Solubility (Y*)

The equilibrium solubility (also known as just solubility) of a specific solute in a solvent is the amount of this solute that is dissolved in the solvent when the system is at thermodynamic equilibrium. In SFE from natural matrices, the solvent is the SC-CO_2 and the solute is a complex multicomponent mixture, which is named as extract. When modeling the mass transfer in SFE, the extract is usually treated as a pseudocomponent. The solubility (Y*) is an essential input data that is requested by Sovová's model (Sovová, 1994). Nonetheless, it is a data that in many cases is not available and that requires a slow, tedious and costly work to be determined experimentally, as can be seen in the work published by Rodrigues et al. (2002) Considering this, when the experimental solubility could not be found in the literature, we used some assumptions to roughly estimate the parameter Y*. So, the values of Y* were determined according to three different strategies:

(1) use the experimental solubility (from literature) measured for the target extract, i.e., the extract of the raw material that is being investigated;

(2) use the experimental solubility (from literature) measured for a similar extract, i.e., an extract (from other raw material) that is somehow similar to the extract of the raw material that is under investigation;

(3) estimate the solubility by determining the slope of the linear part of the investigated OEC, i.e., to assume that the saturation was achieved and thus the calculation procedure described by Rodrigues et al. (2002) could be applied. In this case, the OEC should be constructed by plotting m_{EXT} (kg extract) versus S (kg CO_2).

The values of the parameter Y* are presented in Table 3. The first strategy, that is the ideal one, was adopted for three raw materials: clove, ginger, and grape seed. The solubilities of SFE extracts from clove and ginger have been taken from Rodrigues et al. (2002). These authors used the dynamic method and considered the pseudoternary system (extract + cellulosic structure + solvent) approach, which takes into account the interactions between solute and solid matrix. For grape seed extract, the solubility has been taken from Sovová et al. (2001). These authors first extracted the grape seed oil from ground seeds by SFE. After that, solubility measurements (dynamic method) in different pressures were performed using a bed of ground seeds wetted with the previously extracted oil. The solubility determined by Sovová et al. (2001), for grape seed oil at 313 K/20.5 MPa, has been used as an estimation of Y* for annatto seed extract. So, in this case, the strategy number 2 was adopted. This strategy was chosen because we follow the assumption that the SFE extracts from grape and annatto seeds may have significant similarities in their compositions. In fact, it is known that triglycerides are the major constituents of seed oils (King, 2002). Moreover, concerning the fatty acids (FA) profile, for both grape seed and annatto seed oils the three major constituents are linoleic (C18:2), oleic (C18:1), and palmitic (C16:0) acids. These fatty acids represent about 92%

(Sovová *et al.*, 2001) and 85% (Silva *et al.*, 2008) of the total FA content in grape seed and annatto seed oils, respectively.

Table 3 Input data used for the parameters global yield (X_0) and extract solubility (Y*)

Raw material	**X_0 (kg extract/kg FM)**	**$Y^* \times 10^3$ (kg extract/kg CO_2)**	**T (K) / P (MPa) [a]**
Clove	0.1362	230[b]	308 / 10
Ginger	0.0344	5.97[b]	313 / 30
Grape seed	0.1181	13.3[c]	313 / 29
Lemon verbena	0.0179	2.65[d]	-
Sugarcane residue L-1	0.0264	3.17[d]	-
Sugarcane residue L-2/C-1	0.0224	1.29[d]	-
Sugarcane residue L-2/C-2	0.0300	3.36[d]	-
Annatto seed	0.0300	6.9[c]	313 / 20.5

FM: feed material; L-1: lot used by Prado (2010); L-2: lot used by Shintaku (2006); C-1: curve obtained at 323K/20MPa; C-2: curve obtained at 323K/35MPa.
[a] Temperature (T) and Pressure (P) in which the solubility was experimentally determined.
[b] Data from Rodrigues et al. (2002).
[c] Data from Sovová et al. (2001) for grape seed oil.
[d] Y* was determined according to strategy number 3 (previously described in this section).

In the case of lemon verbena and sugarcane residue, the strategy number 3 was applied due to the lack of experimental data about solubility. The extracts obtained from these raw materials have more particular compositions if compared to vegetable oils, for example. So, we assumed that the third strategy would be more appropriate than the second one. Therefore, although not having an adequate investigation about the solvent flow rate (Q_{CO2}), the values of Y* were calculated according to the method described by Rodrigues et al. (2002). So, the solubility was estimated by using the slope of the linear part of the OEC, which is the slope of the CER period that was determined by spline model. In this case, the value of Y_{CER_SP} (Y_{CER} calculated from spline model) would be equivalent to Y*. We are aware that this strategy is not the conceptually correct approach, because kinetic experiments for solubility determination (dynamic method) must be performed in a very particular solvent flow rate to ensure the saturation of CO_2 at the bed outlet (Sovová *et al.*, 2001; Rodrigues *et al.*, 2002). Then, a random value of Q_{CO2} should not be used to measure the solubility. Nonetheless, since a more accurate option was not available, we assumed that the obtained Y_{CER_SP} could be in the same magnitude order of the extract solubility.

2.6 Comparative analysis of the fitting performance

The mean square error (MSE), which is defined by Equation 14, was calculated in order to quantitatively compare the fitted results obtained using the four different models. Moreover, the performance of the fitted models was compared through the analysis of the residuals distribution (see Section 3 – Figures 2, 4, 6, 8, 10, 12, 14 and 16).

$$MSE = \frac{1}{n_e}\sum_{i=1}^{n_e}\left(m_{i\_MOD} - m_{i\_EXP}\right)^2 \qquad (14)$$

Where n_e is the number of experimental observations (that is, two times the number of points of the OEC); m_{i_MOD} is the modeled mass of extract; m_{i_EXP} is the experimental mass of extract.

3 Results and Discussion

The modeled curves and respective experimental data are presented in Figures 1, 3, 5, 7, 9, 11, 13, and 15. The adjustable parameters and MSEs obtained for each model are compiled in Table 4. The kinetic parameters of the CER period and some additional parameters (described in Section 2.4) of the spline model are presented in Tables 5 and 6, respectively.

Table 4 Results of the mathematical modeling: adjustable parameters[a] and mean square error (MSE)

Model	Clove	Ginger	Grape seed	Lemon verbena	Sugarcane residue (L-1)	Sugarcane residue (L-2) C-1	Sugarcane residue (L-2) C-2	Annatto seed
Diffusion (Crank, 1975)								
D_{ef} (m^2/min)	1.76E-10	2.38E-10	3.64E-11	7.13E-11	1.18E-10	1.28E-11	2.30E-11	3.61E-09
MSE [b]	4.06	0.047	23.8	0.0182	0.0294	1.95E-03	0.0025	0.045
Logistic (Martínez et al., 2003)								
C_m (min^{-1})	0.0159	0.0340	0.0108	0.0098	0.0144	0.0119	0.0211	0.0211
t_m (min)	-2524	-1295	132	-413	-190	-3509	-2091	-2086
MSE [b]	3.12	0.141	1.02	0.0098	0.0079	4.02E-04	0.0039	0.110
Spline (Meireles, 2008)								
b_0 (g) [c]	0.6799	0.2249	-0.0043	0.0988	0.0722	-0.00208	0.0199	0.3020
a_1 (g/min)	0.4459	0.1457	0.0949	0.0163	0.0229	0.00538	0.0141	0.0887
a_2 (g/min)	-0.3365	-0.1329	-0.0278	-0.0109	-0.0134	-0.00406	-0.0116	-0.0735
a_3 (g/min)	-0.0916	-0.0101	-0.0455	-0.0038	-0.0082	-0.00091	-0.0020	-0.0121
$t_1 = t_{CER-SP}$ (min)	33	22	271	63	51	61	31	30
$t_2 = t_{FER-SP}$ (min)	141	107	351	195	136	189	97	129
MSE [b]	2.29	0.017	0.54	0.0071	0.0088	2.77E-04	0.0019	0.039
Sovová (1994)								
(X_K/X_0)	0.58	0.32	0.08	0.60	0.57	0.51	0.39	0.49
k_f (s^{-1})	1.98E-04	8.79E-03	1.00E-03	1.50E-03	1.97E-03	2.64E-03	2.52E-03	3.80E-03
k_s (s^{-1})	2.02E-04	1.08E-04	8.16E-04	7.38E-05	8.80E-05	5.81E-05	4.29E-05	1.55E-04
$t_{CER-SOV}$ (min)	21	6	141	15	11	18	10	8
MSE [b]	2.07	0.012	0.56	0.0108	0.0102	3.05E-04	0.0021	0.107

L-1: lot used by Prado (2010); L-2: lot used by Shintaku (2006); C-1: curve obtained at 323K/20MPa; C-2: curve obtained at 323K/35MPa. [a] The description of the adjustable parameters is presented in the nomenclature chart. [b] MSE: Mean Square Error. [c] The parameter b_0 was not forced to be zero, as explained in Section 2.2.3.

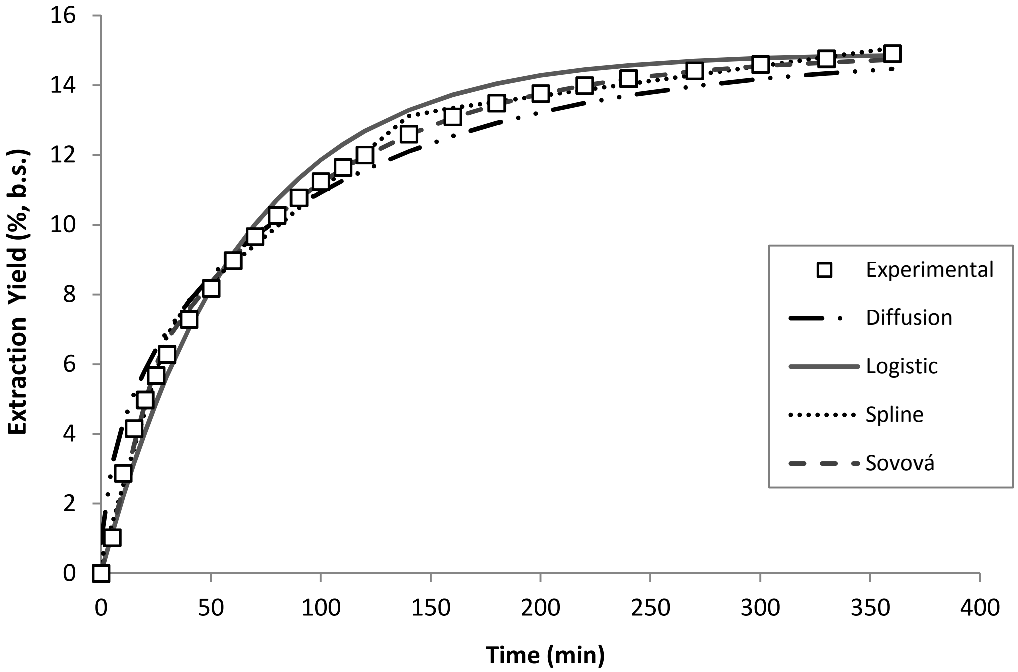

Figure 1. Experimental data of SFE from clove (15 MPa/313 K) and modeled extraction curves obtained using the applied models: diffusion (Crank, 1975), logistic (Martínez et al., 2003), spline (Meireles, 2008), and Sovová (1994)

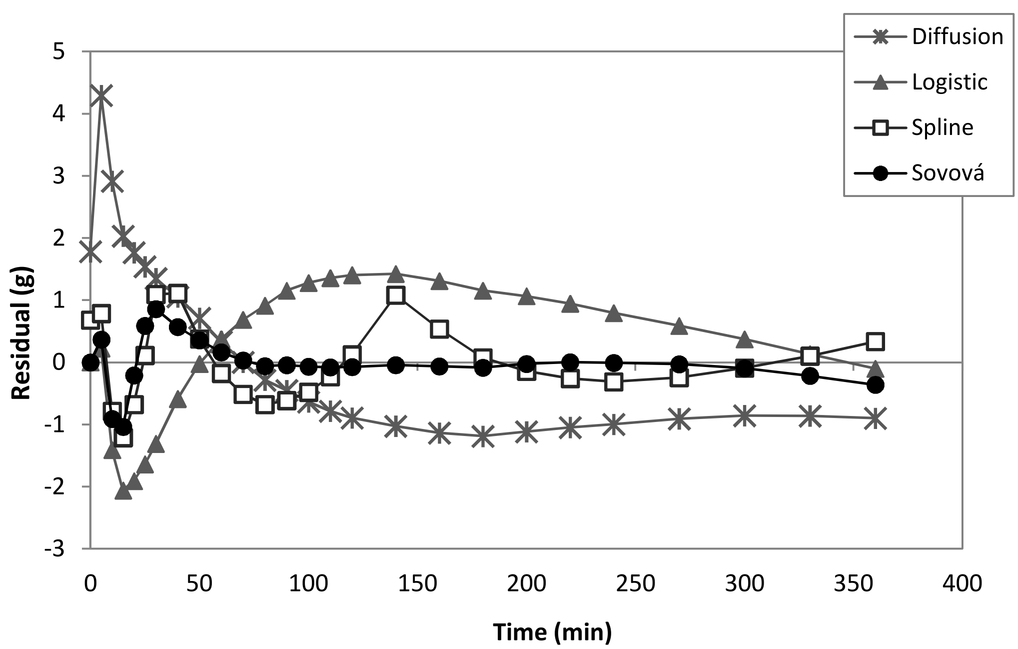

Figure 2. Distribution of the residuals obtained in the modeling of SFE from clove (15 MPa/313 K) using the following models: diffusion (Crank, 1975), logistic (Martínez et al., 2003), spline (Meireles, 2008), and Sovová (1994)

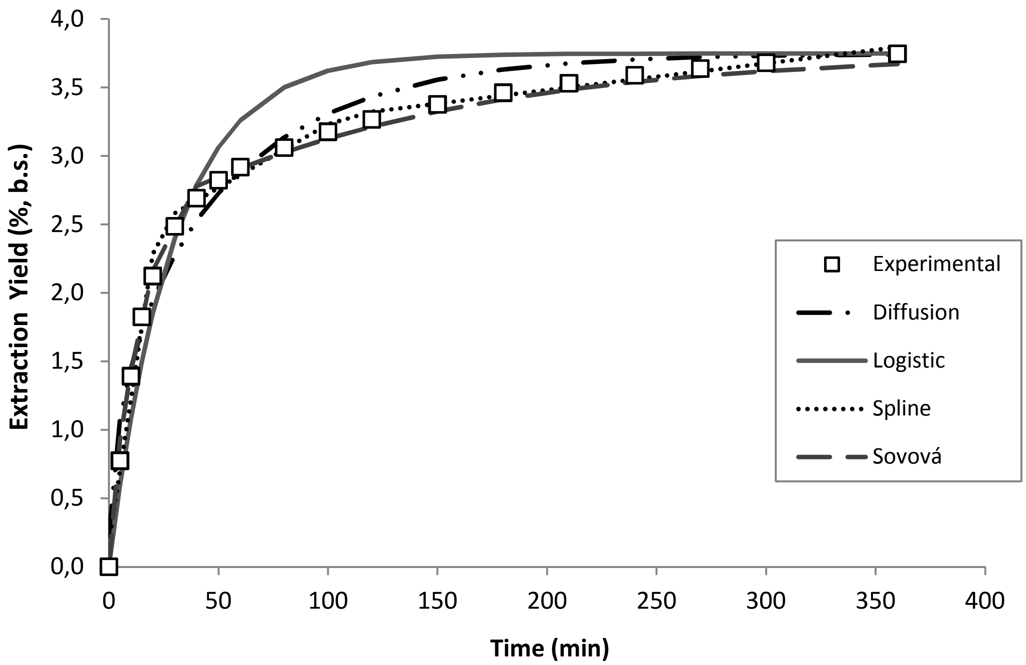

Figure 3. Experimental data of SFE from ginger (30 MPa/313 K) and modeled extraction curves obtained using the applied models: diffusion (Crank, 1975), logistic (Martínez et al., 2003), spline (Meireles, 2008), and Sovová (1994)

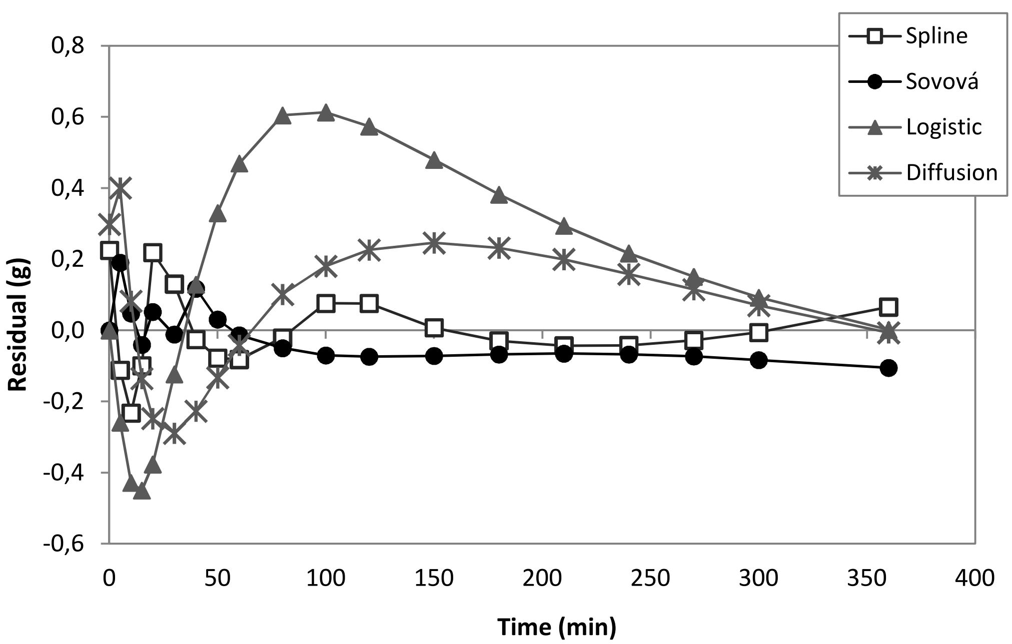

Figure 4. Distribution of the residuals obtained in the modeling of SFE from ginger (30 MPa/313 K) using the following models: diffusion (Crank, 1975), logistic (Martínez et al., 2003), spline (Meireles, 2008), and Sovová (1994)

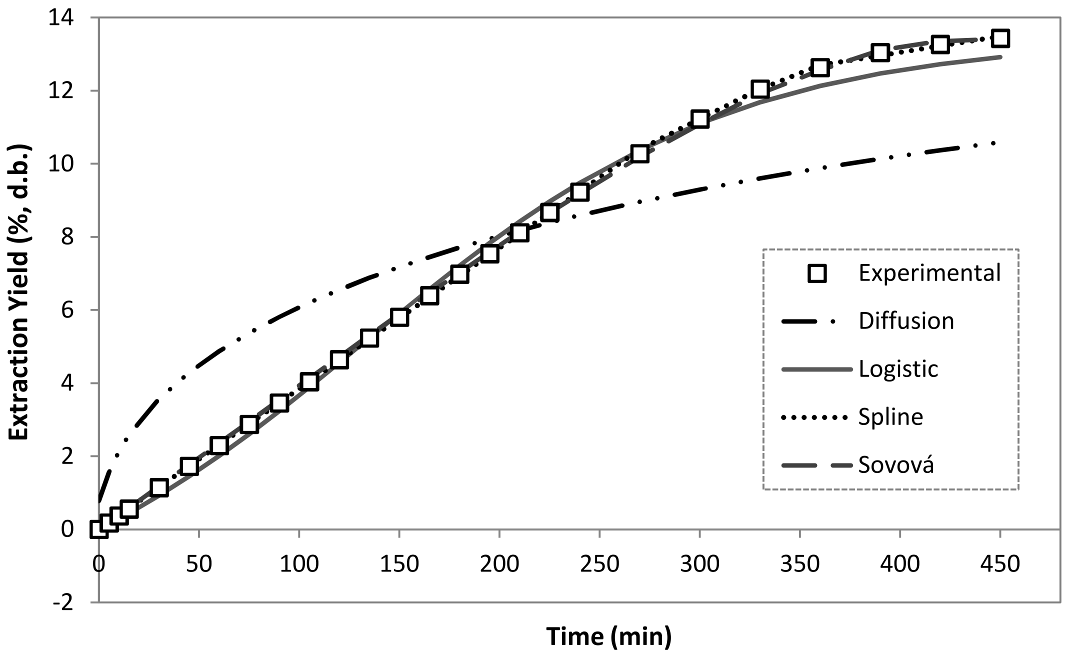

Figure 5. Experimental data of SFE from grape seed (35 MPa/313 K) and modeled extraction curves obtained using the applied models: diffusion (Crank, 1975), logistic (Martínez et al., 2003), spline (Meireles, 2008), and Sovová (1994)

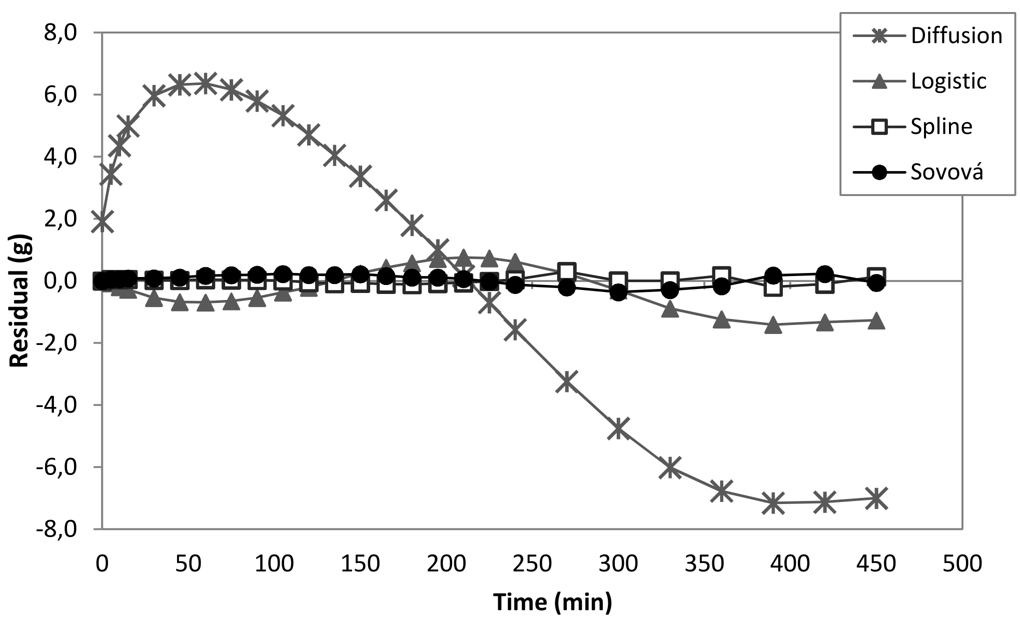

Figure 6. Distribution of the residuals obtained in the modeling of SFE from grape seed (35 MPa/313 K) using the following models: diffusion (Crank, 1975), logistic (Martínez et al., 2003), spline (Meireles, 2008), and Sovová (1994)

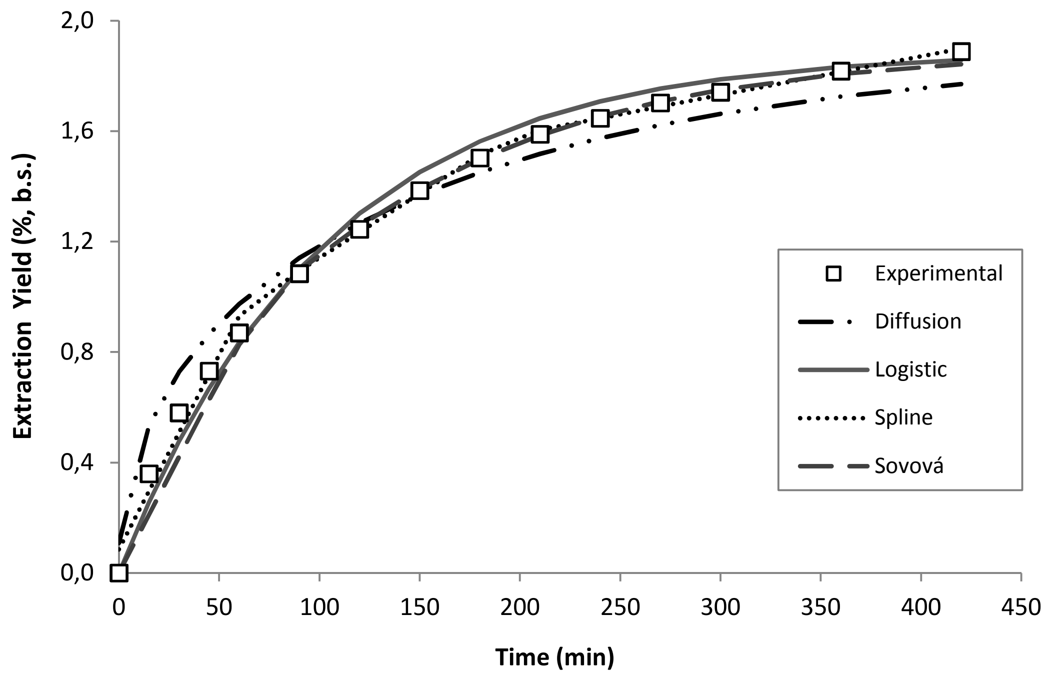

Figure 7. Experimental data of SFE from lemon verbena (35 MPa/333 K) and modeled extraction curves obtained using the applied models: diffusion (Crank, 1975), logistic (Martínez et al., 2003), spline (Meireles, 2008), and Sovová (1994)

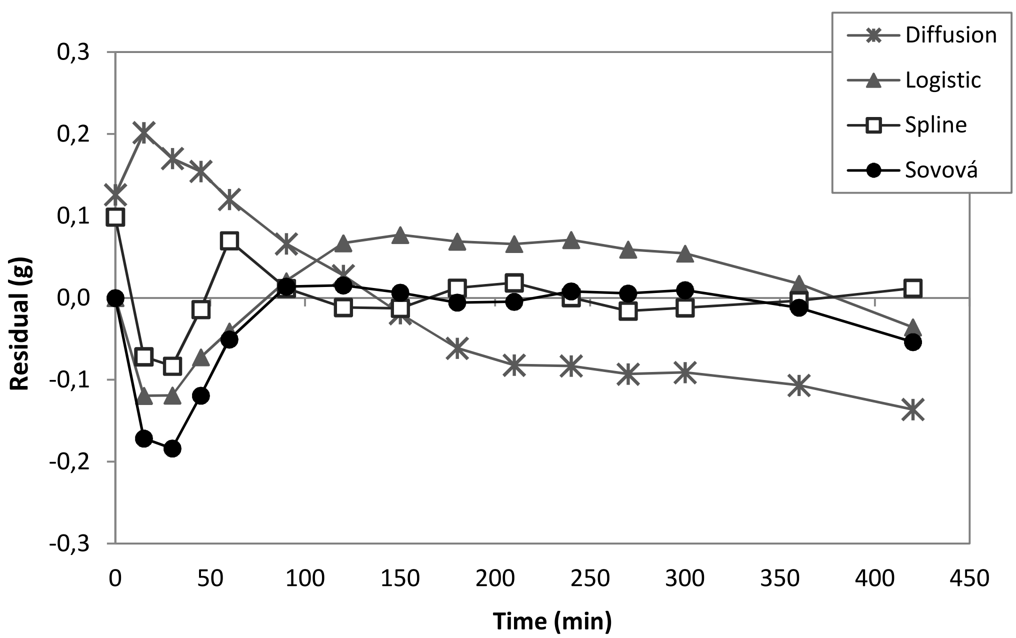

Figure 8. Distribution of the residuals obtained in the modeling of SFE from lemon verbena (35 MPa/333 K) using the following models: diffusion (Crank, 1975), logistic (Martínez et al., 2003), spline (Meireles, 2008), and Sovová (1994)

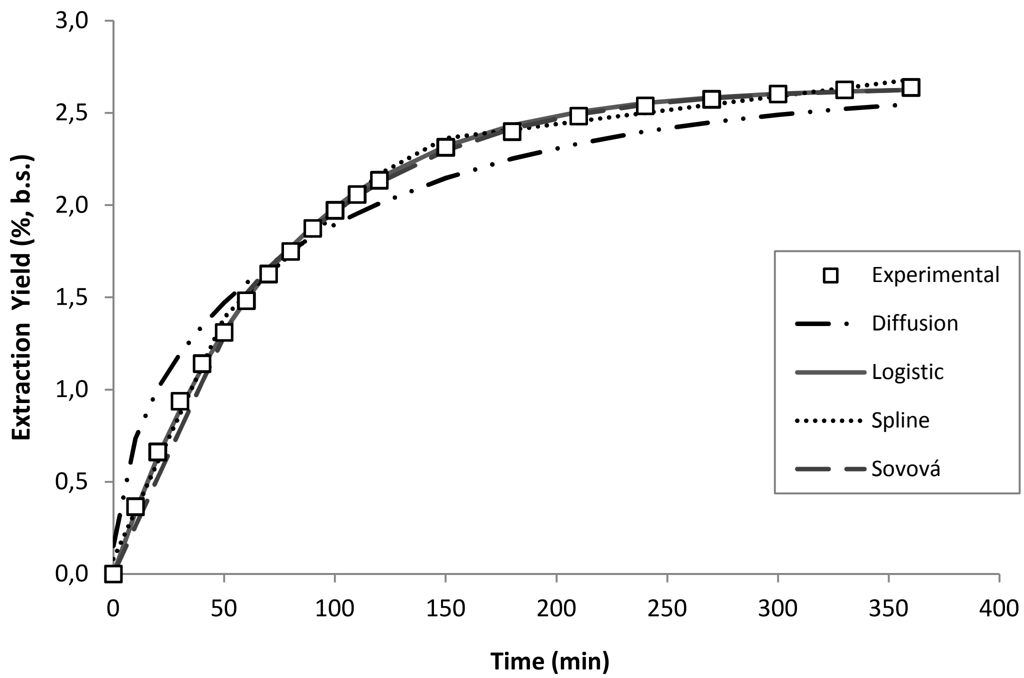

Figure 9. Experimental data of SFE from sugarcane residue L-1 (35 MPa/333 K) and modeled extraction curves obtained using the applied models: diffusion (Crank, 1975), logistic (Martínez et al., 2003), spline (Meireles, 2008), and Sovová (1994).

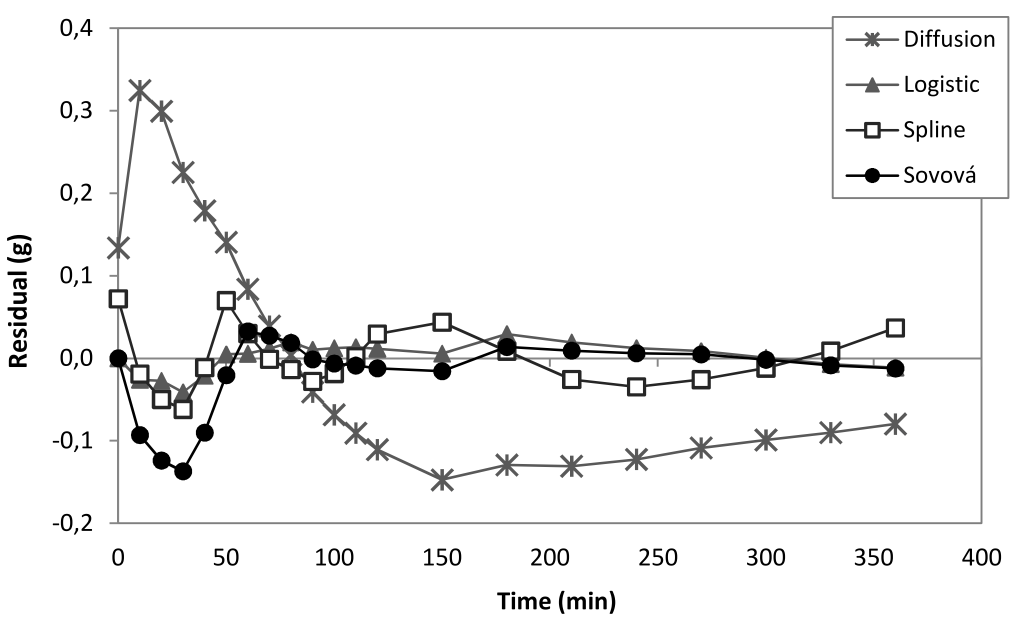

Figure 10. Distribution of the residuals obtained in the modeling of SFE from sugarcane residue L-1 (35 MPa/333 K) using the following models: diffusion (Crank, 1975), logistic (Martínez et al., 2003), spline (Meireles, 2008), and Sovová (1994)

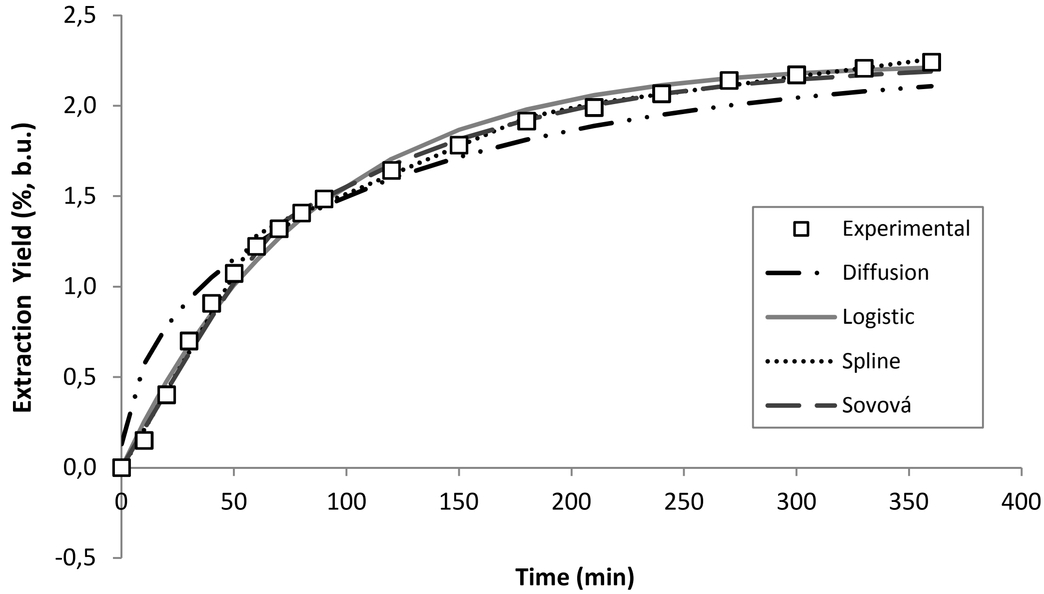

Figure 11. Experimental data of SFE from sugarcane residue L-2/C-1 (20 MPa/323 K) and modeled extraction curves obtained using the applied models: diffusion (Crank, 1975), logistic (Martínez et al., 2003), spline (Meireles, 2008), and Sovová (1994)

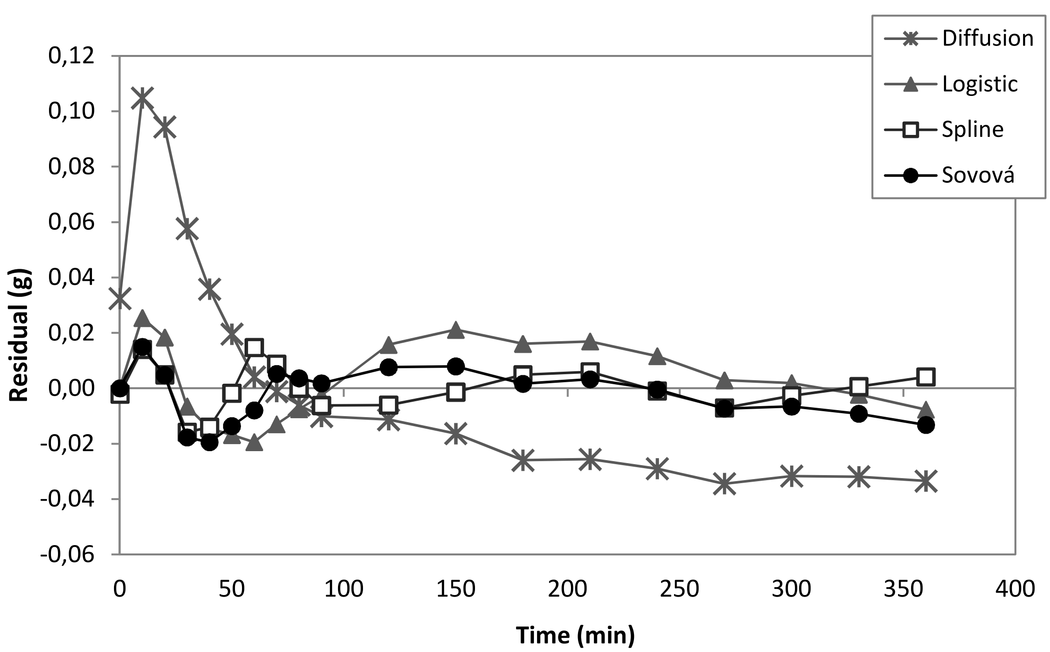

Figure 12. Distribution of the residuals obtained in the modeling of SFE from sugarcane residue L-2/C-1 (20 MPa/323 K) using the following models: diffusion (Crank, 1975), logistic (Martínez et al., 2003), spline (Meireles, 2008), and Sovová (1994)

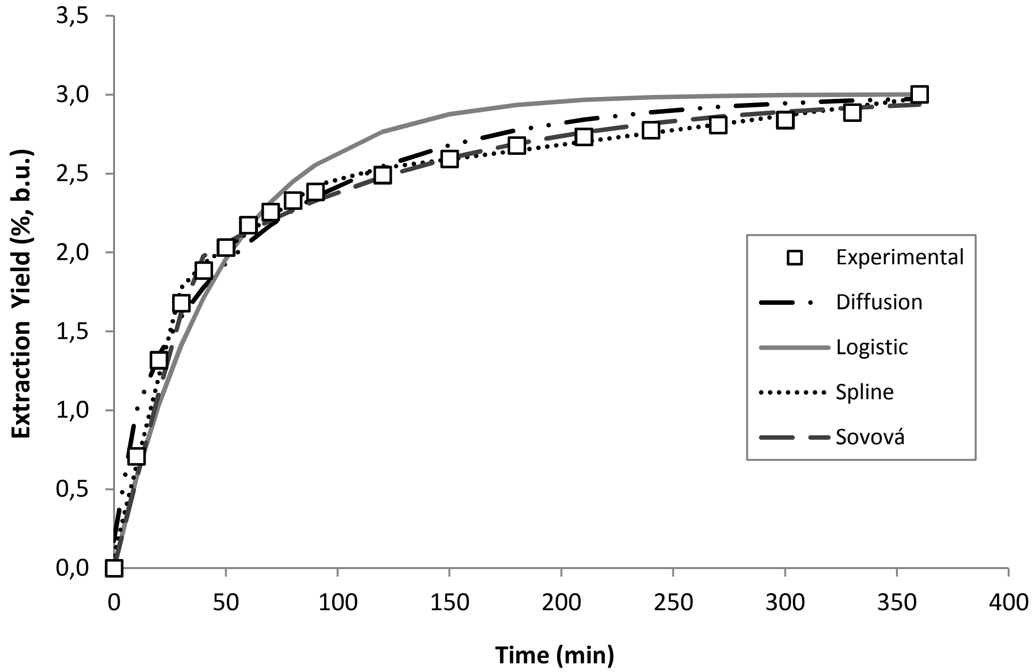

Figure 13. Experimental data of SFE from sugarcane residue L-2/C-2 (35 MPa/323 K) and modeled extraction curves obtained using the applied models: diffusion (Crank, 1975), logistic (Martínez et al., 2003), spline (Meireles, 2008), and Sovová (1994)

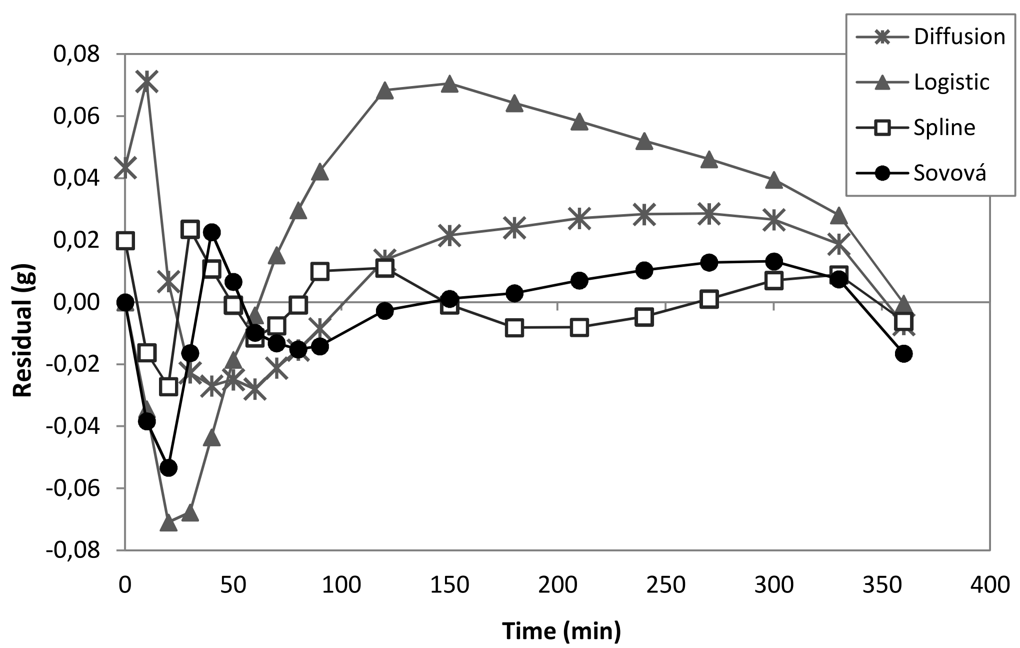

Figure 14. Distribution of the residuals obtained in the modeling of SFE from sugarcane residue L-2/C-2 (35 MPa/323 K) using the following models: diffusion (Crank, 1975), logistic (Martínez et al., 2003), spline (Meireles, 2008), and Sovová (1994)

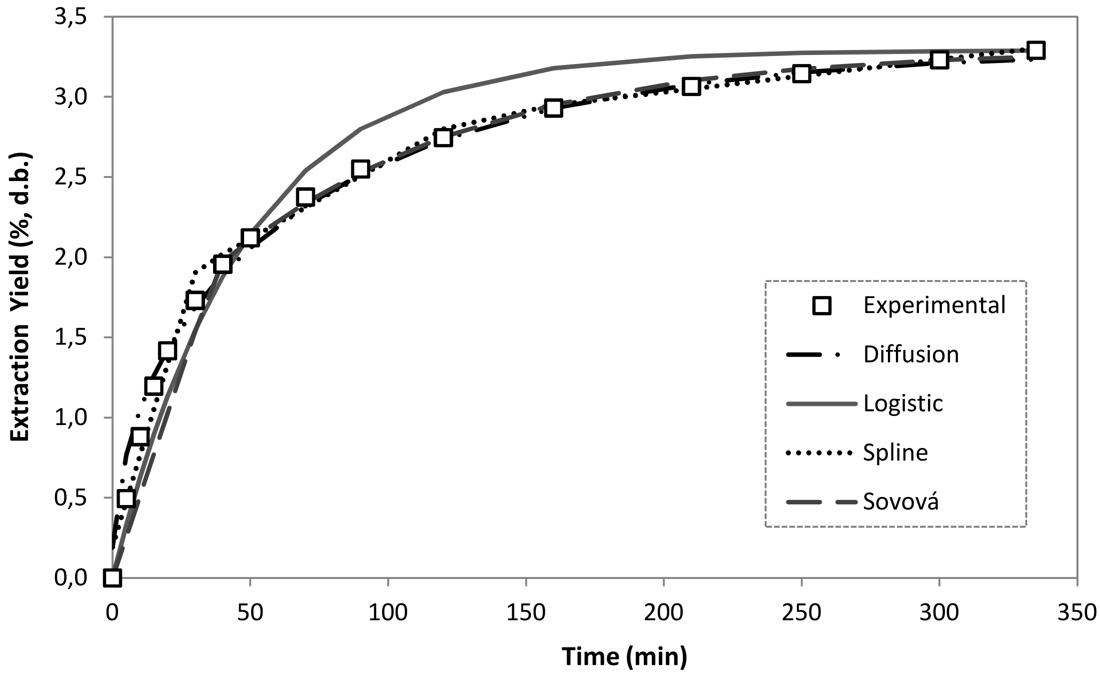

Figure 15. Experimental data of SFE from annatto seed (20 MPa/313 K) and modeled extraction curves obtained using the applied models: diffusion (Crank, 1975), logistic (Martínez et al., 2003), spline (Meireles, 2008), and Sovová (1994)

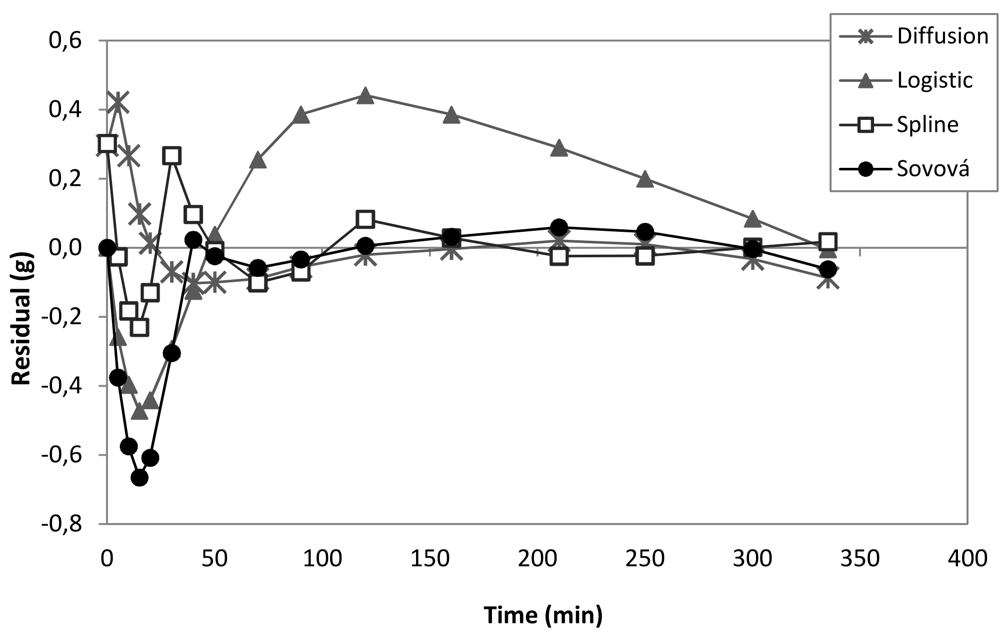

Figure 16. Distribution of the residuals obtained in the modeling of SFE from annatto seed (20 MPa/313 K) using the following models: diffusion (Crank, 1975), logistic (Martínez et al., 2003), spline (Meireles, 2008), and Sovová (1994)

The diffusion model presented the worst fit in most of the cases (5 of 8 curves), as can be seen in the MSE values from Table 4. In general, the behavior of this model follows a pattern: on the one hand, the mass of extract is overestimated in the early stages of the process; on the other hand, the mass of extract is underestimated in the middle and final stages of the extraction. The exceptions for this pattern are the modeled curves from ginger, sugarcane residue (L-2/C-2), and annatto seed, that are the three OECs for which the diffusion model had its better performance. The results prove that the diffusion is not a versatile model since it can only describe well a very specific OEC shape, which is the case of the extraction curve obtained for annatto seed. In fact, the poor fits of diffusion model were expected because it considers that the extraction is limited solely by the mechanism of intraparticle diffusion, as explained in Section 2.2.1.

Thus, this model cannot provide a reliable description of the mass transfer phenomenon that occurs during the SFE. Indeed, it is well known that the convective mechanism plays an important role in SFE, especially in the beginning of the process. Then, one could expect a particularly poor agreement between diffusion model and the experimental data for the CER period. This actually happens and can be clearly noticed in the dispersion graphs (Figures 2, 4, 6, 8, 10, 12, 14, and 16), which show that the highest peaks of residual errors are located in the CER region of all OECs. Regarding the adjustable parameter, that is the effective diffusion coefficient (D_{ef}), the obtained values could be reasonable considering the typical order of magnitude of diffusion coefficients in solids. Nonetheless, these values are not trustworthy since the model provides bad fits and also an inadequate phenomenological description.

The logistic model had the most variable performance, going from good to bad fits, depending on the OEC type. Unlike the diffusion model, the logistic can describe curves with different shapes, such as the OECs from sugarcane residue (L-1) and grape seed. However, it can also provide poor fits, thus showing no consistency and limited versatility. In general, this model was better than diffusion but worse than spline and Sovová, as can be noticed by analyzing the MSE values (Table 4) as well as the dispersion graphs (Figures 2, 4, 6, 8, 10, 12, 14, and 16). The worst fits presented by logistic model were obtained for ginger, sugarcane residue (L-2/C-2), and annatto seed. These raw materials are exactly the same for which the diffusion model had its better performance. In most cases, the behavior of logistic model was the opposite of that cited for diffusion model, so the extracted mass was underestimated in early stages and overestimated during middle to final stages of the extraction. Since the logistic model has an empirical character (see Section 2.2.2), the adjustable parameters have no physical meaning. Besides, these parameters do not bring any practical information about the SFE process and have no direct application in terms of process design.

The spline model was very effective in describing the quantitative behavior of all the OECs. It presented the lowest MSE values in most of the cases (5 of 8 curves), thus providing the best fits. The residual plots (Figures 2, 4, 6, 8, 10, 12, 14, and 16) show that the residuals from spline model are generally distributed in all extraction regions, and there are error peaks in the transitions between different extraction periods (CER – FER – DC). Although having an empirical basis, the spline model can be related to the mass transfer by creating an analogy between the three straight lines and the three extraction regions of a typical OEC. In this case, each one of the lines may be associated with a different mass transfer behavior. Then, the first, second, and third lines represent the CER, FER, and DC periods, respectively. This approach is particularly interesting to describe/characterize the CER, which is indeed known to be the linear region of the OEC. Considering the mentioned analogy, the adjustable parameters t_1, t_2, and b_1 are defined as the duration of the CER period (t_{CER}), the time that ends the FER period (t_{FER}), and the extraction rate of the CER period (M_{CER}), respectively. The spline model, and thus the description of the CER period by a straight line, was used to estimate the kinetic parameters that are presented in Table 5.

The extraction yields of the CER period (R_{CER}) varied from 50 to 77% (Table 5) of the total extraction yields obtained at the end of the OECs. These values are in accordance with the range mentioned by Pereira and Meireles (2010), who claimed that 50 – 90 % of the total amount of extract can be recovered during the CER period. The high amount of solute extracted in a relatively short time justifies why the CER is the most important period in terms of process design. Therefore, when optimizing a SFE process, the best operational conditions (such as solvent flow rate, particle diameter, bed geometry, among others) tend to be those that lead to the highest M_{CER} value. However, the extract composition is a crucial factor that must always be considered, because a high extraction rate will only be valuable if the extract is enriched with the target compounds.

According to Pereira and Meireles (2010), for many industrial applications the SFE process could end shortly after the CER period, except in particular cases where the target compounds are only or mainly extracted during the middle and/or final stages of the extraction. In general, the values of t_{CER} and R_{CER} roughly represent the minimum time a SFE cycle should last and the minimum extraction yield expected at a given process condition (Meireles, 2008). Then, the parameters t_{CER}, S/F_{CER}, and R_{CER} can be used in preliminary studies of economic feasibility by estimating the cost of manufacturing (COM), which may be calculated as described by Rosa and Meireles (2005). In order to do that, the scale-up criterion proposed by Prado and co-workers (Prado *et al.*, 2011; Prado *et al.*, 2012) can be applied to predict the industrial-scale data of the process under investigation. An additional parameter of time, which is defined as the intersection point between the lines of CER and DC periods (Leal, 2008), can be calculated from the spline model. This parameter is named t_{CER2} and it can also be used as a good estimation of the process time in preliminary studies of COM prediction (Albuquerque and Meireles, 2012). The values of the parameter t_{CER2} are presented in Table 6, where the RP_{CER2} results show that the mass of extract obtained at this point varied from 58 to 88 % of the total mass recovered at the final time of extraction. When performing exploratory investigations of economic viability, the parameters t_{CER} and t_{CER2} may be chosen as an initial estimative of the cycle time of the SFE process.

Sovová's model presented a good agreement with experimental data in most cases. It was very accurate to describe the DC periods and also most part of the FER periods, but less accurate to model the CER regions. In fact, the residual plots (Figures 2, 4, 6, 8, 10, 12, 14, and 16) of this model show that the highest errors are largely concentrated at the beginning of the extraction, particularly in the CER. The worst fits of Sovová's model were found for lemon verbena, sugarcane residue (L-1), and annatto seed, because for these raw materials the modeled curves showed poor agreement with experimental points of the CER period. Such poor agreements may be associated with unreliable values of Y*, which have been roughly estimated (see details in Section 2.5) since the experimental solubilities were not available. Indeed, the greatest difficulty in applying Sovová's model is to find a reliable value for the parameter Y*. This happens because for many systems this parameter cannot be found in the literature and, more importantly, the accurate measurement of Y* is not a trivial or quick task. Although the methodology for determining the solubility is already well established (Rodrigues *et al.*, 2002), it requires a lot of experimental work. So, in researches that are focused in process design, it would be much more useful to spend experimental efforts on scale-up assays than on solubility measurements. Taking all into account, finding ways of estimating the solubility may be the most practical alternative. However, when using an estimated value for the parameter Y*, all the uncertainties will be directly propagated to the adjustable parameters of the model (k_F, k_S, and X_K).

Table 5 Kinetic parameters of the constant extraction rate (CER) period

Kinetic parameter [a]	**Clove**	**Ginger**	**Grape seed**	**Lemon verbena**	**Sugarcane residue (L-1)**	**Sugarcane residue (L-2)**		**Annatto seed**
						C-1	**C-2**	
M_{CER} x 10^7 (kg extract/s)	74.32	24.28	15.82	2.72	3.82	0.90	2.35	14.78
Y_{CER} x 10^3 (kg extract/kg CO_2)	77.45	23.92	12.12	2.65	3.17	1.29	3.36	7.63
R_{CER} (%, kg extract/kg dry feed) [b]	7.45	2.51	10.44	0.97	1.42	1.31[c]	1.84[c]	1.92
S/F_{CER} (kg CO2/kg dry feed) [b]	0.92	0.98	8.61	3.33	4.22	10.20[c]	5.24[c]	2.27

[a]obtained using the spline model (t_{CER-SP}); [b]dry basis; [c]result is expressed in wet basis.

Table 6 Additional parameters [a] obtained using the spline model

Parameter	**Clove**	**Ginger**	**Grape seed**	**Lemon verbena**	**Sugercane residue (L-1)**	**Sugarcane residue (L-2)**		**Annatto seed**
						C-1	**C-2**	
t_{CER-2} (min)	56	28	321	96	83	85	41	44
$[S/F]_{CER-2}$ (db)	1.57	1.25	10.20	5.13	6.89	14.09[b]	6.88[b]	3.30
$[S/F]_{FER}$ (db)	3.94	4.74	11.16	10.40	11.22	31.40[b]	16.26[b]	9.63
RP_{CER} (%)	49.4	66.1	77.4	50.8	53.2	57.9	61.1	58.4
RP_{CER-2} (%)	57.6	67.6	87.4	59.0	66.3	63.3	64.3	62.5
RP_{FER} (%)	87.5	86.9	93.6	83.3	87.6	87.6	82.9	87.6

db: dry basis; [a]according to Section 2.4; [b]result is expressed in wet basis.

Even if the experimental solubility is known and an excellent fit is achieved by Sovová's model, not much can be concluded by analyzing the values of the adjustable parameters (Table 4) when only one extraction condition has been modeled. On the other hand, the evaluation of these parameters can bring useful information if the model is used to fit OECs obtained in distinct extraction conditions (different solvent flow rates, particle diameters or bed geometries, among others), as well explored by Silva and Martínez (2014). In the last case, the comparison of the adjustable parameters from different OECs can indicate which extraction condition is the most efficient in terms of mass transfer (note that the same logic can be applied to the analysis of the parameter M_{CER} from spline model). Nonetheless, in both situations (one or more OECs), there is no guarantee that the obtained values for k_F, k_S, and X_K are in accordance with the real values of these phenomenological parameters. In other words, it is quite hard to know if the values of the fitted parameters are reliable and really reflect their attributed physical meanings. This must be evaluated by considering how close the model assumptions are from the physical phenomena that take place inside the extraction vessel.

The ability of Sovová's model to describe the main mass transfer mechanisms of a SFE process will depend on specific characteristics of each system (solid matrix + solute + solvent) under investigation. Indeed, a key point about the mass transfer, which may be related with the significant residual errors found in the CER period of some modeled curves, is the intensity of the interactions between solute and solid matrix. In the model proposed by Sovová (1994), the easily accessible solute is assumed to behave as a free solute, that is, this solute fraction would have no interaction with the solid matrix. In a more refined model proposed years later by Sovová (2005), these interactions can somehow be taken into account by using the partition coefficient in the description of the phase equilibrium between fluid and solid phases. However, this model has two additional parameters, thus requiring extra data about the system. As a consequence, its complexity is highly increased, and very few published works use it (Silva and Martínez, 2014).

There is no doubt that the phenomenological models are of central importance in many scientific contexts. In SFE, they play a fundamental role in understanding the physical phenomena (including thermodynamic and mass transfer aspects) that occur in the extraction vessel. Nonetheless, these models and respective phenomenological parameters have not been helpful in supporting the decision-making for scale-up and economic analysis, which are basic aspects to be considered in the very early stages of process design. Moreover, most of the works that deal with mathematical modeling suggest the applicability of the models for scale-up prediction, but do not prove it by providing pilot-scale data. Although the available scale-up data in the open literature are still inconclusive, some works developed by our research group have demonstrated that the extraction yields and kinetic behaviors observed in laboratory assays can be reproduced on pilot-scale experiments (Prado *et al.*, 2011; Prado *et al.*, 2012; Albuquerque, 2013). These works applied a very simple scale-up criterion, which is based on keeping constant the S/F ratio and respective residence time, as explained by Prado and co-workers (Prado *et al.*, 2011; Prado *et al.*, 2012). Using this simple criterion, the OECs presented very similar shape in pilot and laboratory scales. Therefore, when this scale-up criterion is valid, it is possible to assume that any mathematical model (even being empirical) that can quantitatively describe the small-scale OEC may be able to estimate the kinetic behavior in a larger scale. In order to illustrate this assumption, some pilot data were used to build the OECs presented in Figures 17 and 18.

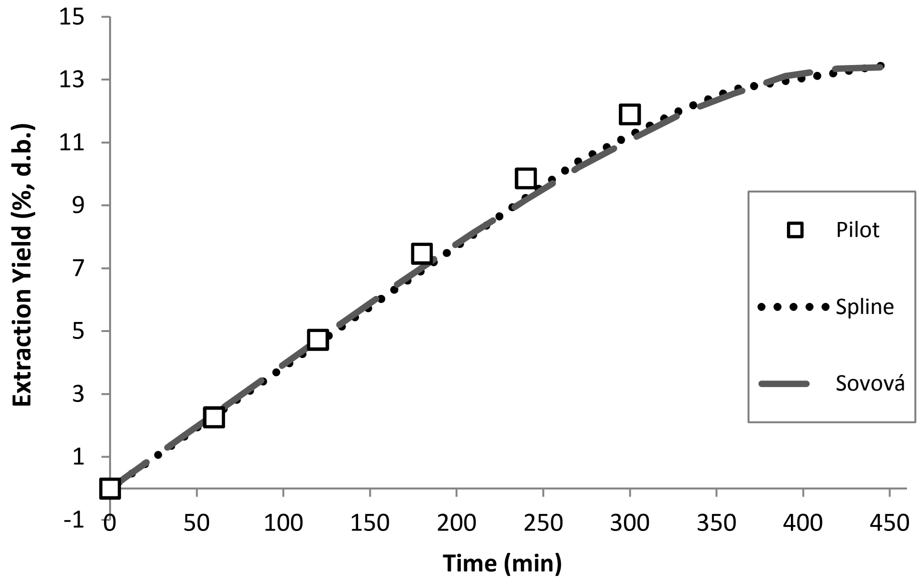

Figure 17. Pilot-scale OEC for grape seed (313 K/35 MPa): experimental pilot[a] data from Prado (2010) and estimated curves obtained by modeling the laboratory-scale OEC (presented in Figure 5) using spline and Sovová's models. [a]The scale-up criterion in the pilot experiment – as described by Prado et al. (2012) – was to keep constant the S/F ratio and respective residence time (t_{RES}) (*note that a pilot-scale SFE assay implies using the exact same solid matrix and same values for bed porosity and bed apparent density*)

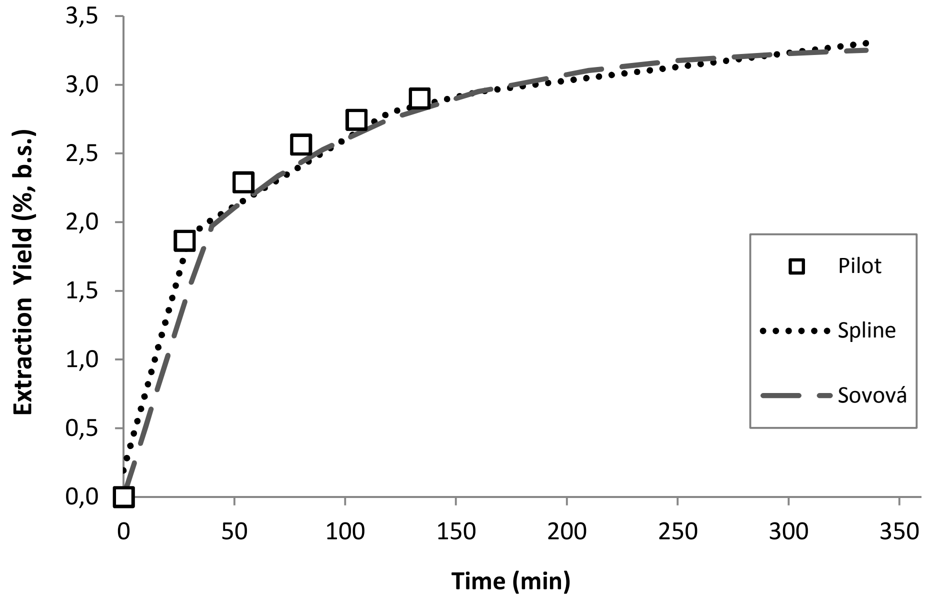

Figure 18. Pilot-scale OEC for annatto seed (313 K/20 MPa): experimental pilot[a] data from Albuquerque (2013) and estimated curves obtained by modeling the laboratory-scale OEC (presented in Figure 15) using spline and Sovová's models. [a]The scale-up criterion in the pilot experiment – as described by Albuquerque (2013) – was to keep constant the S/F ratio and respective residence time (t_{RES}) (*note that a pilot-scale SFE assay implies using the exact same solid matrix and same values for bed porosity and bed apparent density*)

4 CONCLUSIONS

In the present work, some mathematical models were successfully applied to describe the OECs of six different raw materials. For all the studied models, the highest error peaks are located in the CER region. In most cases, the spline model presented the best fits and also the most accurate agreement with experimental data during the CER region, which is the most important one in terms of process design. The spline and Sovová's models provided a good quantitative description of the investigated curves, and may possibly be used to estimate the kinetic behavior in a larger scale (as long as the previously cited scale-up criterion can be adopted). The spline model showed consistency and versatility since it described very well the various curve shapes. Besides, one advantage of the spline model is that only the kinetic data (m_{EXT} and t) is enough to perform the mathematical modeling of the OEC.

Acknowledgements

S. P. Jesus thanks CNPq (141828/2010-2) for her PhD fellowship. M. A. A. Meireles thanks CNPq (301301/2010-7) for her productivity grant. The authors thank Prof. Dr. Julian Martínez for many contributions to this work, in particular for kindly providing the algorithm that was used to fit the Sovová's model.

References

AGUIAR, A. C.; VISENTAINER, J. V.; MARTÍNEZ, J. Extraction from striped weakfish (*Cynoscion striatus*) wastes with pressurized CO_2: Global yield, composition, kinetics and cost estimation. **The Journal of Supercritical Fluids,** v. 71, p. 1-10, 2012.

ALBUQUERQUE, C. L. C. **Obtenção de sementes desengorduradas e de óleo rico em tocotrienóis de urucum por extração supercrítica: estudo dos parâmetros de processo, do aumento de escala e da viabilidade econômica**. 2013. (PhD). FEA (School of Food Engineering), UNICAMP (University of Campinas), Brazil.

ALBUQUERQUE, C. L. C.; MEIRELES, M. A. A. Defatting of annatto seeds using supercritical carbon dioxide as a pretreatment for the production of bixin: Experimental, modeling and economic evaluation of the process. **The Journal of Supercritical Fluids,** v. 66, p. 86-95, 2012.

BRUNNER, G. **Gas extraction: an introduction to fundamentals of supercritical fluids and the application to separation processes**. Darmstadt: Steinkopff, 1994. 387 p.

BRUNNER, G. Supercritical fluids: technology and application to food processing. **Journal of Food Engineering,** v. 67, n. 1–2, p. 21-33, 2005.

CORREIA, J.; MICHIELIN, E. M. Z.; FERREIRA, S. R. S. **Estudo de modelos de transferência de massa para processos de extração supercrítica**. 2006. (Scientific initiation report - PIBIC/CNPQ). EQA

(Department of Chemical and Food Engineering), UFSC (Federal University of Santa Catarina), Brazil.

CRANK, J. **The Mathematics of Diffusion**. 2. Oxford: Oxford University Press, 1975.

FERREIRA, S. R. S.; MEIRELES, M. A. A. Modeling the supercritical fluid extraction of black pepper (*Piper nigrum* L.) essential oil. **Journal of Food Engineering,** v. 54, n. 4, p. 263-269, 2002.

FREUND, R. J.; LITTELL, R. C. **SAS System for Regression**. 3rd. SAS Publishing, 2000. 254 p.

JESUS, S. P. et al. A Simplified Model to Describe the Kinetic Behavior of Supercritical Fluid Extraction from a Rice Bran Oil Byproduct. **Food and Public Health,** v. 3, n. 4, p. 215-222, 2013.

JESUS, S. P.; MEIRELES, M. A. A. Supercritical fluid extraction: a global perspective of the fundamental concepts of this eco-friendly extraction technique. In: CHEMAT, F. e VIAN, M. A. (Ed.). **Alternative Solvents for Natural Products Extraction**: Springer Berlin Heidelberg, 2014. cap. 3, p.39-72.

KING, J. W. Supercritical fluid extraction: present status and prospects. **Grasas y Aceites,** v. 53, n. 1, p. 8-21, 2002.

LEAL, P. F. **Estudo comparativo entre os custos de manufatura e as propriedades funcionais de óleos voláteis obtidos por extração supercrítica e destilação por arraste a vapor**. 2008. (PhD). FEA (School of Food Engineering), UNICAMP (University of Campinas), Brazil

MARTÍNEZ, J. et al. Multicomponent model to describe extraction of ginger oleoresin with supercritical carbon dioxide. **Industrial & engineering chemistry research,** v. 42, n. 5, p. 1057-1063, 2003.

MARTÍNEZ, J.; ROSA, P. T. V.; MEIRELES, M. A. A. Extraction of clove and vetiver oils with supercritical carbon dioxide: modeling and simulation. **The Open Chemical Engineering Journal,** v. 1, n. 1, p. 1-7, 2007.

MEIRELES, M. A. A. Supercritical extraction from solid: process design data (2001–2003). **Current Opinion in Solid State and Materials Science,** v. 7, n. 4–5, p. 321-330, 2003.

MEIRELES, M. A. A. Extraction of bioactive compounds from Latin American plants. In: MARTINEZ, J. L. (Ed.). **Supercritical fluid extraction of nutraceuticals and bioactive compounds**. Boca Raton: CRC Press –Taylor & Francis Group, 2008. cap. 8, p.243-274.

MEZZOMO, N.; MARTÍNEZ, J.; FERREIRA, S. R. S. Supercritical fluid extraction of peach (*Prunus persica*) almond oil: Kinetics, mathematical modeling and scale-up. **The Journal of Supercritical Fluids,** v. 51, n. 1, p. 10-16, 2009.

PEREIRA, C. G.; MEIRELES, M. A. A. Supercritical fluid extraction of bioactive compounds: fundamentals, applications and economic perspectives. **Food and Bioprocess Technology,** v. 3, n. 3, p. 340-372, 2010.

PRADO, J. M. **Estudo do aumento de escala do processo de extração supercrítica em leito fixo**. 2010. (PhD). FEA (School of Food Engineering), UNICAMP (University of Campinas), Brazil

PRADO, J. M. et al. Supercritical fluid extraction of grape seed: Process scale-up, extract chemical composition and economic evaluation. **Journal of Food Engineering,** v. 109, n. 2, p. 249-257, 2012.

PRADO, J. M.; PRADO, G. H. C.; MEIRELES, M. A. A. Scale-up study of supercritical fluid extraction process for clove and sugarcane residue. **The Journal of Supercritical Fluids,** v. 56, n. 3, p. 231-237, 2011.

REVERCHON, E. Supercritical fluid extraction and fractionation of essential oils and related products. **The Journal of Supercritical Fluids,** v. 10, n. 1, p. 1-37, 1997.

REVERCHON, E.; MARRONE, C. Supercritical extraction of clove bud essential oil: isolation and mathematical modeling. **Chemical Engineering Science,** v. 52, n. 20, p. 3421-3428, 1997.

RODRIGUES, V. M. et al. Determination of the solubility of extracts from vegetable raw material in pressurized CO_2: a pseudo-ternary mixture formed by cellulosic structure+solute+solvent. **The Journal of Supercritical Fluids,** v. 22, n. 1, p. 21-36, 2002.

ROSA, P. T. V.; MEIRELES, M. A. A. Rapid estimation of the manufacturing cost of extracts obtained by supercritical fluid extraction. **Journal of Food Engineering,** v. 67, n. 1–2, p. 235-240, 2005.

ROSA, P. T. V.; MEIRELES, M. A. A. Fundamentals of supercritical extraction from solid matrices. In: MEIRELES, M. A. A. (Ed.). **Extracting Bioactive Compounds for Food Products: Theory and Application**. Boca Raton: CRC Press –Taylor & Francis Group, 2009. p.272-288.

SANDLER, S. I. **Chemical and engineering thermodynamics**. 3rd ed. New York, NY: John Wiley, 1999. 772 p.

SHINTAKU, A. **Obtenção de extrato proveniente do aproveitamento de resíduo da indústria sucroalcooleira, utilizando CO_2 supercrítico: parâmetros de processo e estimativa do custo de manufatura**. 2006. 358 (Master). FEA (School of Food Engineering), UNICAMP (University of Campinas), Brazil.

SILVA, G. F. et al. Extraction of bixin from annatto seeds using supercritical carbon dioxide. **Brazilian Journal of Chemical Engineering,** v. 25, p. 419-426, 2008.

SILVA, L. P. S.; MARTÍNEZ, J. Mathematical modeling of mass transfer in supercritical fluid extraction of oleoresin from red pepper. **Journal of Food Engineering,** v. 133, p. 30-39, 2014.

SOVOVÁ, H. Rate of the vegetable oil extraction with supercritical CO_2—I. Modelling of extraction curves. **Chemical Engineering Science,** v. 49, n. 3, p. 409-414, 1994.

SOVOVÁ, H. Mathematical model for supercritical fluid extraction of natural products and extraction curve evaluation. **The Journal of Supercritical Fluids,** v. 33, n. 1, p. 35-52, 2005.

SOVOVÁ, H. Modeling the supercritical fluid extraction of essential oils from plant materials. **Journal of Chromatography A,** v. 1250, n. 0, p. 27-33, 2012.

SOVOVÁ, H. et al. Solubility of two vegetable oils in supercritical CO2. **The Journal of Supercritical Fluids,** v. 20, n. 1, p. 15-28, 2001.

CAPÍTULO 5 – CONCLUSÕES GERAIS

Tendo em vista a revisão de literatura apresentada no Capítulo 1, é possível perceber que a extração supercrítica (SFE) já está consolidada em termos de conhecimento científico (descrição fenomenológica), viabilidade técnica e disponibilidade comercial da tecnologia para aplicação em escala industrial. Em relação à viabilidade econômica, os pesquisadores da área afirmam que a SFE pode ser, em diversas situações, competitiva frente a outros processos convencionais. Contudo, em muitos países (como é o caso do Brasil e demais membros da América Latina) a utilização do processo SFE ainda não faz parte da realidade industrial. Portanto, investigar e validar a viabilidade econômica da SFE continua sendo um desafio para os pesquisadores da área, especialmente nos países onde a tecnologia ainda não é aplicada em escala comercial. Diante de tal contexto, considera-se fundamental concentrar esforços no sentido de desenvolver métodos práticos a fim de predizer o custo de manufatura do produto (COM) utilizando o mínimo possível de informações experimentais. Uma vez estimado o COM, pode-se fazer uma predição sobre o tempo de retorno do investimento, fator que é crucial para despertar o interesse dos potenciais investidores e tornar a SFE uma técnica a ser considerada nas etapas iniciais de design de processo.

A partir do estudo de caso apresentado no Capítulo 3, pode-se concluir que o modelo *spline* é capaz de descrever muito bem o comportamento quantitativo da curva global de extração (OEC). No entanto, há de se considerar que este é um modelo empírico, portanto não possui parâmetros ajustáveis que sejam diretamente relacionados à descrição fenomenológica da SFE. Apesar disso, a descrição da OEC por meio de três linhas retas permite que uma analogia seja feita com relação às etapas CER (*Constant Extraction Rate*), FER (*Falling Extraction Rate*) e DC (*Diffusion-Controlled rate*), sendo que cada etapa está associada a um comportamento distinto em termos de transferência de massa. Assim sendo, as três retas do modelo podem ser associadas a três regiões distintas no que diz respeito aos mecanismos de transporte de massa. Tal analogia é especialmente válida para a etapa CER, uma vez que fenomenologicamente espera-se um comportamento linear no período inicial da OEC, fato que ocorre porque a resistência à transferência de massa tende a ser constante no estágio inicial do processo de SFE. Uma das vantagens do modelo *spline* é que apenas os dados do experimento cinético (massa de extrato versus tempo) são necessários, o que permite a modelagem da OEC mesmo quando informações adicionais (como solubilidade, densidade da matriz sólida, rendimento global, entre outros) não estão disponíveis para um determinado sistema de interesse. Desta forma, apesar da simplicidade do modelo e dos poucos dados requeridos sobre o sistema em questão, é possível ter uma boa estimativa do tempo de processo (t_{CER} e/ou t_{CER2}) a ser utilizado em estudos preliminares de análise econômica.

O estudo apresentado no Capítulo 4 teve como foco descrever a OEC usando modelos de complexidade matemática relativamente baixa. A partir da análise global dos resultados deste capítulo, pode-se concluir que tanto o modelo *spline*[1] quanto o modelo de Sovová[2] são capazes de descrever o comportamento quantitativo de curvas de formatos diversificados. Os melhores ajustes, em termos quantitativos (menores valores para os MSEs – *Mean Square Errors*), foram obtidos para o modelo *spline* na maioria dos casos estudados. Como vantagens do modelo *spline* destacam-se: versatilidade (pode ser ajustado a qualquer formato de curva); facilidade de aplicação (além de matematicamente pouco complexo, também não exige dados cuja determinação experimental é difícil ou trabalhosa); possibilidade de obter uma estimativa inicial para o tempo de processo (estudos realizados no LASEFI têm demonstrado que a região da OEC onde o COM atinge valor mínimo está localizada no intervalo entre t_{CER} e t_{FER}, em geral próximo de t_{CER} ou t_{CER2}); possibilidade de aplicação para estimar dados em maior escala

---

[1] MEIRELES, M. A. A. Extraction of bioactive compounds from Latin American plants. In: MARTINEZ, J. L. (Ed.). Supercritical fluid extraction of nutraceuticals and bioactive compounds. Boca Raton: CRC Press – Taylor & Francis Group, 2008. cap. 8, p.243-274.
[2] SOVOVÁ, H. Rate of the Vegetable Oil Extraction with Supercritical CO_2: I. Modeling of Extraction Curves. Chemical Engineering Science, v. 3, n. 49, 1994, p. 409-414.

(desde que, e somente se, o critério de aumento de escala proposto por Prado[3] seja válido).

Nos ajustes usando o modelo de Sovová (Capítulo 4) também foram obtidos baixos valores para os MSEs (em geral próximos aos do modelo *spline*). Além disso, a grande vantagem do modelo de Sovová consiste na explicação fenomenológica da transferência de massa, visto que este é baseado no balanço diferencial de massa dentro do leito de extração. Portanto, tal modelo possui parâmetros ajustáveis com significados físicos bem definidos, o que em teoria permite a aplicação destes na predição do aumento de escala. Contudo, a maior dificuldade associada à aplicação do modelo de Sovová está na necessidade de conhecer a solubilidade do extrato (Y*), que é um parâmetro cuja determinação experimental é muito trabalhosa e que, para diversos sistemas de interesse, ainda não se encontra disponível na literatura. Nos casos em que o valor experimental de Y* não seja conhecido, é possível aplicar o modelo de Sovová baseando-se em estimativas para tal parâmetro (por exemplo: usar a solubilidade de algum extrato semelhante, cujo valor experimental esteja disponível). Porém, se o valor de Y* não refletir a solubilidade real do sistema em estudo, então os valores ajustados para os coeficientes de transferência de massa (k_{YA} e k_{XA}) também não refletirão uma visão realista de tais coeficientes. Neste caso, os parâmetros ajustáveis do modelo passam a ter valores questionáveis no que diz respeito à coerência de seus significados físicos.

Por fim, considera-se importante ressaltar que os modelos fenomenológicos são, sem dúvida, de grande importância para auxiliar no entendimento dos fenômenos físicos que ocorrem dentro do leito de extração. De fato, a descrição fenomenológica é essencial para conhecer as características e limitações do sistema em termos de termodinâmica (equilíbrio de fases) e transferência de massa. Porém, na prática, tais modelos e seus parâmetros não fornecem informações que auxiliem diretamente na tomada de decisões

[3] PRADO, J. M. Estudo do aumento de escala do processo de extração supercrítica em leito fixo. Tese (Doutorado), Universidade Estadual de Campinas, Faculdade de Engenharia de Alimentos, Campinas, 2010, 250p.

associadas a estudos preliminares de simulação e análise econômica da SFE em escala industrial. Nos trabalhos publicados sobre modelagem matemática da OEC, é comum que os autores sugiram que os modelos ajustados podem ter potencial para predizer dados em maior escala. Entretanto, na grande maioria dos casos, nenhum dado em escala piloto é apresentado para demonstrar a validade do potencial sugerido. De fato, há poucos dados de transposição de escala disponíveis na literatura aberta, sendo este um tema que ainda é controverso e que possui muitos aspectos não esclarecidos. Apesar disso, é interessante mencionar que um critério de aumento de escala simples (manter S/F e t_{RES} constantes, conforme discutido na Seção 3.8 do Capítulo 2) tem se mostrado eficiente ao reproduzir em escala piloto os mesmos rendimentos e comportamentos cinéticos previamente obtidos em escala de laboratório. Portanto, uma vez que tal critério seja válido para determinado sistema (matriz sólida + CO_2), a curva de extração tende a manter seu formato na transposição de escala. Assim sendo, qualquer modelo (inclusive empírico) teria potencial de ser aplicado para estimar dados em maior escala, desde que o mesmo forneça uma boa descrição quantitativa da OEC.

APÊNDICES

APÊNDICE A1. DESCRIÇÃO DA BASE DE DADOS

Inicialmente, dados de experimentos cinéticos para seis matérias-primas selecionadas (cravo, gengibre, semente de uva, cidrão, resíduo de cana-de-açúcar e semente de urucum) foram coletados nas teses desenvolvidas por Alberto Shintaku (2006), Juliana Martin do Prado (2010) e Carolina Lima Cavalcanti de Albuquerque (2013). Tal conjunto de dados foi escolhido em função de dois motivos principais: (1) por formar um grupo heterogêneo de matrizes vegetais; (2) porque o processo SFE dessas matérias-primas foi estudado de forma global (incluindo aumento de escala) nos trabalhos de Prado (2010) e Albuquerque (2013). Diante dos motivos mencionados, este conjunto de dados mostrou-se interessante para ser utilizado na elaboração e validação das metodologias de cálculo empregadas no presente projeto.

Tendo em vista o interesse na curva global de extração (OEC), foram coletadas as seguintes informações para cada uma das matérias-primas selecionadas:

(a) descrição e preparo da matéria-prima: parte utilizada e forma de pré-tratamento;

(b) caracterização das partículas sólidas: umidade, diâmetro médio de partícula, densidade real;

(c) caracterização do leito fixo de extração: densidade aparente, porosidade, geometria;

(d) dados dos experimentos cinéticos: parâmetros de processo e pontos experimentais da OEC.

Os dados experimentais coletados (ver Tabela A1) foram utilizados para o cálculo de dados adicionais por meio das fórmulas apresentadas nas equações a seguir:

$$m_{seca} = m_{MP}\left(\frac{100 - U}{100}\right) \qquad (A1)$$

$$m_{CO2[total]} = m_{MP}\left(\frac{S}{F}\right)_{[total]} \qquad (A2)$$

$$Q_{CO2} = \frac{m_{CO2[total]}}{(60)(1000)\ t_{[total]}} \qquad (A3)$$

$$X_{0\left(\frac{S}{F}\right)} = \frac{m_{EXT}}{m_{seca}} \qquad (A4.1)$$

$$X_{0\left(\frac{S}{F}\right)}(\%) = 100\,\frac{m_{EXT}}{m_{seca}} \qquad (A4.2)$$

$$m_{CO2} = (60)(1000)\ Q_{CO2}\ t \qquad (A5)$$

$$\left(\frac{S}{F}\right)_{[b.u]} = \frac{m_{CO2}}{m_{MP}} \qquad (A6)$$

$$\left(\frac{S}{F}\right)_{[b.s]} = \frac{m_{CO2}}{m_{seca}} \qquad (A7)$$

Onde:

m_{seca} = massa de matéria seca na alimentação (g);

m_{MP} = massa de matéria-prima alimentada no leito (g);

U = umidade da matéria-prima (%, m/m);

$m_{CO2[total]}$ = massa total de CO_2 consumida no experimento (g);

$(S/F)_{[total]}$ = razão S/F total do experimento (base úmida);

Q_{CO2} = vazão média de CO_2 (kg/s);

$t_{[total]}$ = tempo total do experimento (min);

60 = fator de conversão (s/min);

1000 = fator de conversão (g/kg);

$X_{0(S/F)}$ = Rendimento (base seca) expresso na forma de razão mássica (g/g) (Equação A4.1) ou porcentagem (%) (Equação A4.2);

m_{EXT} = massa de extrato (g);

m_{CO2} = massa de CO_2 (g);

$(S/F)_{[b.u.]}$ = razão S/F (base úmida);

$(S/F)_{[b.s.]}$ = razão S/F (base seca).

Para as seis matérias-primas selecionadas fez-se a coleta dos dados de experimentos cinéticos (OEC) conduzidos em duplicata. Os dados experimentais coletados e dados calculados (conforme Tabela A1) estão apresentados nas fichas de dados apresentadas na parte final do apêndice em questão.

Tabela A1. Descrição dos dados (experimentais e calculados) que formam a base de dados de cada matéria-prima selecionada para estudo

DADOS EXPERIMENTAIS [1]	
Símbolo (Unidade)	Descrição
Dados de caracterização das partículas sólidas	
U (%, m/m)	Umidade da matéria-prima
d_P (m)	Diâmetro médio de partícula
ρ_S (kg/m^3)	Densidade real do sólido
Dados de caracterização do leito de extração	
ρ_A (kg/m^3)	Densidade aparente do leito
ε	Porosidade do leito
(H_B/d_B)	Altura do leito/diâmetro do leito
Dados gerais do experimento cinético	
T (K)	Temperatura
P (MPa)	Pressão
ρ_{CO2} (kg/m^3)	Densidade do CO_2
m_{MP} (g)	Massa de matéria-prima alimentada no leito
$(S/F)_{[total]}$ [4]	Razão S/F total do experimento
$t_{[total]}$ (min)	Tempo total do experimento
Dados pontuais do experimento cinético	
m_{EXT} (g) [3]	Massa de extrato
t (min)	Tempo
DADOS CALCULADOS [2]	
Símbolo (Unidade)	Descrição
Dados gerais para o experimento cinético	
m_{seca} (g)	Massa de matéria seca na alimentação
$m_{CO2[total]}$ (g)	Massa total de CO_2 consumida no experimento
Q_{CO2} (kg/s) [4]	Vazão média de CO_2
Dados pontuais para o experimento cinético	
$X_{0(S/F)}$ (g/g ou %; b.s.) [3]	Rendimento em base seca
m_{CO2} (g)	Massa de CO_2
$S/F_{[b.u.]}$	Razão S/F em base úmida
$S/F_{[b.s.]}$	Razão S/F em base seca

[1] Dados experimentais coletados nas teses originais (SHINTAKU, 2006; PRADO, 2010; ALBUQUERQUE, 2013). [2] Dados calculados utilizando as equações A1 a A7.
[3] Para os dados de urucum coletados na tese de Albuquerque (2013), X_0 é dado experimental e m_{EXT} é dado calculado.
[4] Para os dados de resíduo de cana-de-açúcar coletados na tese de Shintaku (2006), Q_{CO2} é dado experimental e $(S/F)_{[TOTAL]}$ é dado calculado.

FICHA DE DADOS: Cravo - Replicata nº1

Dados gerais de referência

Autor (ano)	Juliana M. Prado (2010)
Grupo de pesquisa	LASEFI/DEA/FEA/Unicamp
Tipo de trabalho	Tese de doutorado

Descrição e preparo da matéria-prima

Nome	cravo-da-índia
Parte utilizada	botões florais
Forma recebida	seco
Modo de preparo	moagem

Caracterização das partículas sólidas

Umidade (%)	8,6
dp (m)	9,08E-04
ρ_R (kg/m^3)	1422

Dados do experimento cinético

ρ_A (kg/m^3)	779
Porosidade	0,452
(H_B/d_B)	2,31
T (K)	313
P (MPa)	15
ρ_{CO2} (kg/m^3)	766,51
m_{MP} (g)	229,54
[S/F]total (b.u.)	8,87
t (total) (min)	360

Dados calculados

m_{seca} (g)	209,80
$m_{CO2\ TOTAL}$ (g)	2036,02
Q_{CO2} (kg/s)	9,43E-05

Dados Experimentais		*Dados calculados*			
tempo (min)	**massa de extrato (g)**	**Rendimento (%, m/m) (b.s.)**	**massa de CO2 (g)**	**S/F (b.u.)**	**S/F (b.s.)**
0	0,00	0,00	0,00	0,00	0,00
5	2,34	1,12	28,28	0,12	0,13
10	6,38	3,04	56,56	0,25	0,27
15	9,35	4,45	84,83	0,37	0,40
20	11,14	5,31	113,11	0,49	0,54
25	12,82	6,11	141,39	0,62	0,67
30	14,28	6,81	169,67	0,74	0,81
40	16,58	7,90	226,22	0,99	1,08
50	18,46	8,80	282,78	1,23	1,35
60	20,19	9,62	339,34	1,48	1,62
70	21,70	10,35	395,89	1,72	1,89
80	22,98	10,95	452,45	1,97	2,16
90	24,07	11,48	509,00	2,22	2,43
100	25,02	11,93	565,56	2,46	2,70
110	25,83	12,31	622,12	2,71	2,97
120	26,56	12,66	678,67	2,96	3,23
140	27,79	13,25	791,79	3,45	3,77
160	28,73	13,69	904,90	3,94	4,31
180	29,45	14,03	1018,01	4,44	4,85
200	29,92	14,26	1131,12	4,93	5,39
220	30,28	14,43	1244,23	5,42	5,93
240	30,58	14,57	1357,35	5,91	6,47
270	30,92	14,74	1527,01	6,65	7,28
300	31,21	14,88	1696,68	7,39	8,09
330	31,44	14,98	1866,35	8,13	8,90
360	31,67	15,10	2036,02	8,87	9,70

FICHA DE DADOS: Cravo - Replicata nº2

Dados gerais de referência

Autor (ano)	Juliana M. Prado (2010)
Grupo de pesquisa	LASEFI/DEA/FEA/Unicamp
Tipo de trabalho	Tese de doutorado

Descrição e preparo da matéria-prima

Nome	cravo-da-índia
Parte utilizada	botões florais
Forma recebida	seco
Modo de preparo	moagem

Caracterização das partículas sólidas

Umidade (%)	8,6
dp (m)	9,08E-04
ρ_R (kg/m^3)	1422

Dados do experimento cinético

ρ_A (kg/m^3)	779
Porosidade	0,452
(H_B/d_B)	2,31
T (K)	313
P (MPa)	15
ρ_{CO2} (kg/m^3)	766,51
m_{MP} (g)	222,35
[S/F]total (b.u.)	9,48
t (total) (min)	360

Dados calculados

m_{seca} (g)	203,23
$m_{CO2\ TOTAL}$ (g)	2107,88
Q_{CO2} (kg/s)	9,76E-05

Dados Experimentais		*Dados calculados*			
tempo (min)	**massa de extrato (g)**	**Rendimento (%, m/m) (b.s.)**	**massa de CO2 (g)**	**S/F (b.u.)**	**S/F (b.s.)**
0	0,00	0,00	0,00	0,00	0,00
5	1,90	0,94	29,28	0,13	0,14
10	5,47	2,69	58,55	0,26	0,29
15	7,81	3,84	87,83	0,40	0,43
20	9,41	4,63	117,10	0,53	0,58
25	10,61	5,22	146,38	0,66	0,72
30	11,64	5,73	175,66	0,79	0,86
40	13,51	6,65	234,21	1,05	1,15
50	15,29	7,52	292,76	1,32	1,44
60	16,85	8,29	351,31	1,58	1,73
70	18,20	8,96	409,87	1,84	2,02
80	19,44	9,57	468,42	2,11	2,30
90	20,40	10,04	526,97	2,37	2,59
100	21,37	10,52	585,52	2,63	2,88
110	22,26	10,95	644,07	2,90	3,17
120	23,01	11,32	702,63	3,16	3,46
140	24,23	11,92	819,73	3,69	4,03
160	25,34	12,47	936,83	4,21	4,61
180	26,26	12,92	1053,94	4,74	5,19
200	26,92	13,25	1171,04	5,27	5,76
220	27,51	13,54	1288,15	5,79	6,34
240	28,02	13,79	1405,25	6,32	6,91
270	28,60	14,07	1580,91	7,11	7,78
300	29,07	14,30	1756,57	7,90	8,64
330	29,52	14,53	1932,22	8,69	9,51
360	29,88	14,70	2107,88	9,48	10,37

FICHA DE DADOS: Gengibre - Replicata nº1

Dados gerais de referência

Autor (ano)	Juliana M. Prado (2010)
Grupo de pesquisa	LASEFI/DEA/FEA/Unicamp
Tipo de trabalho	Tese de doutorado

Descrição e preparo da matéria-prima

Nome	gengibre
Parte utilizada	rizomas
Forma recebida	rasurado
Modo de preparo	moagem

Caracterização das partículas sólidas

Umidade (%)	8,3
dp (m)	7,55E-04
ρ_R (kg/m^3)	1477

Dados do experimento cinético

ρ_A (kg/m^3)	728
Porosidade	0,507
(H_B/d_B)	1,65
T (K)	313
P (MPa)	30
ρ_{CO2} (kg/m^3)	910,47
m_{MP} (g)	149,97
[S/F]total (b.u.)	14,44
t (total) (min)	360

Dados calculados

m_{seca} (g)	137,52
$m_{CO2\ TOTAL}$ (g)	2165,57
Q_{CO2} (kg/s)	1,00E-04

Dados Experimentais		*Dados calculados*			
tempo (min)	**massa de extrato (g)**	**Rendimento (%, m/m) (b.s.)**	**massa de CO2 (g)**	**S/F (b.u.)**	**S/F (b.s.)**
0	0,00	0,00	0,00	0,00	0,00
5	1,01	0,74	30,08	0,20	0,22
10	1,87	1,36	60,15	0,40	0,44
15	2,46	1,79	90,23	0,60	0,66
20	2,88	2,10	120,31	0,80	0,87
30	3,39	2,47	180,46	1,20	1,31
40	3,67	2,67	240,62	1,60	1,75
50	3,83	2,79	300,77	2,01	2,19
60	3,96	2,88	360,93	2,41	2,62
80	4,14	3,01	481,24	3,21	3,50
100	4,28	3,11	601,55	4,01	4,37
120	4,40	3,20	721,86	4,81	5,25
150	4,55	3,31	902,32	6,02	6,56
180	4,66	3,39	1082,78	7,22	7,87
210	4,76	3,46	1263,25	8,42	9,19
240	4,84	3,52	1443,71	9,63	10,50
270	4,90	3,57	1624,18	10,83	11,81
300	4,97	3,61	1804,64	12,03	13,12
360	5,06	3,68	2165,57	14,44	15,75

FICHA DE DADOS: Gengibre - Replicata nº2

Dados gerais de referência

Autor (ano)	Juliana M. Prado (2010)
Grupo de pesquisa	LASEFI/DEA/FEA/Unicamp
Tipo de trabalho	Tese de doutorado

Descrição e preparo da matéria-prima

Nome	gengibre
Parte utilizada	rizomas
Forma recebida	rasurado
Modo de preparo	moagem

Caracterização das partículas sólidas

Umidade (%)	8,3
dp (m)	7,55E-04
ρ_R (kg/m^3)	1477

Dados do experimento cinético

ρ_A (kg/m^3)	728
Porosidade	0,507
(H_B/d_B)	1,65
T (K)	313
P (MPa)	30
ρ_{CO2} (kg/m^3)	910,47
m_{MP} (g)	149,96
[S/F]total (b.u.)	14,87
t (total) (min)	360

Dados calculados

m_{seca} (g)	137,51
$m_{CO2\ TOTAL}$ (g)	2229,91
Q_{CO2} (kg/s)	1,03E-04

Dados Experimentais		***Dados calculados***			
tempo (min)	**massa de extrato (g)**	**Rendimento (%, m/m) (b.s.)**	**massa de CO2 (g)**	**S/F (b.u.)**	**S/F (b.s.)**
0	0,00	0,00	0,00	0,00	0,00
5	1,12	0,81	30,97	0,21	0,23
10	1,96	1,43	61,94	0,41	0,45
15	2,56	1,86	92,91	0,62	0,68
20	2,96	2,15	123,88	0,83	0,90
30	3,45	2,51	185,83	1,24	1,35
40	3,74	2,72	247,77	1,65	1,80
50	3,93	2,86	309,71	2,07	2,25
60	4,07	2,96	371,65	2,48	2,70
80	4,28	3,12	495,53	3,30	3,60
100	4,46	3,24	619,42	4,13	4,50
120	4,59	3,34	743,30	4,96	5,41
150	4,74	3,45	929,13	6,20	6,76
180	4,86	3,53	1114,95	7,44	8,11
210	4,95	3,60	1300,78	8,67	9,46
240	5,03	3,66	1486,60	9,91	10,81
270	5,10	3,71	1672,43	11,15	12,16
300	5,16	3,75	1858,25	12,39	13,51
360	5,25	3,82	2229,91	14,87	16,22

FICHA DE DADOS: Semente de uva - Replicata nº1

Dados gerais de referência

Autor (ano)	Juliana M. Prado (2010)
Grupo de pesquisa	LASEFI/DEA/FEA/Unicamp
Tipo de trabalho	Tese de doutorado

Descrição e preparo da matéria-prima

Nome	resíduo de uva (fermentação do vinho)
Parte utilizada	sementes
Forma recebida	seca
Modo de preparo	moagem

Caracterização das partículas sólidas

Umidade (%)	12
dp (m)	7,79E-04
ρ_R (kg/m^3)	1408

Dados do experimento cinético

ρ_A (kg/m^3)	966
Porosidade	0,314
(H_B/d_B)	2,31
T (K)	313
P (MPa)	35
ρ_{CO2} (kg/m^3)	935,34
m_{MP} (g)	274,89
[S/F]total (b.u.)	12,32
t (total) (min)	450

Dados calculados

m_{seca} (g)	241,90
$m_{CO2\ TOTAL}$ (g)	3386,64
Q_{CO2} (kg/s)	1,25E-04

Dados Experimentais		*Dados calculados*			
tempo (min)	**massa de extrato (g)**	**Rendimento (%, m/m) (b.s.)**	**massa de CO2 (g)**	**S/F (b.u.)**	**S/F (b.s.)**
0	0,00	0,00	0,00	0,00	0,00
5	0,41	0,17	37,63	0,14	0,16
10	0,90	0,37	75,26	0,27	0,31
15	1,37	0,57	112,89	0,41	0,47
30	2,74	1,13	225,78	0,82	0,93
45	4,13	1,71	338,66	1,23	1,40
60	5,48	2,26	451,55	1,64	1,87
75	6,84	2,83	564,44	2,05	2,33
90	8,21	3,39	677,33	2,46	2,80
105	9,57	3,96	790,22	2,87	3,27
120	11,00	4,55	903,11	3,29	3,73
135	12,41	5,13	1015,99	3,70	4,20
150	13,79	5,70	1128,88	4,11	4,67
165	15,22	6,29	1241,77	4,52	5,13
180	16,60	6,86	1354,66	4,93	5,60
195	17,97	7,43	1467,55	5,34	6,07
210	19,34	8,00	1580,43	5,75	6,53
225	20,69	8,55	1693,32	6,16	7,00
240	22,03	9,11	1806,21	6,57	7,47
270	24,59	10,17	2031,99	7,39	8,40
300	26,95	11,14	2257,76	8,21	9,33
330	28,94	11,97	2483,54	9,03	10,27
360	30,20	12,49	2709,32	9,86	11,20
390	30,88	12,77	2935,09	10,68	12,13
420	31,05	12,84	3160,87	11,50	13,07
450	31,12	12,87	3386,64	12,32	14,00

FICHA DE DADOS: Semente de uva - Replicata nº2

Dados gerais de referência

Autor (ano)	Juliana M. Prado (2010)
Grupo de pesquisa	LASEFI/DEA/FEA/Unicamp
Tipo de trabalho	Tese de doutorado

Descrição e preparo da matéria-prima

Nome	resíduo de uva (fermentação do vinho)
Parte utilizada	sementes
Forma recebida	seca
Modo de preparo	moagem

Caracterização das partículas sólidas

Umidade (%)	12
dp (m)	7,79E-04
ρ_R (kg/m^3)	1408

Dados do experimento cinético

ρ_A (kg/m^3)	966
Porosidade	0,314
(H_B/d_B)	2,31
T (K)	313
P (MPa)	35
ρ_{CO2} (kg/m^3)	935,34
m_{MP} (g)	285,04
[S/F]total (b.u.)	12,86
t (total) (min)	450

Dados calculados

m_{seca} (g)	250,84
$m_{CO2\ TOTAL}$ (g)	3665,61
Q_{CO2} (kg/s)	1,36E-04

Dados Experimentais		*Dados calculados*			
tempo (min)	**massa de extrato (g)**	**Rendimento (%, m/m) (b.s.)**	**massa de CO2 (g)**	**S/F (b.u.)**	**S/F (b.s.)**
0	0,00	0,00	0,00	0,00	0,00
5	0,44	0,18	40,73	0,14	0,16
10	0,91	0,36	81,46	0,29	0,32
15	1,37	0,55	122,19	0,43	0,49
30	2,90	1,16	244,37	0,86	0,97
45	4,37	1,74	366,56	1,29	1,46
60	5,82	2,32	488,75	1,71	1,95
75	7,32	2,92	610,94	2,14	2,44
90	8,83	3,52	733,12	2,57	2,92
105	10,33	4,12	855,31	3,00	3,41
120	11,88	4,73	977,50	3,43	3,90
135	13,38	5,33	1099,68	3,86	4,38
150	14,81	5,91	1221,87	4,29	4,87
165	16,29	6,50	1344,06	4,72	5,36
180	17,79	7,09	1466,25	5,14	5,85
195	19,19	7,65	1588,43	5,57	6,33
210	20,62	8,22	1710,62	6,00	6,82
225	22,03	8,78	1832,81	6,43	7,31
240	23,43	9,34	1954,99	6,86	7,79
270	26,04	10,38	2199,37	7,72	8,77
300	28,35	11,30	2443,74	8,57	9,74
330	30,39	12,11	2688,12	9,43	10,72
360	32,02	12,77	2932,49	10,29	11,69
390	33,37	13,30	3176,87	11,15	12,67
420	34,30	13,68	3421,24	12,00	13,64
450	35,05	13,97	3665,61	12,86	14,61

FICHA DE DADOS: Cidrão - Replicata nº1

Dados gerais de referência

Autor (ano)	Juliana M. Prado (2010)
Grupo de pesquisa	LASEFI/DEA/FEA/Unicamp
Tipo de trabalho	Tese de doutorado

Descrição e preparo da matéria-prima

Nome	cidrão
Parte utilizada	folhas
Forma recebida	seco
Modo de preparo	moagem

Caracterização das partículas sólidas

Umidade (%)	5,3
dp (m)	6,72E-04
ρ_R (kg/m^3)	1453

Dados do experimento cinético

ρ_A (kg/m^3)	420
Porosidade	0,711
(H_B/d_B)	2,31
T (K)	333
P (MPa)	35
ρ_{CO2} (kg/m^3)	863,49
m_{MP} (g)	119,27
[S/F]total (b.u.)	19,45
t (total) (min)	420

Dados calculados

m_{seca} (g)	112,95
$m_{CO2\ TOTAL}$ (g)	2319,80
Q_{CO2} (kg/s)	9,21E-05

Dados Experimentais		***Dados calculados***			
tempo (min)	**massa de extrato (g)**	**Rendimento (%, m/m) (b.s.)**	**massa de CO2 (g)**	**S/F (b.u.)**	**S/F (b.s.)**
0	0,00	0,00	0,00	0,00	0,00
15	0,38	0,34	82,85	0,69	0,73
30	0,59	0,53	165,70	1,39	1,47
45	0,75	0,66	248,55	2,08	2,20
60	0,89	0,79	331,40	2,78	2,93
90	1,11	0,98	497,10	4,17	4,40
120	1,32	1,17	662,80	5,56	5,87
150	1,51	1,34	828,50	6,95	7,34
180	1,68	1,49	994,20	8,34	8,80
210	1,80	1,59	1159,90	9,73	10,27
240	1,87	1,65	1325,60	11,11	11,74
270	1,94	1,72	1491,30	12,50	13,20
300	1,98	1,76	1657,00	13,89	14,67
360	2,07	1,84	1988,40	16,67	17,60
420	2,17	1,92	2319,80	19,45	20,54

FICHA DE DADOS: Cidrão - Replicata nº2

Dados gerais de referência

Autor (ano)	Juliana M. Prado (2010)
Grupo de pesquisa	LASEFI/DEA/FEA/Unicamp
Tipo de trabalho	Tese de doutorado

Descrição e preparo da matéria-prima

Nome	cidrão
Parte utilizada	folhas
Forma recebida	seco
Modo de preparo	moagem

Caracterização das partículas sólidas

Umidade (%)	5,3
dp (m)	6,72E-04
ρ_R (kg/m^3)	1453

Dados do experimento cinético

ρ_A (kg/m^3)	420
Porosidade	0,711
(H_B/d_B)	2,31
T (K)	333
P (MPa)	35
ρ_{CO2} (kg/m^3)	863,49
m_{MP} (g)	124,61
[S/F]total (b.u.)	22,82
t (total) (min)	420

Dados calculados

m_{seca} (g)	118,01
$m_{CO2\ TOTAL}$ (g)	2843,60
Q_{CO2} (kg/s)	1,13E-04

Dados Experimentais		*Dados calculados*			
tempo (min)	**massa de extrato (g)**	**Rendimento (%, m/m) (b.s.)**	**massa de CO2 (g)**	**S/F (b.u.)**	**S/F (b.s.)**
0	0,00	0,00	0,00	0,00	0,00
15	0,45	0,38	101,56	0,82	0,86
30	0,75	0,63	203,11	1,63	1,72
45	0,94	0,80	304,67	2,45	2,58
60	1,12	0,95	406,23	3,26	3,44
90	1,39	1,18	609,34	4,89	5,16
120	1,56	1,32	812,46	6,52	6,88
150	1,68	1,43	1015,57	8,15	8,61
180	1,79	1,51	1218,69	9,78	10,33
210	1,87	1,58	1421,80	11,41	12,05
240	1,93	1,64	1624,91	13,04	13,77
270	1,99	1,69	1828,03	14,67	15,49
300	2,04	1,73	2031,14	16,30	17,21
360	2,12	1,80	2437,37	19,56	20,65
420	2,19	1,86	2843,60	22,82	24,10

FICHA DE DADOS: Resíduo de cana-de-açúcar (Lote 1) - Replicata nº1

Dados gerais de referência

Autor (ano)	Juliana M. Prado (2010)
Grupo de pesquisa	LASEFI/DEA/FEA/Unicamp
Tipo de trabalho	Tese de doutorado

Descrição e preparo da matéria-prima

Nome	resíduo de cana-de-açúcar
Parte utilizada	torta de filtro
Forma recebida	seco
Modo de preparo	moagem

Caracterização das partículas sólidas

Umidade (%)	~ 0 (menor que 0,6 %)
dp (m)	7,69E-04
ρ_R (kg/m^3)	1731

Dados do experimento cinético

ρ_A (kg/m^3)	302
Porosidade	0,826
(H_B/d_B)	2,31
T (K)	333
P (MPa)	35
ρ_{CO2} (kg/m^3)	863,49
m_{MP} (g)	88,27
[S/F]total (b.u.)	28,64
t (total) (min)	360

Dados calculados

m_{seca} (g)	88,27
$m_{CO2\ TOTAL}$ (g)	2528,05
Q_{CO2} (kg/s)	1,17E-04

Dados Experimentais		***Dados calculados***			
tempo (min)	**massa de extrato (g)**	**Rendimento (%, m/m) (b.s.)**	**massa de CO2 (g)**	**S/F (b.u.)**	**S/F (b.s.)**
0	0,00	0,00	0,00	0,00	0,00
10	0,29	0,33	70,22	0,80	0,80
20	0,53	0,60	140,45	1,59	1,59
30	0,77	0,87	210,67	2,39	2,39
40	0,98	1,12	280,89	3,18	3,18
50	1,15	1,30	351,12	3,98	3,98
60	1,32	1,49	421,34	4,77	4,77
70	1,47	1,66	491,57	5,57	5,57
80	1,60	1,81	561,79	6,36	6,36
90	1,72	1,95	632,01	7,16	7,16
100	1,82	2,06	702,24	7,96	7,96
110	1,90	2,15	772,46	8,75	8,75
120	1,98	2,24	842,68	9,55	9,55
150	2,14	2,43	1053,36	11,93	11,93
180	2,21	2,51	1264,03	14,32	14,32
210	2,30	2,60	1474,70	16,71	16,71
240	2,35	2,66	1685,37	19,09	19,09
270	2,38	2,70	1896,04	21,48	21,48
300	2,41	2,73	2106,71	23,87	23,87
330	2,42	2,74	2317,38	26,25	26,25
360	2,43	2,75	2528,05	28,64	28,64

FICHA DE DADOS: Resíduo de cana-de-açúcar (Lote 1) - Replicata nº2

Dados gerais de referência

Autor (ano)	Juliana M. Prado (2010)
Grupo de pesquisa	LASEFI/DEA/FEA/Unicamp
Tipo de trabalho	Tese de doutorado

Descrição e preparo da matéria-prima

Nome	resíduo de cana-de-açúcar
Parte utilizada	torta de filtro
Forma recebida	seco
Modo de preparo	moagem

Caracterização das partículas sólidas

Umidade (%)	~ 0 (menor que 0,6 %)
dp (m)	7,69E-04
ρ_R (kg/m^3)	1731

Dados do experimento cinético

ρ_A (kg/m^3)	302
Porosidade	0,826
(H_B/d_B)	2,31
T (K)	333
P (MPa)	35
ρ_{CO2} (kg/m^3)	863,49
m_{MP} (g)	87,03
[S/F]total (b.u.)	30,75
t (total) (min)	360

Dados calculados

m_{seca} (g)	87,03
$m_{CO2\ TOTAL}$ (g)	2676,17
Q_{CO2} (kg/s)	1,24E-04

Dados Experimentais		***Dados calculados***			
tempo (min)	**massa de extrato (g)**	**Rendimento (%, m/m) (b.s.)**	**massa de CO2 (g)**	**S/F (b.u.)**	**S/F (b.s.)**
0	0,00	0,00	0,00	0,00	0,00
10	0,35	0,40	74,34	0,85	0,85
20	0,63	0,73	148,68	1,71	1,71
30	0,87	1,00	223,01	2,56	2,56
40	1,02	1,17	297,35	3,42	3,42
50	1,15	1,32	371,69	4,27	4,27
60	1,28	1,47	446,03	5,13	5,13
70	1,38	1,59	520,37	5,98	5,98
80	1,47	1,69	594,71	6,83	6,83
90	1,57	1,80	669,04	7,69	7,69
100	1,64	1,89	743,38	8,54	8,54
110	1,71	1,97	817,72	9,40	9,40
120	1,77	2,03	892,06	10,25	10,25
150	1,91	2,20	1115,07	12,81	12,81
180	1,99	2,29	1338,09	15,38	15,38
210	2,06	2,36	1561,10	17,94	17,94
240	2,10	2,41	1784,12	20,50	20,50
270	2,13	2,45	2007,13	23,06	23,06
300	2,15	2,47	2230,14	25,63	25,63
330	2,18	2,51	2453,16	28,19	28,19
360	2,20	2,53	2676,17	30,75	30,75

FICHA DE DADOS: Resíduo de cana-de-açúcar (Lote 2 / Curva 1) - Replicata nº1

Dados gerais de referência

Autor (ano)	Alberto Shintaku (2006)
Grupo de pesquisa	LASEFI/DEA/FEA/Unicamp
Tipo de trabalho	Dissertação de mestrado

Descrição e preparo da matéria-prima

Nome	resíduo de cana-de-açúcar
Parte utilizada	torta de filtro
Forma recebida	seco
Modo de preparo	moagem

Caracterização das partículas sólidas

Umidade (%)	não informada
dp (m)	2,80E-04
ρ_R (kg/m^3)	1740

Dados do experimento cinético

ρ_A (kg/m^3)	261,8
Porosidade	0,85
(H_B/d_B)	0,78
T (K)	323
P (MPa)	20
ρ_{CO2} (kg/m^3)	785,16
m_{MP} (g)	25
Q_{CO2} (kg/s)	6,91E-05
t (total) (min)	360

Dados calculados

m_{seca} (g)	não calculada
$m_{CO2\ TOTAL}$ (g)	1492,56
[S/F]total (b.u.)	59,70

Dados Experimentais		***Dados calculados***		
tempo (min)	**massa de extrato (g)**	**Rendimento (%, m/m) (b.u.)**	**massa de CO2 (g)**	**S/F (b.u.)**
0	0,0000	0,00	0,00	0,00
10	0,0290	0,12	41,46	1,66
20	0,0818	0,33	82,92	3,32
30	0,1504	0,60	124,38	4,98
40	0,2057	0,82	165,84	6,63
50	0,2499	1,00	207,30	8,29
60	0,2878	1,15	248,76	9,95
70	0,3134	1,25	290,22	11,61
80	0,3384	1,35	331,68	13,27
90	0,3593	1,44	373,14	14,93
120	0,4066	1,63	497,52	19,90
150	0,4416	1,77	621,90	24,88
180	0,4758	1,90	746,28	29,85
210	0,4944	1,98	870,66	34,83
240	0,5042	2,02	995,04	39,80
270	0,5193	2,08	1119,42	44,78
300	0,5258	2,10	1243,80	49,75
330	0,5356	2,14	1368,18	54,73
360	0,5432	2,17	1492,56	59,70

FICHA DE DADOS: Resíduo de cana-de-açúcar (Lote 2 / Curva 1) - Replicata nº2

Dados gerais de referência

Autor (ano)	Alberto Shintaku (2006)
Grupo de pesquisa	LASEFI/DEA/FEA/Unicamp
Tipo de trabalho	Dissertação de mestrado

Descrição e preparo da matéria-prima

Nome	resíduo de cana-de-açúcar
Parte utilizada	torta de filtro
Forma recebida	seco
Modo de preparo	moagem

Caracterização das partículas sólidas

Umidade (%)	não informada
dp (m)	2,80E-04
ρ_R (kg/m^3)	1740

Dados do experimento cinético

ρ_A (kg/m^3)	261,8
Porosidade	0,85
(H_B/d_B)	0,78
T (K)	323
P (MPa)	20
ρ_{CO2} (kg/m^3)	785,16
m_{MP} (g)	25
Q_{CO2} (kg/s)	6,97E-05
t (total) (min)	360

Dados calculados

m_{seca} (g)	não calculada
$m_{CO2\ TOTAL}$ (g)	1505,52
[S/F]total (b.u.)	60,22

Dados Experimentais		*Dados calculados*		
tempo (min)	**massa de extrato (g)**	**Rendimento (%, m/m) (b.u.)**	**massa de CO2 (g)**	**S/F (b.u.)**
0	0,0000	0,00	0,00	0,00
10	0,0462	0,18	41,82	1,67
20	0,1193	0,48	83,64	3,35
30	0,1997	0,80	125,46	5,02
40	0,2483	0,99	167,28	6,69
50	0,2870	1,15	209,10	8,36
60	0,3236	1,29	250,92	10,04
70	0,3467	1,39	292,74	11,71
80	0,3655	1,46	334,56	13,38
90	0,3834	1,53	376,38	15,06
120	0,4148	1,66	501,84	20,07
150	0,4495	1,80	627,30	25,09
180	0,4819	1,93	752,76	30,11
210	0,5010	2,00	878,22	35,13
240	0,5294	2,12	1003,68	40,15
270	0,5509	2,20	1129,14	45,17
300	0,5600	2,24	1254,60	50,18
330	0,5680	2,27	1380,06	55,20
360	0,5777	2,31	1505,52	60,22

FICHA DE DADOS: Resíduo de cana-de-açúcar (Lote 2 / Curva 2) - Replicata nº1

Dados gerais de referência

Autor (ano)	Alberto Shintaku (2006)
Grupo de pesquisa	LASEFI/DEA/FEA/Unicamp
Tipo de trabalho	Dissertação de mestrado

Descrição e preparo da matéria-prima

Nome	resíduo de cana-de-açúcar
Parte utilizada	torta de filtro
Forma recebida	seco
Modo de preparo	moagem

Caracterização das partículas sólidas

Umidade (%)	não informada
dp (m)	2,80E-04
ρ_R (kg/m^3)	1740

Dados do experimento cinético

ρ_A (kg/m^3)	261,8
Porosidade	0,85
(H_B/d_B)	0,78
T (K)	323
P (MPa)	35
ρ_{CO2} (kg/m^3)	899,77
m_{MP} (g)	25
Q_{CO2} (kg/s)	7,00E-05
t (total) (min)	360

Dados calculados

m_{seca} (g)	não calculada
$m_{CO2\ TOTAL}$ (g)	1512,00
[S/F]total (b.u.)	60,48

Dados Experimentais		*Dados calculados*		
tempo (min)	**massa de extrato (g)**	**Rendimento (%, m/m) (b.u.)**	**massa de CO2 (g)**	**S/F (b.u.)**
0	0,0000	0,00	0,00	0,00
10	0,2128	0,85	42,00	1,68
20	0,3179	1,27	84,00	3,36
30	0,3886	1,55	126,00	5,04
40	0,4311	1,72	168,00	6,72
50	0,4588	1,84	210,00	8,40
60	0,4922	1,97	252,00	10,08
70	0,5117	2,05	294,00	11,76
80	0,5285	2,11	336,00	13,44
90	0,5458	2,18	378,00	15,12
120	0,5729	2,29	504,00	20,16
150	0,6007	2,40	630,00	25,20
180	0,6235	2,49	756,00	30,24
210	0,6405	2,56	882,00	35,28
240	0,6526	2,61	1008,00	40,32
270	0,6625	2,65	1134,00	45,36
300	0,6721	2,69	1260,00	50,40
330	0,6809	2,72	1386,00	55,44
360	0,7218	2,89	1512,00	60,48

FICHA DE DADOS: Resíduo de cana-de-açúcar (Lote 2 / Curva 2) - Replicata nº2

Dados gerais de referência

Autor (ano)	Alberto Shintaku (2006)
Grupo de pesquisa	LASEFI/DEA/FEA/Unicamp
Tipo de trabalho	Dissertação de mestrado

Descrição e preparo da matéria-prima

Nome	resíduo de cana-de-açúcar
Parte utilizada	torta de filtro
Forma recebida	seco
Modo de preparo	moagem

Caracterização das partículas sólidas

Umidade (%)	não informada
dp (m)	2,80E-04
ρ_R (kg/m^3)	1740

Dados do experimento cinético

ρ_A (kg/m^3)	261,8
Porosidade	0,85
(H_B/d_B)	0,78
T (K)	323
P (MPa)	35
ρ_{CO2} (kg/m^3)	899,77
m_{MP} (g)	25
Q_{CO2} (kg/s)	7,00E-05
t (total) (min)	360

Dados calculados

m_{seca} (g)	não calculada
$m_{CO2\ TOTAL}$ (g)	1512,00
[S/F]total (b.u.)	60,48

Dados Experimentais		*Dados calculados*		
tempo (min)	**massa de extrato (g)**	**Rendimento (%, m/m) (b.u.)**	**massa de CO2 (g)**	**S/F (b.u.)**
0	0,0000	0,00	0,00	0,00
10	0,1419	0,57	42,00	1,68
20	0,3411	1,36	84,00	3,36
30	0,4513	1,81	126,00	5,04
40	0,5119	2,05	168,00	6,72
50	0,5571	2,23	210,00	8,40
60	0,5943	2,38	252,00	10,08
70	0,6165	2,47	294,00	11,76
80	0,6359	2,54	336,00	13,44
90	0,6464	2,59	378,00	15,12
120	0,6723	2,69	504,00	20,16
150	0,6960	2,78	630,00	25,20
180	0,7156	2,86	756,00	30,24
210	0,7260	2,90	882,00	35,28
240	0,7349	2,94	1008,00	40,32
270	0,7412	2,96	1134,00	45,36
300	0,7473	2,99	1260,00	50,40
330	0,7626	3,05	1386,00	55,44
360	0,7793	3,12	1512,00	60,48

FICHA DE DADOS: Urucum - Replicata nº1

Dados gerais de referência

Autor (ano)	Carolina L. C. de Albuquerque (2013)
Grupo de pesquisa	LASEFI/DEA/FEA/Unicamp
Tipo de trabalho	Tese de doutorado

Descrição e preparo da matéria-prima

Nome	urucum
Parte utilizada	sementes (inteiras)
Forma recebida	seco
Modo de preparo	nenhum

Caracterização das partículas sólidas

Umidade (%)	8,9
dp (m)	3,65E-03
ρ_R (kg/m^3)	1330

Dados do experimento cinético

ρ_A (kg/m^3)	655,17
Porosidade	0,51
(H_B/d_B)	2,10
T (K)	313
P (MPa)	20
ρ_{CO2} (kg/m^3)	840,61
m_{MP} (g)	173
[S/F]total (b.u.)	22,55
t (total) (min)	335

Dados calculados

m_{seca} (g)	157,60
$m_{CO2\ TOTAL}$ (g)	3901,15
Q_{CO2} (kg/s)	1,94E-04

Dados Experimentais		***Dados calculados***			
tempo (min)	**Rendimento (%, m/m) (b.s.)**	**massa de extrato (g)**	**massa de CO2 (g)**	**S/F (b.u.)**	**S/F (b.s.)**
0	0,00	0,00	0,00	0,00	0,00
5	0,53	0,84	58,23	0,34	0,37
10	0,95	1,50	116,45	0,67	0,74
15	1,30	2,05	174,68	1,01	1,11
20	1,55	2,44	232,90	1,35	1,48
30	1,85	2,92	349,36	2,02	2,22
40	2,06	3,25	465,81	2,69	2,96
50	2,21	3,48	582,26	3,37	3,69
70	2,44	3,85	815,17	4,71	5,17
90	2,60	4,10	1048,07	6,06	6,65
120	2,80	4,41	1397,43	8,08	8,87
160	2,96	4,67	1863,24	10,77	11,82
210	3,08	4,85	2445,50	14,14	15,52
250	3,16	4,98	2911,31	16,83	18,47
300	3,25	5,12	3493,57	20,19	22,17
335	3,32	5,23	3901,15	22,55	24,75

FICHA DE DADOS: Urucum - Replicata nº2

Dados gerais de referência

Autor (ano)	Carolina L. C. de Albuquerque (2013)
Grupo de pesquisa	LASEFI/DEA/FEA/Unicamp
Tipo de trabalho	Tese de doutorado

Descrição e preparo da matéria-prima

Nome	urucum
Parte utilizada	sementes (inteiras)
Forma recebida	seco
Modo de preparo	nenhum

Caracterização das partículas sólidas

Umidade (%)	8,9
dp (m)	3,65E-03
ρ_R (kg/m^3)	1330

Dados do experimento cinético

ρ_A (kg/m^3)	639,97
Porosidade	0,52
(H_B/d_B)	2,10
T (K)	313
P (MPa)	20
ρ_{CO2} (kg/m^3)	840,61
m_{MP} (g)	169
[S/F]total (b.u.)	23,01
t (total) (min)	335

Dados calculados

m_{seca} (g)	153,96
$m_{CO2\ TOTAL}$ (g)	3888,69
Q_{CO2} (kg/s)	1,93E-04

Dados Experimentais		*Dados calculados*			
tempo (min)	**Rendimento (%, m/m) (b.s.)**	**massa de extrato (g)**	**massa de CO2 (g)**	**S/F (b.u.)**	**S/F (b.s.)**
0	0,00	0,00	0,00	0,00	0,00
5	0,46	0,71	58,04	0,34	0,38
10	0,81	1,25	116,08	0,69	0,75
15	1,09	1,68	174,12	1,03	1,13
20	1,28	1,97	232,16	1,37	1,51
30	1,61	2,48	348,24	2,06	2,26
40	1,85	2,85	464,32	2,75	3,02
50	2,03	3,13	580,40	3,43	3,77
70	2,31	3,56	812,56	4,81	5,28
90	2,50	3,85	1044,72	6,18	6,79
120	2,69	4,14	1392,96	8,24	9,05
160	2,90	4,46	1857,28	10,99	12,06
210	3,05	4,70	2437,69	14,42	15,83
250	3,13	4,82	2902,01	17,17	18,85
300	3,21	4,94	3482,41	20,61	22,62
335	3,26	5,02	3888,69	23,01	25,26

APÊNDICE A2. ESTUDO PRELIMINAR DO MODELO *SPLINE*

Na literatura específica da área (SFE) é possível encontrar diversos modelos matemáticos que foram propostos para a descrição da OEC. Entre os modelos elaborados por diferentes autores, existem tanto equações muito simples quanto equações altamente complexas. Um exemplo de abordagem simplificada é o modelo *spline*, conforme apresentado por Meireles (2008). Tal modelo consiste basicamente na descrição da OEC por meio de um conjunto de "N" linhas retas. A forma genérica do modelo *spline* está apresentada abaixo, sendo que as equações das "N" retas do modelo são obtidas aplicando-se a Equação A8 para a 1ª, 2ª, 3ª e N-ésima linha reta.

$$m_{EXT} = \left(b_0 - \sum_{i=1}^{i=N-1} t_i a_{i+1} \right) + \sum_{i=1}^{i=N} a_i t \qquad \text{(A8)}$$

Onde:

m_{EXT} = massa acumulada de extrato (kg);

t = tempo de extração (s);

N = número de linhas retas do modelo *spline*;

b_0 = coeficiente linear da reta 1 (kg);

$\sum a_i$ (para $i=1$ a $i=N$) = coeficiente angular da reta 1 a N (kg/s);

t_i (para $i=1$ a $i=N-1$) = ponto do eixo das abscissas (tempo) correspondente ao cruzamento (intercepto) entre a reta i e a reta $i+1$ (s). *Observação: quando se admite N=3, os interceptos t_1 e t_2 correspondem aos parâmetros t_{CER} e t_{FER} da curva de extração, respectivamente*.

O modelo *spline* tem sido extensivamente usado pelo grupo de pesquisa LASEFI (DEA/FEA/UNICAMP) nas últimas décadas. Nos trabalhos do LASEFI é comum a aplicação do modelo *spline* utilizando-se duas ou três linhas retas, dependendo do formato da OEC obtida em pequena escala. Portanto, cada pesquisador faz sua própria análise em relação ao formato da curva obtida e, a partir disso, escolhe se vai usar o modelo com duas ou três linhas retas. O formato da OEC depende da composição do sistema em questão (matriz sólida + solvente) e também das condições operacionais do processo (tais como vazão mássica de solvente e geometria do leito, por exemplo).

Um dos objetivos do presente trabalho foi estudar a aplicação do modelo *spline* para curvas de diferentes formatos (assunto abordado no Capítulo 4). Para tanto, diversos testes preliminares foram feitos buscando-se investigar em detalhes a forma de aplicação deste modelo, bem como avaliar quais os principais fatores que podem influenciar nos resultados da modelagem. Os testes preliminares foram conduzidos com o intuito de definir critérios que possam (ou não) ser utilizados para estabelecer, da forma mais padronizada possível, um procedimento de cálculo para o ajuste *spline* no software SAS. Cabe ressaltar que o propósito do estudo preliminar foi definir uma metodologia padrão para aplicação do modelo *spline* na descrição de curvas de extração diversificadas, independentemente das características peculiares inerentes à OEC de cada tipo distinto de matéria-prima.

O principal critério avaliado foi a definição do número de retas a serem usadas para a descrição da OEC. Para tanto, fez-se uma análise comparativa dos resultados obtidos para os ajustes usando o modelo *spline* com duas e três retas, conforme apresentado no esquema da Figura A1. Além disso, fez-se também uma investigação do impacto que as estimativas iniciais (valores a serem definidos pelo operador do ajuste) exercem sobre os resultados obtidos na modelagem *spline* realizada no software SAS.

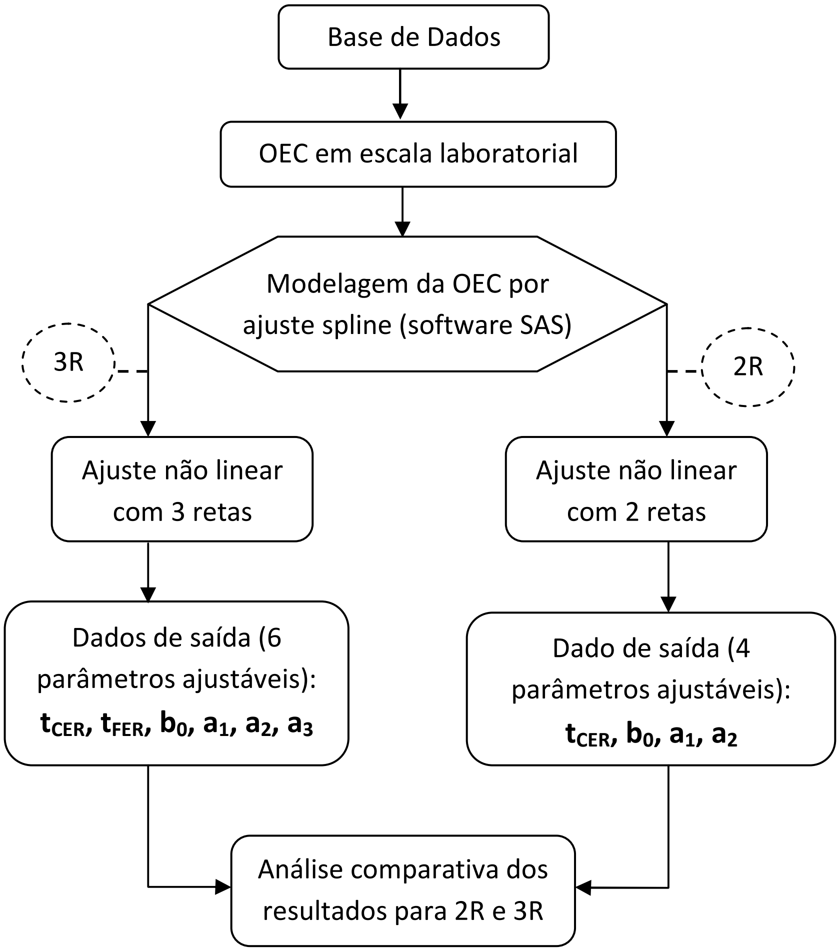

Figura A1. Diagrama esquemático da análise comparativa feita entre os ajustes com duas e três linhas retas (2R: duas retas; 3R: três retas; t_{CER}, t_{FER}, b_0, a_1, a_2, a_3: parâmetros ajustáveis do modelo *spline*)

A2.1. Descrição do modelo *spline*

As equações usadas na modelagem matemática da OEC estão descritas abaixo:

$$m_{EXT} = b_0 + a_1 t \qquad \text{(A9)}$$

$$m_{EXT} = (b_0 - t_1 a_2) + (a_1 + a_2)t \qquad \text{(A10)}$$

$$m_{EXT} = (b_0 - t_1 a_2 - t_2 a_3) + (a_1 + a_2 + a_3)t \qquad \text{(A11)}$$

Onde:

m_{EXT} = massa acumulada de extrato (kg);

t = tempo de extração (s);

b_0, a_1, a_2, a_3, t_1, t_2 = parâmetros ajustáveis do modelo, sendo que:

$t_1 = t_{CER}$ = tempo de duração da etapa CER (s);

$t_2 = t_{FER}$ = tempo que delimita o final da etapa FER (s);

b_0 = coeficiente linear da reta nº 1 (CER) (kg);

(a_1), (a_1+a_2), $(a_1+a_2+a_3)$ = coeficientes angulares das retas nº 1 (CER), nº2 (FER) e nº 3 (DC), respectivamente.

No caso do ajuste com duas retas a Equação A9 é válida para $\mathbf{t \leq t_{CER}}$, enquanto para $\mathbf{t > t_{CER}}$ o modelo é descrito pela Equação A10. Neste caso a Equação A11 não é utilizada e o modelo tem apenas quatro parâmetros ajustáveis (t_{CER}, b_0, a_1, a_2). Já para o ajuste com três retas, as Equações A9, A10 e A11 são válidas, respectivamente, para as etapas CER ($\mathbf{t \leq t_{CER}}$), FER ($\mathbf{t_{CER} < t \leq t_{FER}}$) e DC ($\mathbf{t > t_{FER}}$). Assim sendo, o modelo tem seis parâmetros ajustáveis (t_{CER}, t_{FER}, b_0, a_1, a_2, a_3).

A descrição do procedimento de cálculo utilizado na modelagem *spline* está ilustrada no diagrama esquemático da Figura A2.

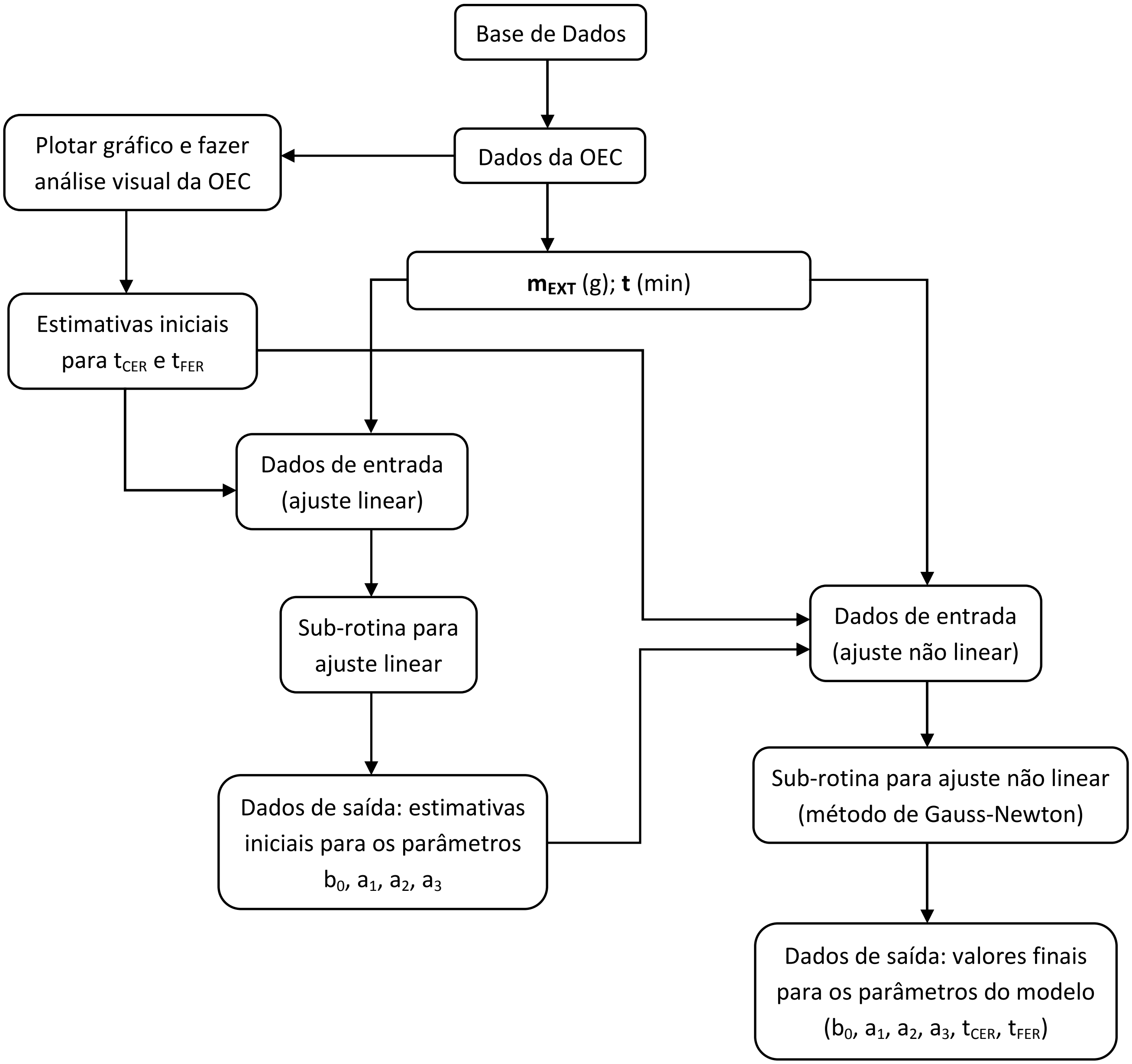

Figura A2. Diagrama esquemático para o ajuste da OEC usando modelo com três retas (*observação: no caso do modelo com duas retas a única diferença é que os parâmetros t_{FER} e a_3 deixam de existir*)

A modelagem foi realizada usando como ferramenta o software SAS (SAS Institute Inc., versão 9.2, Cary, EUA). Para tanto, as sub-rotinas "PROC REG" e "PROC NLIN" foram usadas, respectivamente, para as etapas de ajuste linear e ajuste não linear dos dados (conforme sequência apresentada na Figura A2). As OECs foram expressas na forma de massa acumulada de extrato *versus* tempo de extração. Portanto, os dados experimentais utilizados no ajuste foram $\mathbf{m_{EXT}}$ (em gramas) e tempo (em minutos). Além disso, estimativas iniciais dos parâmetros t_{CER} e t_{FER} foram fornecidas como dados de entrada, sendo estas selecionadas com base em uma avaliação preliminar (análise visual) do formato característico de cada OEC. Os algoritmos utilizados nos ajustes (2 e 3 retas) estão detalhados no Apêndice 3.

A2.2. Avaliação de critérios para a aplicação do modelo *spline*

A2.2.1. Critério A: número de retas

Os resultados da análise comparativa, entre a modelagem com duas e três retas, estão apresentados na Tabela A2.

Tabela A2. Dados para análise comparativa dos resultados[1] obtidos no ajuste *spline* usando 2 e 3 retas

Matéria-prima [2]	**Nº de retas (*spline*)**	**$t_{CER\_inicial}$ (min)**	**$t_{FER\_inicial}$ (min)**	**t_{CER} (min)**	**Erro (SE)[3]**	**t_{FER} (min)**	**Erro (SE) [3]**	**Soma de quadrados**
Gengibre	3	25	120	24	1	107	11	0,0507
	2	50	X	40	3	X	X	0,3463
Cidrão	3	75	230	64	6	195	5	0,0025
	2	160	X	169	8	X	X	0,0161
Semente de uva	3	290	360	276	8	350	3	0,0286
	2	330	X	320	3	X	X	0,1647

[1] Resultados levando em consideração que, na alimentação dos dados experimentais, o ponto zero (origem) não foi utilizado; [2] Dados apresentados no Apêndice 1 (Gengibre – Replicata nº1, Cidrão – Replicata nº1, Semente de uva – Replicata nº1); [3] SE: Erro padrão (*Standard Error).*

Os dados da Tabela A2 demonstram, conforme previamente esperado, que utilizando o modelo de três retas a minimização das somas de quadrados dos resíduos resulta em valores consideravelmente mais baixos. Menores valores para a soma de quadrados estão associados à descrição mais fiel dos dados experimentais em questão. Porém, a análise dos valores obtidos para a soma de quadrados dos resíduos não é condição suficiente para garantir o melhor desempenho de um modelo frente a outro. Na análise do desempenho de um modelo é essencial também levar em consideração a forma de distribuição dos resíduos, a qual pode ser visualizada em gráficos de dispersão. Assim sendo, para uma melhor avaliação dos modelos em estudo (*spline* com 3 e 2 retas), foram elaborados os gráficos apresentados nas Figuras A3, A4 e A8. Cabe ressaltar que para as OECs de gengibre e cidrão (Figuras A3 e A4, respectivamente) os gráficos de dispersão apresentam adicionalmente os resíduos para o modelo *spline* com quatro retas, a fim de demonstrar que quanto maior o número de retas melhor tende a ser a distribuição dos resíduos do modelo.

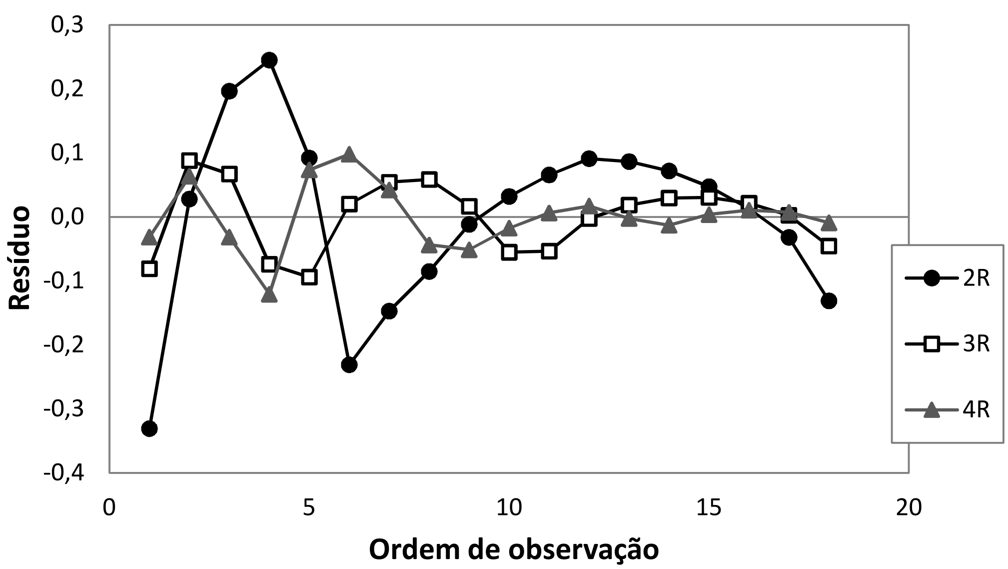

Figura A3. Gráfico de dispersão dos resíduos para a modelagem *spline* (2, 3 e 4 retas) da OEC de gengibre

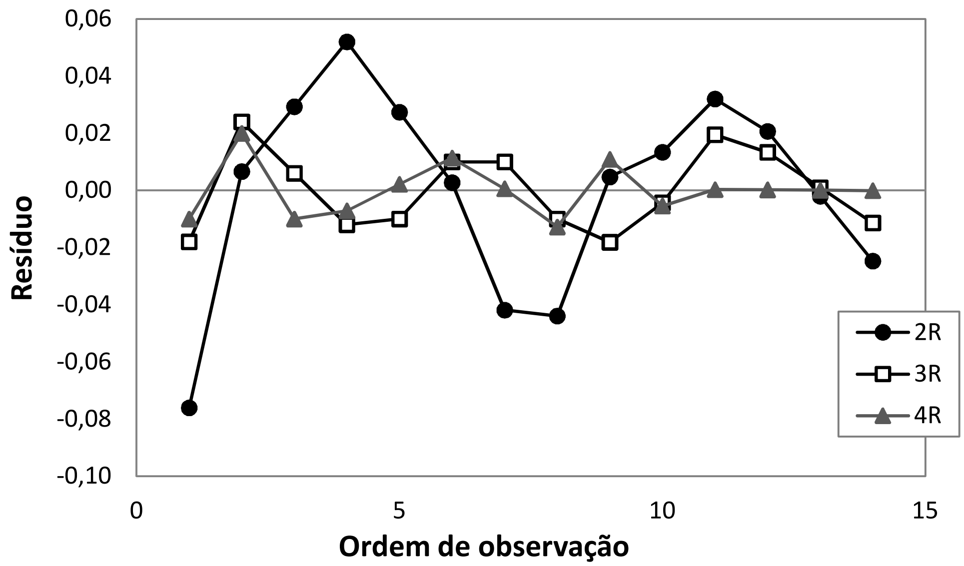

Figura A4. Gráfico de dispersão dos resíduos para a modelagem *spline* (2, 3 e 4 retas) da OEC de cidrão

Nas Figuras A3 e A4 fica claro que, para as OECs em questão (ver formatos das curvas nas Figuras A5 e A6), há uma diferença abrupta entre a distribuição dos resíduos dos modelos de três e duas retas. Portanto, a análise dos gráficos de dispersão dos resíduos demonstra que o ajuste com três retas possui uma qualidade muito superior quando comparado ao ajuste com duas retas. De forma análoga, é possível perceber que o ajuste com quatro retas resulta em melhor distribuição dos resíduos quando comparado ao ajuste de três retas. Porém, neste último caso, é nitidamente visível que a diferença entre a distribuição dos resíduos é muito mais suave, o que indica que ambos os modelos (3 e 4 retas) têm desempenho similares na descrição das OECs avaliadas. A análise das Figuras A5 e A6 comprova que a utilização de um *spline* com três retas já é suficientemente adequado para descrever quantitativamente as curvas em questão. Assim sendo, considera-se não justificável a utilização do ajuste com quatro retas, o que apenas tornaria o modelo mais complexo sem ganhos significativos em termos de qualidade do ajuste. Além disso, outra vantagem importante do modelo de três retas é que o mesmo permite a analogia com a descrição clássica da OEC nas etapas CER (*Constant Extraction Rate*), FER (*Falling Extraction Rate)* e DC (*Diffusion-Controlled Rate)*, conforme modelo descrito por Sovová (1994). Cada uma destas etapas possui características diferenciadas no que diz respeito aos mecanismos de transferência de massa no leito de extração.

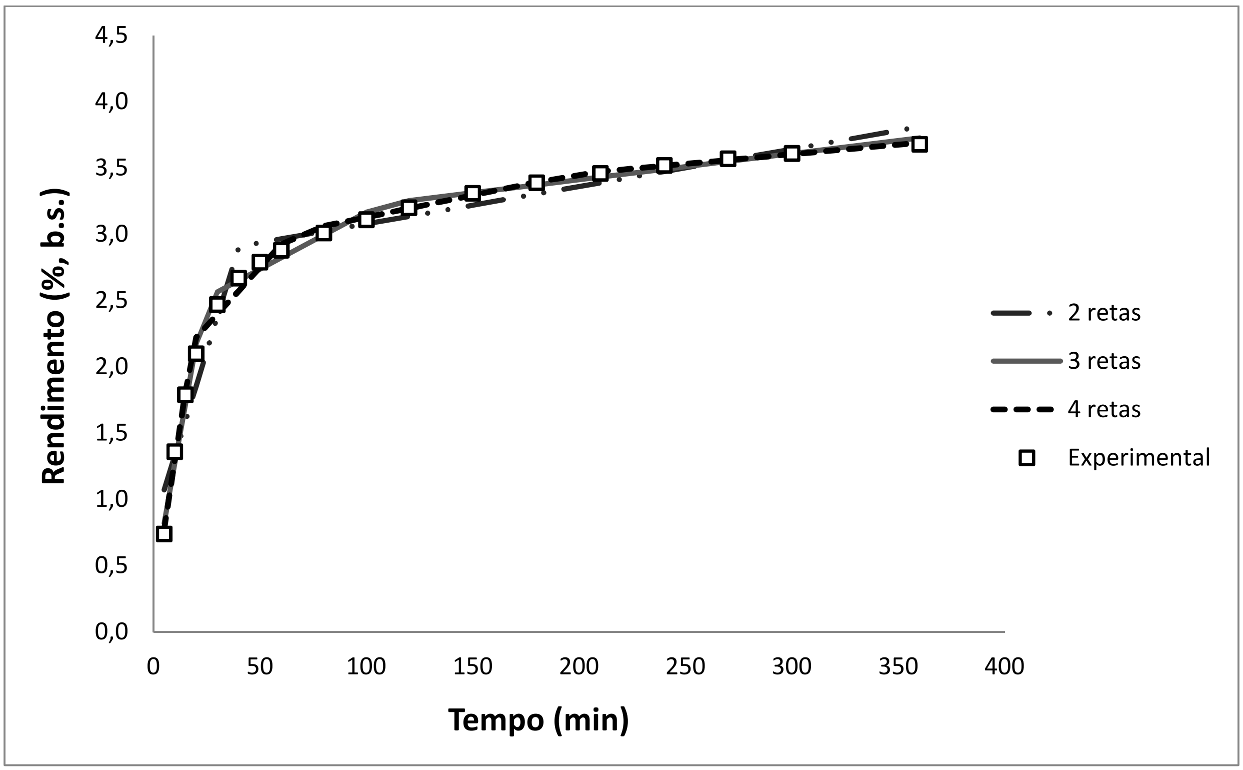

Figura A5. Dados experimentais da OEC de gengibre e valores modelados por ajuste *spline* (2, 3 e 4 retas)

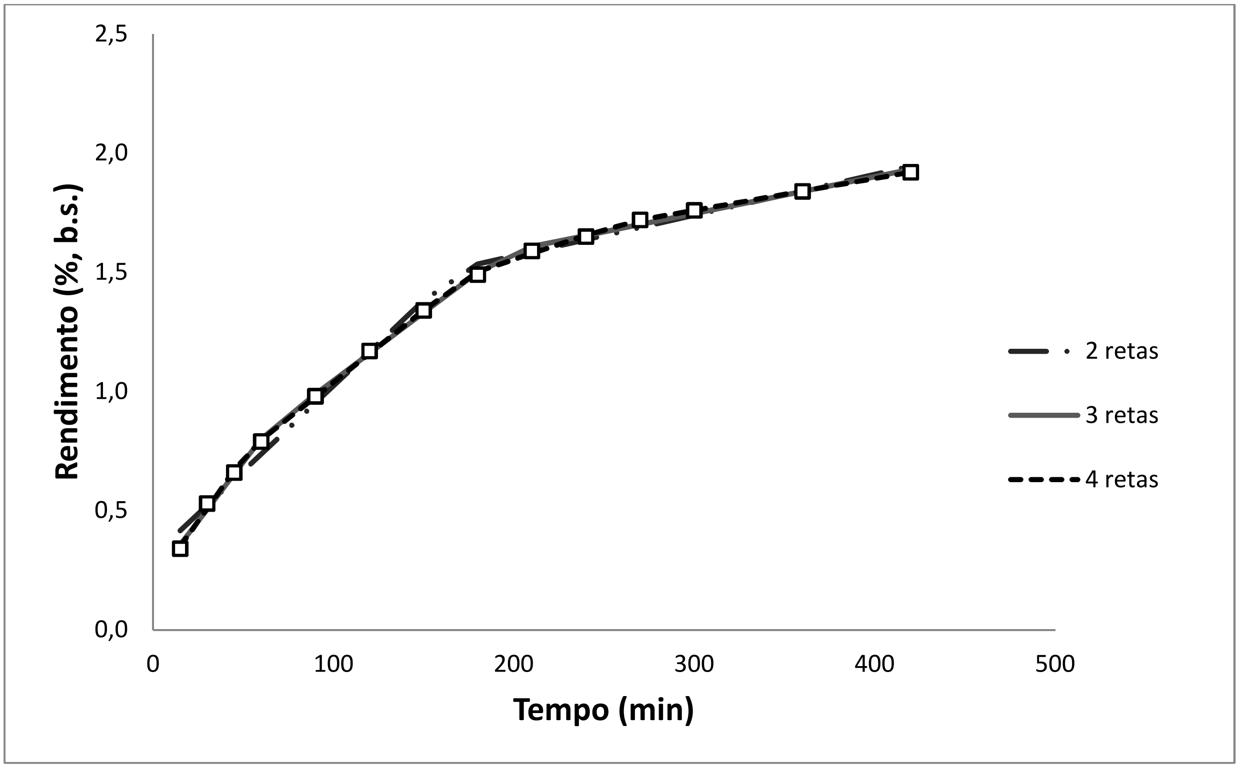

Figura A6. Dados experimentais da OEC de cidrão e valores modelados por ajuste *spline* (2, 3 e 4 retas)

O formato da OEC depende diretamente do tipo de matéria-prima em estudo, pois cada matriz vegetal é um sistema multicomponente complexo e com diversas características próprias. Esta afirmação pode ser demonstrada por meio da análise comparativa das OECs de gengibre, cidrão e semente de uva (Figuras A5, A6 e A7, respectivamente), nas quais é possível identificar três curvas de extração com formatos diferenciados. A OEC obtida para a semente de uva (Prado, 2010) possui um formato bastante peculiar, o qual pode ser aproximado a um *spline* com apenas duas retas. Neste caso específico (Figura A7) é possível observar que o modelo de duas retas já é suficiente para que se obtenha uma boa descrição quantitativa da curva de extração, pois visualmente nota-se pouca diferença com relação à curva modelada com três retas. A análise do gráfico de dispersão dos resíduos (Figura A8) evidencia melhor a distinção entre os modelos de duas e três retas, ao mesmo tempo em que mostra que a diferença entre ambos é suave quando comparada às respectivas diferenças obtidas para gengibre e cidrão (Figuras A3 e A4). De qualquer forma, embora o modelo de duas retas já tenha um desempenho satisfatório para o caso da semente de uva, a utilização do modelo de três retas proporciona melhor distribuição dos resíduos e menor soma de quadrados (ver Tabela A2), sem resultar em nenhum prejuízo à descrição quantitativa da OEC.

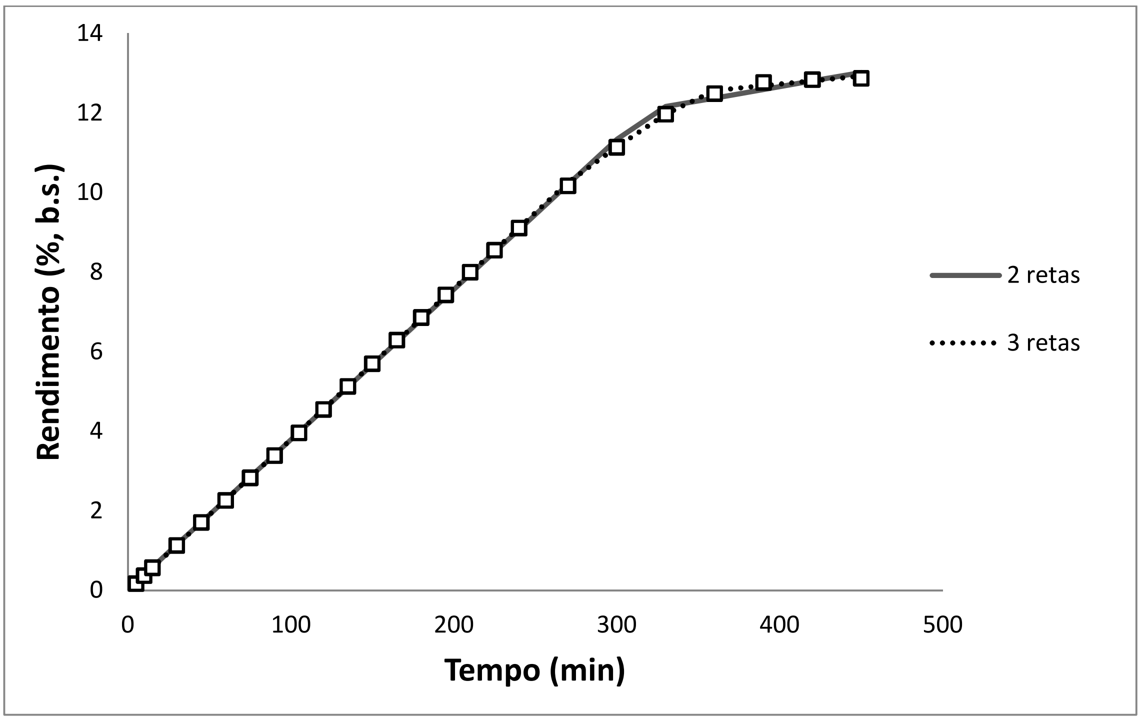

Figura A7. Dados experimentais da OEC de semente de uva e valores modelados por ajuste *spline* (2 e 3 retas)

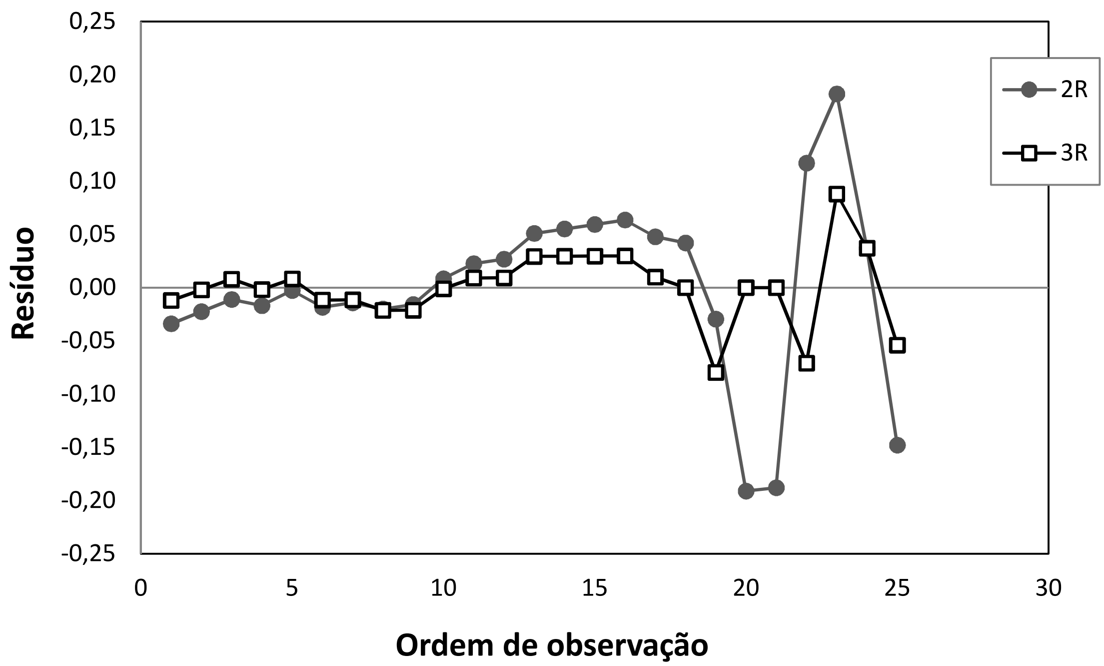

Figura A8. Gráfico de dispersão dos resíduos para a modelagem *spline* (2 e 3 retas) da OEC de semente de uva

Tendo em vista os resultados citados acima, definiu-se como critério a utilização do modelo *spline* com três retas para a descrição das OECs investigadas no presente trabalho. A definição desse critério foi feita a fim de padronizar o máximo possível o procedimento de ajuste, levando em consideração que para determinadas OECs o modelo com apenas duas retas pode não ser adequado. Assim sendo, acredita-se que o modelo selecionado (3 retas) possa ser usado na descrição da OEC de qualquer matéria-prima, independentemente das características próprias de cada matriz vegetal.

A2.2.2. Critério B: estimativas iniciais para t_{CER} e t_{FER}

Sabe-se que, ao realizar o ajuste *spline* da OEC, os dados de saída sofrem influência (moderada a forte, dependendo do formato da curva em questão) direta dos valores adotados como estimativas inicias para os parâmetros t_{CER} e t_{FER}. Em função disso, testes preliminares foram realizados para avaliar a influência que as estimativas iniciais exercem sobre o resultado obtido para os parâmetros ajustados. Os dados das OECs de duas matérias-primas (cravo e gengibre) foram utilizados na realização desses testes. Os resultados obtidos podem ser verificados na Tabela A3.

Diante disso, e visando padronizar o máximo possível a metodologia adotada nos ajustes, buscou-se definir algum critério para escolha dos valores iniciais de t_{CER} e t_{FER}. Para o ajuste com três retas o critério selecionado foi fazer a análise visual do gráfico da OEC baseando-se na descrição física do fenômeno de extração (conforme modelo proposto por Sovová, 1994), levando-se em consideração as características típicas das etapas CER, FER e DC. Portanto, mesmo buscando-se uma padronização, a conclusão foi que a análise visual de cada OEC é etapa essencial para a seleção das estimativas iniciais, fazendo com que o julgamento pessoal do pesquisador exerça influência direta sobre os valores iniciais usados para alimentar os dados de entrada necessários ao ajuste.

Tabela A3. Resultados[1] dos testes preliminares para avaliar a influência que as estimativas iniciais (dados de entrada) exercem sobre os valores obtidos para os parâmetros ajustados

Matéria-prima[2]	**$t_{CER\_inicial}$ (min)**	**$t_{FER\_inicial}$ (min)**	**t_{CER} (min)**	**Erro (SE)[3]**	**t_{FER} (min)**	**Erro (SE)[3]**	**Soma de quadrados**
Cravo (Replicata nº1)	50	160	40	3	132	8	2,5525
	60	180	33	2	129	6	1,8234
	40	150	33	2	129	6	1,8234
	20	130	20	2	121	5	3,1583
	75	175	40	3	132	8	2,5525
Cravo (Replicata nº2)	50	160	42	3	147	9	2,3095
	60	180	51	4	163	12	2,9171
	40	150	34	3	143	7	1,9075
	20	130	19	2	124	5	1,9774
	75	175	51	4	163	12	2,9171
Gengibre (Replicata nº1)	25	120	24	1	107	11	0,0507
	25	110	24	1	107	11	0,0507
	25	100	23	1	90	10	0,0496
	30	120	24	1	107	11	0,0507
	40	150	30	2	132	27	0,1321
Gengibre (Replicata nº2)	25	120	23	1	107	10	0,0546
	25	110	23	1	107	10	0,0546
	25	100	23	1	91	9	0,0540
	30	120	23	1	107	10	0,0546
	40	150	30	2	128	21	0,1385

[1] Resultados levando em consideração que, na alimentação dos dados experimentais, o ponto zero (origem) não foi utilizado; [2] Dados apresentados no Apêndice 1; [3] SE: Erro padrão (*Standard Error).*

APÊNDICE A3. ALGORITMOS UTILIZADOS PARA O AJUSTE DO MODELO *SPLINE*

A3.1. Modelo *Spline* com três retas

```
/* ------------------------------------------------------------------- */
Options NoDate NoNumber PS=100 LS=100 FormDLim='-';
Title'Cravo_R1.e.R2';
FootNote;
/* ------------------------------------------------------------------- */

/* Dados de entrada */
Data DadosOEC;
input tempo_min   mext_g;
            knot1 = 50;       /* estimativa inicial para o tCER */
            knot2 = 160;      /* estimativa inicial para o tFER */
            AL1 = max(tempo_min-knot1,0);
            AL2 = max(tempo_min-knot2,0);
Cards;
0      0.0000
5      2.3414
10     6.3757
15     9.3456
20     11.1393
25     12.8222
30     14.2843
40     16.5803
50     18.4644
60     20.1872
70     21.7045
80     22.9816
90     24.0748
100    25.0219
110    25.8279
120    26.5573
140    27.7943
```

```
160    28.7257
180    29.4452
200    29.9196
220    30.2766
240    30.5766
270    30.9203
300    31.2086
330    31.4366
360    31.6735
0      0.0000
5      1.9025
10     5.4733
15     7.8094
20     9.4093
25     10.6052
30     11.6402
40     13.5128
50     15.2872
60     16.8539
70     18.2005
80     19.4399
90     20.404
100    21.3741
110    22.2592
120    23.0107
140    24.2292
160    25.3418
180    26.2561
200    26.9204
220    27.5072
240    28.0187
270    28.6032
300    29.0704
330    29.5189
360    29.8769
;
```

```
/* Sub-rotina para o Ajuste Linear */

PROC REG DATA=DadosOEC ;
Model mext_g = tempo_min AL1 AL2;
Output out = a p=mext_g_hat r=RES;
Run;
Quit;

/* Observação: os dados de saída do ajuste linear serão utilizados como
dados de entrada na sub-rotina para o ajuste não linear (estimativas
iniciais para os parâmetros b0, a1, a2, a3) */

/* Sub-rotina para o Ajuste Não Linear */

PROC NLIN DATA=DadosOEC METHOD=Gauss;
TITLE 'Cravo_R1.e.R2';
parms       b0 = 2.05821
            a1 = 0.33144
            a2 = -0.24848
            a3 = -0.06662
            knot1 = 50        /* estimativa inicial para o tCER */
            knot2 = 160;      /* estimativa inicial para o tFER */
            AL1 = max(tempo_min-knot1,0);
            AL2 = max(tempo_min-knot2,0);

      Model mext_g = b0 + a1*tempo_min + a2*AL1 + a3*AL2;

      Output out = a p=mext_g_hat r=RES;
      Axis order = (0 to 34 by 2);
      Proc print;
      run;
/* ------------------------------------------------------------------ */
Proc gplot;
      Plot mext_g*mext_g_hat;
Proc gplot;
      Plot RES*mext_g_hat;
```

```
Proc gplot;
Symbol1 value = diamond color = black; Symbol2 value = star color = red;
Plot1 mext_g*tempo_min/legend overlay vaxis = axis1; Plot2
mext_g_hat*tempo_min/legend overlay vaxis = axis1;
RUN;
Quit;
/* ------------------------------------------------------------------ */
```

A3.2. Modelo *Spline* com duas retas

```
/* ------------------------------------------------------------------ */

Options NoDate NoNumber PS=100 LS=100 FormDLim='-';
Title 'Semente.Uva_R1_2.retas';
FootNote;

/* ------------------------------------------------------------------ */

/* Dados de entrada */

Data DadosOEC;
input tempo_min   Rend_BS; /* Rend_BS = dados de rendimento em % (b.s.)
*/
      knot1 = 330;      /* estimativa inicial para o tCER */
      AL1 = max(tempo_min-knot1,0);

Cards;
0      0.00
5      0.17
10     0.37
15     0.57
30     1.13
45     1.71
60     2.26
```

```
75    2.83
90    3.39
105   3.96
120   4.55
135   5.13
150   5.70
165   6.29
180   6.86
195   7.43
210   8.00
225   8.55
240   9.11
270   10.17
300   11.14
330   11.97
360   12.49
390   12.77
420   12.84
450   12.87
;

/* Sub-rotina para o Ajuste Linear */

PROC REG DATA=DadosOEC ;
Model Rend_BS = tempo_min AL1;
Output out = a p=Rend_BS_hat r=RES;
Run;
Quit;

/* Observação: os dados de saída do ajuste linear serão utilizados como
dados de entrada na sub-rotina para o ajuste não linear (estimativas
iniciais para os parâmetros b0, a1, a2) */
```

```
/* Sub-rotina para o Ajuste Não Linear */

PROC NLIN DATA=DadosOEC METHOD=Gauss;
TITLE 'Semente.Uva_ R1_2.retas';
parms       b0 = 0.05514
            a1 = 0.03729
            a2 = -0.03237
            knot1 = 330       /* estimativa inicial para o tCER */
            AL1 = max(tempo_min-knot1,0);

      Model Rend_BS = b0 + a1*tempo_min + a2*AL1;

      Output out = a p=Rend_BS_hat r=RES;
      Axis order = (0 to 15 by 1);
      Proc print;
      run;

/* ------------------------------------------------------------------ */

Proc gplot;
      Plot Rend_BS*Rend_BS_hat;
Proc gplot;
      Plot RES*Rend_BS_hat;
Proc gplot;
Symbol1 value = diamond color = black; Symbol2 value = star color = red;
Plot1 Rend_BS*tempo_min/legend overlay vaxis = axis1;
Plot2 Rend_BS_hat*tempo_min/legend overlay vaxis = axis1;
RUN;
Quit;

/* ------------------------------------------------------------------ */
```

APÊNDICE A4. DADOS DE SAÍDA DO AJUSTE *SPLINE* (REFERENTE AO CAPÍTULO 4)

Cravo_R1.e.R2

The REG Procedure
Model: MODEL1
Dependent Variable: mext_g

Analysis of Variance

Source	DF	Sum of Squares	Mean Square	F Value	Pr > F
Model	3	4278.69345	1426.23115	486.60	<.0001
Error	48	140.68799	2.93100		
Corrected Total	51	4419.38145			

Root MSE	1.71202	R-Square	0.9682
Dependent Mean	20.23482	Adj R-Sq	0.9662
Coeff Var	8.46075		

Parameter Estimates

Variable	DF	Parameter Estimate	Standard Error	t Value	Pr > |t|
Intercept	1	2.05821	0.65682	3.13	0.0029
tempo_min	1	0.33144	0.01970	16.82	<.0001
AL1	1	-0.24848	0.02573	-9.66	<.0001
AL2	1	-0.06662	0.01256	-5.30	<.0001

Cravo_R1.e.R2

The NLIN Procedure
Dependent Variable mext_g
Method: Gauss-Newton

Iterative Phase

Iter	b0	a1	a2	a3	knot1	knot2	Sum of Squares
0	2.0582	0.3314	-0.2485	-0.0666	50.0000	160.0	140.7
1	1.3491	0.3850	-0.2839	-0.0834	38.3867	141.0	137.1
2	0.6799	0.4459	-0.3365	-0.0916	32.0015	141.4	123.3
3	0.6799	0.4459	-0.3365	-0.0916	32.9993	141.4	119.0

NOTE: Convergence criterion met.

Estimation Summary

Method	Gauss-Newton
Iterations	3
R	0
PPC	0
RPC(knot1)	0.03118
Object	0.034458
Objective	119.0403
Observations Read	52
Observations Used	52
Observations Missing	0

Source	DF	Sum of Squares	Mean Square	F Value	Approx Pr > F
Model	5	4300.3	860.1	332.35	<.0001
Error	46	119.0	2.5878		
Corrected Total	51	4419.4			

Parameter	Estimate	Approx Std Error	Approximate 95% Confidence Limits	
b0	0.6799	0.7751	-0.8803	2.2400
a1	0.4459	0.0430	0.3593	0.5324

a2	-0.3365	0.0446	-0.4263	-0.2468
a3	-0.0916	0.0132	-0.1182	-0.0651
knot1	32.9993	3.3966	26.1623	39.8364
knot2	141.4	11.5144	118.2	164.5

Approximate Correlation Matrix

	b0	a1	a2	a3	knot1	knot2
b0	1.0000000	-0.8320503	0.8022179	-0.0000000	0.3546810	0.0000000
a1	-0.8320503	1.0000000	-0.9641460	0.0000000	-0.6770376	-0.0000000
a2	0.8022179	-0.9641460	1.0000000	-0.2379404	0.5071479	-0.1647125
a3	-0.0000000	0.0000000	-0.2379404	1.0000000	0.4919980	0.2873858
knot1	0.3546810	-0.6770376	0.5071479	0.4919980	1.0000000	0.2333081
knot2	0.0000000	-0.0000000	-0.1647125	0.2873858	0.2333081	1.0000000

Cravo_R1.e.R2

Obs	tempo_ min	mext_g	knot1	knot2	AL1	AL2	mext_ g_hat	RES
1	0	0.0000	50	160	0	0	0.6799	-0.67988
2	5	2.3414	50	160	0	0	2.9092	-0.56777
3	10	6.3757	50	160	0	0	5.1385	1.23724
4	15	9.3456	50	160	0	0	7.3677	1.97786
5	20	11.1393	50	160	0	0	9.5970	1.54227
6	25	12.8222	50	160	0	0	11.8263	0.99588
7	30	14.2843	50	160	0	0	14.0556	0.22869
8	40	16.5803	50	160	0	0	16.1584	0.42193
9	50	18.4644	50	160	0	0	17.2518	1.21257
10	60	20.1872	50	160	10	0	18.3453	1.84191
11	70	21.7045	50	160	20	0	19.4388	2.26575
12	80	22.9816	50	160	30	0	20.5322	2.44939
13	90	24.0748	50	160	40	0	21.6257	2.44913
14	100	25.0219	50	160	50	0	22.7191	2.30277
15	110	25.8279	50	160	60	0	23.8126	2.01531
16	120	26.5573	50	160	70	0	24.9060	1.65125
17	140	27.7943	50	160	90	0	27.0930	0.70133
18	160	28.7257	50	160	110	0	27.5707	1.15505
19	180	29.4452	50	160	130	20	27.9246	1.52059
20	200	29.9196	50	160	150	40	28.2786	1.64103
21	220	30.2766	50	160	170	60	28.6325	1.64407
22	240	30.5766	50	160	190	80	28.9865	1.59012
23	270	30.9203	50	160	220	110	29.5174	1.40288
24	300	31.2086	50	160	250	140	30.0484	1.16024
25	330	31.4366	50	160	280	170	30.5793	0.85730
26	360	31.6735	50	160	310	200	31.1102	0.56327
27	0	0.0000	50	160	0	0	0.6799	-0.67988
28	5	1.9025	50	160	0	0	2.9092	-1.00667
29	10	5.4733	50	160	0	0	5.1385	0.33484
30	15	7.8094	50	160	0	0	7.3677	0.44166
31	20	9.4093	50	160	0	0	9.5970	-0.18773
32	25	10.6052	50	160	0	0	11.8263	-1.22112
33	30	11.6402	50	160	0	0	14.0556	-2.41541
34	40	13.5128	50	160	0	0	16.1584	-2.64557
35	50	15.2872	50	160	0	0	17.2518	-1.96463
36	60	16.8539	50	160	10	0	18.3453	-1.49139
37	70	18.2005	50	160	20	0	19.4388	-1.23825
38	80	19.4399	50	160	30	0	20.5322	-1.09231
39	90	20.4040	50	160	40	0	21.6257	-1.22167
40	100	21.3741	50	160	50	0	22.7191	-1.34503
41	110	22.2592	50	160	60	0	23.8126	-1.55339
42	120	23.0107	50	160	70	0	24.9060	-1.89535
43	140	24.2292	50	160	90	0	27.0930	-2.86377
44	160	25.3418	50	160	110	0	27.5707	-2.22885
45	180	26.2561	50	160	130	20	27.9246	-1.66851
46	200	26.9204	50	160	150	40	28.2786	-1.35817
47	220	27.5072	50	160	170	60	28.6325	-1.12533
48	240	28.0187	50	160	190	80	28.9865	-0.96778
49	270	28.6032	50	160	220	110	29.5174	-0.91422
50	300	29.0704	50	160	250	140	30.0484	-0.97796
51	330	29.5189	50	160	280	170	30.5793	-1.06040
52	360	29.8769	50	160	310	200	31.1102	-1.23333

Gengibre_R1.e.R2

The REG Procedure
Model: MODEL1
Dependent Variable: mext_g

Analysis of Variance

Source	DF	Sum of Squares	Mean Square	F Value	Pr > F
Model	3	75.23844	25.07948	1009.56	<.0001
Error	34	0.84462	0.02484		
Corrected Total	37	76.08306			

Root MSE	0.15761	R-Square	0.9889
Dependent Mean	3.73297	Adj R-Sq	0.9879
Coeff Var	4.22220		

Parameter Estimates

Variable	DF	Parameter Estimate	Standard Error	t Value	Pr > |t|
Intercept	1	0.31671	0.07828	4.05	0.0003
tempo_min	1	0.13192	0.00446	29.58	<.0001
AL1	1	-0.12179	0.00512	-23.78	<.0001
AL2	1	-0.00747	0.00136	-5.50	<.0001

Gengibre_R1.e.R2

The NLIN Procedure
Dependent Variable mext_g
Method: Gauss-Newton

Iterative Phase

Iter	b0	a1	a2	a3	knot1	knot2	Sum of Squares
0	0.3167	0.1319	-0.1218	-0.00747	25.0000	120.0	0.8446
1	0.2249	0.1457	-0.1329	-0.0101	21.8681	102.4	0.7846
2	0.2249	0.1457	-0.1329	-0.0101	22.1298	107.0	0.6649

NOTE: Convergence criterion met.

Estimation Summary

Method	Gauss-Newton
Iterations	2
R	0
PPC	0
RPC(knot2)	0.044787
Object	0.152562
Objective	0.664877
Observations Read	38
Observations Used	38
Observations Missing	0

Source	DF	Sum of Squares	Mean Square	F Value	Approx Pr > F
Model	5	75.4182	15.0836	725.96	<.0001
Error	32	0.6649	0.0208		
Corrected Total	37	76.0831			

Parameter	Estimate	Approx Std Error	Approximate 95% Confidence Limits	
b0	0.2249	0.0790	0.0640	0.3857
a1	0.1457	0.00645	0.1326	0.1588

a2	-0.1329	0.00668	-0.1465	-0.1193
a3	-0.0101	0.00181	-0.0138	-0.00641
knot1	22.1298	0.9000	20.2966	23.9630
knot2	107.0	11.3785	83.7909	130.1

Approximate Correlation Matrix

	b0	a1	a2	a3	knot1	knot2
b0	1.0000000	-0.8164966	0.7880384	0.0000000	0.3137575	0.0000000
a1	-0.8164966	1.0000000	-0.9651460	-0.0000000	-0.6537565	-0.0000000
a2	0.7880384	-0.9651460	1.0000000	-0.2523300	0.4861220	-0.1869958
a3	0.0000000	-0.0000000	-0.2523300	1.0000000	0.5336246	0.5535984
knot1	0.3137575	-0.6537565	0.4861220	0.5336246	1.0000000	0.2694689
knot2	0.0000000	-0.0000000	-0.1869958	0.5535984	0.2694689	1.0000000

Gengibre_R1.e.R2

Obs	tempo_ min	mext_g	knot1	knot2	AL1	AL2	mext_ g_hat	RES
1	0	0.0000	25	120	0	0	0.22486	-0.22486
2	5	1.0115	25	120	0	0	0.95334	0.05816
3	10	1.8677	25	120	0	0	1.68181	0.18589
4	15	2.4626	25	120	0	0	2.41029	0.05232
5	20	2.8842	25	120	0	0	3.13876	-0.25456
6	30	3.3935	25	120	5	0	3.54981	-0.15631
7	40	3.6681	25	120	15	0	3.67782	-0.00972
8	50	3.8333	25	120	25	0	3.80584	0.02746
9	60	3.9565	25	120	35	0	3.93385	0.02265
10	80	4.1378	25	120	55	0	4.18988	-0.05208
11	100	4.2782	25	120	75	0	4.44590	-0.16770
12	120	4.3995	25	120	95	0	4.57033	-0.17083
13	150	4.5452	25	120	125	30	4.65142	-0.10622
14	180	4.6647	25	120	155	60	4.73251	-0.06781
15	210	4.7598	25	120	185	90	4.81359	-0.05379
16	240	4.8394	25	120	215	120	4.89468	-0.05528
17	270	4.9048	25	120	245	150	4.97577	-0.07097
18	300	4.9661	25	120	275	180	5.05686	-0.09076
19	360	5.0575	25	120	335	240	5.21904	-0.16154
20	0	0.0000	25	120	0	0	0.22486	-0.22486
21	5	1.1187	25	120	0	0	0.95334	0.16536
22	10	1.9609	25	120	0	0	1.68181	0.27909
23	15	2.5563	25	120	0	0	2.41029	0.14602
24	20	2.9562	25	120	0	0	3.13876	-0.18256
25	30	3.4458	25	120	5	0	3.54981	-0.10401
26	40	3.7387	25	120	15	0	3.67782	0.06088
27	50	3.9339	25	120	25	0	3.80584	0.12806
28	60	4.0746	25	120	35	0	3.93385	0.14075
29	80	4.2840	25	120	55	0	4.18988	0.09412
30	100	4.4618	25	120	75	0	4.44590	0.01590
31	120	4.5897	25	120	95	0	4.57033	0.01937
32	150	4.7429	25	120	125	30	4.65142	0.09148
33	180	4.8591	25	120	155	60	4.73251	0.12659
34	210	4.9540	25	120	185	90	4.81359	0.14041
35	240	5.0343	25	120	215	120	4.89468	0.13962
36	270	5.1027	25	120	245	150	4.97577	0.12693
37	300	5.1595	25	120	275	180	5.05686	0.10264
38	360	5.2492	25	120	335	240	5.21904	0.03016

Semente.Uva_R1.e.R2

The REG Procedure
Model: MODEL1
Dependent Variable: mext_g

Analysis of Variance

Source	DF	Sum of Squares	Mean Square	F Value	Pr > F
Model	3	6254.16693	2084.72231	3528.99	<.0001
Error	48	28.35559	0.59074		
Corrected Total	51	6282.52252			

Root MSE	0.76860	R-Square	0.9955
Dependent Mean	15.64847	Adj R-Sq	0.9952
Coeff Var	4.91164		

Parameter Estimates

Variable	DF	Parameter Estimate	Standard Error	t Value	Pr > |t|
Intercept	1	0.02120	0.20392	0.10	0.9176
tempo_min	1	0.09456	0.00134	70.40	<.0001
AL1	1	-0.03997	0.00808	-4.95	<.0001
AL2	1	-0.03277	0.01362	-2.41	0.0200

Semente.Uva_R1.e.R2

The NLIN Procedure
Dependent Variable mext_g
Method: Gauss-Newton

Iterative Phase

Iter	b0	a1	a2	a3	knot1	knot2	Sum of Squares
0	0.0212	0.0946	-0.0400	-0.0328	290.0	360.0	28.3556
1	-0.00433	0.0949	-0.0278	-0.0455	276.7	347.9	28.1940
2	-0.00433	0.0949	-0.0278	-0.0455	271.0	351.3	28.0902

NOTE: Convergence criterion met.

Estimation Summary

Method	Gauss-Newton
Iterations	2
R	0
PPC	0
RPC(knot1)	0.020874
Object	0.003684
Objective	28.09016
Observations Read	52
Observations Used	52
Observations Missing	0

Source	DF	Sum of Squares	Mean Square	F Value	Approx Pr > F
Model	5	6254.4	1250.9	2048.43	<.0001
Error	46	28.0902	0.6107		
Corrected Total	51	6282.5			

Parameter	Estimate	Approx Std Error	Approximate 95% Confidence Limits	
b0	-0.00433	0.2118	-0.4308	0.4221
a1	0.0949	0.00148	0.0919	0.0979

a2	-0.0278	0.0261	-0.0804	0.0247
a3	-0.0455	0.0273	-0.1005	0.00951
knot1	271.0	44.5169	181.4	360.6
knot2	351.3	25.2389	300.5	402.1

Approximate Correlation Matrix

	b0	a1	a2	a3	knot1	knot2
b0	1.0000000	-0.8122968	0.0460869	-0.0000000	0.0919439	-0.0000000
a1	-0.8122968	1.0000000	-0.0567365	0.0000000	-0.1847656	0.0000000
a2	0.0460869	-0.0567365	1.0000000	-0.9519267	-0.9135282	-0.8218260
a3	-0.0000000	0.0000000	-0.9519267	1.0000000	0.8824315	0.6686040
knot1	0.0919439	-0.1847656	-0.9135282	0.8824315	1.0000000	0.6545296
knot2	-0.0000000	0.0000000	-0.8218260	0.6686040	0.6545296	1.0000000

Semente.Uva_R1.e.R2

Obs	tempo_ min	mext_g	knot1	knot2	AL1	AL2	mext_ g_hat	RES
1	0	0.0000	290	360	0	0	-0.0043	0.00433
2	5	0.4133	290	360	0	0	0.4701	-0.05682
3	10	0.9003	290	360	0	0	0.9446	-0.04428
4	15	1.3670	290	360	0	0	1.4190	-0.05204
5	30	2.7425	290	360	0	0	2.8424	-0.09990
6	45	4.1276	290	360	0	0	4.2658	-0.13817
7	60	5.4779	290	360	0	0	5.6891	-0.21124
8	75	6.8400	290	360	0	0	7.1125	-0.27251
9	90	8.2079	290	360	0	0	8.5359	-0.32798
10	105	9.5735	290	360	0	0	9.9592	-0.38575
11	120	11.0045	290	360	0	0	11.3826	-0.37811
12	135	12.4100	290	360	0	0	12.8060	-0.39598
13	150	13.7895	290	360	0	0	14.2294	-0.43985
14	165	15.2172	290	360	0	0	15.6527	-0.43552
15	180	16.6047	290	360	0	0	17.0761	-0.47139
16	195	17.9714	290	360	0	0	18.4995	-0.52806
17	210	19.3445	290	360	0	0	19.9228	-0.57832
18	225	20.6933	290	360	0	0	21.3462	-0.65289
19	240	22.0312	290	360	0	0	22.7696	-0.73836
20	270	24.5928	290	360	0	0	25.6163	-1.02350
21	300	26.9547	290	360	10	0	27.6545	-0.69980
22	330	28.9449	290	360	40	0	29.6660	-0.72105
23	360	30.2023	290	360	70	0	31.2806	-1.07826
24	390	30.8828	290	360	100	30	31.9276	-1.04478
25	420	31.0510	290	360	130	60	32.5746	-1.52360
26	450	31.1243	290	360	160	90	33.2216	-2.09731
27	0	0.0000	290	360	0	0	-0.0043	0.00433
28	5	0.4440	290	360	0	0	0.4701	-0.02612
29	10	0.9144	290	360	0	0	0.9446	-0.03018
30	15	1.3721	290	360	0	0	1.4190	-0.04694
31	30	2.8989	290	360	0	0	2.8424	0.05650
32	45	4.3705	290	360	0	0	4.2658	0.10473
33	60	5.8169	290	360	0	0	5.6891	0.12776
34	75	7.3212	290	360	0	0	7.1125	0.20869
35	90	8.8343	290	360	0	0	8.5359	0.29842
36	105	10.3319	290	360	0	0	9.9592	0.37265
37	120	11.8755	290	360	0	0	11.3826	0.49289
38	135	13.3788	290	360	0	0	12.8060	0.57282
39	150	14.8138	290	360	0	0	14.2294	0.58445
40	165	16.2922	290	360	0	0	15.6527	0.63948
41	180	17.7859	290	360	0	0	17.0761	0.70981
42	195	19.1856	290	360	0	0	18.4995	0.68614
43	210	20.6229	290	360	0	0	19.9228	0.70008
44	225	22.0297	290	360	0	0	21.3462	0.68351
45	240	23.4341	290	360	0	0	22.7696	0.66454
46	270	26.0391	290	360	0	0	25.6163	0.42280
47	300	28.3543	290	360	10	0	27.6545	0.69980
48	330	30.3870	290	360	40	0	29.6660	0.72105
49	360	32.0236	290	360	70	0	31.2806	0.74304
50	390	33.3723	290	360	100	30	31.9276	1.44472
51	420	34.3040	290	360	130	60	32.5746	1.72941
52	450	35.0484	290	360	160	90	33.2216	1.82679

Cidrao_R1.e.R2

The REG Procedure
Model: MODEL1
Dependent Variable: mext_g

Analysis of Variance

Source	DF	Sum of Squares	Mean Square	F Value	Pr > F
Model	3	12.59384	4.19795	468.84	<.0001
Error	26	0.23280	0.00895		
Corrected Total	29	12.82664			

Root MSE	0.09462	R-Square	0.9819
Dependent Mean	1.39636	Adj R-Sq	0.9798
Coeff Var	6.77652		

Parameter Estimates

Variable	DF	Parameter Estimate	Standard Error	t Value	Pr > |t|
Intercept	1	0.11959	0.04778	2.50	0.0189
tempo_min	1	0.01522	0.00099126	15.35	<.0001
AL1	1	-0.01101	0.00131	-8.39	<.0001
AL2	1	-0.00280	0.00072616	-3.86	0.0007

Cidrao_R1.e.R2

The NLIN Procedure
Dependent Variable mext_g
Method: Gauss-Newton

Iterative Phase

Iter	b0	a1	a2	a3	knot1	knot2	Sum of Squares
0	0.1196	0.0152	-0.0110	-0.00280	75.0000	230.0	0.2328
1	0.0988	0.0163	-0.0114	-0.00336	64.7734	207.0	0.2197
2	0.0988	0.0163	-0.0109	-0.00376	62.6852	193.7	0.2146
3	0.0988	0.0163	-0.0109	-0.00376	62.5897	195.1	0.2144

NOTE: Convergence criterion met.

Estimation Summary

Method	Gauss-Newton
Iterations	3
R	0
PPC	0
RPC(knot2)	0.007344
Object	0.00108
Objective	0.214365
Observations Read	30
Observations Used	30
Observations Missing	0

Source	DF	Sum of Squares	Mean Square	F Value	Approx Pr > F
Model	5	12.6123	2.5225	282.41	<.0001
Error	24	0.2144	0.00893		
Corrected Total	29	12.8266			

Parameter	Estimate	Approx Std Error	Approximate 95% Confidence Limits	
b0	0.0988	0.0518	-0.00802	0.2057

a1	0.0163	0.00141	0.0133	0.0192
a2	-0.0109	0.00173	-0.0144	-0.00732
a3	-0.00376	0.00107	-0.00596	-0.00156
knot1	62.5897	8.8756	44.2715	80.9078
knot2	195.1	22.3150	149.0	241.1

Approximate Correlation Matrix

	b0	a1	a2	a3	knot1	knot2
b0	1.0000000	-0.8164966	0.6666667	0.0000000	0.2095743	0.0000000
a1	-0.8164966	1.0000000	-0.8164966	-0.0000000	-0.4755607	-0.0000000
a2	0.6666667	-0.8164966	1.0000000	-0.5390717	-0.0430773	-0.4116013
a3	0.0000000	-0.0000000	-0.5390717	1.0000000	0.6976197	0.4947419
knot1	0.2095743	-0.4755607	-0.0430773	0.6976197	1.0000000	0.3949367
knot2	0.0000000	-0.0000000	-0.4116013	0.4947419	0.3949367	1.0000000

Cidrao_R1.e.R2

Obs	tempo_ min	mext_g	knot1	knot2	AL1	AL2	mext_ g_hat	RES
1	0	0.0000	75	230	0	0	0.09882	-0.09882
2	15	0.3793	75	230	0	0	0.34266	0.03664
3	30	0.5939	75	230	0	0	0.58650	0.00740
4	45	0.7492	75	230	0	0	0.83034	-0.08114
5	60	0.8868	75	230	0	0	1.07418	-0.18738
6	90	1.1104	75	230	15	0	1.26370	-0.15329
7	120	1.3162	75	230	45	0	1.42504	-0.10884
8	150	1.5132	75	230	75	0	1.58638	-0.07318
9	180	1.6839	75	230	105	0	1.74773	-0.06383
10	210	1.7993	75	230	135	0	1.85297	-0.05367
11	240	1.8683	75	230	165	10	1.90143	-0.03313
12	270	1.9399	75	230	195	40	1.94989	-0.00999
13	300	1.9823	75	230	225	70	1.99835	-0.01605
14	360	2.0733	75	230	285	130	2.09527	-0.02197
15	420	2.1688	75	230	345	190	2.19219	-0.02339
16	0	0.0000	75	230	0	0	0.09882	-0.09882
17	15	0.4494	75	230	0	0	0.34266	0.10674
18	30	0.7453	75	230	0	0	0.58650	0.15880
19	45	0.9395	75	230	0	0	0.83034	0.10916
20	60	1.1216	75	230	0	0	1.07418	0.04742
21	90	1.3933	75	230	15	0	1.26370	0.12961
22	120	1.5569	75	230	45	0	1.42504	0.13186
23	150	1.6846	75	230	75	0	1.58638	0.09822
24	180	1.7872	75	230	105	0	1.74773	0.03947
25	210	1.8695	75	230	135	0	1.85297	0.01653
26	240	1.9334	75	230	165	10	1.90143	0.03197
27	270	1.9916	75	230	195	40	1.94989	0.04171
28	300	2.0382	75	230	225	70	1.99835	0.03985
29	360	2.1238	75	230	285	130	2.09527	0.02853
30	420	2.1918	75	230	345	190	2.19219	-0.00039

Residuo.Cana_Lote1_R1.e.R2

The REG Procedure
Model: MODEL1
Dependent Variable: mext_g

Analysis of Variance

Source	DF	Sum of Squares	Mean Square	F Value	Pr > F
Model	3	19.30761	6.43587	614.67	<.0001
Error	38	0.39787	0.01047		
Corrected Total	41	19.70548			

Root MSE	0.10232	R-Square	0.9798
Dependent Mean	1.56484	Adj R-Sq	0.9782
Coeff Var	6.53898		

Parameter Estimates

Variable	DF	Parameter Estimate	Standard Error	t Value	Pr > |t|
Intercept	1	0.09642	0.04749	2.03	0.0494
tempo_min	1	0.02147	0.00111	19.28	<.0001
AL1	1	-0.01363	0.00160	-8.52	<.0001
AL2	1	-0.00663	0.00093861	-7.07	<.0001

Residuo.Cana_Lote1_R1.e.R2

The NLIN Procedure
Dependent Variable mext_g
Method: Gauss-Newton

Iterative Phase

Iter	b0	a1	a2	a3	knot1	knot2	Sum of Squares
0	0.0964	0.0215	-0.0136	-0.00663	60.0000	150.0	0.3979
1	0.0722	0.0229	-0.0134	-0.00821	51.3366	132.7	0.3812
2	0.0722	0.0229	-0.0134	-0.00821	51.1847	136.0	0.3709

NOTE: Convergence criterion met.

Estimation Summary

Method	Gauss-Newton
Iterations	2
R	0
PPC	0
RPC(knot2)	0.025052
Object	0.026895
Objective	0.37094
Observations Read	42
Observations Used	42
Observations Missing	0

Source	DF	Sum of Squares	Mean Square	F Value	Approx Pr > F
Model	5	19.3345	3.8669	375.29	<.0001
Error	36	0.3709	0.0103		
Corrected Total	41	19.7055			

Parameter	Estimate	Approx Std Error	Approximate 95% Confidence Limits	
b0	0.0722	0.0519	-0.0332	0.1775
a1	0.0229	0.00172	0.0194	0.0264
a2	-0.0134	0.00219	-0.0178	-0.00896

a3	-0.00821	0.00141	-0.0111	-0.00535
knot1	51.1847	5.9655	39.0862	63.2832
knot2	136.0	10.3445	115.0	157.0

Approximate Correlation Matrix

	b0	a1	a2	a3	knot1	knot2
b0	1.0000000	-0.8257228	0.6477503	0.0000000	0.2574055	0.0000000
a1	-0.8257228	1.0000000	-0.7844645	0.0000000	-0.5622419	-0.0000000
a2	0.6477503	-0.7844645	1.0000000	-0.5984064	0.0324275	-0.4560150
a3	0.0000000	0.0000000	-0.5984064	1.0000000	0.6357717	0.5735916
knot1	0.2574055	-0.5622419	0.0324275	0.6357717	1.0000000	0.3759828
knot2	0.0000000	-0.0000000	-0.4560150	0.5735916	0.3759828	1.0000000

Residuo.Cana_Lote1_R1.e.R2

Obs	tempo_ min	mext_g	knot1	knot2	AL1	AL2	mext_ g_hat	RES
1	0	0.00000	60	150	0	0	0.07217	-0.07217
2	10	0.29400	60	150	0	0	0.30138	-0.00738
3	20	0.52910	60	150	0	0	0.53059	-0.00149
4	30	0.77080	60	150	0	0	0.75981	0.01099
5	40	0.98480	60	150	0	0	0.98902	-0.00422
6	50	1.14670	60	150	0	0	1.21823	-0.07153
7	60	1.31840	60	150	0	0	1.32936	-0.01096
8	70	1.46770	60	150	10	0	1.42462	0.04308
9	80	1.59630	60	150	20	0	1.51988	0.07642
10	90	1.71860	60	150	30	0	1.61514	0.10346
11	100	1.81590	60	150	40	0	1.71040	0.10550
12	110	1.89600	60	150	50	0	1.80566	0.09034
13	120	1.97710	60	150	60	0	1.90092	0.07618
14	150	2.14330	60	150	90	0	2.07193	0.07137
15	180	2.21480	60	150	120	30	2.11154	0.10326
16	210	2.29530	60	150	150	60	2.15115	0.14415
17	240	2.34950	60	150	180	90	2.19076	0.15874
18	270	2.38050	60	150	210	120	2.23038	0.15012
19	300	2.41000	60	150	240	150	2.26999	0.14001
20	330	2.41930	60	150	270	180	2.30960	0.10970
21	360	2.42700	60	150	300	210	2.34921	0.07779
22	0	0.00000	60	150	0	0	0.07217	-0.07217
23	10	0.34700	60	150	0	0	0.30138	0.04562
24	20	0.63170	60	150	0	0	0.53059	0.10111
25	30	0.87250	60	150	0	0	0.75981	0.11269
26	40	1.01580	60	150	0	0	0.98902	0.02678
27	50	1.15000	60	150	0	0	1.21823	-0.06823
28	60	1.28040	60	150	0	0	1.32936	-0.04896
29	70	1.38410	60	150	10	0	1.42462	-0.04052
30	80	1.47070	60	150	20	0	1.51988	-0.04918
31	90	1.56770	60	150	30	0	1.61514	-0.04744
32	100	1.64173	60	150	40	0	1.71040	-0.06867
33	110	1.71133	60	150	50	0	1.80566	-0.09433
34	120	1.76600	60	150	60	0	1.90092	-0.13492
35	150	1.91283	60	150	90	0	2.07193	-0.15910
36	180	1.99093	60	150	120	30	2.11154	-0.12061
37	210	2.05813	60	150	150	60	2.15115	-0.09302
38	240	2.10133	60	150	180	90	2.19076	-0.08943
39	270	2.13210	60	150	210	120	2.23038	-0.09828
40	300	2.15370	60	150	240	150	2.26999	-0.11629
41	330	2.18240	60	150	270	180	2.30960	-0.12720
42	360	2.19800	60	150	300	210	2.34921	-0.15121

Residuo.Cana_Lote2_50C/200bar_R1.e.R2

The REG Procedure
Model: MODEL1
Dependent Variable: mext_g

Analysis of Variance

Source	DF	Sum of Squares	Mean Square	F Value	Pr > F
Model	3	1.14147	0.38049	1038.72	<.0001
Error	34	0.01245	0.00036631		
Corrected Total	37	1.15392			

Root MSE	0.01914	R-Square	0.9892
Dependent Mean	0.35303	Adj R-Sq	0.9883
Coeff Var	5.42141		

Parameter Estimates

Variable	DF	Parameter Estimate	Standard Error	t Value	Pr > |t|
Intercept	1	-0.00104	0.00860	-0.12	0.9040
tempo_min	1	0.00532	0.00018277	29.11	<.0001
AL1	1	-0.00429	0.00021963	-19.55	<.0001
AL2	1	-0.00091023	0.00019138	-4.76	<.0001

Residuo.Cana_Lote2_50C/200bar_R1.e.R2

The NLIN Procedure
Dependent Variable mext_g
Method: Gauss-Newton

Iterative Phase

Iter	b0	a1	a2	a3	knot1	knot2	Sum of Squares
0	-0.00104	0.00532	-0.00429	-0.00091	65.0000	260.0	0.0125
1	-0.00208	0.00538	-0.00428	-0.00081	63.3960	235.7	0.0116
2	-0.00208	0.00538	-0.00418	-0.00085	62.3784	209.5	0.0110
3	-0.00208	0.00538	-0.00406	-0.00091	61.2994	187.0	0.0105
4	-0.00208	0.00538	-0.00406	-0.00091	61.2670	188.5	0.0105

NOTE: Convergence criterion met.

Estimation Summary

Method	Gauss-Newton
Iterations	4
R	0
PPC	0
RPC(knot2)	0.00821
Object	0.001851
Objective	0.01051
Observations Read	38
Observations Used	38
Observations Missing	0

Source	DF	Sum of Squares	Mean Square	F Value	Approx Pr > F
Model	5	1.1434	0.2287	696.27	<.0001
Error	32	0.0105	0.000328		
Corrected Total	37	1.1539			

Parameter	Estimate	Approx Std Error	Approximate 95% Confidence Limits	
b0	-0.00208	0.00873	-0.0199	0.0157

a1	0.00538	0.000242	0.00488	0.00587
a2	-0.00406	0.000276	-0.00462	-0.00350
a3	-0.00091	0.000167	-0.00125	-0.00057
knot1	61.2670	3.1058	54.9407	67.5934
knot2	188.5	17.2368	153.4	223.6

Approximate Correlation Matrix

	b0	a1	a2	a3	knot1	knot2
b0	1.0000000	-0.8320503	0.7299065	0.0000000	0.2866959	0.0000000
a1	-0.8320503	1.0000000	-0.8772385	-0.0000000	-0.6007429	-0.0000000
a2	0.7299065	-0.8772385	1.0000000	-0.3802720	0.2557841	-0.2977476
a3	0.0000000	-0.0000000	-0.3802720	1.0000000	0.4475271	0.1084836
knot1	0.2866959	-0.6007429	0.2557841	0.4475271	1.0000000	0.2121668
knot2	0.0000000	-0.0000000	-0.2977476	0.1084836	0.2121668	1.0000000

Residuo.Cana_Lote2_50C/200bar_R1.e.R2

Obs	tempo_ min	mext_g	knot1	knot2	AL1	AL2	mext_ g_hat	RES
1	0	0.0000	65	260	0	0	-0.00208	0.002084
2	10	0.0290	65	260	0	0	0.05168	-0.022675
3	20	0.0818	65	260	0	0	0.10543	-0.023634
4	30	0.1504	65	260	0	0	0.15919	-0.008793
5	40	0.2057	65	260	0	0	0.21295	-0.007252
6	50	0.2499	65	260	0	0	0.26671	-0.016811
7	60	0.2878	65	260	0	0	0.32047	-0.032670
8	70	0.3134	65	260	5	0	0.33879	-0.025387
9	80	0.3384	65	260	15	0	0.35196	-0.013562
10	90	0.3593	65	260	25	0	0.36514	-0.005837
11	120	0.4066	65	260	55	0	0.40466	0.001937
12	150	0.4416	65	260	85	0	0.44419	-0.002588
13	180	0.4758	65	260	115	0	0.48371	-0.007913
14	210	0.4944	65	260	145	0	0.50366	-0.009257
15	240	0.5042	65	260	175	0	0.51584	-0.011644
16	270	0.5193	65	260	205	10	0.52803	-0.008731
17	300	0.5258	65	260	235	40	0.54022	-0.014419
18	330	0.5356	65	260	265	70	0.55241	-0.016806
19	360	0.5432	65	260	295	100	0.56459	-0.021393
20	0	0.0000	65	260	0	0	-0.00208	0.002084
21	10	0.0462	65	260	0	0	0.05168	-0.005475
22	20	0.1193	65	260	0	0	0.10543	0.013866
23	30	0.1997	65	260	0	0	0.15919	0.040507
24	40	0.2483	65	260	0	0	0.21295	0.035348
25	50	0.2870	65	260	0	0	0.26671	0.020289
26	60	0.3236	65	260	0	0	0.32047	0.003130
27	70	0.3467	65	260	5	0	0.33879	0.007913
28	80	0.3655	65	260	15	0	0.35196	0.013538
29	90	0.3834	65	260	25	0	0.36514	0.018263
30	120	0.4148	65	260	55	0	0.40466	0.010137
31	150	0.4495	65	260	85	0	0.44419	0.005312
32	180	0.4819	65	260	115	0	0.48371	-0.001813
33	210	0.5010	65	260	145	0	0.50366	-0.002657
34	240	0.5294	65	260	175	0	0.51584	0.013556
35	270	0.5509	65	260	205	10	0.52803	0.022869
36	300	0.5600	65	260	235	40	0.54022	0.019781
37	330	0.5680	65	260	265	70	0.55241	0.015594
38	360	0.5777	65	260	295	100	0.56459	0.013107

Residuo.Cana_Lote2_50C/350bar_R1.e.R2

The REG Procedure
Model: MODEL1
Dependent Variable: mext_g

Analysis of Variance

Source	DF	Sum of Squares	Mean Square	F Value	Pr > F
Model	3	1.37616	0.45872	159.30	<.0001
Error	34	0.09791	0.00288		
Corrected Total	37	1.47406			

Root MSE	0.05366	R-Square	0.9336
Dependent Mean	0.54701	Adj R-Sq	0.9277
Coeff Var	9.81002		

Parameter Estimates

Variable	DF	Parameter Estimate	Standard Error	t Value	Pr > |t|
Intercept	1	0.07159	0.02644	2.71	0.0105
tempo_min	1	0.00968	0.00071696	13.50	<.0001
AL1	1	-0.00875	0.00089842	-9.74	<.0001
AL2	1	-0.00052206	0.00044367	-1.18	0.2475

Residuo.Cana_Lote2_50C/350bar_R1.e.R2

The NLIN Procedure
Dependent Variable mext_g
Method: Gauss-Newton

Iterative Phase

Iter	b0	a1	a2	a3	knot1	knot2	Sum of Squares
0	0.0716	0.00968	-0.00875	-0.00052	50.0000	165.0	0.0979
1	0.0571	0.0108	-0.00966	-0.00071	44.0288	148.7	0.0870
2	0.0447	0.0117	-0.0102	-0.00107	39.7434	116.5	0.0854
3	0.0327	0.0129	-0.0109	-0.00153	35.0331	98.6572	0.0805
4	0.0221	0.0139	-0.0115	-0.00193	31.6282	96.6287	0.0725
5	0.0200	0.0141	-0.0116	-0.00201	31.2147	96.8090	0.0717
6	0.0199	0.0141	-0.0116	-0.00201	31.2044	96.8080	0.0717
7	0.0199	0.0141	-0.0116	-0.00201	31.2043	96.8080	0.0717

NOTE: Convergence criterion met.

Estimation Summary

Method	Gauss-Newton
Iterations	7
Subiterations	2
Average Subiterations	0.285714
R	4.653E-8
PPC(b0)	3.872E-8
RPC(b0)	0.000027
Object	1.051E-9
Objective	0.071661
Observations Read	38
Observations Used	38
Observations Missing	0

Source	DF	Sum of Squares	Mean Square	F Value	Approx Pr > F
Model	5	1.4024	0.2805	125.25	<.0001
Error	32	0.0717	0.00224		
Corrected Total	37	1.4741			

Parameter	Estimate	Approx Std Error	Approximate 95% Confidence Limits	
b0	0.0199	0.0280	-0.0371	0.0769
a1	0.0141	0.00150	0.0111	0.0172
a2	-0.0116	0.00170	-0.0151	-0.00819
a3	-0.00201	0.000813	-0.00367	-0.00036
knot1	31.2043	3.6288	23.8128	38.5958
knot2	96.8080	18.4650	59.1962	134.4

Approximate Correlation Matrix

	b0	a1	a2	a3	knot1	knot2
b0	1.0000000	-0.8017837	0.7071068	0.0000000	0.2235077	0.0000000
a1	-0.8017837	1.0000000	-0.8819171	-0.0000000	-0.5739002	-0.0000000
a2	0.7071068	-0.8819171	1.0000000	-0.4639468	0.2045363	-0.3224541
a3	0.0000000	-0.0000000	-0.4639468	1.0000000	0.6296604	0.5749923
knot1	0.2235077	-0.5739002	0.2045363	0.6296604	1.0000000	0.3188892
knot2	0.0000000	-0.0000000	-0.3224541	0.5749923	0.3188892	1.0000000

Residuo.Cana_Lote2_50C/350bar_R1.e.R2

Obs	tempo_ min	mext_g	knot1	knot2	AL1	AL2	mext_ g_hat	RES
1	0	0.0000	50	165	0	0	0.01990	-0.019900
2	10	0.2128	50	165	0	0	0.16110	0.051700
3	20	0.3179	50	165	0	0	0.30230	0.015600
4	30	0.3886	50	165	0	0	0.44350	-0.054900
5	40	0.4311	50	165	0	0	0.48228	-0.051183
6	50	0.4588	50	165	0	0	0.50704	-0.048243
7	60	0.4922	50	165	10	0	0.53180	-0.039603
8	70	0.5117	50	165	20	0	0.55656	-0.044863
9	80	0.5285	50	165	30	0	0.58132	-0.052823
10	90	0.5458	50	165	40	0	0.60608	-0.060283
11	120	0.5729	50	165	70	0	0.63365	-0.060746
12	150	0.6007	50	165	100	0	0.64749	-0.046794
13	180	0.6235	50	165	130	15	0.66134	-0.037842
14	210	0.6405	50	165	160	45	0.67519	-0.034691
15	240	0.6526	50	165	190	75	0.68904	-0.036439
16	270	0.6625	50	165	220	105	0.70289	-0.040387
17	300	0.6721	50	165	250	135	0.71674	-0.044636
18	330	0.6809	50	165	280	165	0.73058	-0.049684
19	360	0.7218	50	165	310	195	0.74443	-0.022632
20	0	0.0000	50	165	0	0	0.01990	-0.019900
21	10	0.1419	50	165	0	0	0.16110	-0.019200
22	20	0.3411	50	165	0	0	0.30230	0.038800
23	30	0.4513	50	165	0	0	0.44350	0.007800
24	40	0.5119	50	165	0	0	0.48228	0.029617
25	50	0.5571	50	165	0	0	0.50704	0.050057
26	60	0.5943	50	165	10	0	0.53180	0.062497
27	70	0.6165	50	165	20	0	0.55656	0.059937
28	80	0.6359	50	165	30	0	0.58132	0.054577
29	90	0.6464	50	165	40	0	0.60608	0.040317
30	120	0.6723	50	165	70	0	0.63365	0.038654
31	150	0.6960	50	165	100	0	0.64749	0.048506
32	180	0.7156	50	165	130	15	0.66134	0.054258
33	210	0.7260	50	165	160	45	0.67519	0.050809
34	240	0.7349	50	165	190	75	0.68904	0.045861
35	270	0.7412	50	165	220	105	0.70289	0.038313
36	300	0.7473	50	165	250	135	0.71674	0.030564
37	330	0.7626	50	165	280	165	0.73058	0.032016
38	360	0.7793	50	165	310	195	0.74443	0.034868

Urucum_R1.e.R2

The REG Procedure
Model: MODEL1
Dependent Variable: mext_g

Analysis of Variance

Source	DF	Sum of Squares	Mean Square	F Value	Pr > F
Model	3	76.48077	25.49359	388.39	<.0001
Error	28	1.83788	0.06564		
Corrected Total	31	78.31866			

Root MSE	0.25620	R-Square	0.9765
Dependent Mean	3.22574	Adj R-Sq	0.9740
Coeff Var	7.94239		

Parameter Estimates

Variable	DF	Parameter Estimate	Standard Error	t Value	Pr > |t|
Intercept	1	0.45635	0.10858	4.20	0.0002
tempo_min	1	0.07281	0.00413	17.65	<.0001
AL1	1	-0.06270	0.00500	-12.54	<.0001
AL2	1	-0.00807	0.00252	-3.21	0.0034

Urucum_R1.e.R2

The NLIN Procedure
Dependent Variable mext_g
Method: Gauss-Newton

Iterative Phase

Iter	b0	a1	a2	a3	knot1	knot2	Sum of Squares
0	0.4564	0.0728	-0.0627	-0.00807	40.0000	180.0	1.8379
1	0.3792	0.0808	-0.0695	-0.00884	34.9028	164.5	1.4830
2	0.3127	0.0876	-0.0754	-0.00950	31.8065	154.6	1.3546
3	0.3023	0.0887	-0.0736	-0.0120	30.4524	123.0	1.3110
4	0.3020	0.0887	-0.0735	-0.0121	30.3778	129.0	1.2525
5	0.3020	0.0887	-0.0735	-0.0121	30.3773	129.0	1.2525

NOTE: Convergence criterion met.

Estimation Summary

Method	Gauss-Newton
Iterations	5
Subiterations	1
Average Subiterations	0.2
R	5.707E-8
PPC(a3)	3.752E-8
RPC(a3)	0.000034
Object	2.778E-9
Objective	1.252481
Observations Read	32
Observations Used	32
Observations Missing	0

Source	DF	Sum of Squares	Mean Square	F Value	Approx Pr > F
Model	5	77.0662	15.4132	319.96	<.0001
Error	26	1.2525	0.0482		
Corrected Total	31	78.3187			

Approx

Parameter	Estimate	Std Error	Approximate 95% Confidence Limits	
b0	0.3020	0.1066	0.0830	0.5210
a1	0.0887	0.00643	0.0755	0.1019
a2	-0.0735	0.00687	-0.0877	-0.0594
a3	-0.0121	0.00266	-0.0175	-0.00658
knot1	30.3773	2.4305	25.3815	35.3732
knot2	129.0	17.7500	92.4702	165.4

Approximate Correlation Matrix

	b0	a1	a2	a3	knot1	knot2
b0	1.0000000	-0.8040303	0.7525201	-0.0000000	0.2818784	0.0000000
a1	-0.8040303	1.0000000	-0.9359351	0.0000000	-0.6127066	-0.0000000
a2	0.7525201	-0.9359351	1.0000000	-0.3198725	0.3656472	-0.2187455
a3	-0.0000000	0.0000000	-0.3198725	1.0000000	0.5359507	0.2983607
knot1	0.2818784	-0.6127066	0.3656472	0.5359507	1.0000000	0.2405343
knot2	0.0000000	-0.0000000	-0.2187455	0.2983607	0.2405343	1.0000000

Urucum_R1.e.R2

Obs	tempo_ min	mext_g	knot1	knot2	AL1	AL2	mext_ g_hat	RES
1	0	0.0000	40	180	0	0	0.30201	-0.30201
2	5	0.8353	40	180	0	0	0.74571	0.08959
3	10	1.4972	40	180	0	0	1.18942	0.30778
4	15	2.0488	40	180	0	0	1.63313	0.41567
5	20	2.4428	40	180	0	0	2.07683	0.36597
6	30	2.9157	40	180	0	0	2.96425	-0.04855
7	40	3.2466	40	180	0	0	3.14396	0.10264
8	50	3.4830	40	180	10	0	3.29592	0.18708
9	70	3.8455	40	180	30	0	3.59985	0.24565
10	90	4.0977	40	180	50	0	3.90377	0.19393
11	120	4.4129	40	180	80	0	4.35966	0.05324
12	160	4.6650	40	180	120	0	4.59335	0.07165
13	210	4.8542	40	180	170	30	4.75055	0.10365
14	250	4.9803	40	180	210	70	4.87632	0.10398
15	300	5.1221	40	180	260	120	5.03352	0.08858
16	335	5.2324	40	180	295	155	5.14356	0.08884
17	0	0.0000	40	180	0	0	0.30201	-0.30201
18	5	0.7082	40	180	0	0	0.74571	-0.03751
19	10	1.2471	40	180	0	0	1.18942	0.05768
20	15	1.6782	40	180	0	0	1.63313	0.04507
21	20	1.9707	40	180	0	0	2.07683	-0.10613
22	30	2.4787	40	180	0	0	2.96425	-0.48555
23	40	2.8482	40	180	0	0	3.14396	-0.29576
24	50	3.1254	40	180	10	0	3.29592	-0.17052
25	70	3.5565	40	180	30	0	3.59985	-0.04335
26	90	3.8490	40	180	50	0	3.90377	-0.05477
27	120	4.1415	40	180	80	0	4.35966	-0.21816
28	160	4.4648	40	180	120	0	4.59335	-0.12855
29	210	4.6957	40	180	170	30	4.75055	-0.05485
30	250	4.8189	40	180	210	70	4.87632	-0.05742
31	300	4.9421	40	180	260	120	5.03352	-0.09142
32	335	5.0191	40	180	295	155	5.14356	-0.12446

APÊNDICE A5. MEMÓRIA DO PERÍODO DE DOUTORADO

A doutoranda Susana Pereira de Jesus concluiu graduação (2007) e mestrado (2010) em Engenharia de Alimentos, ambos cursados na Universidade Federal de Santa Catarina (UFSC). O curso de doutorado foi iniciado em março de 2010, sendo este financiado pelo CNPq por meio de bolsa de projeto (processo nº 141828/2010-2) cuja vigência é de 05/2010 a 04/2014.

A carga horária total cursada foi de 25 créditos, incluindo disciplinas e estágios de capacitação docente (PED C), sendo que a aprovação com conceito “A” foi obtida em todos os créditos completados. As disciplinas cursadas, no período de 2010 a 2012, foram as seguintes: Termodinâmica; Fenômenos de Transporte I; Tópicos Especiais em Físico-Química X (Tecnologia de Fluidos Supercríticos); Fenômenos de Transporte II; Seminários; Tópicos em Engenharia de Alimentos (Ciclo de Melhoria PDSA); Tópicos em Engenharia de Alimentos (Métodos Estatísticos). O estágio de docência (PED C) foi realizado, por dois semestres seguidos (2011/1 e 2011/2), na disciplina Termodinâmica (TA331), a qual faz parte do currículo obrigatório do curso de graduação em Engenharia de Alimentos da FEA/Unicamp. Nesta mesma disciplina e curso, a doutoranda foi colaboradora ministrando aula teórica no semestre 2013/2. Além disto, participou como avaliadora de trabalhos (área de Tecnológicas) no Congresso Interno de Iniciação Científica da Unicamp nas edições realizadas nos anos de 2011, 2012 e 2013.

Os exames de qualificação de área e qualificação geral foram apresentados no 2º semestre de 2010 e 2º semestre de 2013, respectivamente. Cabe informar que em abril de 2012, por motivos de ordem pessoal e técnica, fez-se a troca do tema do projeto de doutorado. A produção científica, até o momento, inclui a publicação de dois capítulos de livro (um deles – referente ao tema do projeto inicial – está apresentado no Apêndice A6), um artigo científico e um trabalho em anais de evento (resumo), conforme referências citadas a seguir:

JESUS, S. P.; SANTOS, D. T.; MEIRELES, M. A. A. Environmentally Friendly Technologies for Obtaining Anthocyanins from an Unusual Source. In: MOTOHASHI, N. (Ed.). **Anthocyanins: Structure, Biosynthesis and Health Benefits**. New York: Nova Science Publishers Inc., 2012. p. 139-152.

JESUS, S. P.; MEIRELES, M. A. A. Supercritical Fluid Extraction: A Global Perspective of the Fundamental Concepts of this Eco-Friendly Extraction Technique. In: CHEMAT, F.; VIAN, M. A. (Eds.). **Alternative Solvents for Natural Products Extraction**. Springer Berlin Heidelberg, 2014. p. 39-72.

JESUS, S. P.; CALHEIROS, M. N.; HENSE, H.; MEIRELES, M. A. A. A Simplified Model to Describe the Kinetic Behavior of Supercritical Fluid Extraction from a Rice Bran Oil Byproduct. **Food and Public Health**, v. 3, n. 4, p. 215-222, 2013.

JESUS, S. P.; MEIRELES, M. A. A. Supercritical Fluid Extraction from Natural Products: an Overview of the Mathematical Modeling, Scale-up, Simulation and Economic Analysis of the Process. In: WORKSHOP ON SUPERCRITICAL FLUIDS AND ENERGY (SFE'13), 2013, Campinas. **Anais…** Campinas: Mercado de Letras, 2013. p. 307-309.

APÊNDICE A6. CAPÍTULO PUBLICADO

"ENVIRONMENTALLY FRIENDLY TECHNOLOGIES FOR OBTAINING ANTHOCYANINS FROM AN UNUSUAL SOURCE"

Susana P. Jesus, Diego T. Santos and M. Angela A. Meireles

Capítulo publicado no livro *Anthocyanins: Structure, Biosynthesis and Health Benefits*, Editora: Nova Science Publishers, 2012.

e-ISBN: 978-1-62257-356-1

AVISO DE DIREITO DE AUTOR

In: Anthocyanins: Structure, Biosynthesis and Health Benefits
Editor: Noboru Motohashi
ISBN: 978-1-62257-329-5

Chapter 7

Environmentally Friendly Technologies for Obtaining Anthocyanins from an Unusual Source

S. P. Jesus, D. T. Santos and M. A. A. Meireles*
LASEFI (LAboratory of Supercritical technology: Extraction, Fractionation, and Identification of vegetable extracts) / DEA (Department of Food Engineering) / FEA (School of Food Engineering) / UNICAMP (University of Campinas), Campinas, São Paulo, Brazil

Abstract

The consumers' constantly growing interest in healthier products has been motivating the search for new sources of bioactive compounds such as anthocyanins. Academic and industrial researches have been intensively investigating the anthocyanins due to their valuable functional properties. Although these natural pigments are widely spread in nature, their extraction procedure demands special attention to avoid degradation. For this reason, the extraction method plays a fundamental role in the recovery of anthocyanins from natural sources. Conventional extraction techniques are both time- and solvent-consuming, besides that they usually have a negative impact on the environment since they generate large amounts of organic solvent waste. On the other hand, there is an increasing demand for developing alternative methods in order to achieve faster, more efficient, cost-effective and environmentally friendly extraction processes. This chapter presents the recent work done by our research group (LASEFI/DEA/FEA/UNICAMP) for obtaining anthocyanins from skins of a Brazilian fruit named jabuticaba (*Myrciaria cauliflora*). Several results from conventional and innovative extraction technologies are summarized and discussed with the aim of comparing extraction performances in terms of anthocyanins recovery. This chapter provides a more complete understanding about the influence of different extraction methods on the recovery of anthocyanins.

* E-mail address: meireles@fea.unicamp.br.

Introduction

The consumers' desire for a healthier lifestyle has motivated the search for new sources of natural ingredients [1]. Anthocyanins are water-soluble pigments found in many fruits, vegetables and flowers [2]. Besides being colorants, anthocyanins have other bioactive properties, of which the strong antioxidant capacity is one of the most significant ones [3]. It is known that anthocyanins may promote important health benefits because they present antioxidant, anti-inflammatory and antimutagenic activities [4]. Therefore, the academic and industrial interest in anthocyanins has been increasing in recent decades since these substances have a high potential for application in food, cosmetic and pharmaceutical products.

Jabuticaba (*Myrciaria cauliflora*) is a Brazilian native fruit that seems to be a promising source for anthocyanins extraction. This fruit has a white gelatinous flesh covered by a dark purple to almost black skin, of which the intense color is attributed to the high content of anthocyanins [1]. The extraction method is a key factor for obtaining anthocyanins from natural sources. Taking into account that conventional extraction methods are commonly time- and solvent-consuming [5], there is an increasing demand for developing faster, more efficient and environmentally friendly extraction procedures [6]. An efficient extraction method should maximize anthocyanins recovery with concomitant minimal degradation of these unstable pigments [1].

This chapter presents some fundamental aspects about anthocyanins extraction and degradation, considering the influence of different extraction techniques on anthocyanins recovery. The focus is on discussing some environmentally friendly extraction methods that have been recently used by our research group (LASEFI/DEA/FEA/UNICAMP) in order to recover anthocyanins from jabuticaba skins.

Anthocyanins Degradation

Anthocyanins are highly unstable compounds, being very susceptible to degradation. Their stability is affected by many factors, such as temperature, pH, light, oxygen, anthocyanins concentration, enzymes, and the presence of accompanying substances (metallic ions, sugars, copigments, among others) [7, 8]. It is known that anthocyanins are particularly sensitive to heat, alkaline pH, and light exposure. Thus, in order to minimize thermal degradation, conventional extraction techniques are generally conducted at low temperatures combined with long processing times. Besides time-consuming, these methods have a negative impact on the environment because they generate large amounts of solvent wastes [9].

It is well established that anthocyanins degradation is particularly dependent of both temperature and time [9]. Low temperature and short extraction time tend to result in poor efficiency in extracting anthocyanins. On the other hand, high temperature and long extraction time lead to significant anthocyanins degradation. Therefore, an optimal combination between temperature and time must be found in order to achieve maximum anthocyanins extraction together with minimum anthocyanins degradation [10].

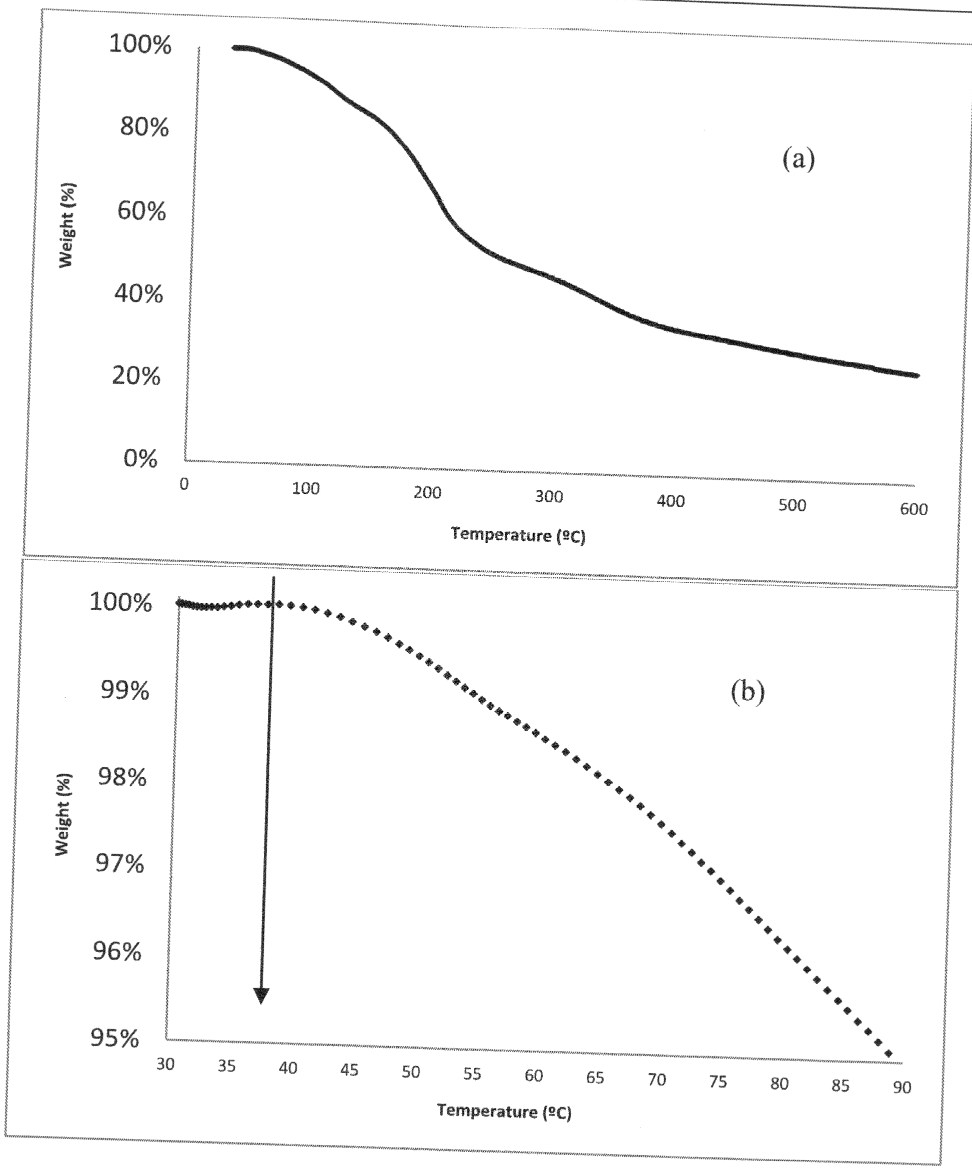

Figure 1. (a) Thermogravimetric analysis (TGA) of an ethanolic extract obtained from jabuticaba skins (analysis was conducted in nitrogen atmosphere). (b) Image zoom.

Santos and co-authors [1] used thin layer chromatography (TLC) to fractionate some ethanolic extracts obtained from jabuticaba skins. The results from qualitative TLC analysis indicated that cyanidin-3-glucoside and delphinidin-3-glucoside were the anthocyanins possibly present in the extracts [1]. The thermal stability of an anthocyanin-rich extract obtained from jabuticaba skins was determined by thermogravimetric analysis (TGA), which is presented in Figure 1. The TGA curve showed that the thermal degradation started at approximately 45 ºC and increased continually as the temperatures increased.

The total yield of a target compound will remain constant (if no degradation occurs) after some time of extraction, when the available compound has been entirely exhausted from the sample. Actually, when working with unstable substances, the yield of the extraction process will be a function of both extraction and degradation phenomena. Since anthocyanins are particularly unstable, a maximum level of anthocyanins will be reached after a certain time of extraction. After this time, degradation effects will probably overcome the extraction effects, decreasing the total anthocyanins content [9].

Petersson and co-authors [9] investigated the extraction/degradation curves of anthocyanins from extracts of red onion. They used an elevated temperature to perform a batch extraction in a pressurized vessel at 2–4 bar. These authors successfully distinguished extraction and degradation effects and proposed a model to predict the real extraction curve, which might be similar to the theoretical one if there was no degradation phenomenon competing with extraction. The obtained curves are schematically represented in Figure 2. The experimental data demonstrated that a very short extraction time (13–25 min, including pre-heating period) must be used in order to avoid significant degradation effects when extracting anthocyanins at high temperature (110ºC). A dynamic extraction process may probably result in less degradation at the same temperature, because residence time of the solvent is shorter in a semi-continuous solid-liquid extraction [9]. Thus, to avoid significant thermal degradation, anthocyanins extraction techniques performed at elevated temperature should always be associated with short process time.

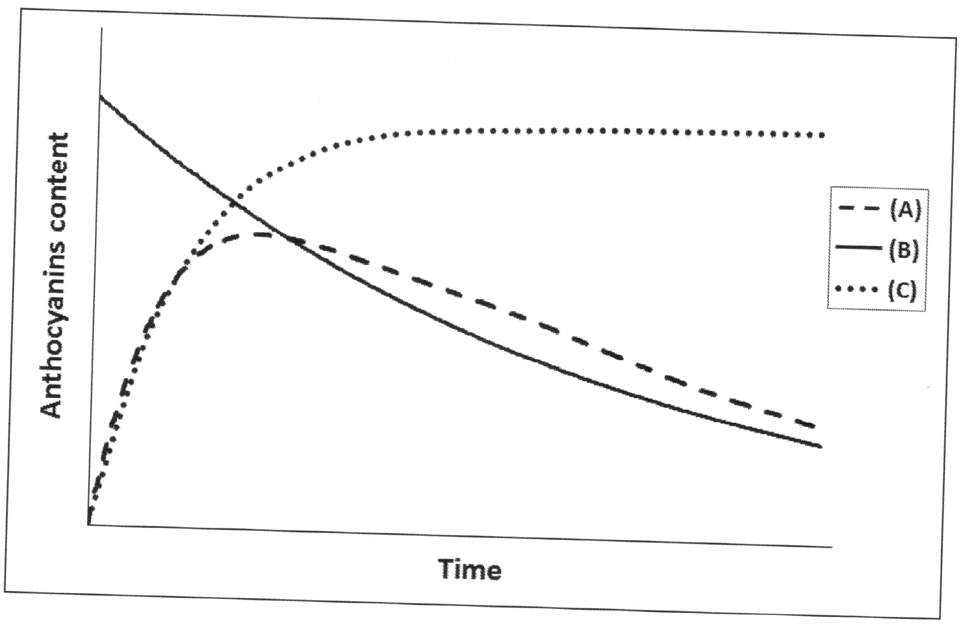

Figure 2. Extraction and degradation phenomena competing during high temperature extraction of anthocyanins: (A) combined extraction/degradation curve; (B) degradation curve; (C) total extraction curve (predicted). (Schematic figure based on the hypothesis proposed by Petersson and co-authors [9].

Anthocyanins Extraction Methods

The recovery of anthocyanins from plant materials has been traditionally performed by conventional solid-liquid extraction, which usually requires a long processing time that demands large amounts of organic solvents. Because anthocyanins are polar molecules, the most common solvents are ethanol, methanol, and acetone, or aqueous solutions of these solvents [5,7]. The solvents are commonly acidified in order to increase both extraction efficiency and anthocyanins stability [2,5]. The extraction efficiency is improved because acidified solvents denature cellular membranes and facilitate solubilization of anthocyanins

[2]. The pH decrease also enhances stability since in acidic conditions (pH < 2), anthocyanins are in their most stable form (flavylium cation) [5,8].

There are several extraction techniques that have been used for obtaining target compounds from plant matrices. These methods may be divided into two main groups: Low Pressure Solvent Extraction (LPSE) and High Pressure Solvent Extraction (HPSE). As the names indicate, the LPSE is conducted at atmospheric pressure, while HPSE requires a pressurized system (pressure ranges vary according to the applied method). The LPSE group includes a wide variety of extraction methods, from very traditional (Soxhlet, agitation, maceration, percolation, centrifugation, among others) to more recent ones (ultrasound, microwave, and pulsed electric field assisted extractions). The HPSE group involves modern developed technologies, of which Supercritical Fluid Extraction (SFE) is the most studied and industrially consolidated. The HPSE includes also emerging technologies such as Pressurized Liquid Extraction (PLE), High Hydrostatic Pressure Extraction (HHPE), and High Pressure Carbon Dioxide Assisted Extraction (HPCDAE).

Although various procedures for anthocyanins extraction have been investigated by different research groups [11–18], in this chapter our focus is to discuss some methods that have been recently used by our research group (LASEFI/DEA/FEA/UNICAMP) for recovering anthocyanins from jabuticaba skins. The evaluated LPSE methods were agitated bed extraction (ABE), ultrasound-assisted extraction (UAE), Soxhlet, and percolation. Beyond that, a novel extraction process was developed applying an ultrasound treatment followed by agitated bed extraction (UAE + ABE). In the HPSE group, the applied methods were pressurized liquid extraction (PLE) and high pressure carbon dioxide assisted extraction (HPCDAE). A schematic summary showing important parameters of the investigated LPSE and HPSE methods is presented in Table 1.

Influence of Extraction Methods on Anthocyanins Recovery

The composition of a natural plant extract is strongly dependent on three fundamental factors: plant material characteristics, solvent properties and extraction process conditions. The characteristics (yield and chemical profile) of extracts obtained by different techniques should only be effectively compared when using both the same solvent and plant material. According to literature information, special attention should be dedicated to plant material, since it is essential to minimize the possible significant influence of origin, year of production, storage conditions and pretreatment of the plant material [6].

This section presents recently published data [1,6,10] concerning the anthocyanins extraction from jabuticaba skins. Table 2 and Table 3 contain a data compilation including experimental LPSE and HPSE results expressed in terms of anthocyanins recovery. It is important to highlight that only "green" solvents were used in all extraction procedures. Since the focus was the extraction technique, and not particularly the solvent composition optimization, different solvent mixtures were not tested. It is well established that the quality of a natural extract is directly associated to its functional properties, which are a function of chemical composition [6]. For this reason, we considered that the most efficient extraction process would be the one which leaded to the highest anthocyanins content in the extract.

Table 1. General process parameters according to the extraction method

Extraction Group	Extraction method	Combination of temperature and time	Operation mode	Solid (plant material) configuration	Solvent residence time	Specific characteristics
LPSE	UAE	low T + long t	batch	dispersed particles	long t_R	ultrasonic frequency (cavitation bubbles)
LPSE	ABE	low T + long t	batch	dispersed particles	long t_R	continuous agitation
LPSE	UAE + ABE	low T + long t	batch	dispersed particles	long t_R	ultrasonic frequency + agitation
LPSE	Soxhlet	high T + long t	batch	compact fixed bed	long t_R	solvent recirculation; exhaustive extraction
LPSE	Percolation	low T + long t	semi-continuous	compact fixed bed	short t_R	solvent recirculation
HPSE	PLE	high T + short t	semi-continuous	compact fixed bed	short t_R	dynamic extraction; combination of T + P + t
HPSE	HPCDAE	high T + short t	batch	dispersed particles	long t_R	explosive effect (CO_2 expansion); pH decrease

LPSE, Low Pressure Solvent Extraction; HPSE, High Pressure Solvent Extraction; UAE, Ultrasound Assisted Extraction; ABE, Agitated Bed Extraction; PLE, Pressurized Liquid Extraction; HPCDAE, High Pressure Carbon Dioxide-Assisted Extraction; CO_2, carbon dioxide; T, temperature; P, pressure; t, time; t_R, residence time of solvent.

Table 2. LPSE of anthocyanins from jabuticaba skins using ethanol as solvent and solvent to feed ratio equal to 10: compilation of experimental results from LASEFI/DEA/FEA/UNICAMP

IC	Extraction method	Plant material moisture (%, w/w)	Process parameters	TMA (mg cy-3-glu eq/g dry material)[(a)]	Ref.
E1	UAE	80.8	T = 25 °C; t_E = 2 h; f = 40 kHz	4.7 ± 0.2	[1]
E2	ABE	80.8	T = 30 °C; t_E = 2 h; AGR = 150 rpm	6.2 ± 0.3	[1]
E3	Combined UAE + ABE	80.8	UAE (10 min) + ABE (2 h)	5.3 ± 0.2	[1]
E4	Soxhlet	80.8	t_E = 8 h	5.0 ± 0.2	[1]
E5	Percolation	80.8	T = 23 °C; t_E = 2 h; SFR = 28 mL/min	1.90 ± 0.09	[26]
E6	Percolation	66.5	T = 23 °C; t_E = 2 h; SFR = 28 mL/min	1.2 ± 0.2	[10]

LPSE, Low Pressure Solvent Extraction; IC, identification code; UAE, Ultrasound-Assisted Extraction; ABE, Agitated Bed Extraction; PM, Plant Material; S/F, solvent to feed ratio; T, temperature; tE, extraction time; f, frequency; AGR, agitation rate; SFR, solvent flow rate; (mg cy-3-glu eq/g dry material), mg of cyanidin-3-glucoside equivalent/g of jabuticaba skins (dry basis).

[(a)] The content of anthocyanins is expressed in terms of Total Monomeric Anthocyanins (TMA), which was determined using the pH differential method as described by Santos and co-authors [1]. A detailed discussion about methods of anthocyanins analysis can be found in the reference [27].

The LPSE experiments E1 to E5 (Table 2) were conducted using both the same plant material (fresh jabuticaba skins, 80.8 % moisture) and solvent. Therefore, this data may be compared in order to evaluate the extraction methods performances. Taking into account the anthocyanins content, the most efficient LPSE method was ABE. The high-temperature and long-time characteristics of Soxhlet process probably induced significant anthocyanins degradation, resulting in lower anthocyanins recovery than ABE. When comparing percolation and ABE, although both were conducted in low temperature and had the same extraction time, the two important differences (the solid material configuration and the residence time of solvent) may have affected the anthocyanins extraction. The compact fixed bed and the short residence time are factors that imply disadvantages for mass transfer in the percolation method. These process differences may explain why percolation provided much lower anthocyanins recovery than ABE.

Ultrasound has been shown to improve the extraction of target compounds from various plant materials by reducing extraction times and increasing yields [19]. The enhancement of extraction efficiency of organic compounds by UAE is attributed to the phenomenon of cavitation, which is produced when an ultrasonic wave passes through the solvent. Cavitation bubbles are produced and compressed during the application of ultrasound treatment. When the bubbles and the gas within them are compressed, there is an important increase in temperature and pressure causing the collapse of the bubble. This collapse results in a significant disruption of cells and produces a "shock wave" that passes through the solvent enhancing the mixing. Ultrasound also exerts a mechanical effect, allowing a more intense penetration of solvent into the plant matrix. These effects provide enhanced mass transfer and improve the release of intracellular products into the bulk medium [19–21].

Although UAE enhances mass transfer and may improve the extraction of organic compounds [19–21], the experimental data (Table 2) showed that ultrasound did not have a positive influence on anthocyanins recovery from jabuticaba skins. Considering results from E1 and E3 (Table 2), the applied ultrasonic frequency may have favored the degradation of highly sensitive anthocyanins. This effect justifies why the short time ultrasonic treatment (UAE + ABE) was less aggressive to anthocyanins recovery than UAE.

Table 3. HPSE of anthocyanins from jabuticaba skins: compilation of experimental results from LASEFI/DEA/FEA/UNICAMP

IC	Extraction method	PM moisture (%, w/w)	Solvent	S/F	Process parameters	TMA (mg cy-3-glu eq/g dry material)[(a)]	Ref.
E7	PLE	66.5	Ethanol	4.4	T = 80 °C; P = 50 bar; t_S = 9 min; t_D = 12 min; SFR = ~ 1.7 mL/min	2.4 ± 0.5	[10]
E8	PLE	59.2	Ac. water[(b)] (pH = 2.5)	4.4	T = 80 °C; P = 117 bar; t_S = 5 min; t_D = 20 min; SFR = ~ 1.0 mL/min	0.58 ± 0.02	[6]
E9	HPCDAE	59.2	Ac. water[(b)] (pH = 2.5)	10	T = 80 °C; P = 117 bar; $R_{S\text{-}L/CO2}$ = 20 %; t_E = 20 min	2.2 ± 0.3	[6]
E10	HPCDAE Control[(c)]	59.2	Ac. water[(b)] (pH = 2.5)	10	T = 80 °C; P = 1 bar; t_E = 20 min	1.6 ± 0.1	[6]

HPSE, High Pressure Solvent Extraction; IC, identification code; PLE, Pressurized Liquid Extraction; HPCDAE, High Pressure Carbon Dioxide Assisted-Extraction; PM, Plant Material; S/F, solvent to feed ratio; T, temperature; P, pressure; SFR, solvent flow rate; t_S, static extraction time; t_D, dynamic extraction time; t_E, extraction time; $R_{S\text{-}L/CO2}$, volume ratio of solid-liquid mixture/pressurized CO_2; (mg cy-3-glu eq/g dry material), mg of cyanidin-3-glucoside equivalent/g of jabuticaba skins (dry basis).

(a) The content of anthocyanins is expressed in terms of Total Monomeric Anthocyanins (TMA), which was determined using the pH differential method as described by Santos and co-authors [1]. A detailed discussion about methods of anthocyanins analysis can be found in the reference [27].

(b) Distilled water acidified by hydrochloric acid addition.

(c) HPCDAE Control: an extraction under atmospheric pressure using the HPCDAE system without CO_2 addition and pressurization.

The PLE is an emerging technology that has been intensively studied in recent years [2,5,11,12,22–25]. The major advantage of PLE process is that the pressurized solvent remains in the liquid state well above its boiling point, allowing for high-temperature extraction [2]. It is known that increasing temperature improves extraction efficiency by enhancing solubility and diffusion rate of compounds into the solvent, reducing solute-matrix interactions, decreasing viscosity and surface tension of the solvent [9,12]. If water or aqueous solutions are used as solvents, a particularly important effect is that elevated temperatures modify the dielectric constant of the water resulting in the possibility of tuning its polarity [24]. However, elevation of temperature simultaneously results in increasing degradation rates of thermolabile compounds such as anthocyanins [1, 2, 9]. Therefore, a high-temperature process must be combined with short extraction time because anthocyanins degradation rates are temperature and time dependent [9].

In the case of anthocyanins recovery from jabuticaba skins by PLE, a process parameters optimization study has been recently published by Santos and co-authors [10]. The evaluated independent variables were temperature (T), pressure (P), and static extraction time (t_S). The data from PLE experiment (E7 – Table 3) represent the optimal extraction conditions considering the investigated range of each variable (T = 40–120°C, P = 50 –100 bar, t_S = 3–15 min). The optimization study demonstrated that extraction temperature strongly affected the anthocyanins recovery, being clearly the most significant extraction variable. In the lowest range (T=40–80°C), the temperature presented a positive influence on anthocyanins extraction, while in the highest range (T=80–120°C), the influence was negative since increasing temperature caused a decrease in anthocyanins recovery. In addition, when working in the highest temperature range studied (T=80–120°C), the elevation of static extraction time presented a negative influence on anthocyanins extraction [10].

In order to compare PLE (E7 – Table 3) to a LPSE technique, a percolation (E6– Table 2) extraction was conducted using the same plant material (dried jabuticaba skins, 66.5% moisture) and solvent. This LPSE method was chosen for comparison because PLE and percolation are semi-continuous processes, in which the solvent flows through a solid fixed bed. The experimental data demonstrated that the PLE procedure was more effective in extracting anthocyanins from jabuticaba skins, since the PLE extract presented significantly higher anthocyanins content than the percolation extract [10]. The better performance presented by PLE is probably due to the use of elevated temperature combined with system pressurization and short extraction time. Several published research articles have demonstrated that the above mentioned combination enhances the extraction of anthocyanins from various sources [2,5,11,12].

The HPCDAE is an innovative technique that exploits the explosive effect of high pressure carbon dioxide (CO_2) combined with its ability to acidify the extraction medium. The pH decrease is attributed to the generation of "in situ" carbonic acid and/or alkyl carbonic acid when CO_2 is inserted into the water or aqueous solution solvent [6]. The rapid release of gas pressure results in the explosive effect of high pressure CO_2, which may improve the extraction efficiency of target compounds by modifying cell membranes, decreasing the intracellular pH, disordering the intracellular electrolyte balance and removing vital constituents from cells and cells membranes [6, 18]. According to Xu and co-authors [18], in HPCDAE, there are probably five forms associated with CO_2, including supercritical CO_2, H_2CO_3 and its dissociated products such as H^+, HCO_3^-, and CO_3^{-2}. These different forms may play important roles in anthocyanins extraction, which were not fully understood until now [6].

Santos and Meireles [6] have published a work concerning the optimization of HPCDAE process parameters in order to achieve anthocyanin-rich extracts. The investigated independent variables were temperature (T=40–80°C), pressure (P=65–135 bar), and volume ratio of solid-liquid mixture/pressurized CO_2 ($R_{S\text{-}L/CO2}$ = 20–80%). The experimental results demonstrated that the recovery of anthocyanins was significantly affected by both temperature and pressure. However, the effect of the volume ratio of solid- liquid mixture/pressurized CO_2 was not significant in terms of anthocyanins extraction. The

HPCDAE data from Table 3 (E9) present the determined optimal conditions for anthocyanins recovery from jabuticaba skins [6].

A comparison between HPCDAE and PLE was conducted using the same plant material (dried jabuticaba skins, 59.2% moisture), solvent, temperature and pressure in both techniques [6]. Results (Table 3, E8 and E9) showed that HPCDAE provides much higher anthocyanins recovery than PLE in similar process conditions. The better performance of HPCDAE is probably due to the explosive effect caused by fast decompression of CO_2, which may have improved mass transfer from plant matrix to extracting solvent because of plant cell destruction during CO_2 expansion [6]. Besides that, the pH decrease was possibly favorable for anthocyanins extraction and stability. When considering the comparison between HPCDAE and HPCDAE-control (E9 and E10, respectively), the positive influence of pressure and CO_2 addition was confirmed since the extract obtained by HPCDAE presented significant higher anthocyanins content [6].

It is possible that the anthocyanins recovery by PLE with acidified water (Table 3, E8) might be improved if a study for temperature optimization had been performed. Some authors have demonstrated that the optimal extraction condition may be achieved in temperatures higher than 80ºC when using acidified water or acidified water solutions as PLE solvents [11,12].

The HPSE procedures are certainly promising techniques for obtaining anthocyanins from various sources. HPSE techniques usually require smaller amounts of solvents (S/F, solvent to feed ratio) and shorter extraction times than LPSE, which are important factors from an industrial point of view.

The plant material plays a noticeable influence on the extraction process as can be demonstrated by comparing data from E5 and E6 (Table 2). Although applying the same process parameters (temperature, time, and solvent) in both extractions, the percolation experiments E5 and E6 were conducted using jabuticaba skins with different moisture contents (80.8 and 66.5 %, respectively). The results showed that a better recovery of anthocyanins was achieved when using fresh jabuticaba skins, revealing the possible adverse effects of the drying pre-treatment [6, 10]. The heating applied in the drying process (conducted at T = 45 ºC) may have caused anthocyanins degradation [6, 10]. According to Monrad and co-authors [12], a certain water quantity is necessary to facilitate anthocyanins extraction. Therefore, the water from plant material possibly acted as a co-solvent improving anthocyanins recovery.

Conclusion

It is well established that the extraction method exerts a strongly influence over the recovery of anthocyanins from plant matrices. In general, from all discussed extraction process parameters, the temperature seems to be the most significant one. Therefore, despite working with LPSE or HPSE processes, the temperature always plays a fundamental role in anthocyanins extraction. Since degradation of anthocyanins is temperature- and time-dependent, the extraction time also requires special attention, particularly when working with high temperature processes.

Anthocyanins extraction has been traditionally conducted by LPSE at low temperatures, probably because in conventional techniques it is usual to utilize long extraction times. The HPSE procedures are certainly promising techniques for obtaining anthocyanins from various sources. One of the major advantages of HPSE methods is the possibility of using only "green" solvents (such as water, ethanol and CO_2) still providing a high recovery of anthocyanins. In addition, HPSE techniques usually require smaller amounts of solvents and shorter extraction times than LPSE, which are important factors from an industrial point of view.

Acknowledgment

The authors are grateful to CNPq and FAPESP for financial support. Susana P. Jesus thanks CNPq (141828/2010-2); Diego T. Santos thanks CNPq (141894/2009-1) for the doctorate fellowships and FAPESP (10/16485-5) for the Postdoc fellowship.

References

[1] Santos, D.T., Veggi, P.C., Meireles, M.A.A. (2010). Extraction of antioxidant compounds from Jabuticaba (*Myrciaria cauliflora*) skins: Yield, composition and economical evaluation. *Journal of Food Engineering*, 101, 23-31.

[2] Ju, Z.Y., Howard, L.R. (2003). Effects of solvent and temperature on pressurized liquid extraction of anthocyanins and total phenolics from dried red grape skin. *Journal of Agricultural and Food Chemistry*, 51, 5207-5213.

[3] Nicoué, E.E, Savard, S., Belkacemi, K. (2007). Anthocyanins in wild blueberries of Quebec: extraction and identification. *Journal of Agricultural and Food Chemistry*, 55, 5626-5635.

[4] Santos, D.T., Meireles, M.A.A. (2009). Jabuticaba as a source of functional pigments. *Pharmacognosy Reviews*, 3, 127-132.

[5] Gizir, A.M., Turker, N., Artuvan, E. (2008). Pressurized acidified water extraction of black carrot [*Daucus carota* ssp *sativus* var. *atrorubens* Alef.] anthocyanins. *European Food Research and Technology*, 226, 363-370.

[6] Santos, D.T., Meireles, M.A.A. (2011). Optimization of bioactive compounds extraction from jabuticaba (*Myrciaria cauliflora*) skins assisted by high pressure CO2, *Innovative Food Science and Emerging Technologies*, 12, 398-406.

[7] Castañeda-Ovando, A., Pacheco-Hernández, M.L., Páez-Hernández, M.E., Rodríguez, J. A. & Galán-Vidal, C. A. (2009). Chemical studies of anthocyanins: A review. *Food Chemistry*, 113, 859-871.

[8] Cavalcanti, R.N., Santos, D.T., Meireles, M.A.A. (2011). Non-thermal stabilization mechanisms of anthocyanins in model and food systems-An overview. *Food Research International*, 44, 499-509.

[9] Petersson, E.V., Liu, J., Sjöberg, P.J.R., Danielsson, R., Turner, C. (2010). Pressurized Hot Water Extraction of anthocyanins from red onion: A study on extraction and degradation rates. *Analytica Chimica Acta*, 663, 27-32.

[10] Santos, D.T., Veggi, P.C., Meireles, M.A.A. (2011). Optimization and economic evaluation of pressurized liquid extraction of phenolic compounds from jabuticaba skins. *Journal of Food Engineering*, in press.

[11] Arapitsas, P., Turner, C. (2008). Pressurized solvent extraction and monolithic column-HPLC/DAD analysis of anthocyanins in red cabbage. *Talanta*, 74, 1218-1223.

[12] Monrad, J.K., Howard, L.R., King, J.W., Srinivas, K., Mauromoustakos, A. (2010). Subcritical solvent extraction of anthocyanins from dried red grape pomace. *Journal of Agricultural and Food Chemistry*, 58, 2862-2868.

[13] Corrales, M., García, A.F., Butz, P., Tauscher, B. (2009). Extraction of anthocyanins from grape skins assisted by high hydrostatic pressure. *Journal of Food Engineering*, 90, 415-421.

[14] Corrales, M., Toepfl , S., Butz, P., Knorr, D., Tauscher, B. (2008). Extraction of anthocyanins from grape by-products assisted by ultrasonics, high hydrostatic pressure or pulsed electric fields: A comparison. *Innovative Food Science & Emerging Technologies*, 9, 85-91.

[15] Seabra, I.J., Braga, M.E.M., Batista, M.T., Sousa, H.C. (2010). Effect of solvent (CO2/ethanol/H2O) on the fractionated enhanced solvent extraction of anthocyanins from elder berry pomace. *Journal of Supercritical Fluids*, 54, 145-152.

[16] Seabra, I.J., Braga, M.E.M., Batista, M.T.P., Sousa, H.C. (2011). Fractioned high pressure extraction of anthocyanins from elderberry (*Sambucus nigra* L.) pomace. *Food Bioprocess Technology*, 3, 674–683.

[17] Perez-Serradilla, J.A., Luque de Castro, M.D. (2011). Microwave-assisted extraction of phenolic compounds from wine lees and spray-drying of the extract. *Food Chemistry*, 124, 1652-1659.

[18] Xu, Z., Wu, J., Zhang, Y., Hu, X., Liao, X., Wang, Z. (2010). Extraction of anthocyanins from red cabbage using high pressure CO2. *Bioresource Technology*, 101, 7151-7157.

[19] Paniwnyk, L., Beaufoy, E., Lorimer, J.P., Mason, T.J. (2001). The extraction of rutin from flower buds of *Sophora japonica*. *Ultrasonics Sonochemistry*, 8, 299-301.

[20] Rostagno, M.A.; Palma, M., Barroso, C.G. (2003). Ultrasound-assisted extraction of soy isoflavones. *Journal of Chromatography A*, 1012, 119-128.

[21] Wu, J., Lin, L., Chau, F. (2001). Ultrasound-assisted extraction of ginseng saponins from ginseng roots and cultured ginseng cells. *Ultrasonics Sonochemistry*, 8, 347-352.

[22] Ibáñez, E., Kubátová, A., Señoráns, F.J., Cavero, S., Reglero, G., Hawthorn, S.B. (2003). Subcritical water extraction of antioxidant compounds from rosemary plants. *Journal of Agricultural and Food Chemistry*, 51, 375-382.

[23] García-Marino, M., Rivas-Gonzalo, J.C., Ibáñez, E., García-Moreno, C. (2006). Recovery of catechins and proanthocyanidins from winery by-products using subcritical water extraction. *Analytica Chimica Acta*, 563, 44-50.

[24] Rodríguez-Meizoso, I., Jaime, L., Santoyo, S., Señoráns, F.J., Cifuentes, A., Ibáñez, E. (2010). Subcritical water extraction and characterization of bioactive compounds from *Haematococcus pluvialis* microalga. *Journal of Pharmaceutical and Biomedical Analysis*, 51, 456-463.

[25] Teo, C.C., Tan, S.N., Yong, J.W.H., Hew, C.S., Ong, E.S. (2010). Review: Pressurized hot water extraction (PHWE). *Journal of Chromatography A*, 1217, 2484-2494.

[26] Santos, D.T., Veggi, P.C., Meireles, M.A.A. (2009). "Avaliação Técnico-Econômica da Extração de Antocianinas por Percolação em Leito Fixo". In *Proceedings of the XXXIV Brazilian Congress on Particulate Systems*, Oct. 2009 (Campinas, Brazil).
[27] Giusti, M.M., Jing, P. (2008). Analysis of Anthocyanins. In C. Socaciu (Ed.), *Food Colorants: Chemical and Functional Properties* (pp. 479-505). Boca Raton, FL: CRC Press.

REFERÊNCIAS

ALBUQUERQUE, C. L. C. **Obtenção de sementes desengorduradas e de óleo rico em tocotrienóis de urucum por extração supercrítica: estudo dos parâmetros de processo, do aumento de escala e da viabilidade econômica**. 2013. (PhD). UNICAMP (University of Campinas), Brazil.

MEIRELES, M. A. A. Extraction of bioactive compounds from Latin American plants. In: MARTINEZ, J. L. (Ed.). **Supercritical fluid extraction of nutraceuticals and bioactive compounds**. Boca Raton: CRC Press –Taylor & Francis Group, 2008. cap. 8, p.243-274.

PRADO, J. M. **Estudo do aumento de escala do processo de extração supercrítica em leito fixo**. 2010. (PhD). FEA (School of Food Engineering), UNICAMP (University of Campinas), Brazil

SHINTAKU, A. **Obtenção de extrato proveniente do aproveitamento de resíduo da indústria sucroalcooleira, utilizando CO_2 supercrítico: parâmetros de processo e estimativa do custo de manufatura**. 2006. 358 (Master). FEA (School of Food Engineering), UNICAMP (University of Campinas), Brazil.

SOVOVÁ, H. Rate of the vegetable oil extraction with supercritical CO_2—I. Modelling of extraction curves. **Chemical Engineering Science,** v. 49, n. 3, p. 409-414, 1994.